

Pediatric Radiology Online Course

University of Virginia Health Sciences Center

Department of Radiology

Jonathan Ciambotti M.D., Wei-Shin Lai M.D., Christopher D. Cook M.D.,
Talissa Altes M.D., Ellen Casey S.M.D., Tatiana Pirttima M.D.,
Steven Pirttima M.D., Kimiknu Mentore, Jack W. Higginbotham M.D.,
Atul Gupta S.M.D., Joan McIlhenny M.D., Spencer B. Gay M.D.

All materials were downloaded from the Website

<https://www.med-ed.virginia.edu/courses/rad/peds/index.html>

By

DR/ ASHRAF ABOTALEB

Consultant, Pediatric Emergency Medicine



Pediatric Radiology Online Course

University of Virginia Health Sciences Center

Department of Radiology

Jonathan Ciambotti M.D., Wei-Shin Lai M.D., Christopher D. Cook M.D.,
Talissa Altes M.D., Ellen Casey S.M.D., Tatiana Pirttima M.D.,
Steven Pirttima M.D., Kimiknu Mentore, Jack W. Higginbotham M.D.,
Atul Gupta S.M.D., Joan McIlhenny M.D., Spencer B. Gay M.D.

All materials were downloaded from the Website

<https://www.med-ed.virginia.edu/courses/rad/peds/index.html>

By

DR/ ASHRAF ABOTALEB

Consultant, Pediatric Emergency Medicine

Learning Objectives

Chest:

1. Know the components of the pediatric CXR study.
2. Know the approach to reading a pediatric CXR.
3. Identify pneumothorax, pneumomediastinum, and pneumoperitoneum.
4. Identify the medical causes of respiratory distress syndrome (transient tachypnea, meconium aspiration, neonatal pneumonia, and respiratory distress syndrome).
5. Identify the surgical causes of respiratory distress syndrome (congenital diaphragmatic hernia, congenital cystic adenomatoid malformation, congenital lobar emphysema, and sequestration).
6. Identify laryngomalacia, acute epiglottitis, croup, and retropharyngeal abscess.
7. Identify and classify pulmonary inflammatory disease.

Abdominal:

1. Identify the radiographic features of esophageal atresia, tracheoesophageal fistula, duodenal atresia, jejunal-ileal atresia, meconium ileus, meconium plug syndrome, hirschsprung disease, and necrotizing enterocolitis.
2. Identify the radiographic features of esophageal foreign bodies, esophageal stricture, and hypertonic pyloric stenosis.
3. Identify the radiographic features of malrotation, midgut volvulus, Meckel's diverticulum, appendicitis, and intussusception colonic atresia.
4. Identify the radiographic features of biliary atresia, neonate hepatitis, choledochal cyst.

Genitourinary:

- 1- Know how to identify and grade vesicoureteral reflux.
- 2- Identify cystic renal diseases (autosomal recessive polycystic kidney disease and autosomal dominant polycystic kidney disease).
- 3- Identify congenital urinary abnormalities.
- 4- Identify hydronephrosis and its causes.
- 5- Identify genitourinary tumors.

Musculoskeletal:

- 1- Identify common types of pediatric trauma.**
- 2- Identify common pediatric hip abnormalities and pathologies.**
- 3- Identify common pediatric lower extremity abnormalities.**
- 4- Identify benign pediatric musculoskeletal lesions.**
- 5- Identify aggressive pediatric musculoskeletal lesions.**
- 6- Identify congenital orthopedic disorders.**
- 7- Identify metabolic disorders on traditional radiographic studies.**

Neurological:

- 1- Know the normal appearance of a pediatric head US.**
- 2- Identify germinal matrix hemorrhage and its grade.**
- 3- Identify neurological developmental abnormalities on radiographic studies.**
- 4- Identify neurofibromatosis, tuberous sclerosis, and Sturge-Weber syndrome.**
- 5- Identify TORCH syndrome, encephalitis, subacute sclerosing panencephalitis, acute disseminated encephalomyelitis, meningitis, and cysticercosis.**
- 6- Identify cerebellar astrocytoma, medulloblastoma, brainstem glioma, and ependymoma.**
- 7- Identify craniopharyngioma, suprasellar astrocytoma, hypothalamic hamartoma, and germ cell tumors**
- 8- Identify pineocytoma and pineoblastoma, germinoma, and tectal glioma**
- 9- Identify intraventricular and hemispheric supratentorial tumors.**

Pediatric Chest X Rays

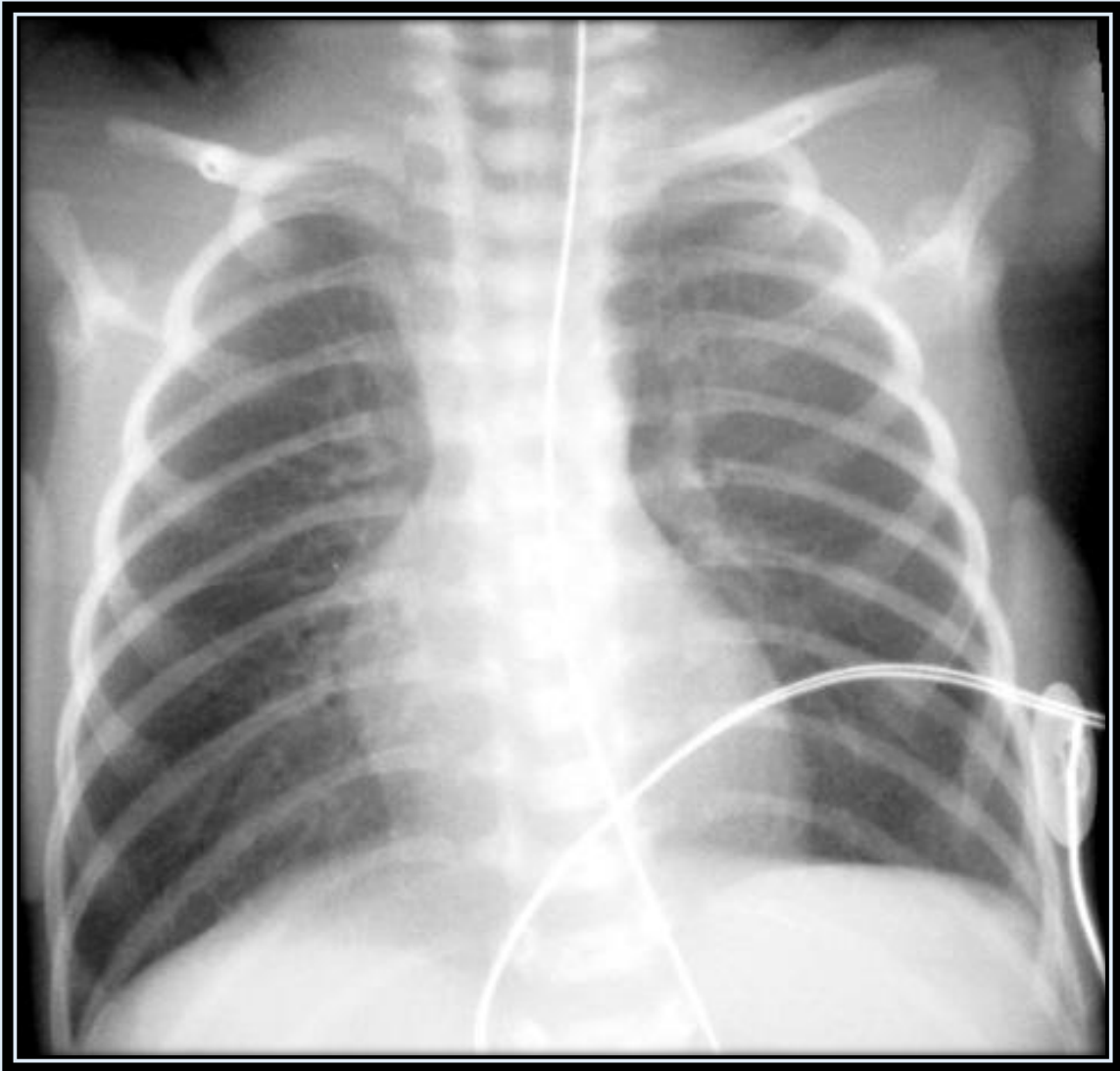
Pediatric Chest X Rays

Comprehensive Outline for Pediatric Chest Section

- **Introduction to Pediatric Chest Imaging**
 - **Inspiratory and Expiratory CXR**
 - **Thymic Tissue**
 - **Tubes and Lines**
- **Pneumothorax, Pneumomediastinum, Pneumoperitoneum**
- **Respiratory Neonatal Distress**
 - **Medical Causes**
 - Transient Tachypnea of the Newborn
 - Meconium Aspiration
 - Neonatal Pneumonia
 - Respiratory Distress Syndrome
 - **Complications**
 - Pulmonary Interstitial Emphysema
 - Patent Ductus Arteriosus
 - Chronic Lung Disease/Bronchopulmonary Dysplasia
 - **Surgical Causes**
 - Congenital Diaphragmatic Hernia
 - Congenital Cystic Adenomatoid Malformation
 - Congenital Lobar Emphysema
 - Sequestration
- **Pediatric Airway**
 - **Laryngomalacia**
 - **Acute Epiglottitis**
 - **Croup**
 - **Retropharyngeal Abscess**
- **Pulmonary Inflammatory Disease**
 - **Viral Pulmonary Infections**
 - **Bacterial Pulmonary Infections**
 - Pneumatocele

- Pleural Effusion
 - Empyema
- **Specific Organisms**
 - Bordetella pertussis
 - Mycoplasma
 - Tuberculosis
- **Swyer-James Syndrome**
- **Sickle Cell Acute Chest Syndrome**
- **Cystic Fibrosis**
- **Post-Test**

Introduction to Pediatric Chest Imaging

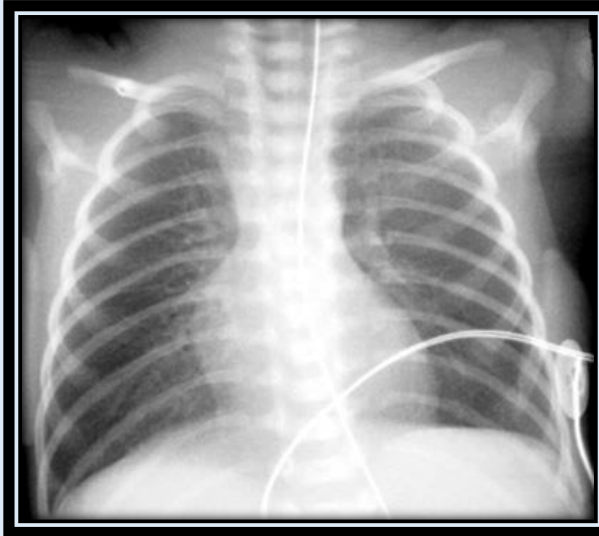


The initial assessment of the pediatric CXR should include:

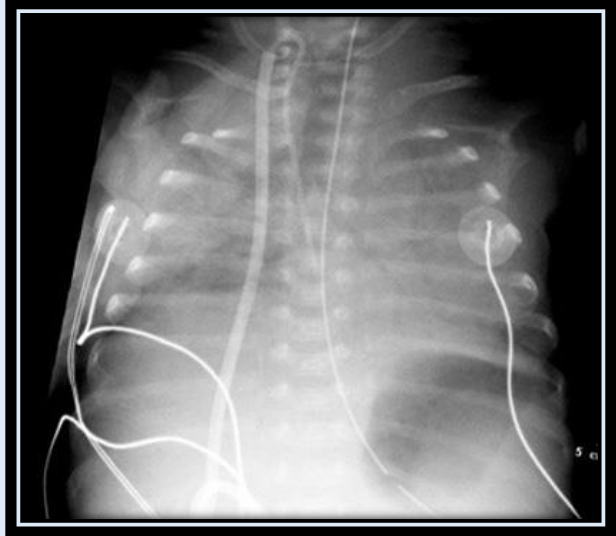
- Technique of the exam, to include patient positioning, proper exposure and the degree of inspiration
- Position of all tubes and lines and evaluation for pneumothorax, pneumomediastinum, and pneumoperitoneum
- Mediastinal and cardiac silhouettes
- Airway and lungs
- Pulmonary vascular pattern

Inspiratory and Expiratory CXR

The initial assessment of the pediatric chest radiograph should include an evaluation of the degree of inspiration. It is difficult to obtain a full inspiratory film in the younger pediatric patient, and the radiologist should not confuse an expiratory film with pulmonary pathology.



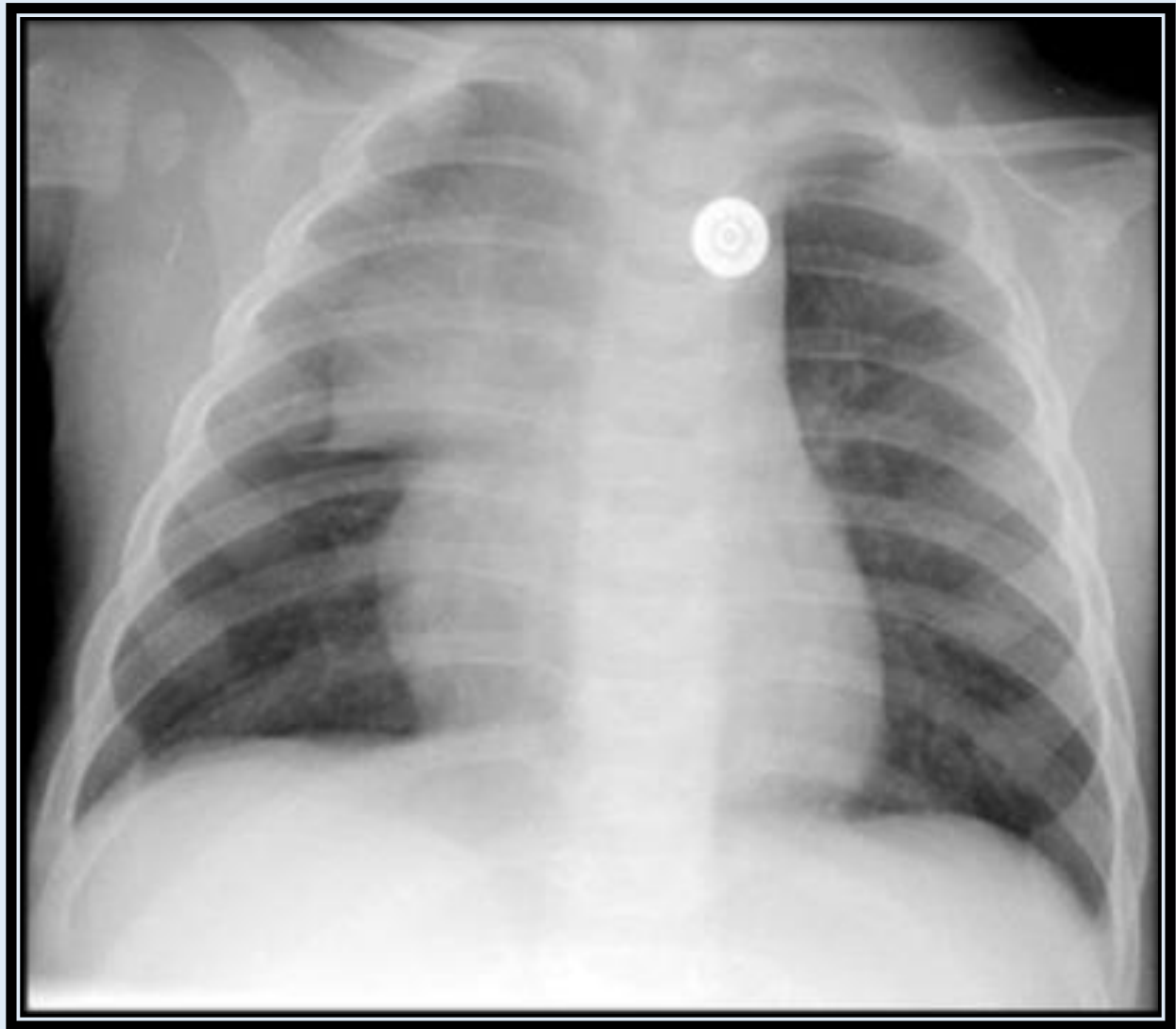
Normal Inspiratory CXR



Example of an Expiratory Exam

Thymic Tissue

Another important feature to recognize in the pediatric chest is the normal thymic tissue in the anterior mediastinum. Normal thymic tissue, as demonstrated on this image, should not be confused with a mediastinal or pulmonary mass.



Tubes and Lines

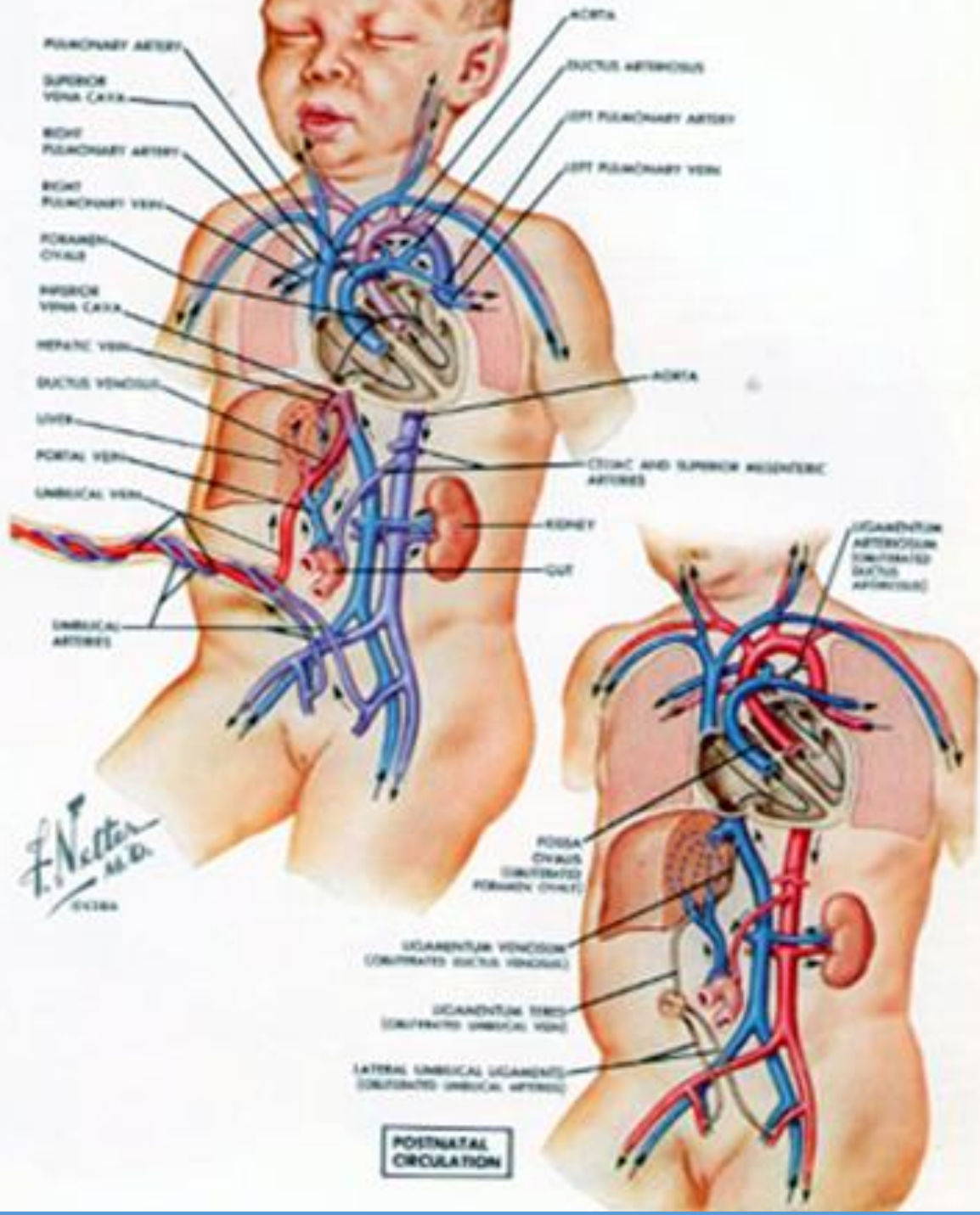
The ideal position of the endotracheal tube is in the mid trachea, 1.2 cm below the vocal cords and 2.0 cm above the carina. This is usually at the level of the inferior border of the head of the clavicle.

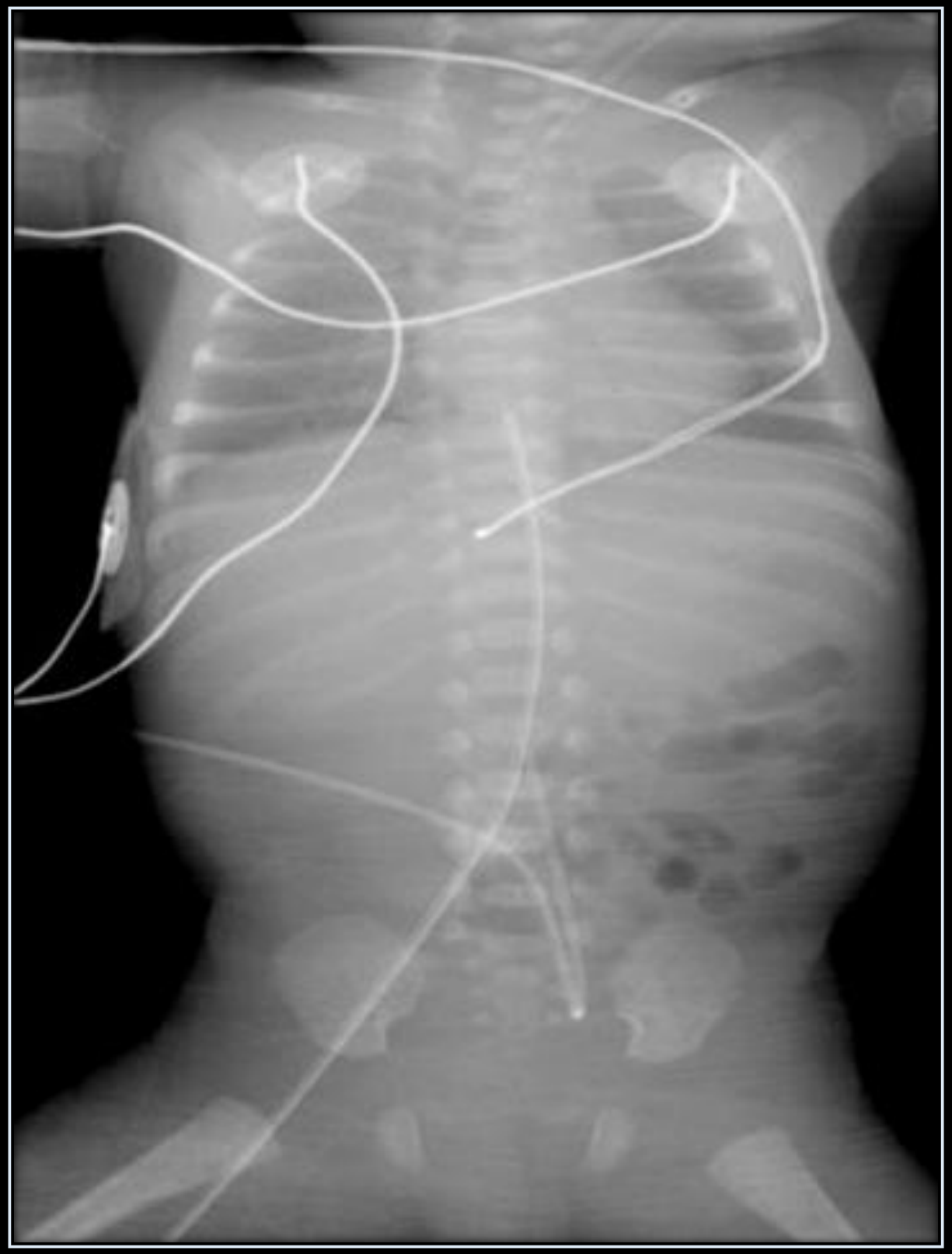
Chest tubes are ideally positioned anterior and apical for treatment of pneumothorax. It may be necessary to obtain a second view such as a cross table lateral to determine if the chest tube is anterior or posterior. The chest tube should be positioned posterior and inferior for drainage of pleural fluid.

Peripherally inserted central catheters (PICC) should terminate in the SVC if placed in the upper extremity or in the IVC within 1 cm of the diaphragm if placed in the lower extremity.

Umbilical arterial catheters (UAC) are differentiated from umbilical venous catheters (UVC) by the initial downward course from the umbilical insertion into the internal iliac artery. UVC's will extend immediately superior from the umbilicus. The UVC tip should be positioned within 1 cm of the diaphragm for ideal placement in the IVC. The UAC should be positioned below L2 to prevent mesenteric or renal complications. Another school of thought is to keep the UAC above the diaphragm in the thoracic aorta.

PRENATAL CIRCULATION





Quiz - Tubes and Lines

Q_1: The chest tube is placed in which direction in order to drain pleural fluid?

- A. Superior
- B. Inferior
- C. Superior and Anterior
- D. Inferior and Posterior

Q_2: Both UVC's and UAC's extend immediately superior from the umbilicus.

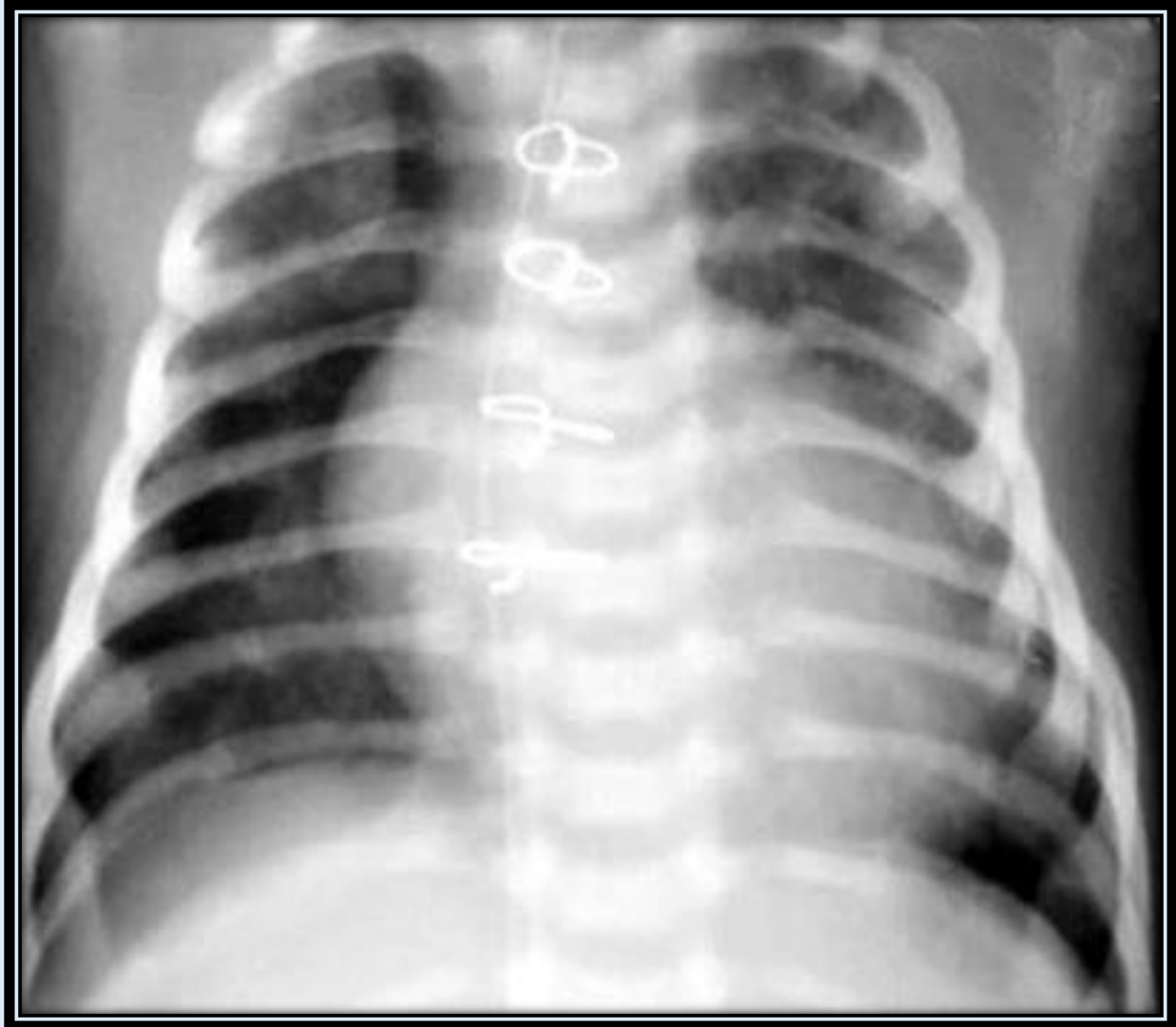
- A. True
- B. False

Pneumothorax, Pneumomediastinum, Pneumoperitoneum

The presence of free air either in the chest or abdomen is a frequent complication of disease and therapy in the neonatal setting. All exams should be thoroughly scrutinized for the presence of pneumothorax, pneumo-mediastinum, or pneumoperitoneum. If there is any question in this regard, a decubitus CXR, with the side of interest upright, should be obtained to evaluate for a pneumothorax. If free intraperitoneal air is a question then a left side down decubitus abdomen exam should be obtained. If the child cannot be positioned for the decubitus exam then a cross table lateral chest XR or abdominal XR will suffice.

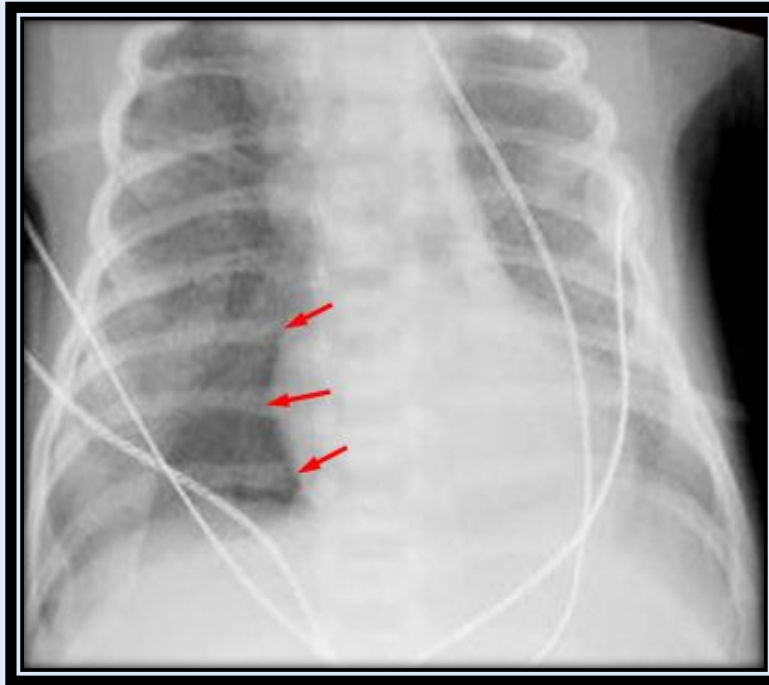
Pneumothorax

Most exams in the neonate will be performed in the supine position, so the air will rise to the least dependent portion of the body. The least dependent portion of the chest is the anterior, lower chest. This is where you should look for a pneumothorax, which will appear as an unusually sharp heart border or an unusually sharp and lucent costophrenic angle on a supine CXR. The **hyperlucent costophrenic angle** is known as the **deep sulcus sign**.

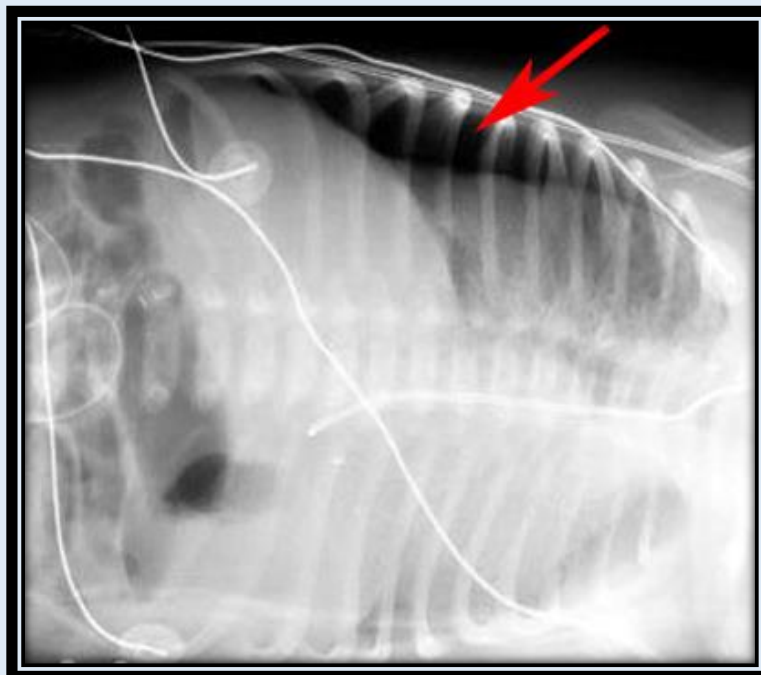


Right anterior **pneumothorax** demonstrating a sharp right heart border and a hyperlucent costophrenic angle.

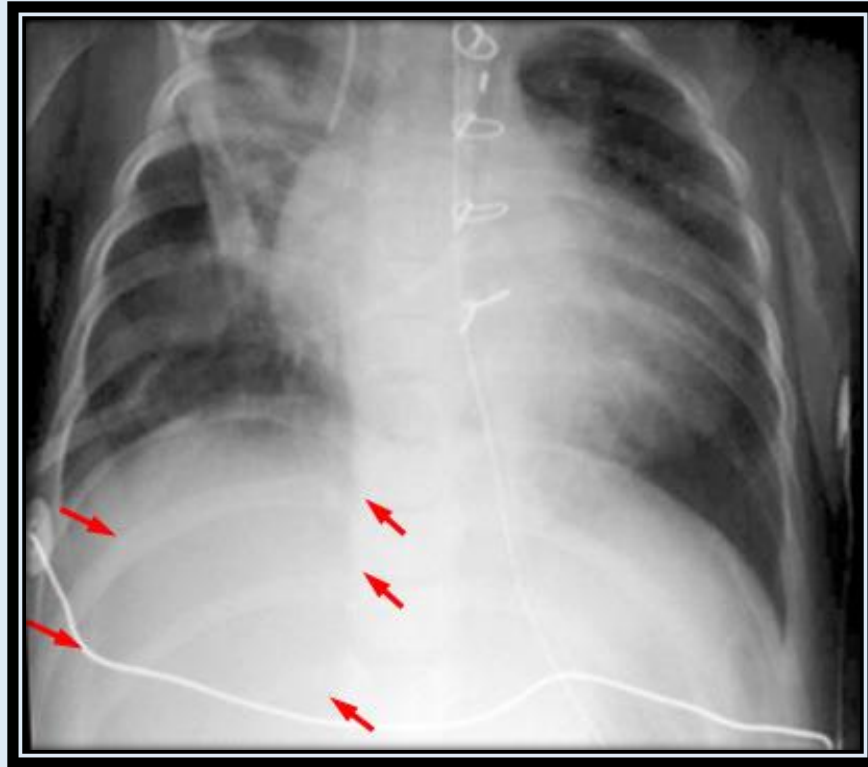
The following illustrates one case of a pneumothorax shown on supine CXR and confirmed by decubitus CXR, and one case of pneumoperitoneum confirmed on left side down decubitus view.



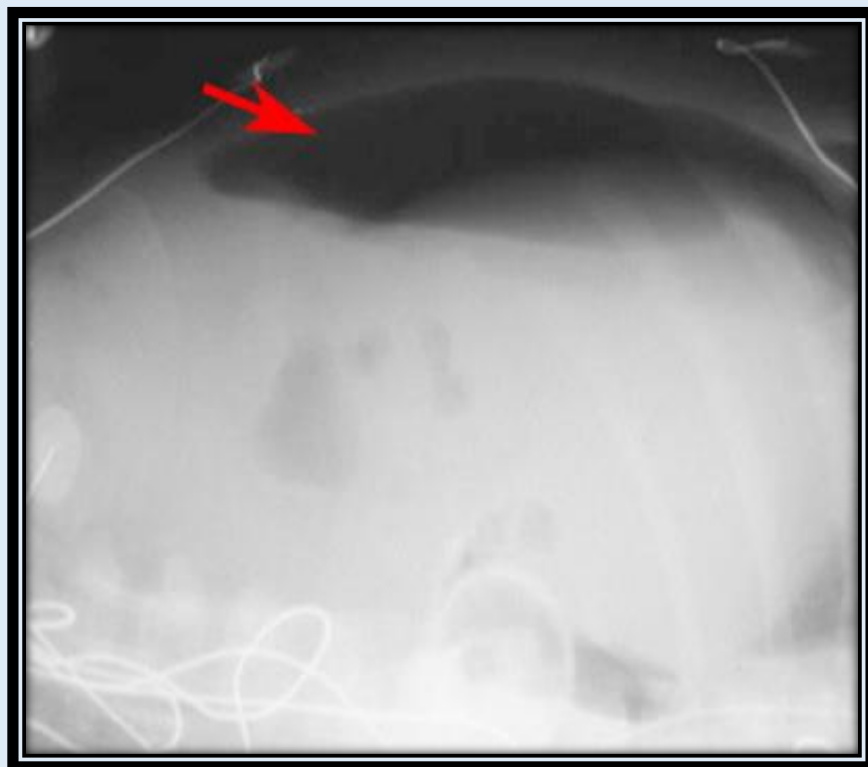
Supine CXR demonstrating a hyperlucent right heart border indicating a **right anterior pneumothorax**.



Right pneumothorax confirmed with a left decubitus CX

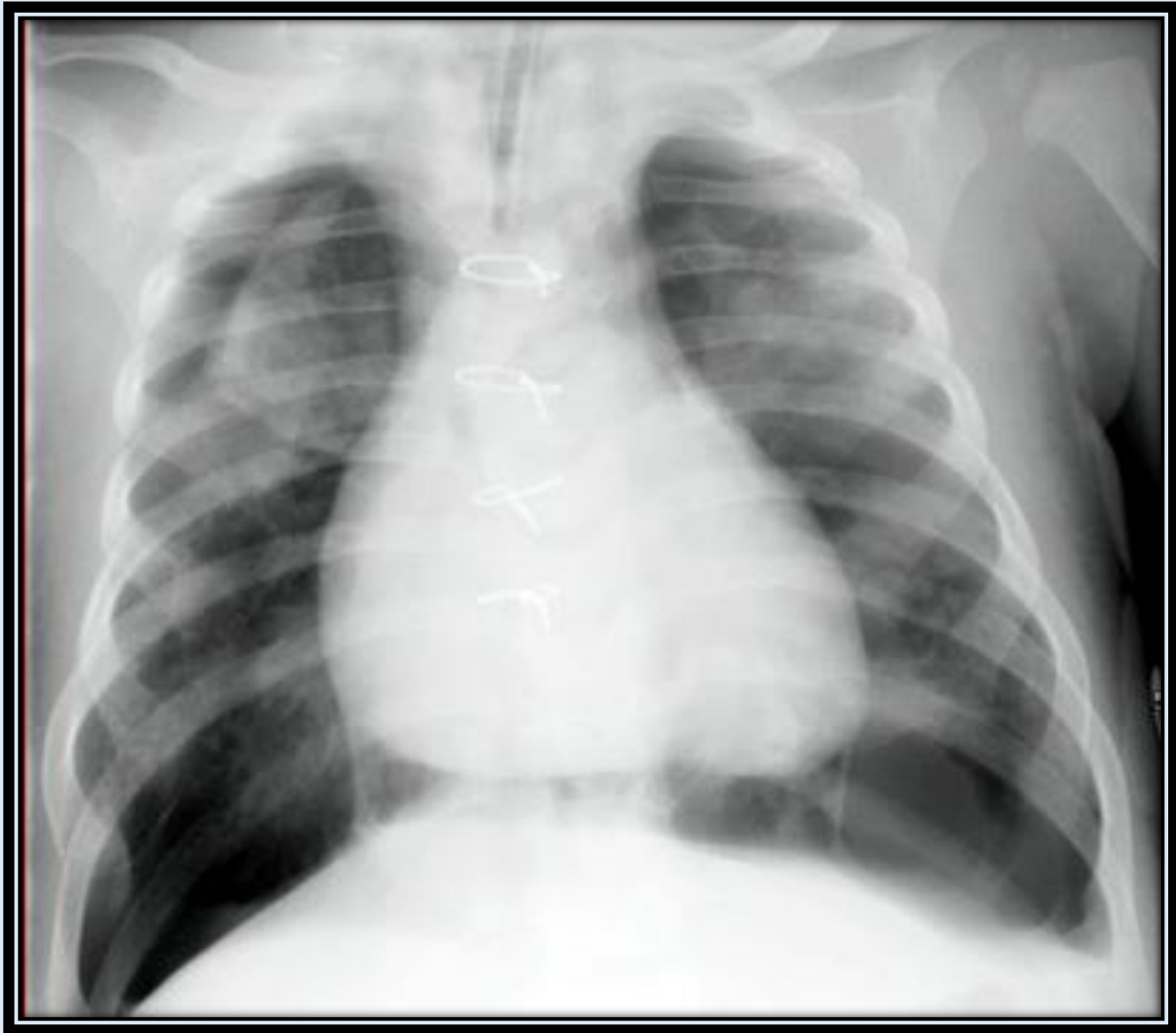


Supine CXR demonstrating hyperlucency over the anterior abdomen.



Left side down decubitus CXR confirms the free **intraperitoneal air**

Quiz - Pneumothorax



1. What is the most likely diagnosis?
2. What type of XR will confirm the diagnosis?

Answer:

1. Supine CXR demonstrating bilateral pneumothoraces with hyperlucency of the anterior chest.
2. This diagnosis can be confirmed with a decubitus CXR.

Respiratory Neonatal Distress

Excluding congenital heart disease, neonatal respiratory distress can be broken down into two broad categories: medical and surgical. Medical causes are managed by the neonatologist. Surgical causes need the immediate care of a pediatric surgeon because of mass effect on the developing lungs and possible acute airway compromise. Congenital heart disease is suspected when external oxygenation does not raise the oxygen saturation. The oxygen saturation will respond to external oxygenation if lung disease is the cause.

Medical Causes of Neonatal Respiratory Distress
Transient Tachypnea of the Newborn
Meconium Aspiration
Neonatal Pneumonia
Respiratory Distress Syndrome (Surfactant Deficiency)

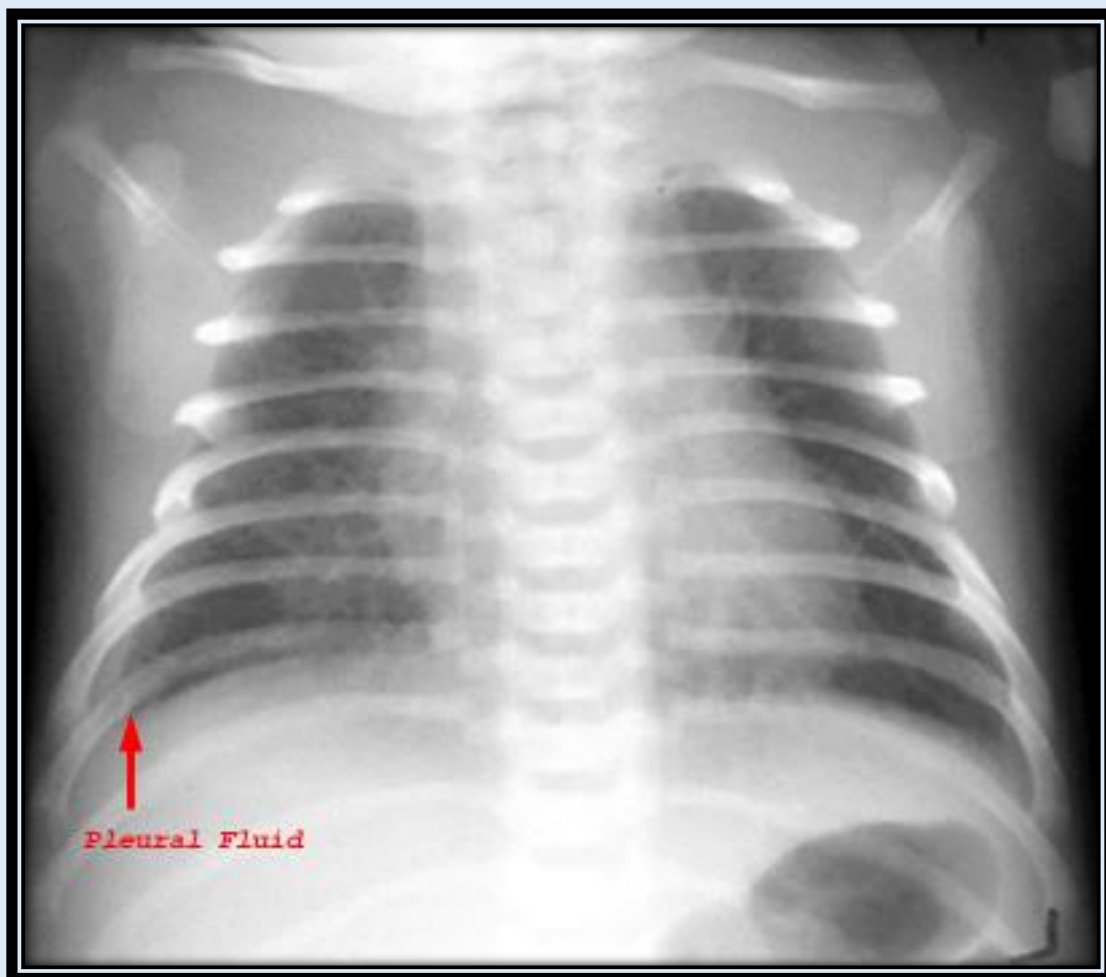
Surgical Causes of Neonatal Respiratory Distress
Congenital Diaphragmatic Hernia
Congenital Cystic Adenomatoid Malformation
Congenital Lobar Emphysema
Sequestration

Medical Respiratory Neonatal Distress

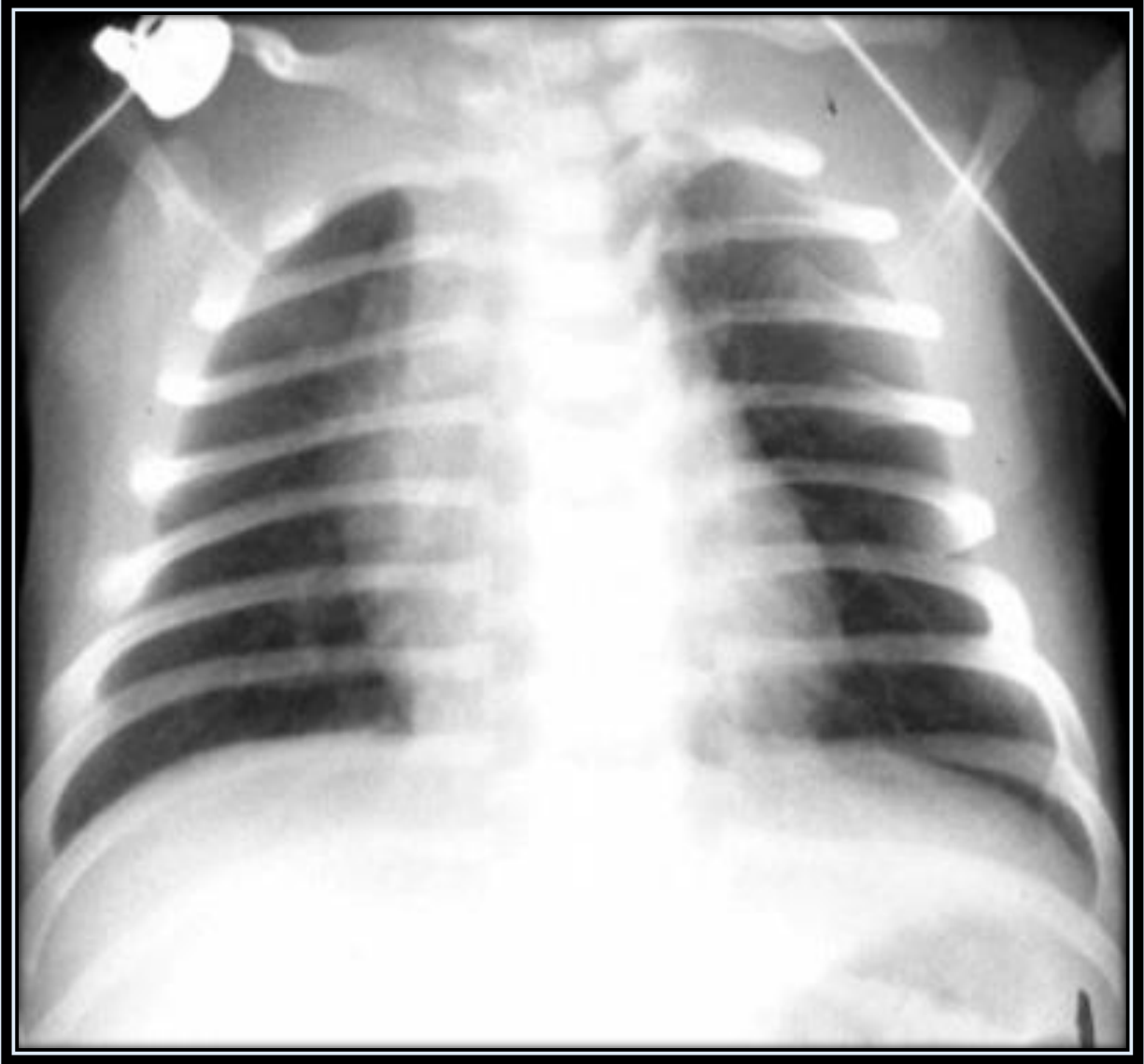
Transient Tachypnea of the Newborn (TTN)

Transient tachypnea of the newborn is delayed clearance of intrauterine pulmonary fluid. The thoracic squeeze of a normal vaginal delivery will clear 30% of the pulmonary fluid. Therefore, either C-section or a precipitous vaginal delivery may lead to TTN. The infant has normal respiration during the first hours of life but then gradually develops mild respiratory distress which begins around 4-6 hours and peaks at 24 hours with rapid recovery by 48-72 hours. Since the respiratory distress is mild, intubation is usually not required.

The chest radiograph will follow the clinical course with the abnormalities peaking during the first day of life then rapidly clearing. The CXR will demonstrate the findings of fluid overload with vascular congestion and small pleural effusions. The CXR is nearly always normal by 48-72 hours.



TTN on day one of life with mild vascular congestion and small pleural effusions



On day two of life the fluid overload has resolved and the CXR is normal

Neonatal Pneumonia

Neonatal pneumonia can be a difficult clinical and radiographic diagnosis. Frequently, the child will be covered with antibiotics without positive confirmation of pneumonia. However, pneumonia can be confirmed with positive blood cultures. Many different organisms can cause neonatal pneumonia but group B streptococcus is one of the most common infecting agents as 25% of women are colonized.

The radiographic presentation of neonatal pneumonia is frequently nonspecific. Neonatal pneumonia can present with either diffuse reticulonodular densities similar to respiratory distress syndrome or with patchy, asymmetric infiltrates with hyperaeration similar to meconium aspiration. The presence of a small pleural effusion is a useful distinguishing feature as it is a common finding in neonatal pneumonia (up to 2/3) and is uncommon in respiratory distress syndrome.

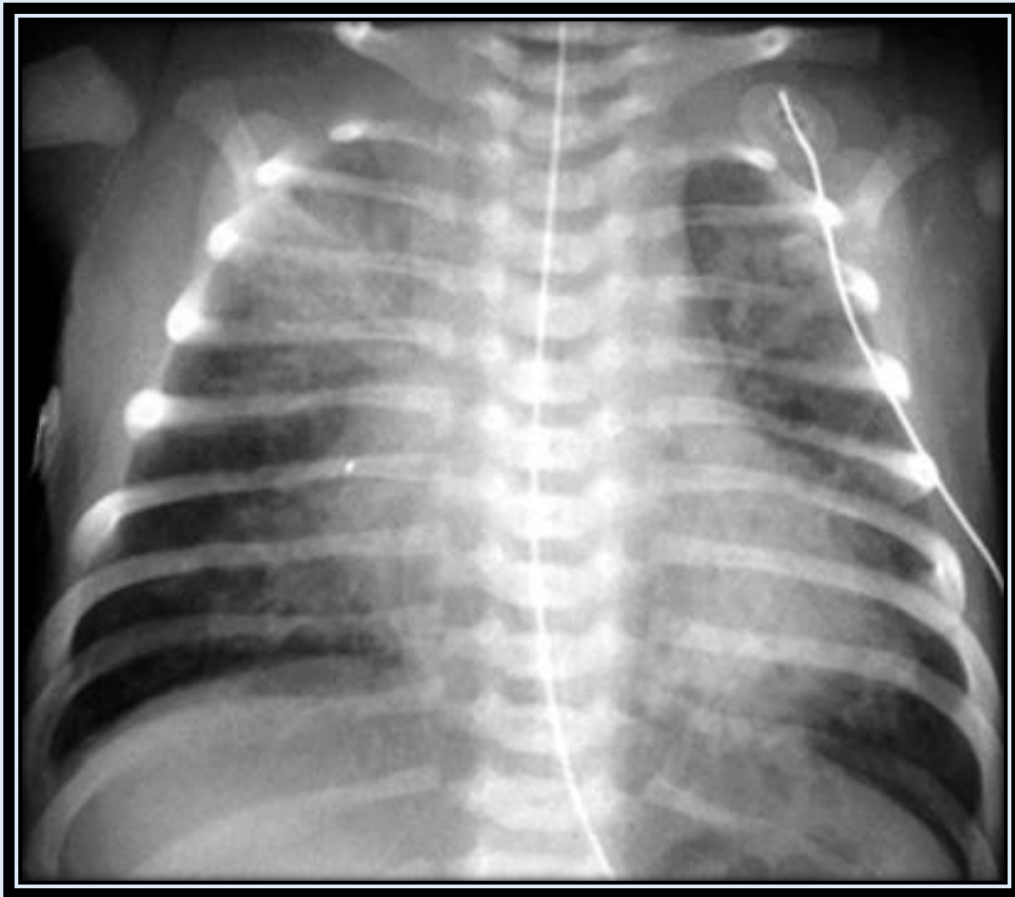


Example of neonatal pneumonia presenting as patchy, asymmetric opacities with a small right pleural effusion.

Meconium Aspiration Syndrome

Meconium staining of the amniotic fluid is relative common, affecting approximately 10% of live births, but only 1% will have meconium aspiration syndrome. The diagnosis is confirmed with visualization of meconium below the vocal cords. Because of the thick tenacious properties of meconium, aspiration into the tracheobronchial tree will result in significant respiratory compromise and can be complicated by persistent pulmonary hypertension. The child will usually be intubated and not infrequently extracorporeal membrane oxygenation is necessary. The mortality can approach 25% despite these supportive measures.

The radiology of meconium aspiration reflects the underlying pathophysiology. The aspirated meconium results in complete obstruction of the bronchi, resulting in atelectasis and compensatory hyperinflation of the remaining patent airways. Overall the lungs appear hyperinflated. Barotrauma is a frequent complication.

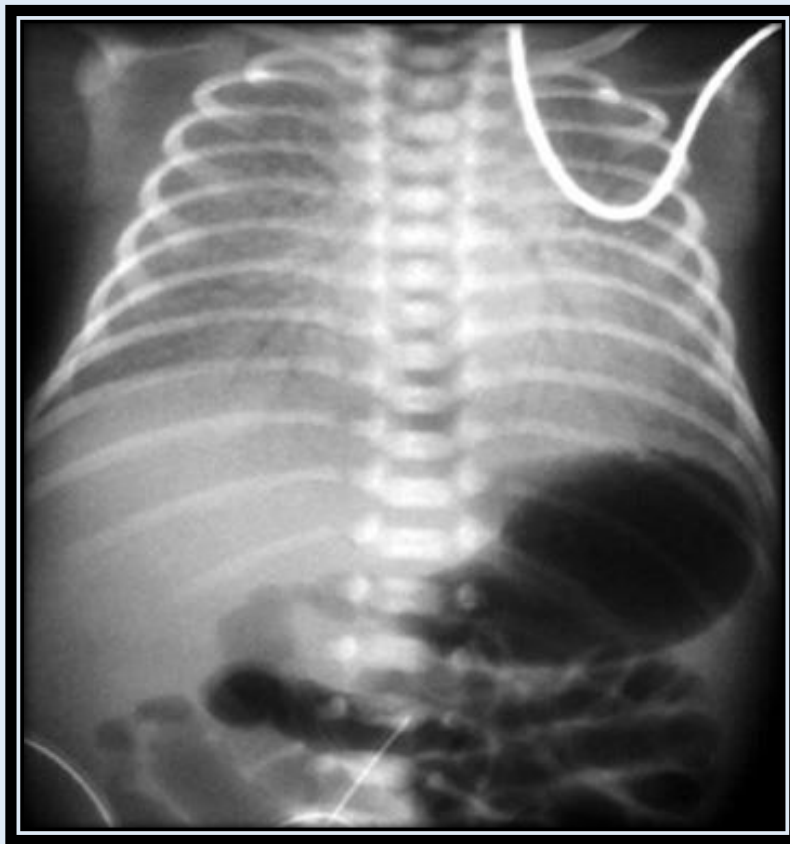


CXR shows hyperinflation and patchy asymmetric airspace disease that is typical of meconium aspiration

Respiratory Distress Syndrome (RDS)

Respiratory distress syndrome is the term used to describe the clinical manifestations of surfactant deficiency, and it is synonymous with hyaline membrane disease (HMD). RDS is seen in children less than 36 weeks old and is obviously more prevalent and more severe the younger the premature infant. Surfactant production from type 2 pneumatocytes begins at 24 weeks. Surfactant lowers the surface tension of the alveoli, and without it, the alveoli lose their compliance, collapse and have difficulty ventilating. RDS presents immediately at birth with respiratory compromise. Synthetic surfactant is now administered in the delivery room to high-risk infants and has greatly improved the survival of premature infants.

The classic radiographic findings of RDS include diffuse symmetric reticulogranular densities, prominent central air bronchograms and generalized hypoventilation. Neonatal pneumonia can have a similar appearance. The classic findings may not be present because of the early intervention with surfactant and ventilatory support with intubation.



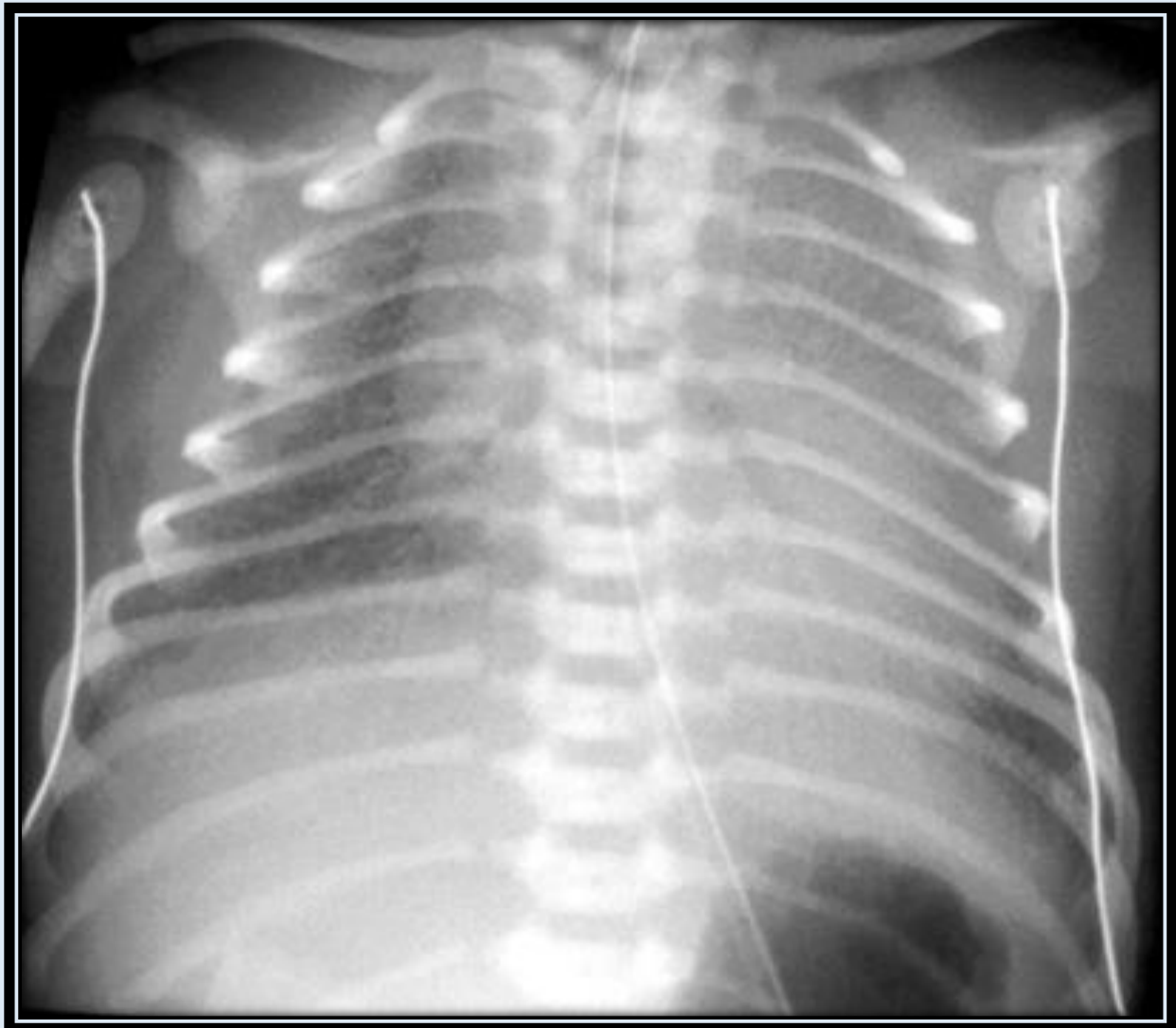
CXR in a premature infant prior to intubation with severe hypoventilation, marked air bronchograms and diffuse symmetric reticulogranular opacities.

Quiz - Medical Respiratory Neonatal Distress

1. Which of the following medical causes of neonatal respiratory distress almost always requires intubation?

- A. TTN
- B. Neonatal Pneumonia
- C. Meconium Aspiration

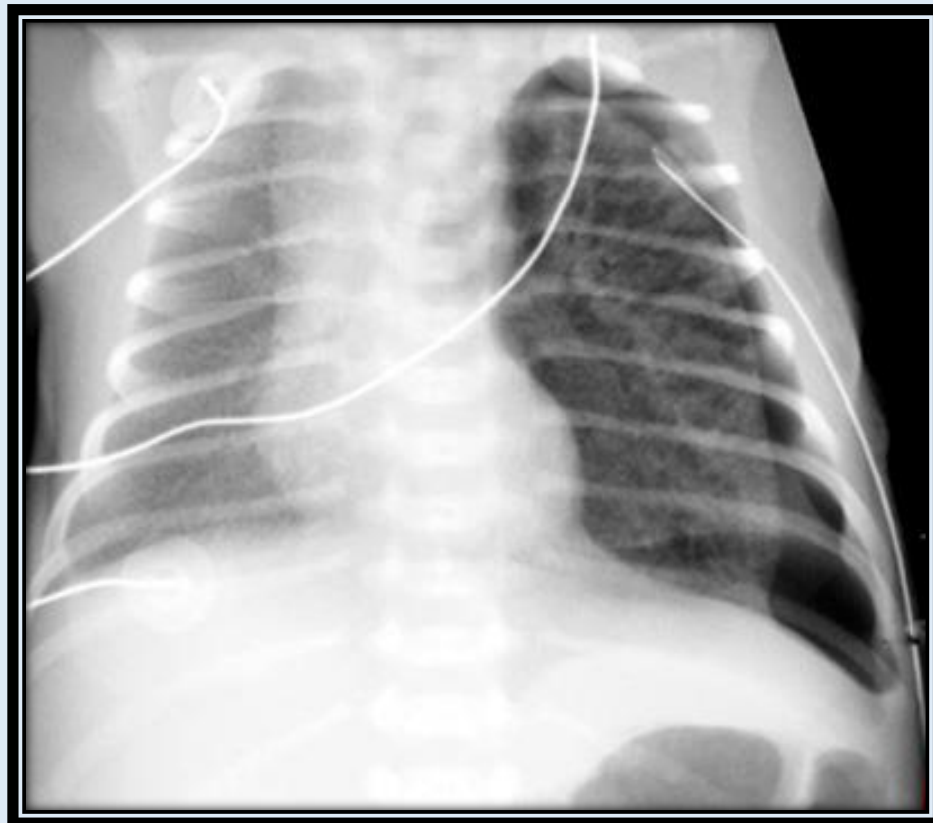
2. What is the diagnosis for this patient?



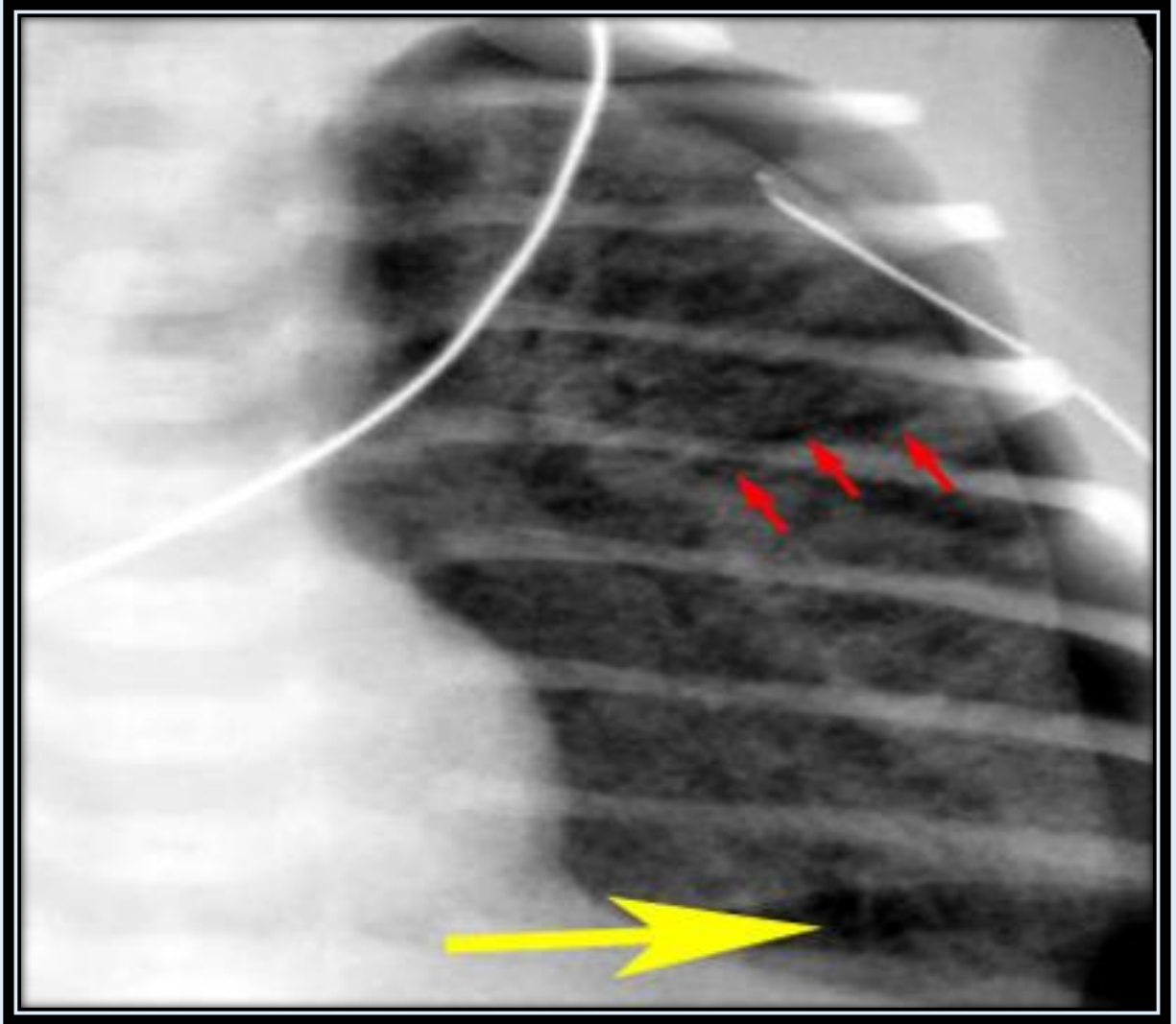
This is RDS. Note the evidence of hypoventilation and marked air bronchograms.

Complications of Respiratory Distress

The neonatologist must maintain a balance between the ventilatory needs of the infant and the complications that can result from positive pressure ventilation. The lung volumes on the daily neonatal CXR are used as a guide to determine the ventilator settings. If the compliance of the lungs is too low, or the mean airway pressure is too high, barotrauma will result. The signs of barotrauma should be identified on the neonatal CXR. Pneumothorax has already been discussed. Pulmonary interstitial emphysema (PIE) results from rupture of the alveoli with air accumulating in the peribronchial and perivascular spaces. PIE is recognized by linear lucencies radiating from the hilum. However, PIE can also be cystic in appearance, which can be difficult to distinguish from chronic lung disease. Correlation with the clinical course is helpful as PIE occurs early and is associated with high ventilatory settings, and chronic lung disease occurs later in the hospital course with lower ventilatory settings. PIE is an ominous sign because it indicates the poor compliance of the lungs and is frequently followed by a pneumothorax. In addition to adjusting the ventilatory settings as much as tolerated, it is helpful to put the most affected side down.



Example of unilateral **PIE** with a pneumothorax

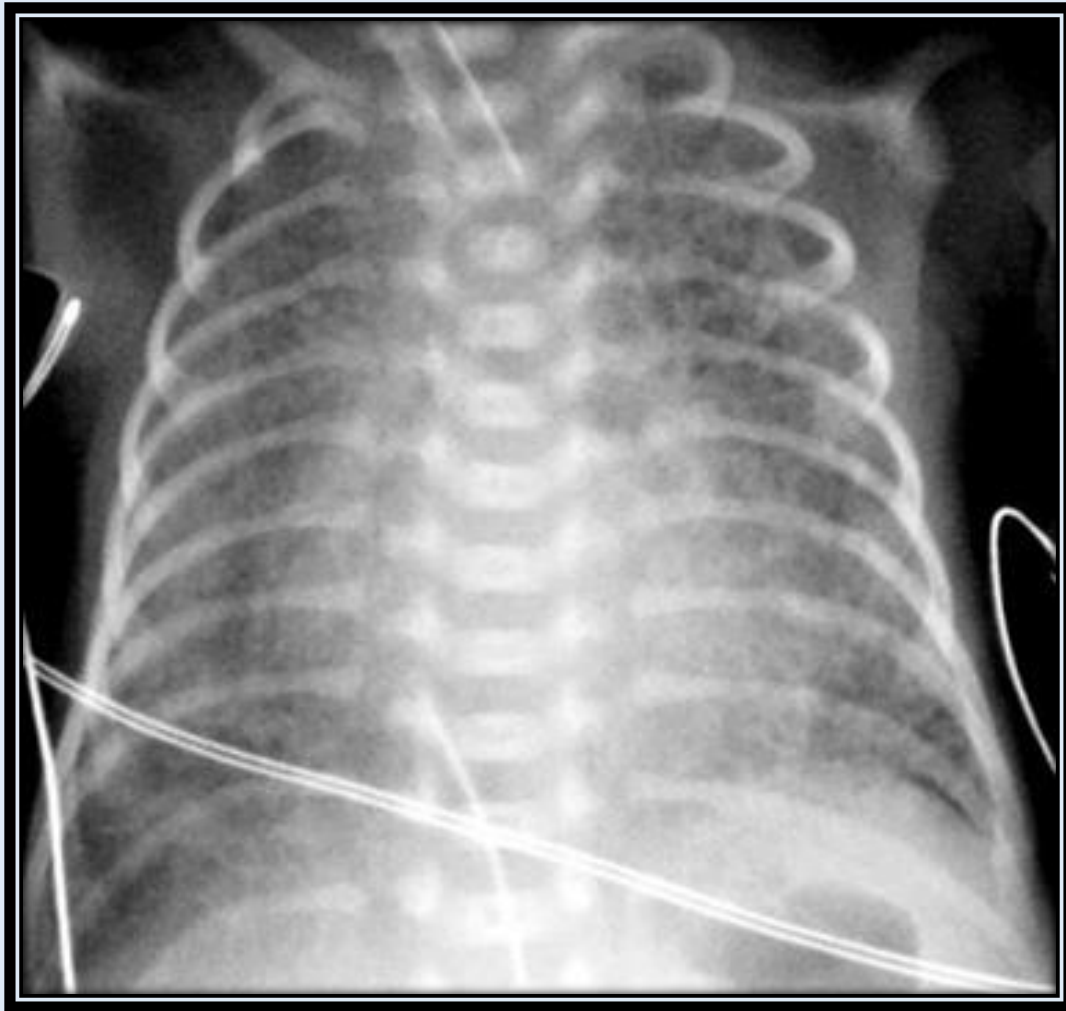


Close up of left lung demonstrating the streaky lucencies of the air in the interstitium (red arrows) complicated by a **pneumothorax** (yellow arrow). This patient was treated with a chest tube and by placing the left side down. The **PIE resolved after 2 days**.

Patent Ductus Arteriosus (PDA)

The ductus is normally open in utero but will close in 1-2 days after birth in response to the decreased pulmonary resistance. If the pulmonary resistance remains high then the ductus may remain open with a right to left shunt. During the first week of life, as the ventilatory therapy decreases the pulmonary resistance, the ductus may switch to a left to right shunt resulting in increased pulmonary blood flow. This is demonstrated on CXR by increased heart size and increased pulmonary vascularity. An echo will confirm the PDA.

PDA is treated with indomethacin, which inhibits prostaglandins. The PDA can be induced to remain open in cases of congenital heart disease with the administration of prostaglandins. If indomethacin does not work, then surgical ligation is necessary.

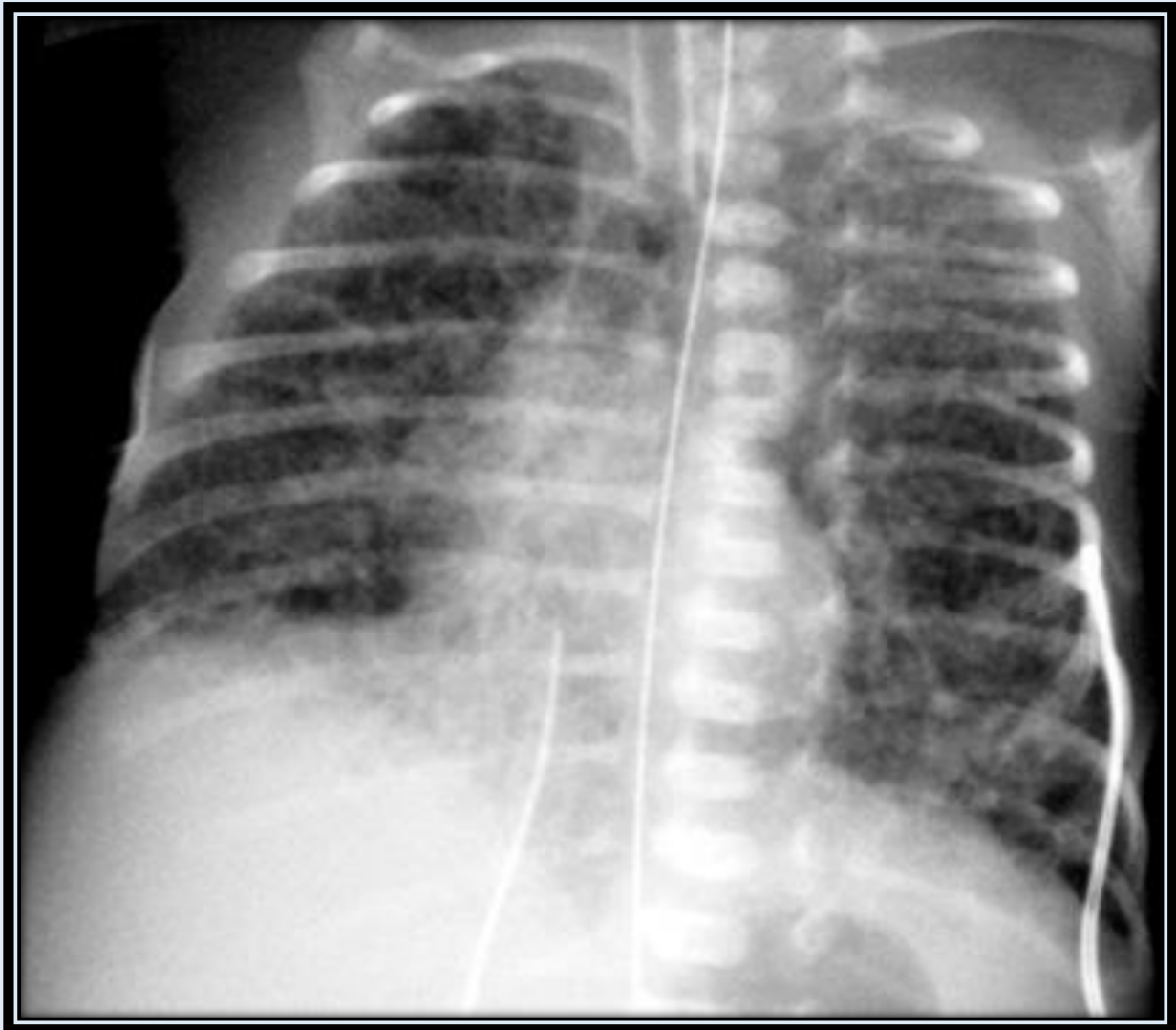


CXR shows an **enlarged heart** and significant vascular congestion with a **pulmonary edema** pattern resulting from a **PDA**

Chronic Lung Disease (CLD)

Bronchopulmonary Dysplasia (BPD)

For our purposes, chronic lung disease and bronchopulmonary dysplasia are synonymous terms referring to the long-term sequelae of respiratory distress syndrome. Oxygen toxicity and positive pressure ventilation are thought to result in pulmonary inflammation with subsequent fibrosis. Clinically, CLD is defined as continued oxygen needs and CXR abnormalities beyond 28 days of life or 36 weeks gestational age. The radiographic manifestations of CLD are diffuse interstitial thickening with hyperinflation. The most severe form manifests in cystic changes in the lungs. Steroid therapy may result in improvement and prevention of CLD.



Cystic interstitial pulmonary disease reflecting the severe form of chronic lung disease.

Quiz - Complications of Respiratory Disease

1. Chronic Lung Disease is defined as continuous oxygen needs and CXR abnormalities beyond:

- A.** 48 Hours
- B.** 12 Days
- C.** 28 Days
- D.** 1 Year

Answer

C: 28 days

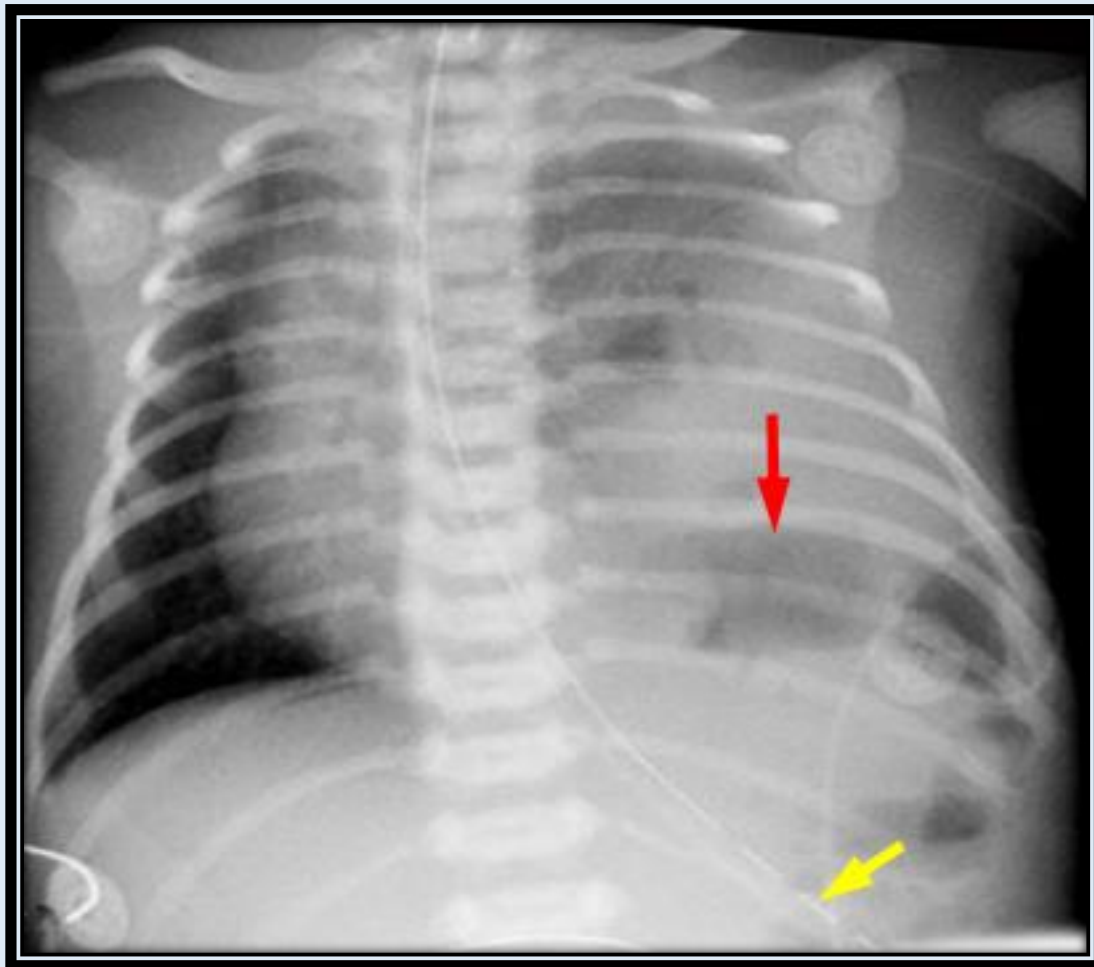
Surgical Respiratory Neonatal Distress

Previously, mass lesions in the chest presented postnatally and were diagnosed with the help of the postnatal CXR. Currently, with the widespread use of prenatal OB US, many chest mass lesions are discovered prior to birth. Prenatal MRI can be helpful in working up the chest mass. Regardless of the prenatal imaging, chest masses will be evident on the postnatal CXR. Chest masses can result in mass effect and shift of the mediastinum. This will result in airway compromise and pulmonary hypoplasia. Additionally, mass effect on the esophagus can result in decreased swallowing and polyhydramnios. The mass effect may be severe enough to limit venous return to the heart and significantly decrease cardiac output.

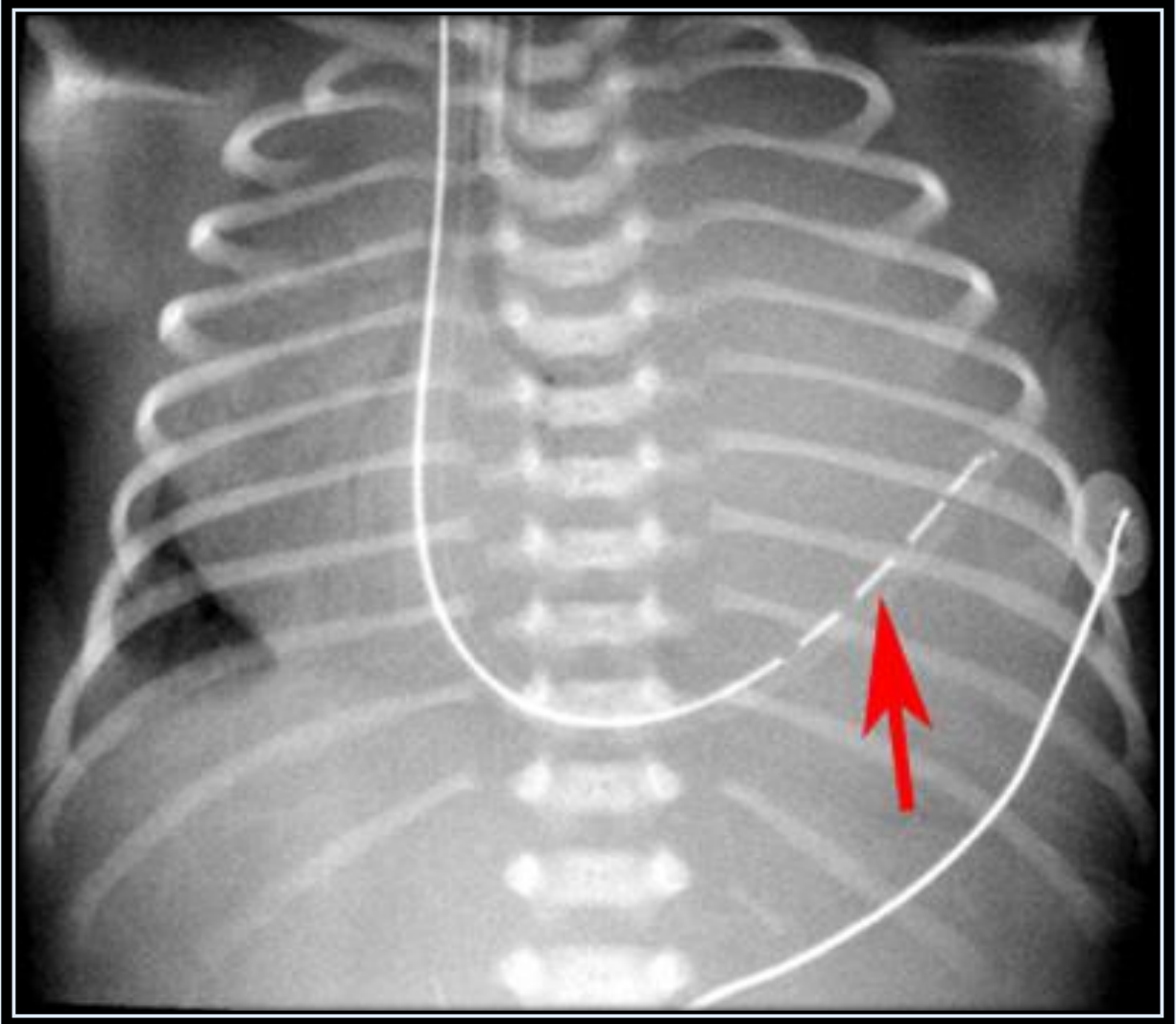
Etiologies of Surgical Neonatal Respiratory Distress
Congenital Diaphragmatic Hernia
Congenital Cystic Adenomatoid Malformation
Congenital Lobar Emphysema
Sequestration

Congenital Diaphragmatic Hernia (CDH)

A defect in the diaphragm will result in herniation of abdominal contents into the thoracic cavity. The mass effect from the abdominal contents in the chest will lead to severe respiratory distress from pulmonary hypoplasia in both the ipsilateral and contralateral lung. The most common defect is in the posterior and lateral diaphragm. This is a Bochdalek hernia, which is more common on the left (75%). A Morgagni hernia is less common and is anterior and medial. Morgagni hernias present later in life and are more common on the right because the heart and pericardium will protect the left side. Congenital diaphragmatic hernia is frequently diagnosed on prenatal US. The postnatal CXR is confirmatory.



Postnatal CXR demonstrates a mass in the lower left chest with shift of the mediastinum. The presence of bowel gas (red arrow) indicates the mass is due to a diaphragmatic hernia. In this case, the stomach remains in the abdominal cavity as indicated by the position of the nasogastric tube (yellow arrow).



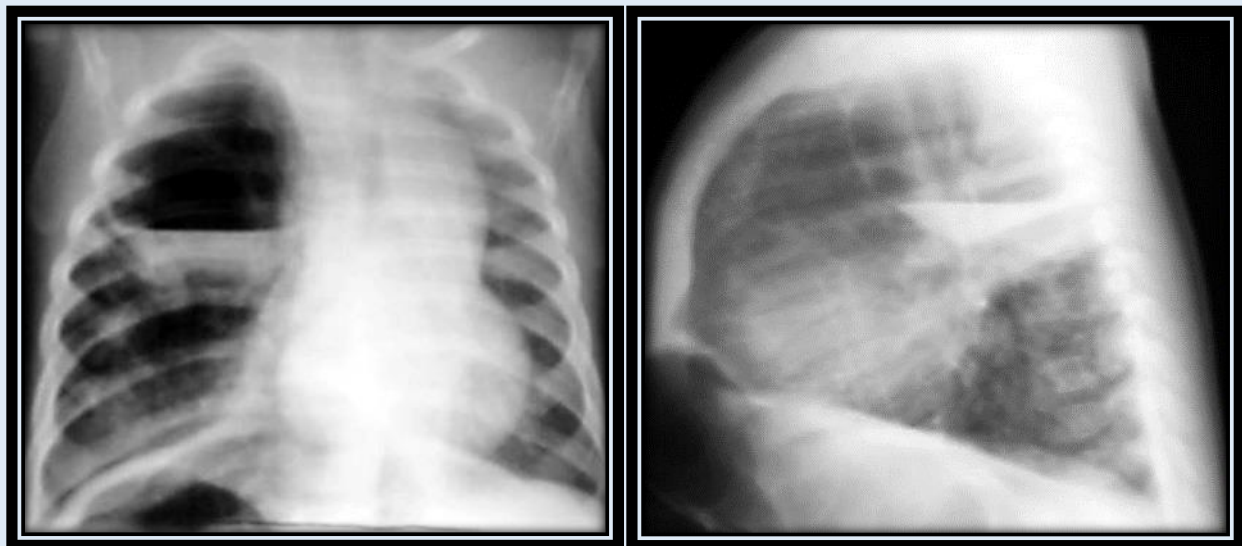
CXR demonstrates a mass in the left chest with shift of the mediastinum. Although no bowel gas is identified, the position of the nasogastric tube (red arrow) indicates the stomach is located in the thoracic cavity.

Congenital Cystic Adenomatoid Malformation (CCAM)

Congenital cystic adenomatoid malformation is a hamartoma of the lung. If there is significant mass effect in the chest, CCAM is surgically resected. Occasionally CCAM can regress. CCAM that is discovered on prenatal US may not be recognized on the postnatal CXR. Chest CT may be necessary to demonstrate the CCAM. If the CCAM is asymptomatic then it is uncertain whether surgical resection is necessary. An argument can be made for surgical resection because of reported cases of lung cancer arising from CCAM.

The presentation can vary from a large cystic lesion to a grossly solid appearing lesion that is composed of microscopic cysts. CCAM has a normal pulmonary arterial supply as opposed to pulmonary sequestration. Three types of CCAM are recognized depending on gross appearance:

- Type I CCAM - Most frequent (2/3 of cases), contains a dominant cyst > 2 cm surrounded by multiple, smaller cysts.
- Type II CCAM - (15-33%) uniform smaller cysts up to 2 cm. Other congenital malformations are associated with Type II CCAM in 50% of cases.
- Type III CCAM - Least common (< 10%), contains microscopic cysts that are not grossly visible. Grossly and on imaging the lesion appears solid. Fetal hydrops and maternal polyhydramnios are frequent complications.



Example of a Type 1 CCAM on CXR with a large dominant cyst containing an air fluid level

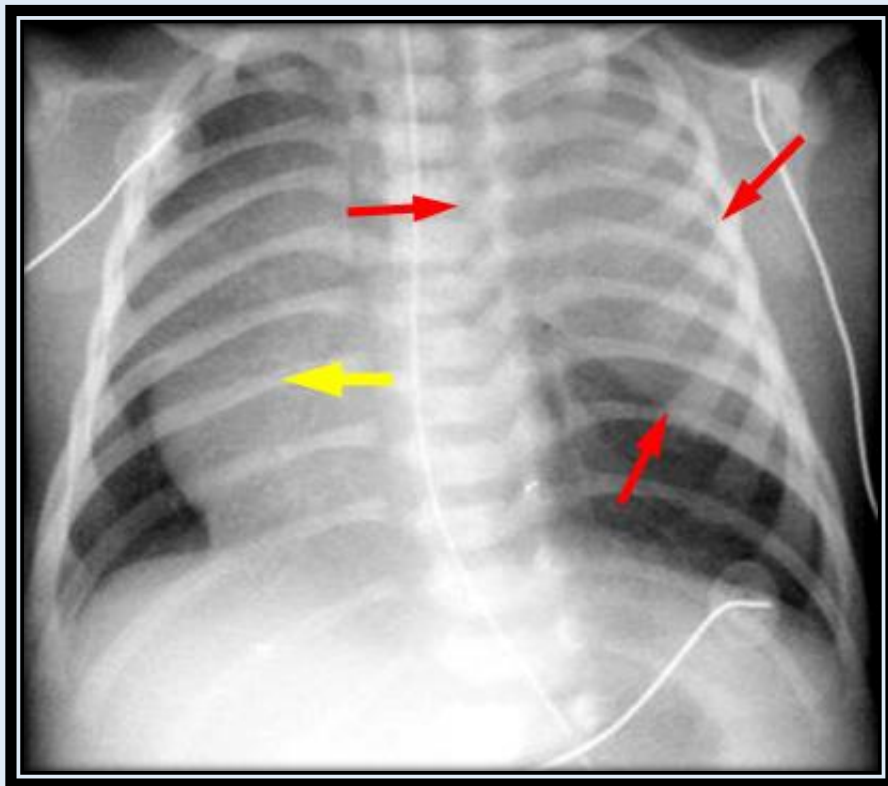


Chest CT on the same patient confirms a Type I CCAM with a large dominant cyst surrounded by multiple smaller cysts

Congenital Lobar Emphysema (CLE)

Congenital lobar emphysema is characterized by overexpansion of one or more lobes. Emphysema is a misnomer as there is no destruction of alveoli. The etiology of CLE is not entirely clear, but it is thought to result from an airway obstruction, which can arise from a myriad of causes. However, even at surgical resection and pathologic examination, the cause is not usually identified. Prior to resection CT and bronchoscopy are helpful to rule out a treatable cause such as a pulmonary sling.

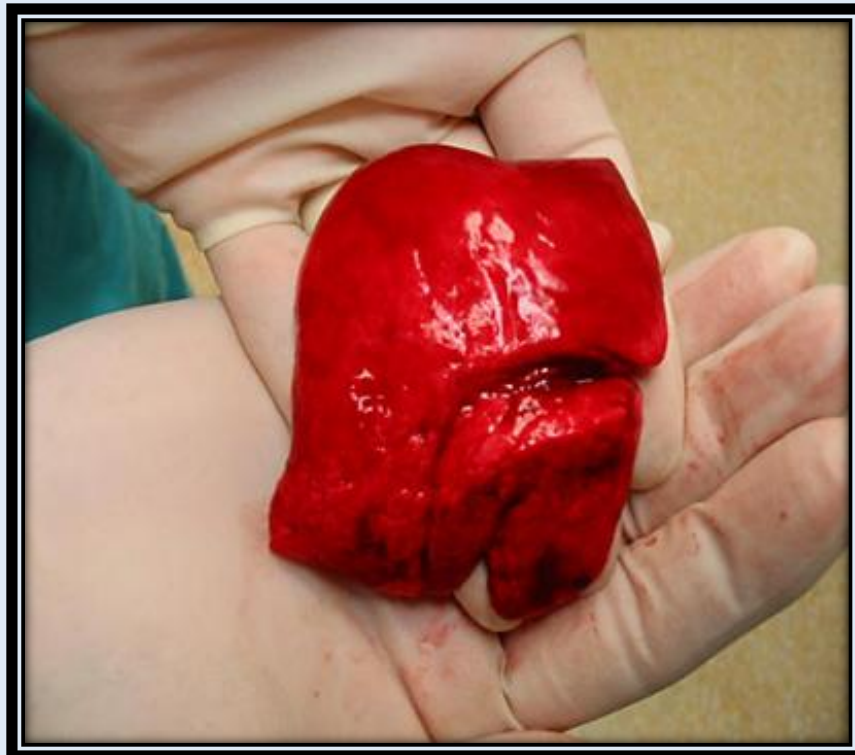
CLE has a distinct anatomic distribution: 43% in the left upper lobe, 32% in the right middle lobe, and 20% in the right upper lobe. CLE is very uncommon in the lower lobes. Initially, CLE will appear as a solid mass on both prenatal US and postnatal CXR because of the delayed clearance of pulmonary fluid. Over several days the fluid will slowly resorb, and the classic findings of a hyperlucent lobe will be present. The initial appearance of a CLE as a solid chest mass may mimic CCAM, sequestration or even a tumor. The appearance of a CLE as a hyperlucent lobe can be confused with a pneumothorax.



Initial postnatal CXR demonstrates a solid appearing mass in the left upper chest (red arrows) with mass effect and shift of the mediastinum (yellow arrow). At this point, the CLE is filled with fluid and thus mimics a solid mas



Chest CT on day 2 of life. The fluid has been absorbed and the left upper lobe is shown to be hyperinflated resulting in mass effect and shift of the mediastinum.

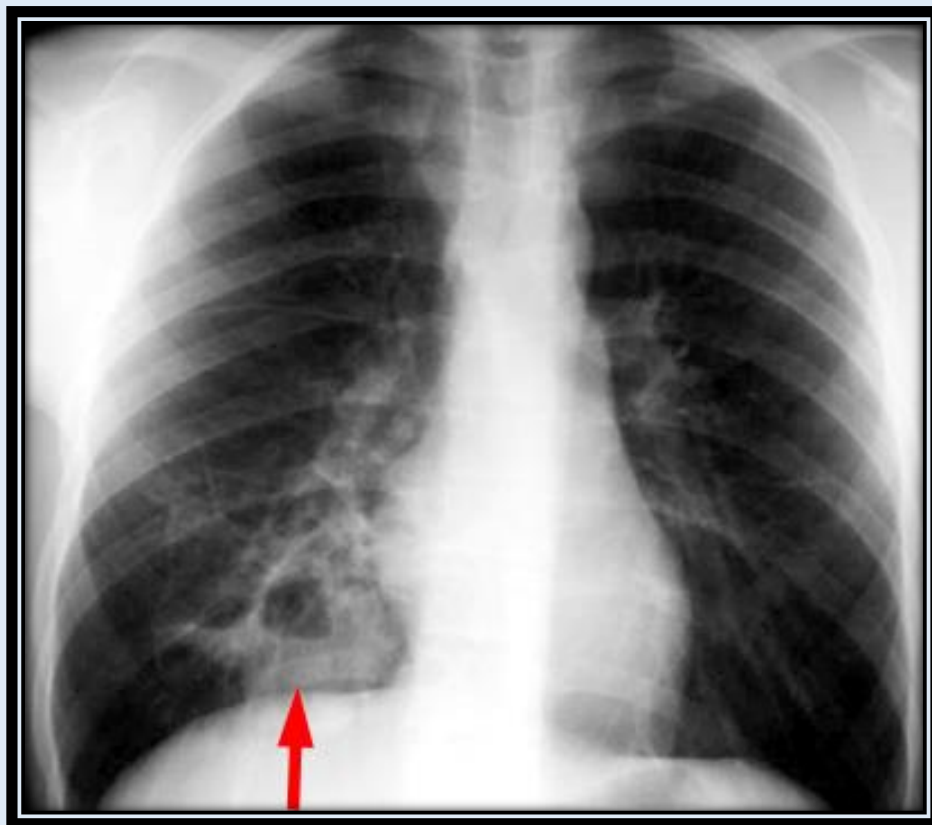


The gross specimen confirms the hyperexpansion of the left upper lobe.

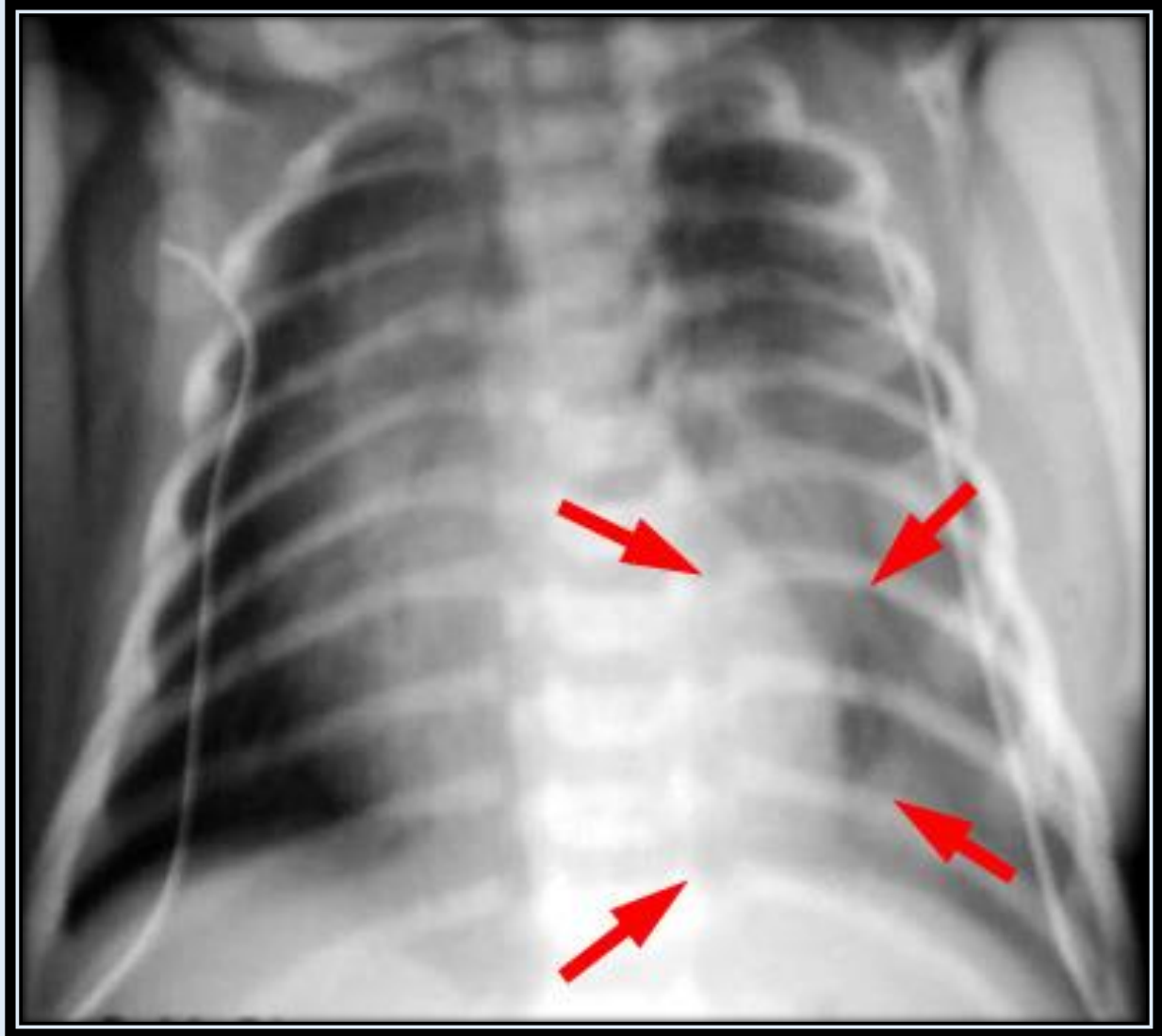
Pulmonary Sequestration

Pulmonary sequestration is lung tissue that is not connected to the tracheobronchial tree. Sequestration has a systemic arterial supply instead of a pulmonary artery supply. The documentation of the systemic arterial supply by US, CT, MRI or arteriography is diagnostic of sequestration. The venous drainage can be either systemic or pulmonary. Two types of sequestration, intralobar and extralobar, are recognized.

- Intralobar sequestration is contained within the normal lung pleura and presents in the 2nd or 3rd decades with recurrent infections. The most common location is the medial left lower lobe.
- Extralobar sequestration is contained in its own separate pleura and commonly presents in the neonatal period with respiratory distress from mass effect. Furthermore, other anomalies are frequently found with extralobar sequestration. As with intralobar sequestration, extralobar sequestration is frequently found in the medial left lower lobe presenting as a soft tissue mass. Extralobar sequestration can be confused with an adrenal mass (neuroblastoma) because it presents as a mass in the medial left lower lobe.



CXR demonstrating a consolidation with cavitation in the medial right lower lobe.



Neonatal CXR demonstrates a mass in the medial left lower lobe. An MRI demonstrated a systemic arterial supply off the aorta which confirmed an extralobar sequestration.

Quiz - Surgical Respiratory Neonatal Distress

1. Congenital diaphragmatic hernia can cause mass effect in the chest from intrathoracic abdominal contents and lead to severe respiratory distress in both lungs as a result of bilateral pulmonary hypoplasia.

- A. True
- B. False

2. Congenital Lobar Emphysema must not be confused with a pneumothorax. What is similar in their appearance?

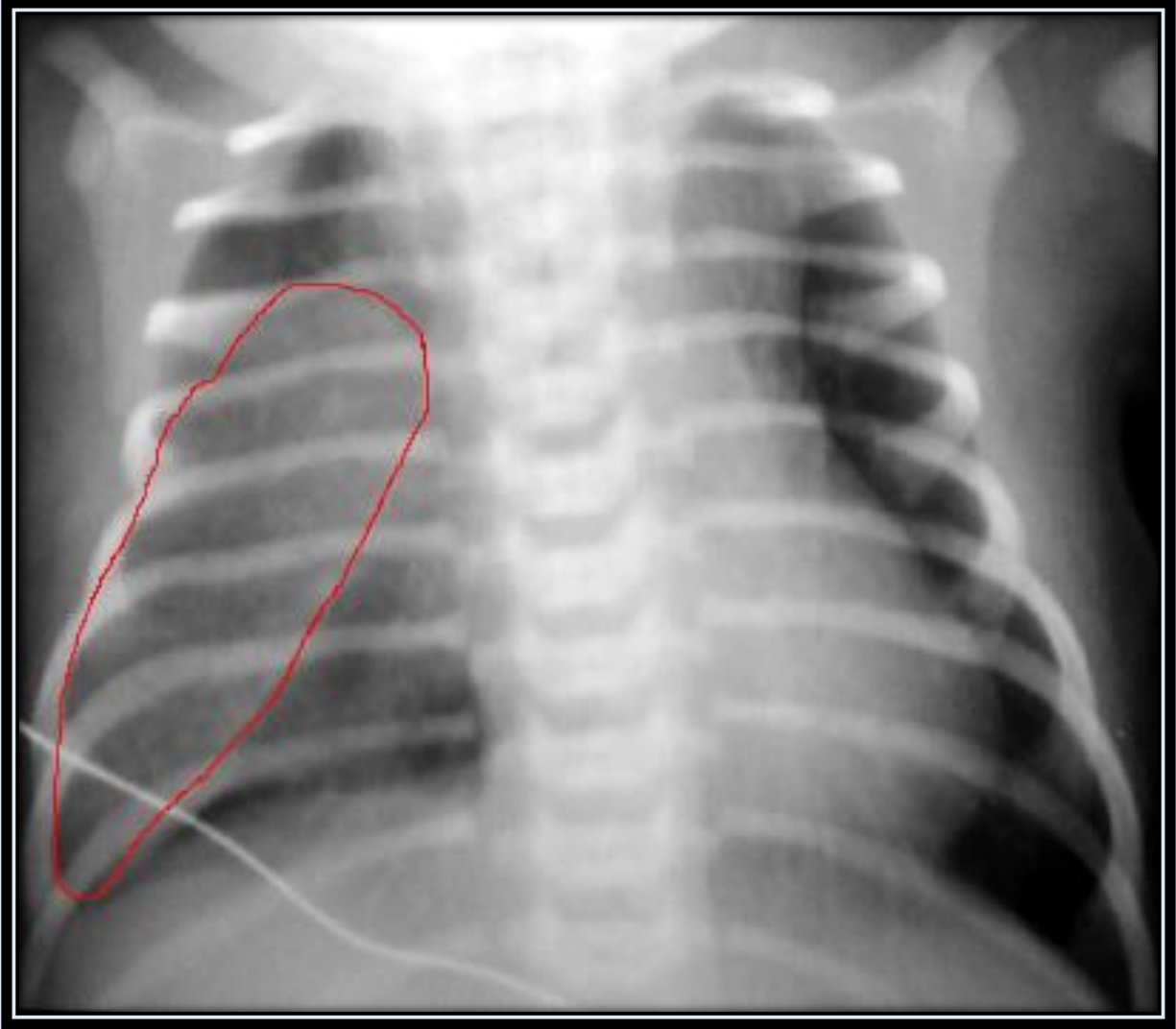
They are both characterized by a hyperlucent chest.

3. CCAM and pulmonary sequestration both have a systemic arterial supply.

Only pulmonary sequestration has a systemic arterial supply.

4. What is the most likely diagnosis?





This is Congenital Lobar Emphysema.

This is a more difficult case because it does not look like typical, hyperlucent CLE. Remember that CLE is more opaque in the initial period due to the retention of fetal pulmonary fluid.

Pediatric Airway

Laryngomalacia

Evaluation of a child with an inspiratory stridor is a frequent request. Most commonly, inspiratory stridor is caused by laryngomalacia. Laryngomalacia is caused by a characteristic infolding of the aryepiglottic folds, which obstruct the airway. This is self-limiting and improves by 1-2 years of age. If laryngomalacia is excluded, tracheomalacia is considered. The diagnosis can be made by bronchoscopy, but the radiologist may be asked to image the child to identify the tracheomalacia and to look for a cause such as a vascular anomaly.

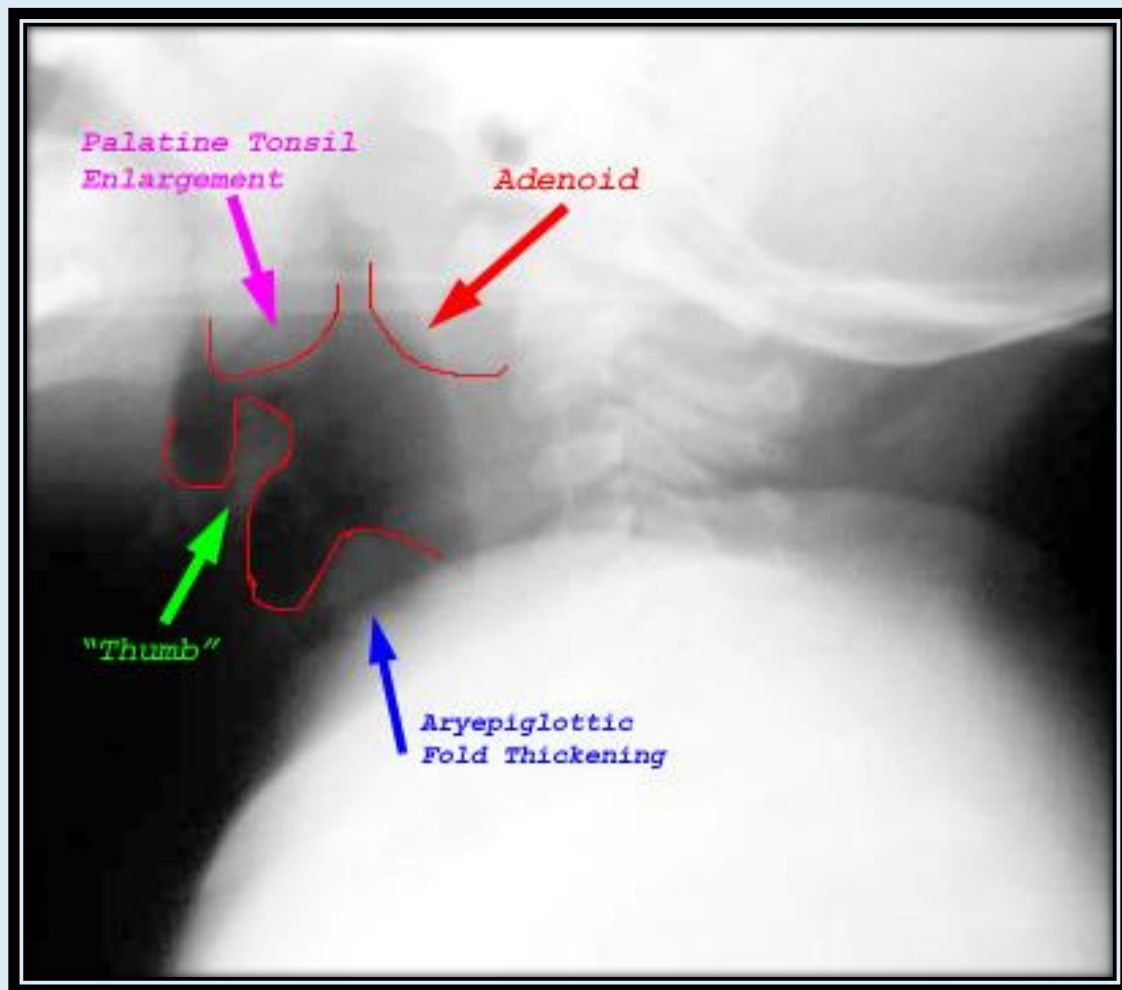
Lateral fluoroscopy can identify the collapse of the trachea with expiration confirming tracheomalacia. Additionally, CT bronchoscopy in both inspiration and expiration with a CTA is very helpful in answering these questions. MRI offers the same advantages as CT in dynamically examining the airway and looking at the vascular anatomy, but does not have the cost of the radiation dose. The disadvantage is that sedation is usually necessary for MRI whereas it is not usually needed for CT. Other etiologies for inspiratory stridor include infectious conditions, which will be discussed in the following section. Neck masses such as hemangiomas and cystic hygromas will not be discussed.

Acute epiglottitis

Acute epiglottitis is seen less commonly now that children are immunized against *Haemophilus influenza* type b. However, the clinical presentation can be striking.

- The child will have a high fever, dysphagia and sore throat.
- The child will be sitting upright with head held forward in severe respiratory distress.

Intubation may be necessary to maintain the airway, so it is best not to take the patient out of the emergency department for imaging. If imaging is obtained, a lateral soft tissue neck film should be taken in an upright position. The hypopharynx will be enlarged with thickening of the epiglottis and aryepiglottic folds. The thickening of the epiglottis results in the "thumb sign". Subglottic edema, as seen in croup, will also be found in 25% of patients with epiglottitis.

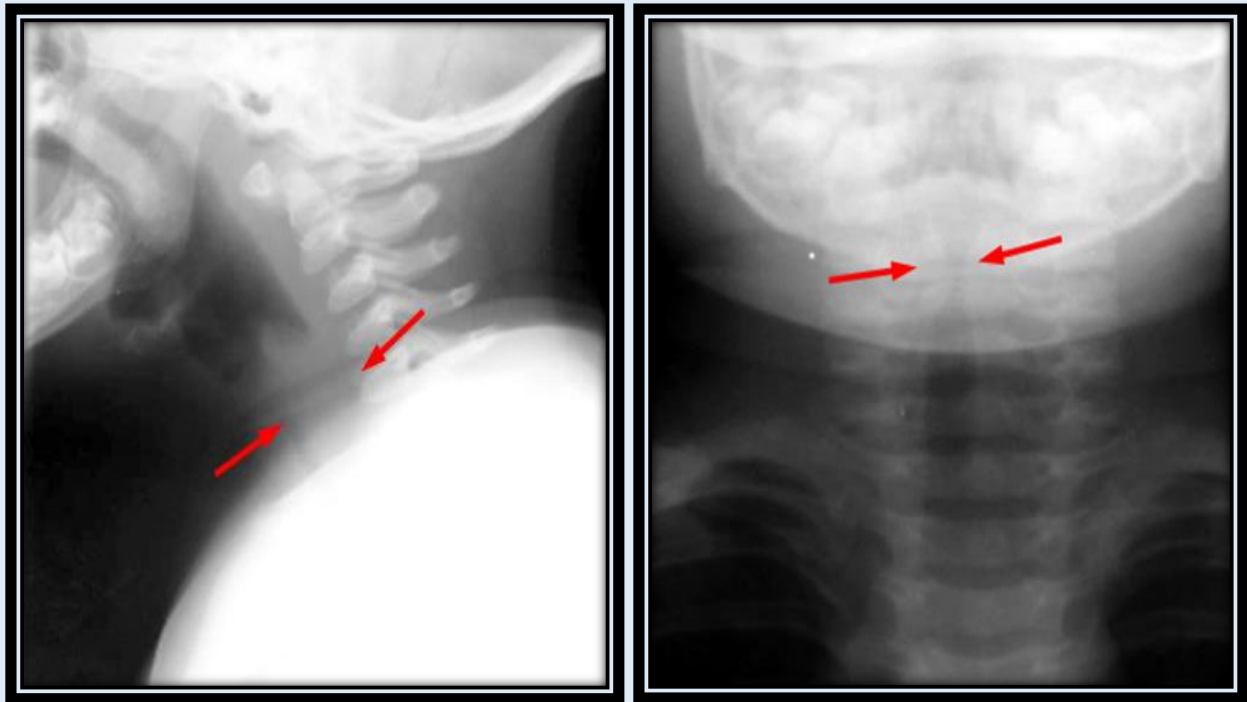


Lateral soft tissue demonstrates thickening of aryepiglottic folds and the epiglottis ("thumb sign"). Also note the enlargement of the palatine tonsil.

Croup

Croup, or acute laryngotracheobronchitis, remains a common cause of upper airway obstruction. Croup is viral, most commonly parainfluenza, and is seen mostly in the fall and winter when parainfluenza is more common. Croup is seen in a younger population than epiglottitis (usually 6 months to 3 years). Croup presents with a distinctive barking cough and is self limited, lasting about a week.

A lateral soft tissue radiograph will show the AP narrowing of the subglottic trachea, which normally should maintain the same AP diameter to the thoracic inlet. An AP soft tissue neck film will also show subglottic narrowing, but this can be confused with normal respiration changes. CXR will usually show signs of the viral bronchitis. Most importantly, the radiographic examination will also determine if there is a retropharyngeal abscess or an airway foreign body.



AP and lateral soft tissue exam of the neck demonstrates the **subglottic edema**.
Note that the epiglottis is not thickened as in epiglottitis.

Retropharyngeal Abscess

Retropharyngeal abscess results from infection with group B streptococcus or staphylococcus infections of the oropharynx. Clinical presentation is with fever, stiff neck, dysphagia and cervical adenopathy. Soft tissue neck radiographs will demonstrate retropharyngeal soft tissue swelling and soft tissue gas. Neck CT is helpful to demonstrate the extent of the disease and to determine if there are drainable fluid collections



Quiz - Pediatric Airway

1. The radiographic examination for a patient with inspiratory stridor is helpful in determining the presence of:

- A. Airway Foreign Body**
- B. Narrowing of the Subglottic Trachea**
- C. Retropharyngeal Abscess**
- D. All of the Above**

Answer: D

Pulmonary Inflammatory Disease

Viral Pulmonary Infections

Community acquired pediatric pulmonary infections are caused by a wide variety of organisms. They are most commonly viral in etiology and present in children less than 5 years old. Bacteria and mycoplasma become more common with increasing age.

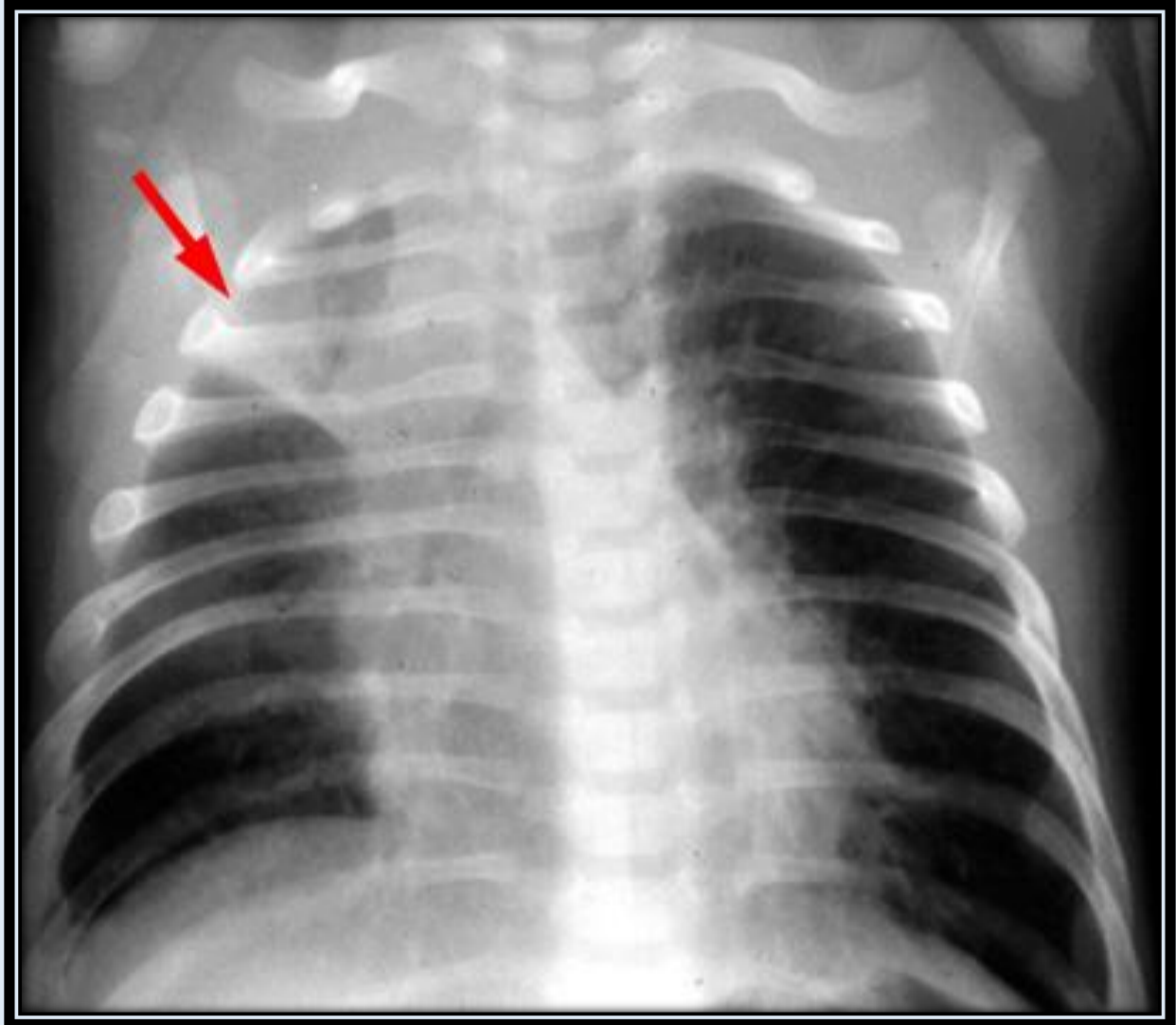
Respiratory syncytial virus (RSV) is the most frequently encountered viral agent in the infant and toddler population, usually presenting in the winter months. Parainfluenza, influenza, and adenovirus are also common viral pathogens. Viral infections tend to most severely affect the tracheobronchial tree, resulting in bronchiolitis and bronchitis, with relative sparing of the lung parenchyma.

The role of the radiologist in interpreting a CXR in a patient with a respiratory infection is to determine if it is viral or bacterial. These differences will be elaborated in the following sections. In summary, viral respiratory infections result in bronchitis, which manifests as peribronchial cuffing, dirty hilum and hyperinflation. Bacterial pneumonia will manifest as focal lobar consolidation with pleural effusion being common.

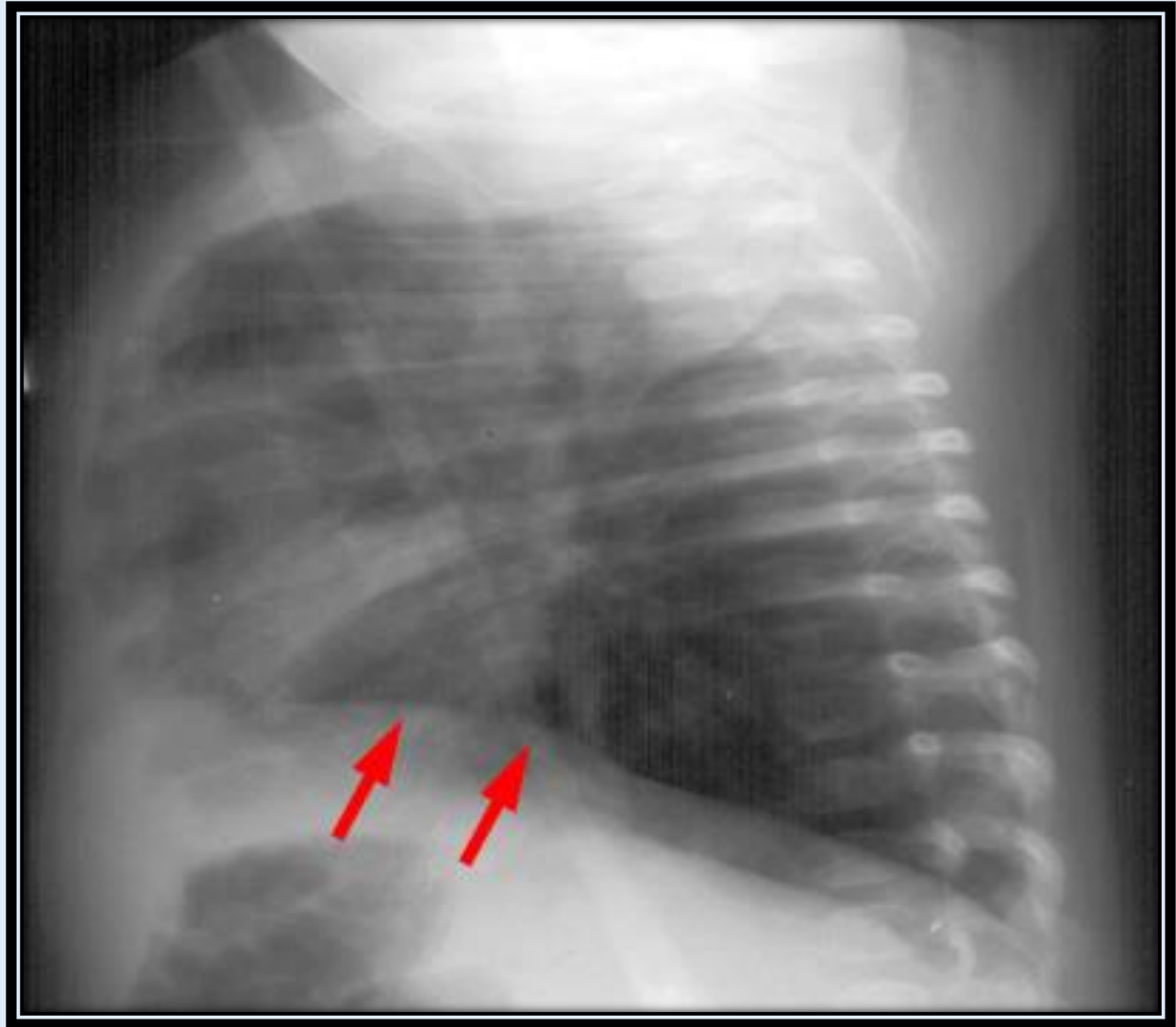
CXR Findings

Bronchitis will manifest on the CXR as peribronchial thickening or "peribronchial cuffing". A bronchus seen on end will show the bronchial wall thickening, and the hilum will demonstrate a dirty appearance, which is well demonstrated on the lateral projection.

The bronchial inflammation results in areas of mucus plugging and atelectasis whereas other areas of the lung will demonstrate hyperinflation from air trapping. The overall lung volumes will be hyperinflated with an increase in the anterior retrosternal space and flattening of the diaphragms. Viral infections do not have pleural effusions, however, these are relatively common in bacterial infections. The CXR findings for viral infection are the same as that for asthma, which is termed reactive airways disease in the preschool population.



PA CXR demonstrates **atelectasis**

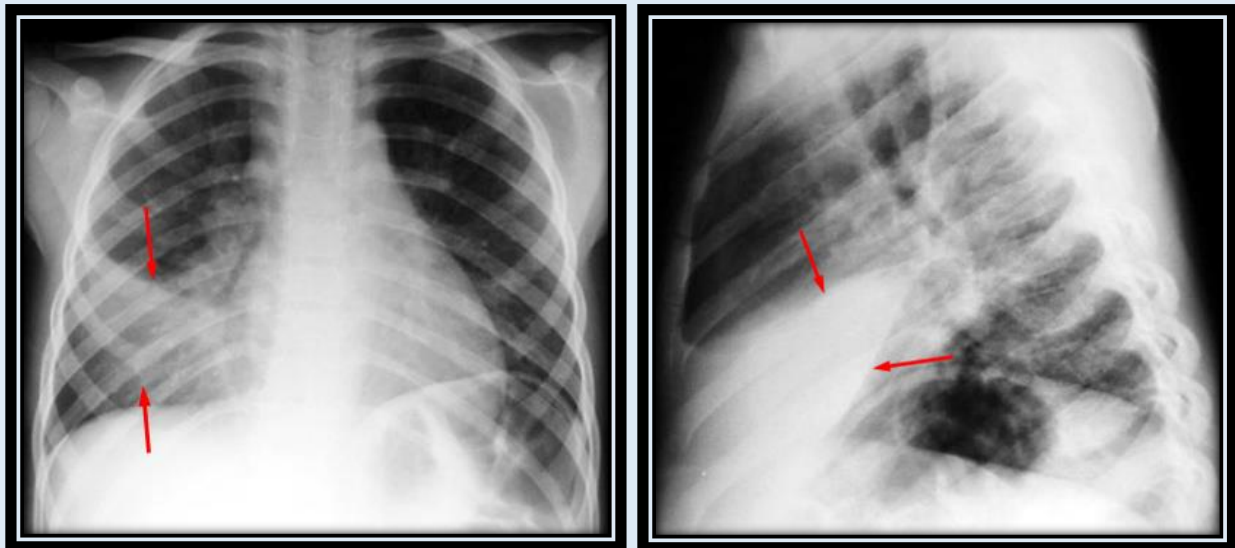


LAT CXR demonstrates **flattening of the diaphragms**.

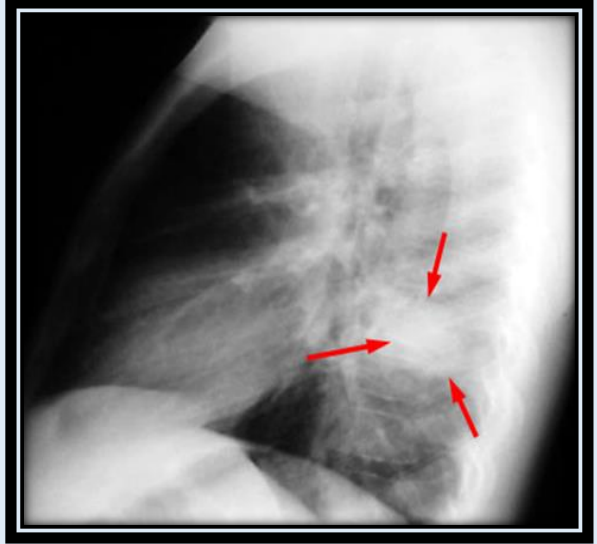
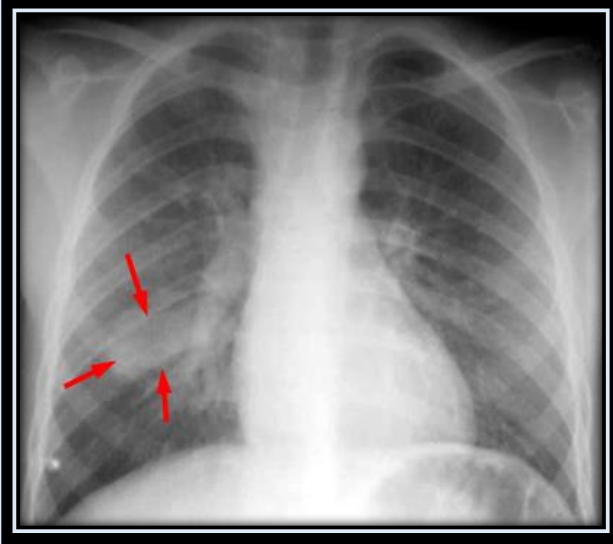
Bacterial Pulmonary Infection

Neonatal pneumonia is frequently caused by group b streptococcus and Chlamydia. Chlamydia tends to present slightly later, around 4 weeks, and the chlamydial conjunctivitis is helpful in making the diagnosis. Other common organisms include staphylococcus aureus, haemophilus influenzae type b, and pneumococcus.

The CXR findings are diagnostic of pneumonia but not specific as to the infecting organism. The most typical presentation is a lobar bronchopneumonia, which manifests on CXR as focal lobar consolidation with air bronchograms. The consolidation may have a round appearance, called **"round pneumonia"**, which can mimic a pulmonary mass.

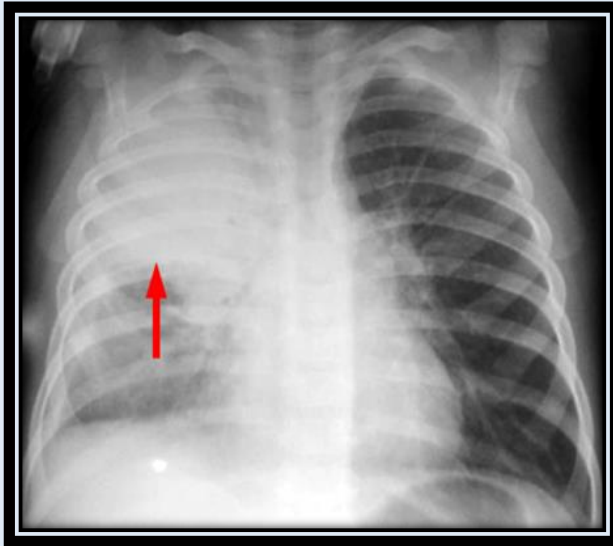


Example of a right middle lobe pneumonia. PA and LAT CXR demonstrate consolidation in the right middle lobe.

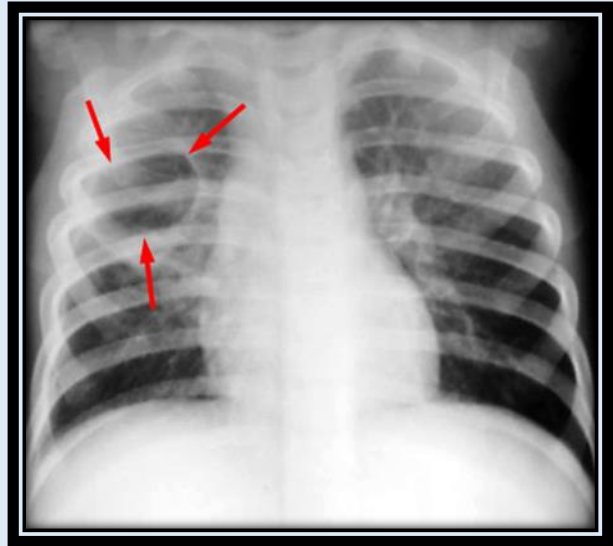


Example of a "round pneumonia." PA and LAT CXR shows a round opacity in the superior segment of the right lower lobe which has the appearance of a mass

Pneumatoceles are frequent with staphylococcal infections, and they should not be confused with a pulmonary abscess. Pneumatoceles have thin, smooth walls and are seen with an improving clinical picture, whereas pulmonary abscesses have thick, irregular walls with an air fluid level and the child tends to be very ill. Pneumatoceles are thought to be a form of localized pulmonary interstitial emphysema and are self-limiting with only the rare case of a large, persisting pneumatocele needing surgery.



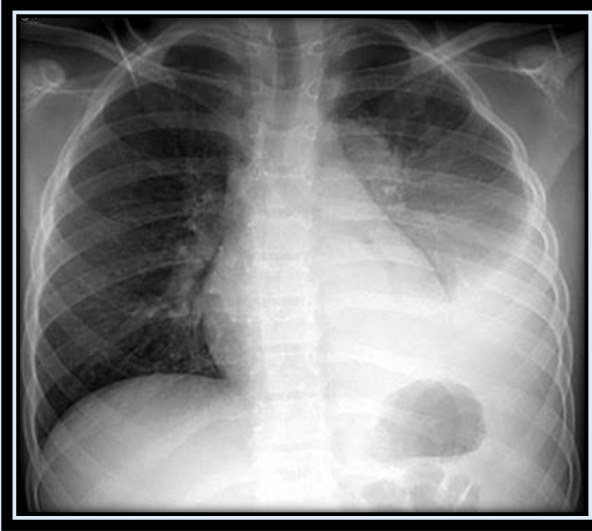
Initial CXR shows a **dense right upper lobe consolidation.**



CXR a week later shows a **round cyst with thin walls** in the right upper lobe

Pleural effusions are common in bacterial pneumonias and should be easily recognized on the CXR. Most pleural effusions are transudative parapneumonic effusions that will resolve with antibiotic treatment of the pneumonia. An empyema will result from spread of the infection into the pleural fluid.

Differentiating sterile transudative parapneumonic pleural fluid from an empyema is difficult with imaging, and therefore a sample of the fluid is usually necessary. Children with pneumonia and empyema that are not responding to antibiotics will require drainage. A chest CT is helpful to plan and monitor the drainage procedure.



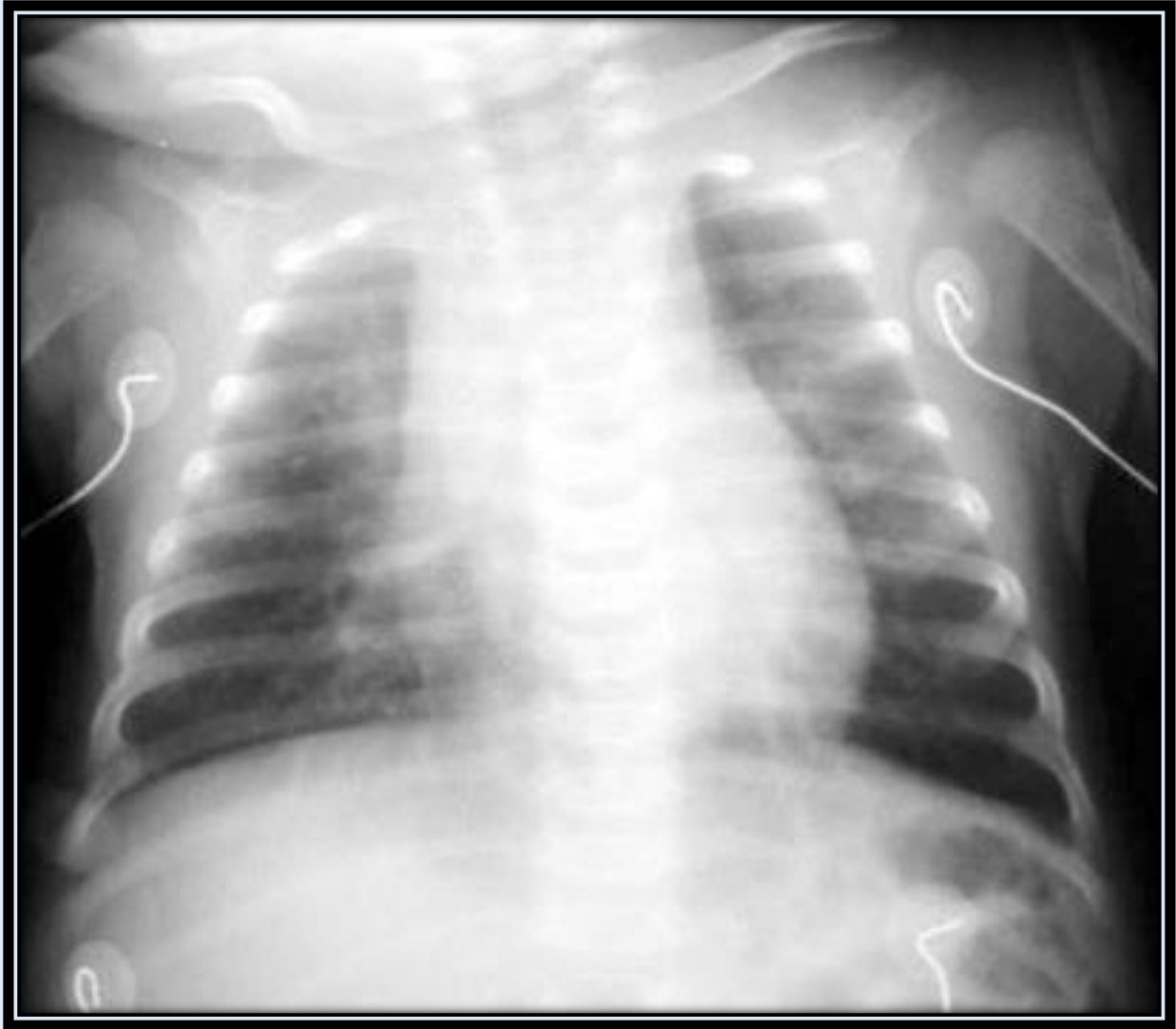
PA and LAT CXR demonstrates a **left lower lobe consolidation**, representing pneumonia. Also note the meniscus in the left costophrenic angle indicating a **parapneumonic left pleural effusion**



Example of an **empyema**. CT through the lower thorax shows a fluid collection in the right lower pleural space with an air fluid level and a thick enhancing wall.

Specific Organisms

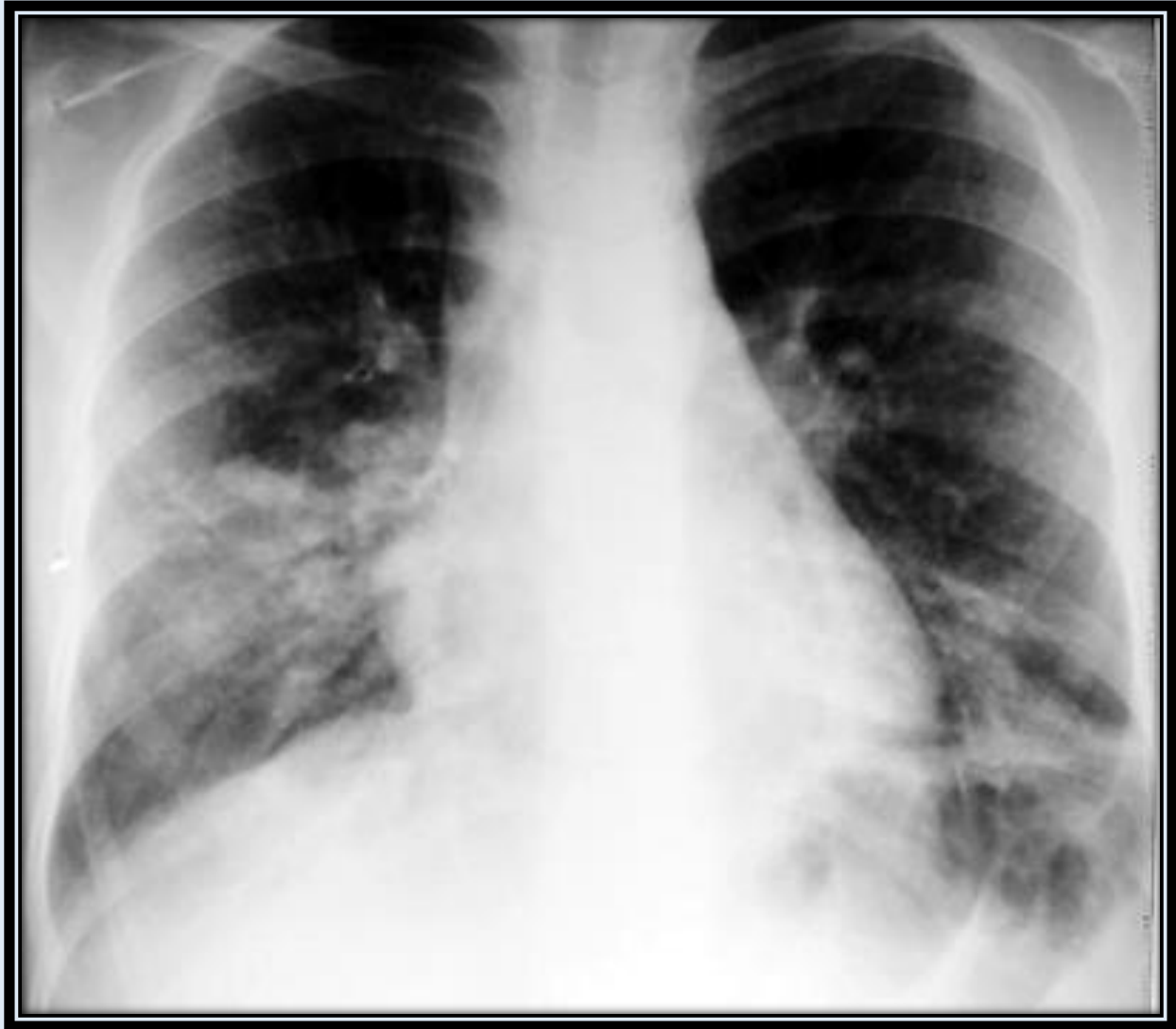
Bordetella pertussis pneumonia is encountered less frequently because of vaccination, but it is still relatively common. In the fall of 2001, there was a small epidemic of 56 cases in Albemarle County, Virginia. The diagnosis is usually made on the basis of the characteristic "whooping cough" and confirmed with a PCR test. The classic finding on CXR is a "shaggy heart".



Example of a "shaggy heart" on CXR in a patient with **Bordetella pertussis pneumonia**.

Mycoplasma pneumoniae is a common cause of epidemic respiratory infections in the school-age child. Symptoms tend to be less severe, and it is sometimes referred to as "walking pneumonia".

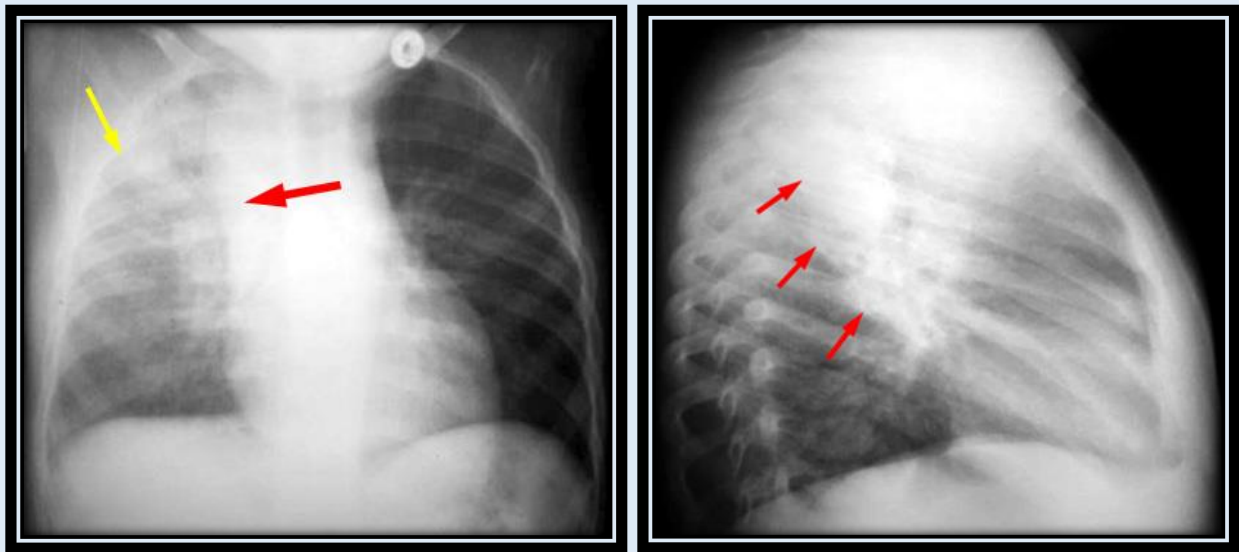
Mycoplasma has a variable presentation on CXR, most commonly presenting as bilateral lower lobe consolidation with small pleural effusions. It may also present with bilateral reticulonodular densities and areas of atelectasis if the infection is predominantly bronchitis.



Example of **bilateral lower lobe opacities** on CXR in a patient with **Mycoplasma pneumoniae**.

Tuberculosis remains a significant pulmonary infection in the 21st century, and the radiologist should maintain a high index of suspicion.

Primary TB in the pediatric population differs from the presentation of reactivation TB seen in adults. Primary TB produces a focal lobar consolidation in any pulmonary lobe. Hilar adenopathy and pleural effusions are common and should alert the radiologist to the possibility of TB. If the lungs are secondarily infected hematogenously, miliary TB will result and present as characteristic, uniform small nodules diffusely through the lungs.



PA and LAT CXR with diffuse air space disease throughout the right upper lobe and significant right paratracheal adenopathy. The red arrow indicates adenopathy; the yellow arrow indicates TB pneumonia.

Swyer-James Syndrome

Post-inflammatory bronchial stenosis results in a hyperlucent, enlarged pulmonary lobe due to air trapping.

Sickle Cell Acute Chest Syndrome

Acute chest pain with fever is a common complication of sickle cell disease. Pulmonary opacities are frequently seen on CXR, and it is unclear if the etiology is ischemic or infectious. Acute chest syndrome is treated with empiric antibiotics and supportive pain therapy.

Cystic Fibrosis (CF)

Cystic Fibrosis is an autosomal recessive disease affecting 1/1500 Caucasian individuals. The pulmonary system is most severely affected, but gastrointestinal complications are also common with meconium ileus in the newborn period and malabsorption that can result in failure to thrive. Supportive care for CF has greatly extended the quality of life and overall life expectancy for these patients. However, recurrent pulmonary infections in combination with malnutrition will eventually lead to pulmonary insufficiency and pulmonary hypertension.

The presence of multiple recurrent pulmonary infections should lead to a test for CF. Meconium ileus is virtually the only diagnostic presentation of CF in the early course of the disease. Eventually, the CXR will demonstrate the characteristic hyperinflation and bronchiectasis. The CXR is used primarily to monitor acute infections and the general progression of the disease.



Quiz - Pulmonary Inflammatory Disease

1. What disease state is associated with "peribronchial cuffing?"

Viral Bronchitis.

2. Pneumatoceles are caused by bacterial pulmonary infections.

A. True

B. False

3. Pediatric and adult patients have identical presentations of TB.

A. True

B. False

Chest Radiology Post-Test

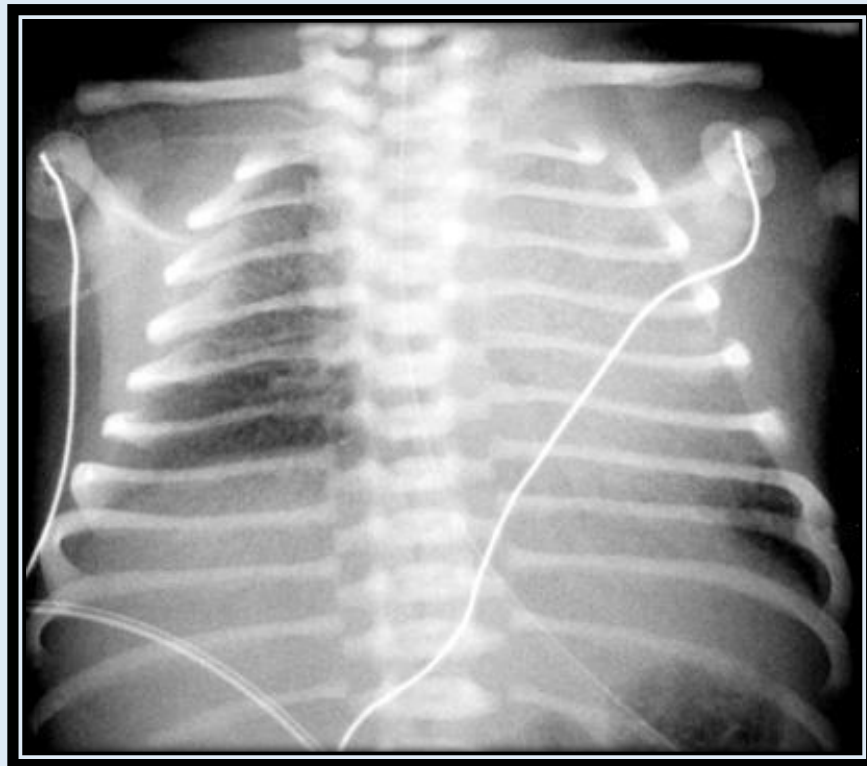
Q_1: The appropriate position of the UAC is at the level of the diaphragm.

- A. True
- B. False

Q_2: The "deep sulcus sign" refers to the following:

- A. Pneumomediastinum
- B. Pneumothorax
- C. Pleural Effusion
- D. Pneumoperitoneum

Q_3: The most likely diagnosis is:

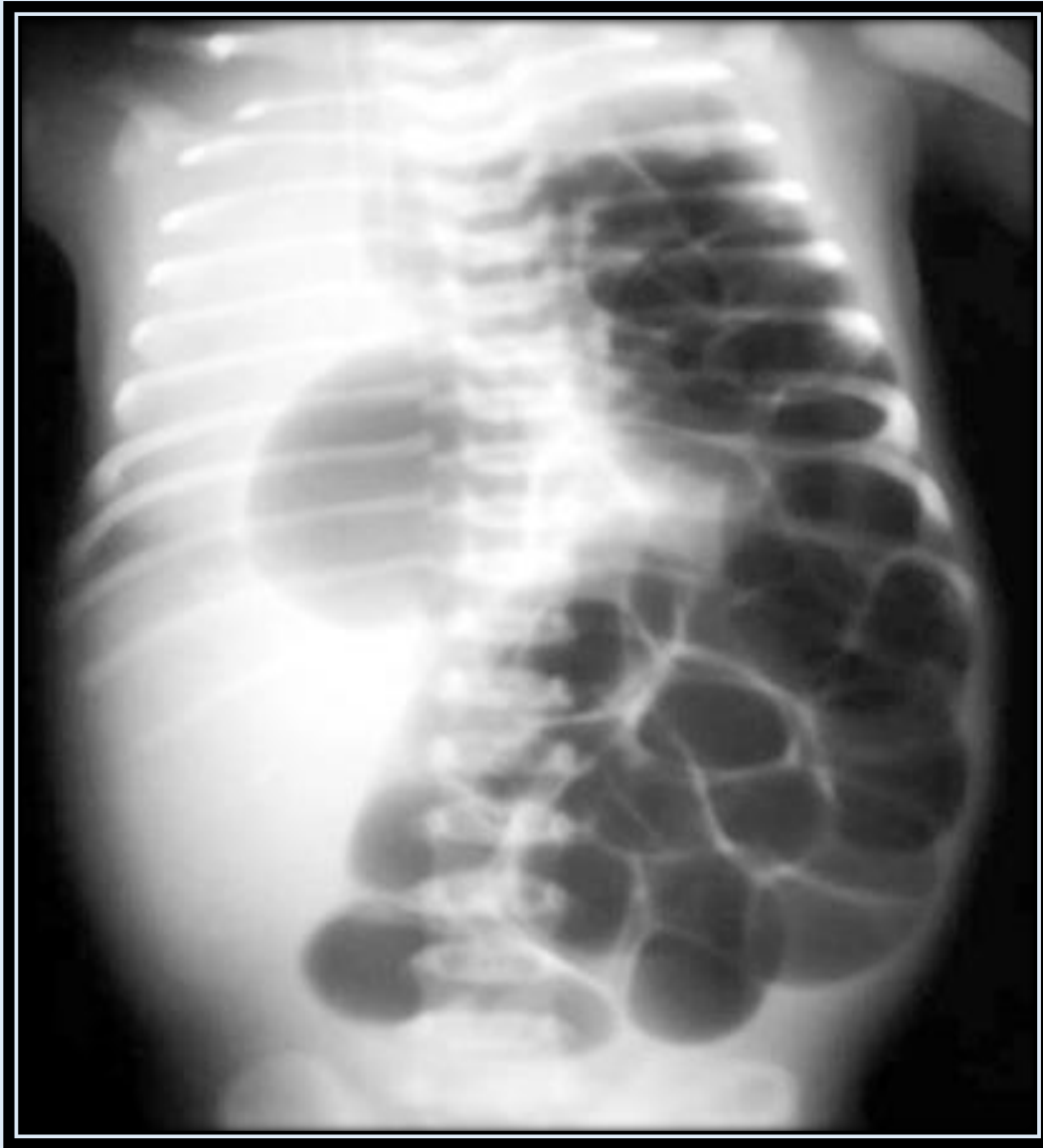


- A. Meconium Aspiration
- B. Respiratory Distress Syndrome
- C. Congenital Diaphragmatic Hernia
- D. Normal CXR

Q_4: Pleural fluid is frequently seen with respiratory distress syndrome.

- A. True
- B. False

Q_5: The most likely diagnosis is:



- A. Congenital Diaphragmatic Hernia
- B. Congenital Cystic Adenomatoid Malformation
- C. Congenital Lobar Emphysema
- D. Respiratory Distress Syndrome

Q_6: Which one is the most common etiology of neonatal pneumonia?

- A. Group B Streptococcus
- B. Chlamydia
- C. Staphylococcus
- D. Haemophilus Influenzae

Q_7: Which of the following induces closure of the ductus arteriosus?

- A. Indomethacin
- B. Steroids
- C. Prostaglandins
- D. Antibiotics

Q_8: The CXR findings of hyperexpansion, peribronchial cuffing, and dirty hila indicate which of the following:

- A. Tuberculosis
- B. Meconium Aspiration
- C. Viral Bronchitis
- D. Staphylococcal Pneumonia

Q_9: A pneumatocele cannot be reliably differentiated from a pulmonary abscess

- A. True
- B. False

Q_10: All of the following require a surgical consult except:

- A. Congenital Diaphragmatic Hernia
- B. Pulmonary Interstitial Emphysema
- C. Congenital Cystic Adenomatoid Malformation
- D. Congenital Lobar Emphysema

Answers

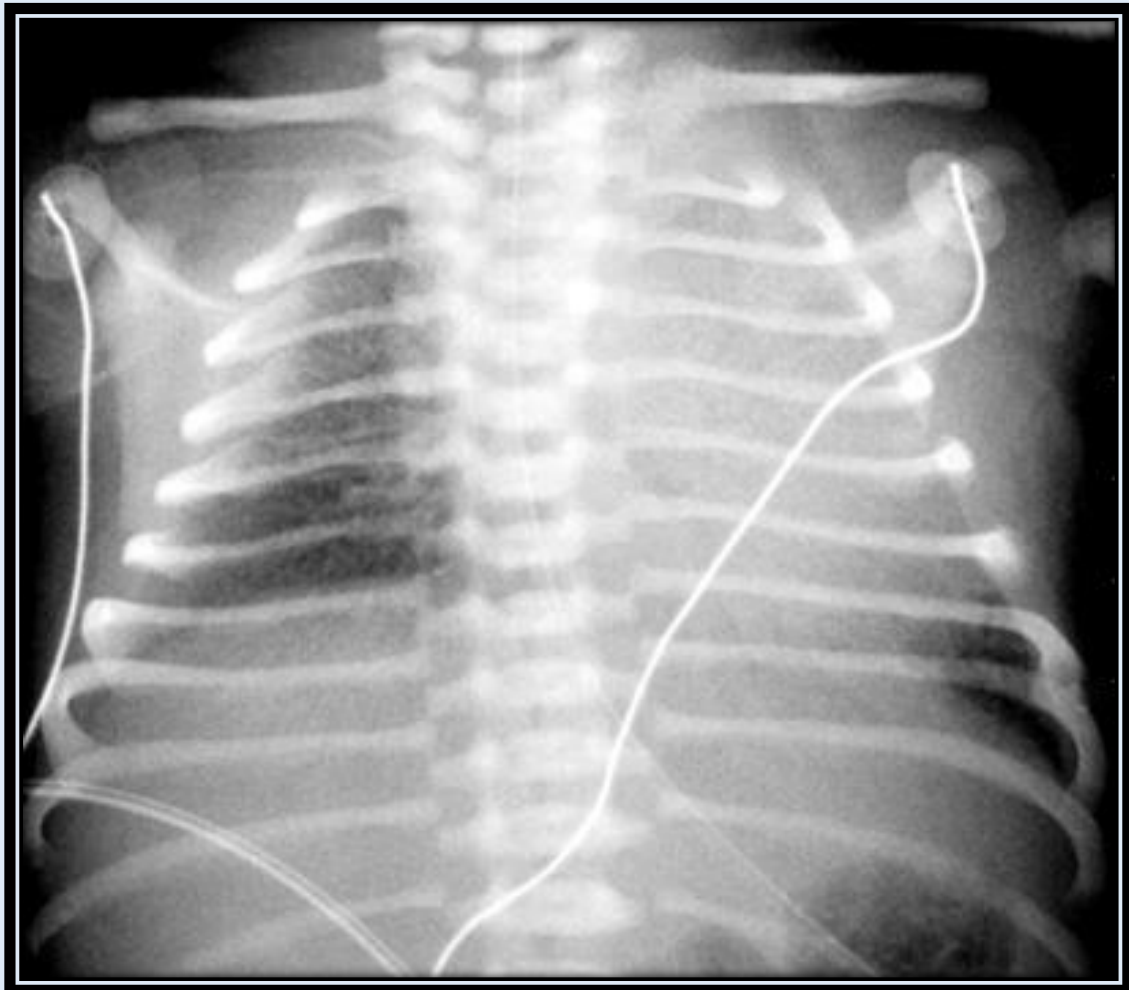
Q_1: The appropriate position of the UAC is at the level of the diaphragm.

False. The appropriate position of the UAC is below the level of the L2 vertebral body to avoid complications with the mesenteric vessels. The UVC should be positioned at the level of the diaphragm to ensure placement in the IVC.

Q_2: The "deep sulcus sign" refers to the following:

Anterior pneumothorax. The "deep sulcus sign" refers to an anterior pneumothorax that is best seen on supine CXR as a hyperlucent costophrenic angle.

Q_3: The most likely diagnosis is:

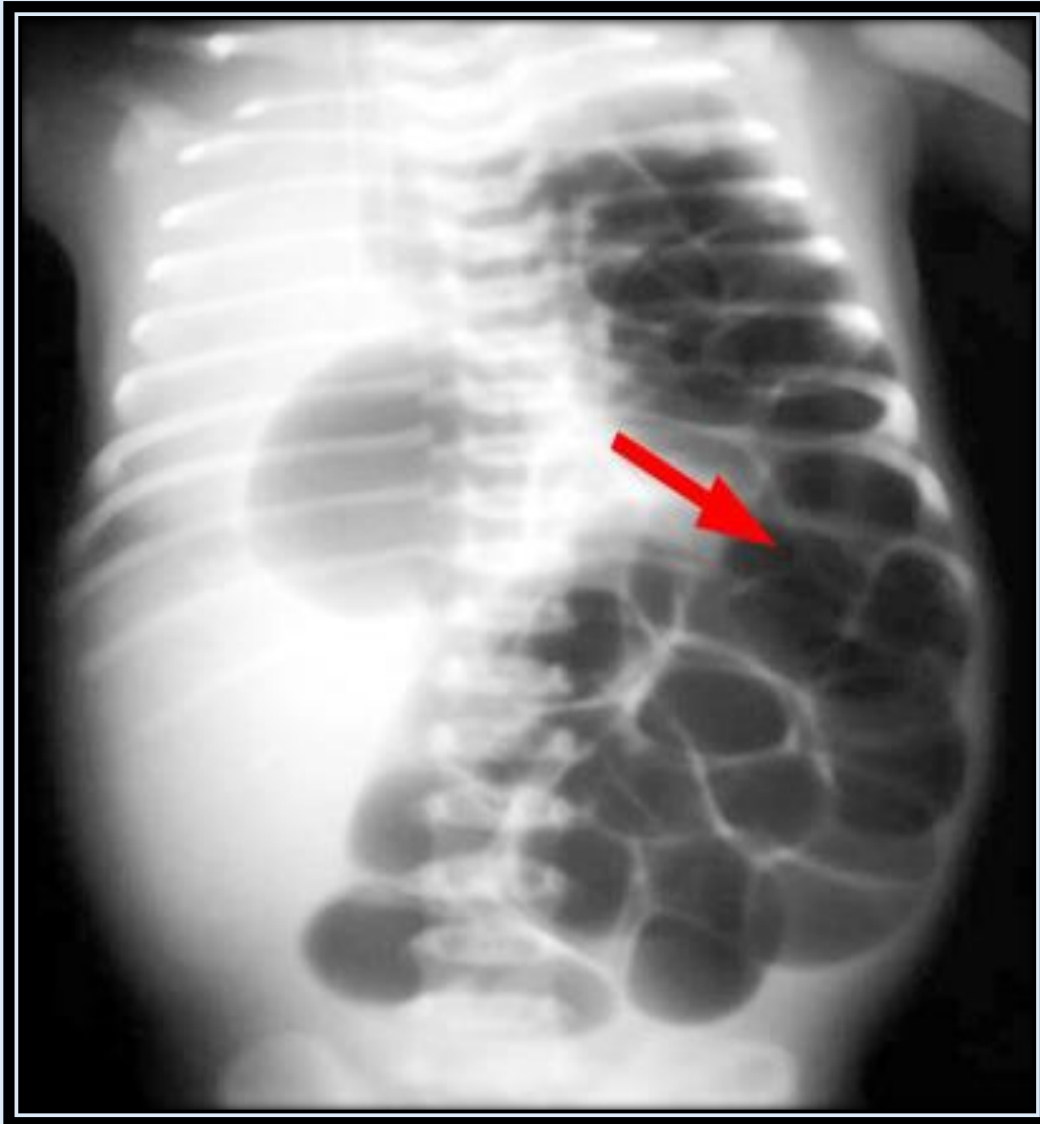


Respiratory distress syndrome is the most likely diagnosis based on the decreased lung volumes and diffuse granular pattern in the lungs.

Q_4: Pleural fluid is frequently seen with respiratory distress syndrome.

False. Pleural fluid is infrequently seen with RDS. Pleural fluid is more commonly seen with neonatal infection.

Q_5: The most likely diagnosis is:



Congenital diaphragmatic hernia. The cystic lucencies in the left chest are shown to be continuous with the bowel gas indicating a defect in the diaphragm with herniation of bowel into the chest.

Q_6: Which of these is the most common etiology of neonatal pneumonia?

The most common cause of neonatal pneumonia is **group B streptococcus** from the vaginal canal.

Q_7: The ductus arteriosus is induced to close by administration of:

Indomethacin will inhibit prostaglandins and thereby induce closure of the ductus arteriosus. Prostaglandins are given in cases of congenital heart disease to keep the ductus open.

Q_8: The CXR findings of hyperexpansion, peribronchial cuffing, and dirty hila indicate which of the following:

Viral bronchitis

Q_9: A pneumatocele cannot be reliably differentiated from a pulmonary abscess.

False. A pneumatocele can be differentiated from a pulmonary abscess based on the clinical status of the patient and the imaging findings.

Q_10: All of the following require a surgical consult EXCEPT:

Pulmonary interstitial emphysema is managed in the NICU with the most affected side positioned downward and adjustment of the ventilator settings.

Pediatric Abdominal Radiology

Pediatric Abdominal Radiology

Comprehensive Outline for Pediatric Abdominal Section

- **Neonatal**

- Esophageal Atresia - Introduction
- Esophageal Atresia - Radiographic Features
- Tracheoesophageal Fistula
- Duodenal Atresia - Introduction
- Duodenal Atresia - Radiographic Features
- Jejunal-Ileal Atresia
- Meconium Ileus - Introduction
- Meconium Ileus - Radiographic Features
- Meconium Plug Syndrome
- Hirschsprung Disease - Introduction
- Hirschsprung Disease - Radiographic Features
- Necrotizing Enterocolitis - Introduction
- Necrotizing Enterocolitis - Radiographic Features

- **Upper GI**

- Esophageal Foreign Body
- Esophageal Strictures
- Hypertrophic Pyloric Stenosis - Introduction
- Hypertrophic Pyloric Stenosis - Radiographic Features
- Hypertrophic Pyloric Stenosis - Sonographic Features

- **Lower GI**

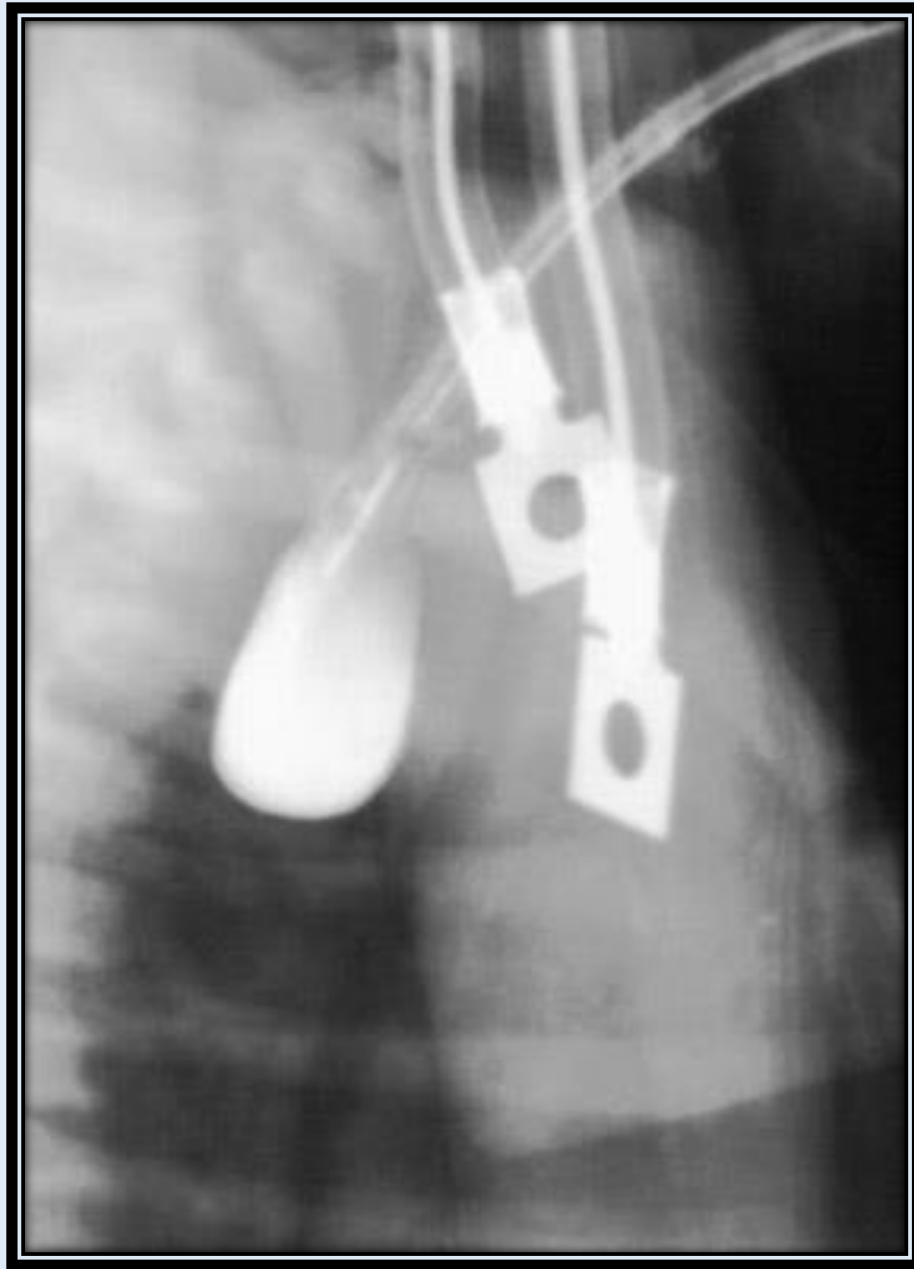
- Malrotation - Introduction
- Malrotation - Radiographic Features
- Midgut Volvulus - Introduction
- Midgut Volvulus - Radiographic Features
- Meckel's Diverticulum
- Appendicitis - Introduction
- Appendicitis - Radiographic Features
- Intussusception - Introduction
- Intussusception - Radiographic Features
- Colonic Atresia

- **Liver and Biliary**

- Biliary Atresia - Introduction
- Biliary Atresia - Radiographic Features
- Neonatal Hepatitis
- Choledochal Cyst - Introduction
- Choledochal Cyst - Radiographic Features

Esophageal Atresia

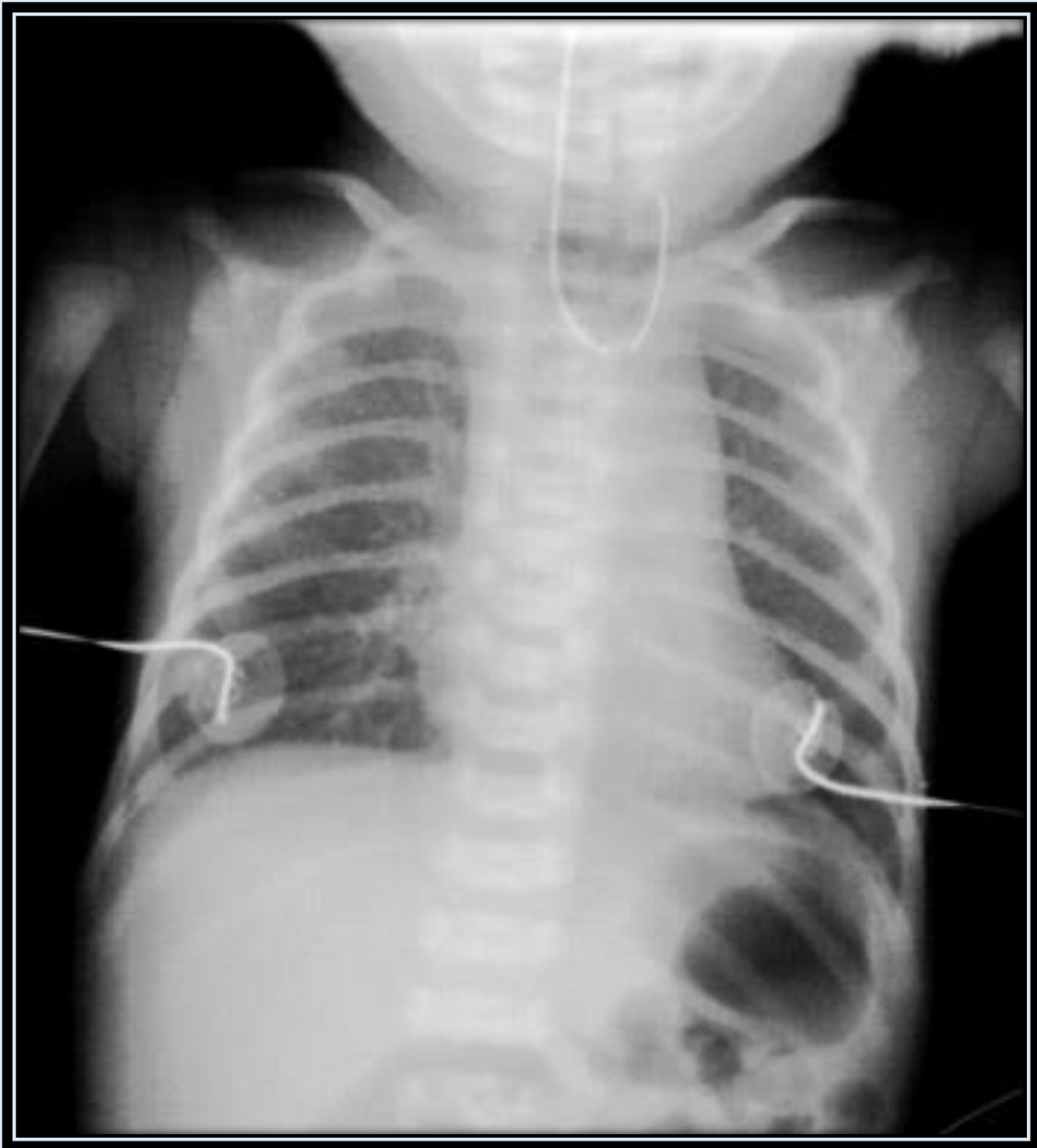
Esophageal atresia is the interruption of the tubular esophagus. Its incidence is 1 in 2,000-4,000 live births. It is associated with the VACTERL disorders. The most common associated anomaly is the tracheoesophageal fistula. Symptoms include drooling due to accumulation of pharyngeal secretions, regurgitation of ingested fluids and frothy sputum. Infants present shortly after birth.



Contrast collecting in **proximal esophageal pouch**. A contrast study of the pouch is rarely indicated. Air injected through the NG tube can be used as very safe, negative contrast agent.

Radiographic Features

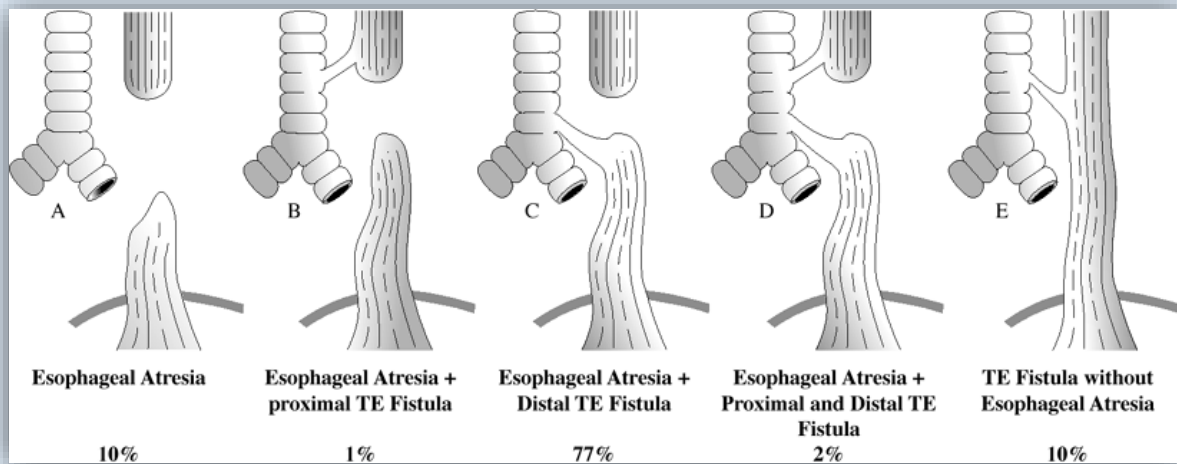
Common radiographic features include the **"Coiled NG Tube"** in the esophageal pouch. If there is bowel gas in the abdomen there must be an associated tracheoesophageal fistula, ~90% of cases of esophageal atresia. A TE fistula can occur without esophageal atresia and may present later in life with wheezing or recurrent pneumonia.



Note the NG tube looped in the upper esophagus. Air in the stomach indicates presence of a tracheoesophageal fistula

Tracheoesophageal Fistula

A tracheoesophageal fistula is secondary to incomplete division of the trachea and esophagus during organogenesis, resulting in an abnormal connection between the esophagus and the trachea. Its incidence is 1 in 2,000-4,000 live births. Symptoms include coughing and choking during feeding, recurrent pneumonia and respiratory distress.





While one would not purposely perform a study in this way, it nicely demonstrates the anatomy of esophageal atresia with TE fistula. Contrast was administered through a G tube into the stomach. The contrast refluxed into the distal esophagus across the tracheoesophageal fistula into the trachea and from the trachea into the esophageal pouch.

Duodenal Atresia

The most common cause of congenital duodenal obstruction is duodenal atresia. Failure of recannulation of the duodenum typically occurs in the region of the ampulla of Vater. It is often diagnosed prenatally on OB ultrasound. The incidence is 1 in 10,000 live births. Associated disorders include Down syndrome (30%), malrotation (20%), heart disease (20%), renal anomalies, tracheoesophageal fistula, and the VACTERL anomalies. Symptoms include bilious vomiting in the first day of life. Treatment is surgery.



Radiographic Features

The most prominent feature is the **"double bubble" sign** (dilated stomach and duodenal bulb) -- dilated stomach and no gas distal to the proximal duodenum. Stated another way, there is no gas in the rest of the small or large bowel.



Double bubble sign



Double bubble sign

Jejunal-Ileal Atresia

Jejunal-ileal atresia is a segmental atresia of the jejunum or the ileum. It is associated with malrotation and volvulus (25%) and cystic fibrosis (10%). Patients present within the first days of life with vomiting or a distended abdomen.



Multiple distended loops of bowel



Barium enema demonstrates unused **microcolon** in a patient with distal ileal atresia

Meconium Ileus

Meconium ileus is caused by thick, tenacious meconium that adheres to the wall of the small bowel and causes obstruction most often at the level of the ileocecal valve in a neonate. Almost all patients with meconium ileus have cystic fibrosis; 10-15% of CF patients present with meconium ileus. Complications include ileal atresia and/or stenosis, volvulus, perforation, and meconium peritonitis (due to obstruction and ischemia from tenacious meconium). It can be treated non-surgically with water-soluble enemas to relieve the obstruction or be treated surgically.



Multiple dilated loops of bowel and an unused **microcolon** on barium enema.

Radiographic Features

- Microcolon (unused colon)
- "Frothy" or "soap-bubble" pattern of bowel gas (air mixed with meconium), often in the right lower quadrant
- Dilated small bowel loops
- Small bowel obstruction
- Calcification due to meconium peritonitis (15%)
- Distal ileum packed with meconium and larger than microcolon on contrast enema



Small bowel obstruction with dilated loops of bowel and soap bubble bowel gas pattern in the right lower quadrant.



On barium enema, there is a **microcolon**

Meconium Plug Syndrome

In meconium plug syndrome, there is meconium obstruction of the colon, often seen in infants of diabetic mothers or mothers who received magnesium sulfate for eclampsia. Meconium forms a cast of the colon, and the colon remains normal in caliber. These patients present within the first 24 hours of life with abdominal distension, vomiting, and failure to pass meconium.

Differential diagnosis includes Hirschsprung Disease.

Treatment is with water-soluble enemas.



Meconium cast filling defect in colon on barium enema.

Hirschsprung Disease

Hirschsprung Disease is aganglionosis of the colon with absence of parasympathetic ganglia in mucosal and submucosal layers of colon. This is a result of the failure of normal cranial-caudal migration of ganglion cells. The most common transition site is the rectosigmoid colon. Total colonic aganglionosis is rare.

The incidence is 1 in 5,000-8,000 live births, with a male to female ratio of 4-9 to 1. Patients may present with failure to pass meconium within the first 24 hours of life or later with constipation and paradoxical diarrhea (25%). The treatment is a surgical pull-through procedure.



The **transition zone** is near the splenic flexure.

Radiographic Features

Normally, the rectum is larger than the colon. In Hirschsprung Disease, there is an abnormal rectosigmoid ratio with the rectum smaller than the sigmoid due to denervation hyperspasticity. Therefore, one sees dilation of large and small bowel proximal to the "transition zone." The "Transition Zone" is the junction between the proximal normally innervated colon and the distal aganglionic segment. The normally innervated proximal colon becomes dilated. In 33% of cases, there is a normal-appearing rectum.



The **transition zone** is in the mid-descending colon.

Necrotizing Enterocolitis

Necrotizing enterocolitis is the most common acquired gastrointestinal emergency of premature infants. It occurs less frequently in older children who are under great stress (e.g., congenital heart disease). Necrotizing enterocolitis is related to infection and ischemia, commonly affecting the ileum and ascending colon. It usually presents during the first or second week of life with bloody stools (50%), explosive diarrhea, bilious emesis, mild respiratory distress, generalized sepsis, distention of the abdomen, and feeding difficulties. It requires an immature gut and time for gut to become colonized in order to develop. These patients typically have been fed. The treatment is bowel rest and antibiotics and surgery for bowel perforation.

Radiographic Features

A definitive radiographic finding is **pneumatosis**, gas in the bowel wall. There is a "frothy" or "soap-bubble" bowel gas pattern. Linear or crescent shaped gas collections in the bowel wall may also be seen. Another sign is unchanged bowel gas pattern over several films indicating an ileus. More worrisome signs include gas in portal venous system and ascites. Infants can have an occult perforation without free intraperitoneal air in the setting of a gasless abdomen. Pneumoperitoneum used to be considered a surgical emergency. However, a percutaneous drain may now be placed instead of surgery.



Multiple dilated loops of bowel with pneumatosis



Extensive **pneumatosis** throughout the abdomen.

Quiz - Neonatal

Q_1: Failure to pass an NG tube is associated with which of the following?

- A. Esophageal Atresia
- B. H-Type TE Fistula
- C. Malrotation
- D. Duodenal Atresia

Q_2: The "double bubble" sign indicates which of the following?

- A. Esophageal Atresia
- B. TE Fistula
- C. Jejunal-Ileal Atresia
- D. Duodenal Atresia

Q_3: Almost all Cystic Fibrosis patients have Meconium Ileus.

- A. True
- B. False

Q_4: Which of the following is a definitive radiographic finding for NEC?

- A. Caterpillar Sign
- B. Pneumatosis
- C. Double-Bubble Sign
- D. TE Fistula

Q_5: There is always an abnormal rectosigmoid ratio in Hirschsprung Disease.

- A. True
- B. False

Answers

Q_1: Failure to pass an NG tube is associated with which of the following?

Esophageal Atresia.

Q_2: The "double bubble" sign indicates which of the following?

Duodenal Atresia.

Q_3: Almost all Cystic Fibrosis patients have Meconium Ileus.

False. Only 10 to 15 percent of CF patients have Meconium Ileus, but almost all patients with Meconium Ileus have CF.

Q_4: Which of the following is a definitive radiographic finding for NEC?

Pneumatosis.

Q_5: There is always an abnormal rectosigmoid ratio in Hirschsprung Disease.

False. There is a normal appearing rectum in 33 percent of cases.

Esophageal Foreign Body

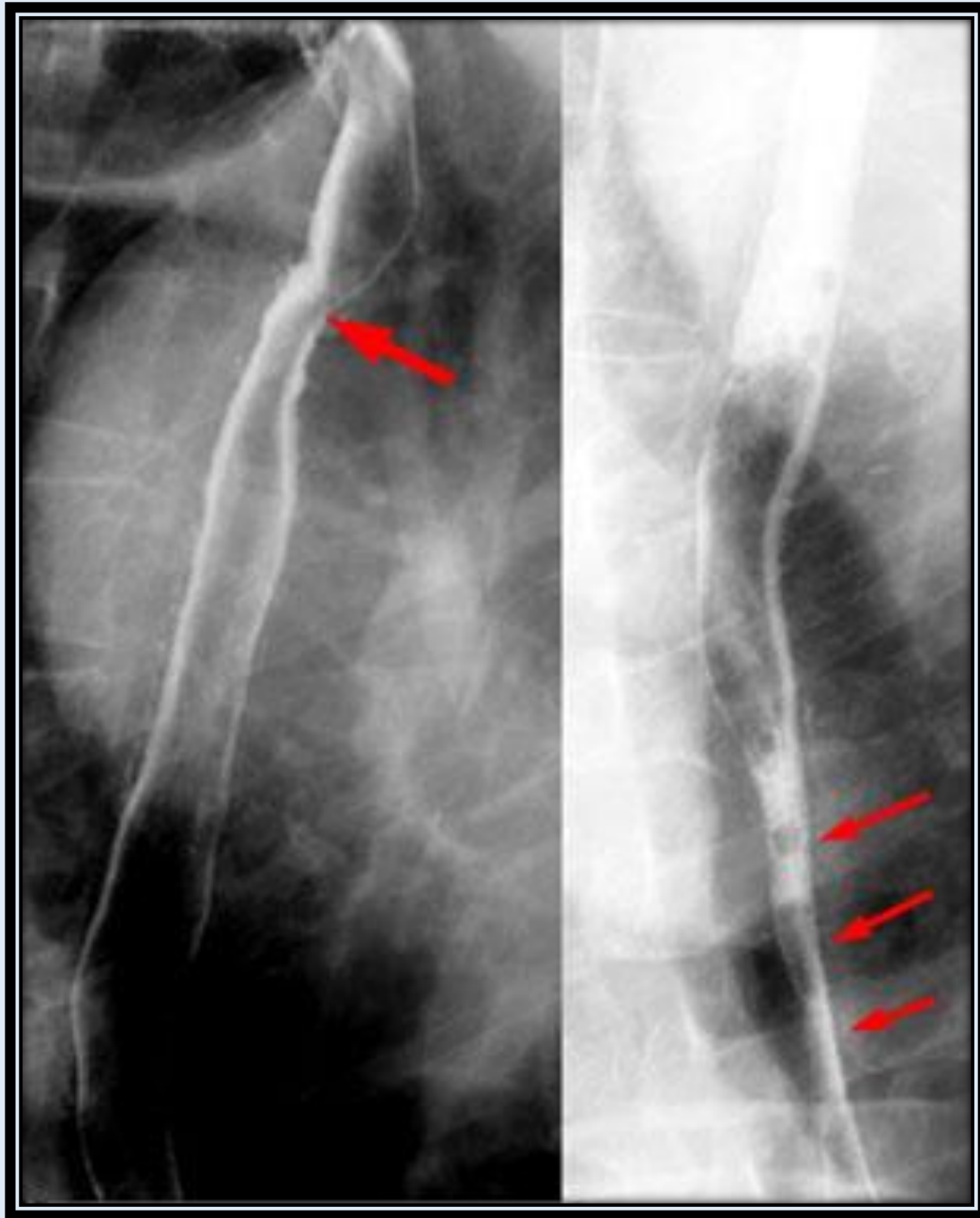
Most swallowed foreign bodies, especially the round ones, pass through the entire gastrointestinal tract successfully, but some lodge in the esophagus, usually proximally at the thoracic inlet or at the level of the aortic arch. The most common foreign body is a coin. Batteries can cause mucosal damage. The treatment is endoscopic removal or fluoroscopically guided removal. Complications of chronic foreign bodies include traumatic tracheoesophageal fistula or an inflamed mass that compresses the trachea resulting in respiratory symptoms. On XR, a coin lodged in the esophagus has its widest dimension on the AP view and a coin in the trachea has its widest dimension on the lateral view.



Coin in mid-thoracic esophagus

Esophageal Structures

Esophageal strictures are areas of local esophageal narrowing. They can result from ingestion of corrosive agents, previous esophageal atresia repair, epidermolysis bullosa or gastroesophageal reflux. A commonly used therapy is using balloon catheters under fluoroscopic guidance to dilate the esophagus.



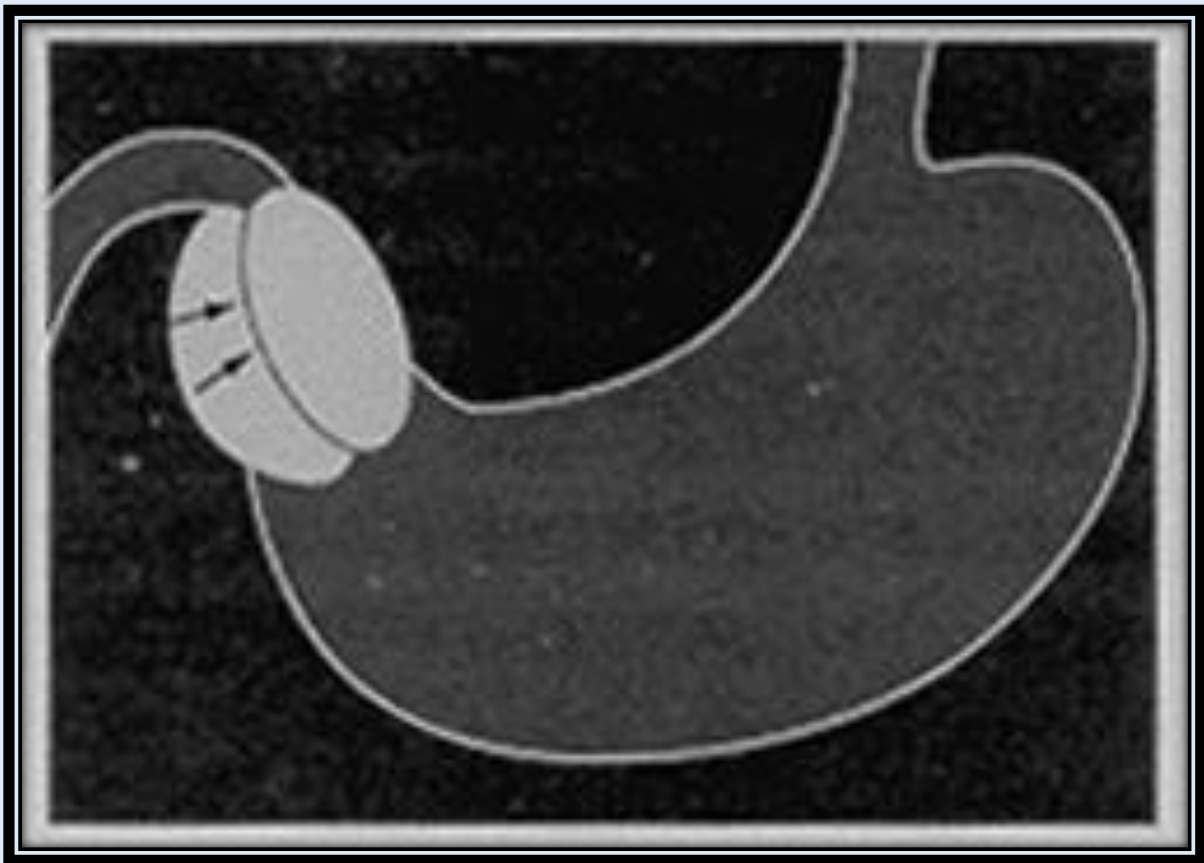
Two visible **esophageal strictures**



Contrast study of **esophageal strictures**

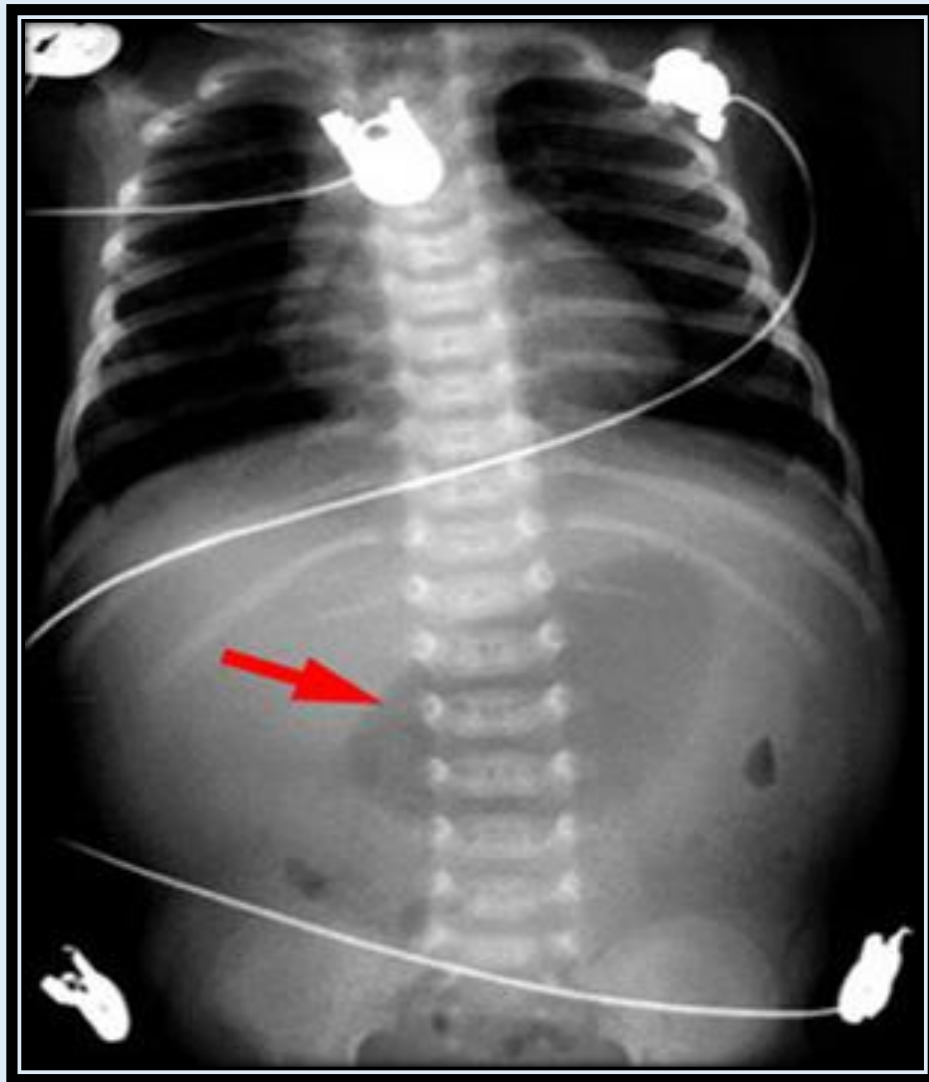
Hypertrophic Pyloric Stenosis

Hypertrophic pyloric stenosis is the thickening of the muscle of the pylorus resulting in an obstruction. Its incidence is 3 in 1,000 live births, with a male to female ratio of 4-5:1, and an increased incidence with firstborn male children. Signs and symptoms include non-bilious, projectile vomiting and a palpable mass. Treatment usually includes surgery. Associated abnormalities include esophageal atresia, tracheoesophageal fistula, renal abnormalities, Turner's syndrome, trisomy 18, and rubella.



Radiographic Features

The plain XR will show a **"single bubble"** with air in a distended stomach. An elongated and narrowed pyloric canal (2-4cm in length) results in a "string" sign when a small amount of barium streaks through the pyloric canal. A transient triangular tent-like cleft/niche in the middle of the pyloric canal is called the "diamond" sign. There is an outpouching along the lesser curvature because of antral peristalsis disruption. Active gastric hyperperistaltic waves is the "caterpillar sign." A mass impression upon the antrum with a streak of barium pointing toward the pyloric canal is known as "antral beaking." Indentation of the base of the bulb (occurring in 50%) is called the **Kirklin sign** or **"mushroom" sign**. There is gastric distension with fluid and/or air.



"Single Bubble" sign of dilated stomach.



Upper GI study with barium demonstrating the "**mushroom**" sign.

Sonographic Features

- Hypoechoic ring of hypertrophic pyloric muscle around echogenic mucosa centrally on cross section
- Indentation of muscle mass on fluid-filled antrum on longitudinal section
- Pyloric length (mm) >14mm
- Pyloric muscle wall thickness > 4mm - measured from outer wall to mucosa
- Exaggerated peristaltic waves
- Delayed or no gastric emptying of fluid into duodenum



Thick pyloric muscle

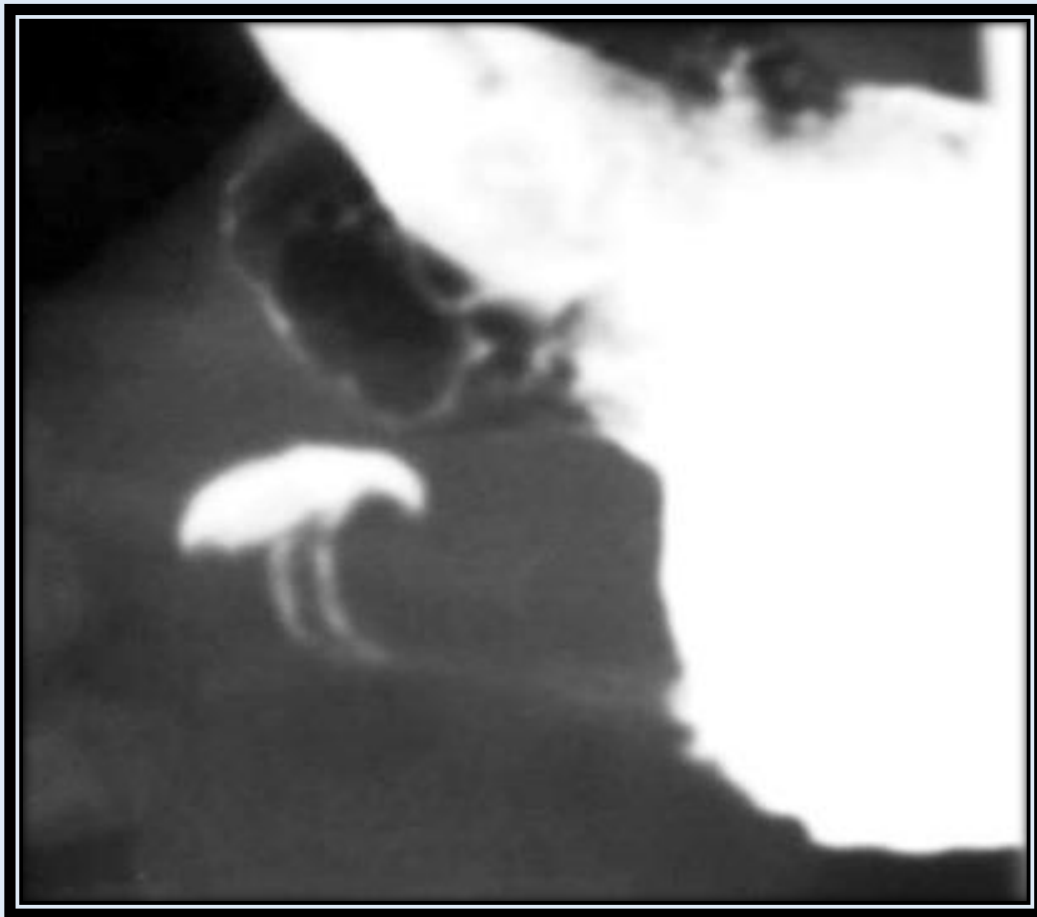


Elongated pyloric muscle

Quiz - Upper GI

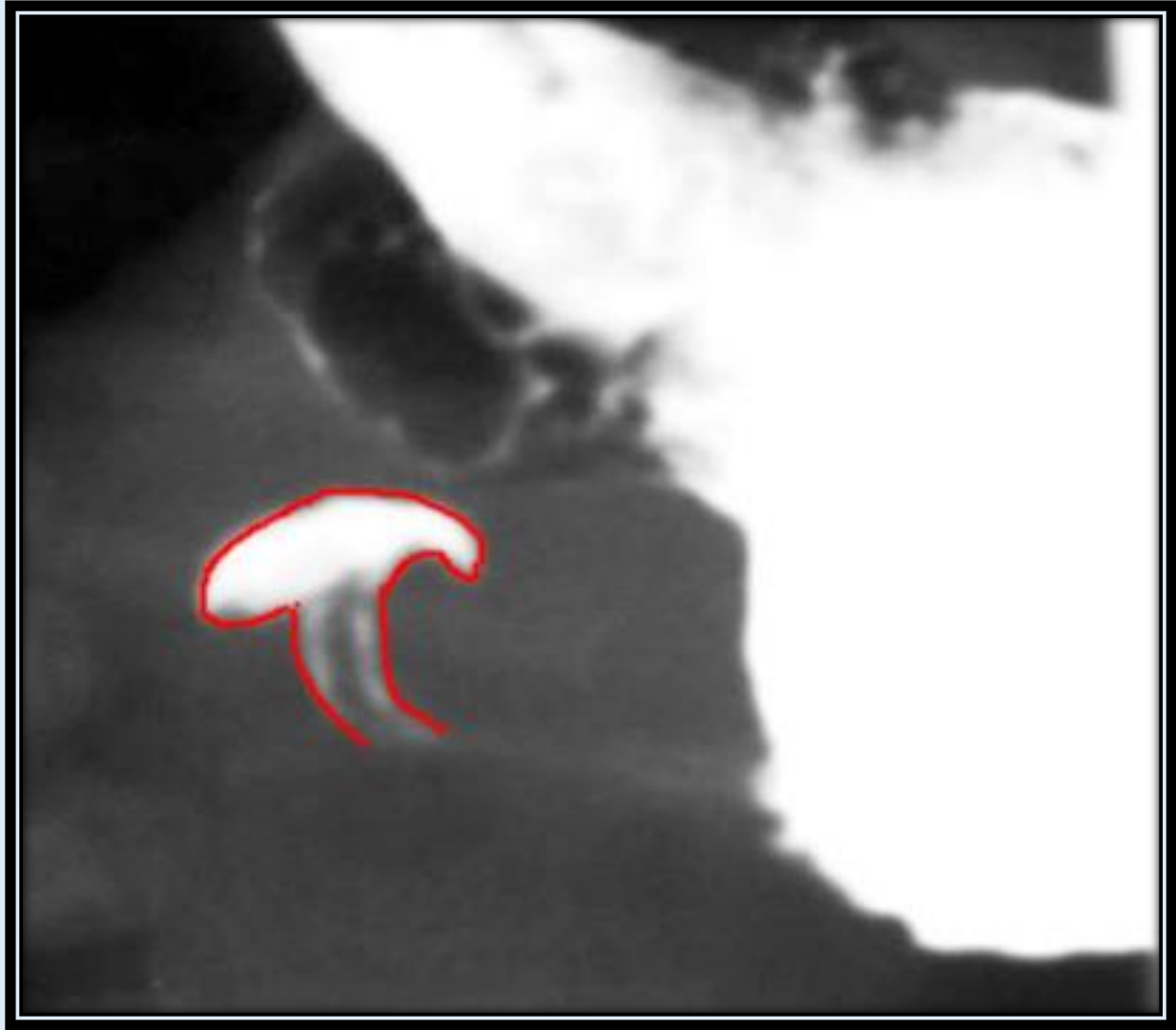
1. Which of the following is an associated abnormality with Hypertrophic Pyloric Stenosis?
 - A. Cystic Fibrosis
 - B. Turner's Syndrome
 - C. Down's Syndrome
2. Which of the following would you expect to see on an ultrasound of a patient with pyloric thickening?
 - A. Exaggerated peristaltic waves
 - B. Diminished peristaltic waves
 - C. Increased gastric emptying
 - D. Shortened pyloric muscle
3. What is the most likely diagnosis?

Can you identify the "mushroom" sign?



Answers

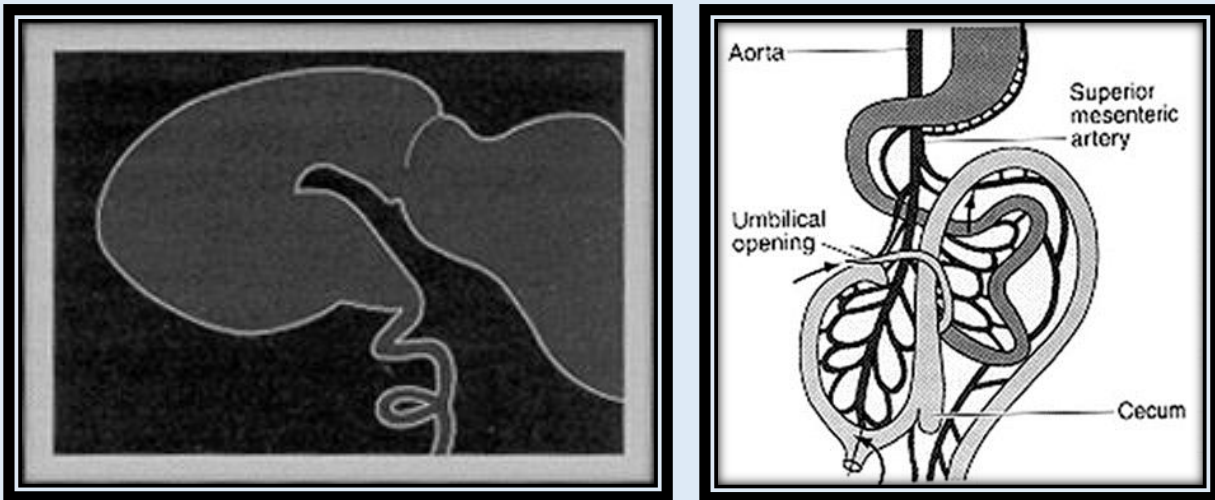
1. Turner's Syndrome
2. Exaggerated peristaltic waves
3. Upper GI study demonstrating hypertrophic pyloric stenosis.



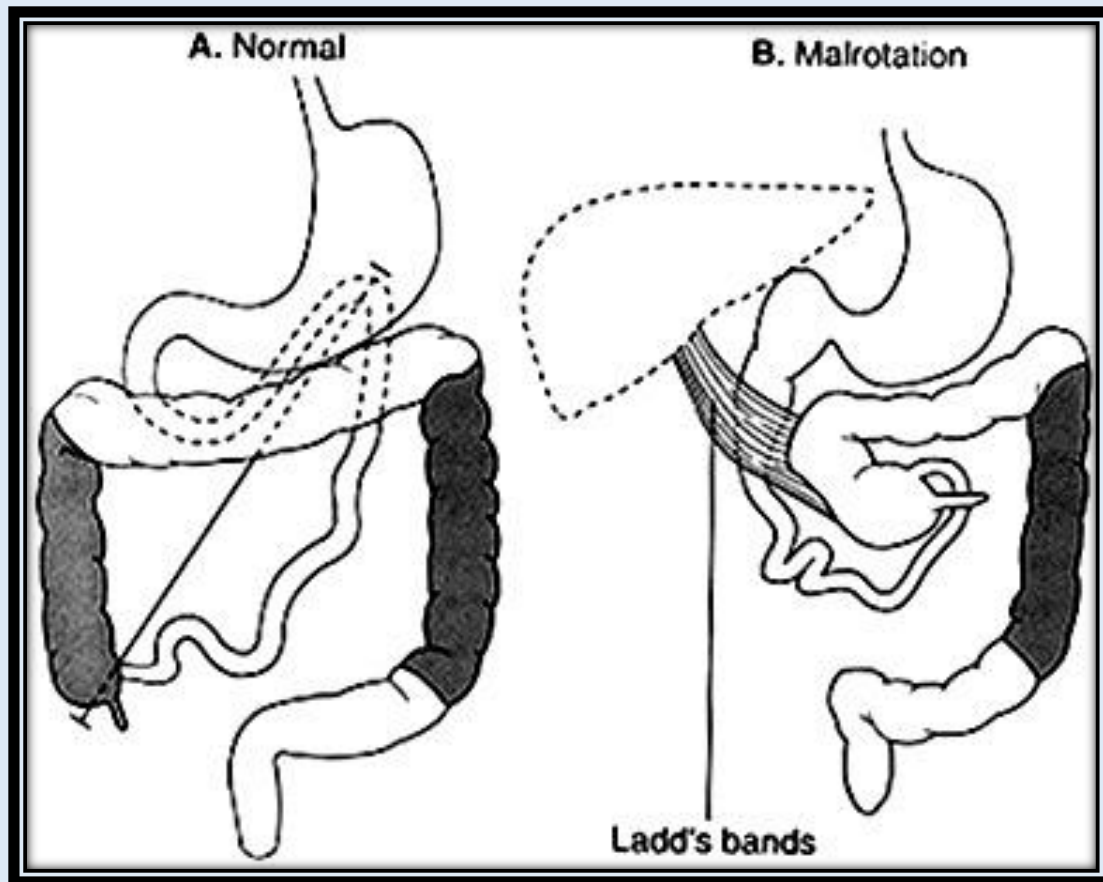
The **"mushroom" or Kirklin sign** (outlined in red) is indicative of indentation of the base of the bulb

Malrotation

Malrotation is the failure of the normal embryonic rotation of the bowel, which results in suspension of the small bowel on a narrow vascular pedicle. The duodenal-jejunal junction does not reach its expected location to the left of the spine at the level of the duodenal bulb. Malposition of the cecum may result in its location in the left side of the abdomen. Complications include obstruction and midgut volvulus. Most present at early age with bilious vomiting, but symptoms can occur at any age. Midgut volvulus is a surgical emergency, because it can lead to bowel necrosis. Ladd Bands are dense peritoneal bands, which cross the duodenum from the malpositioned cecum to the hilum of the liver. They may cause partial obstruction.

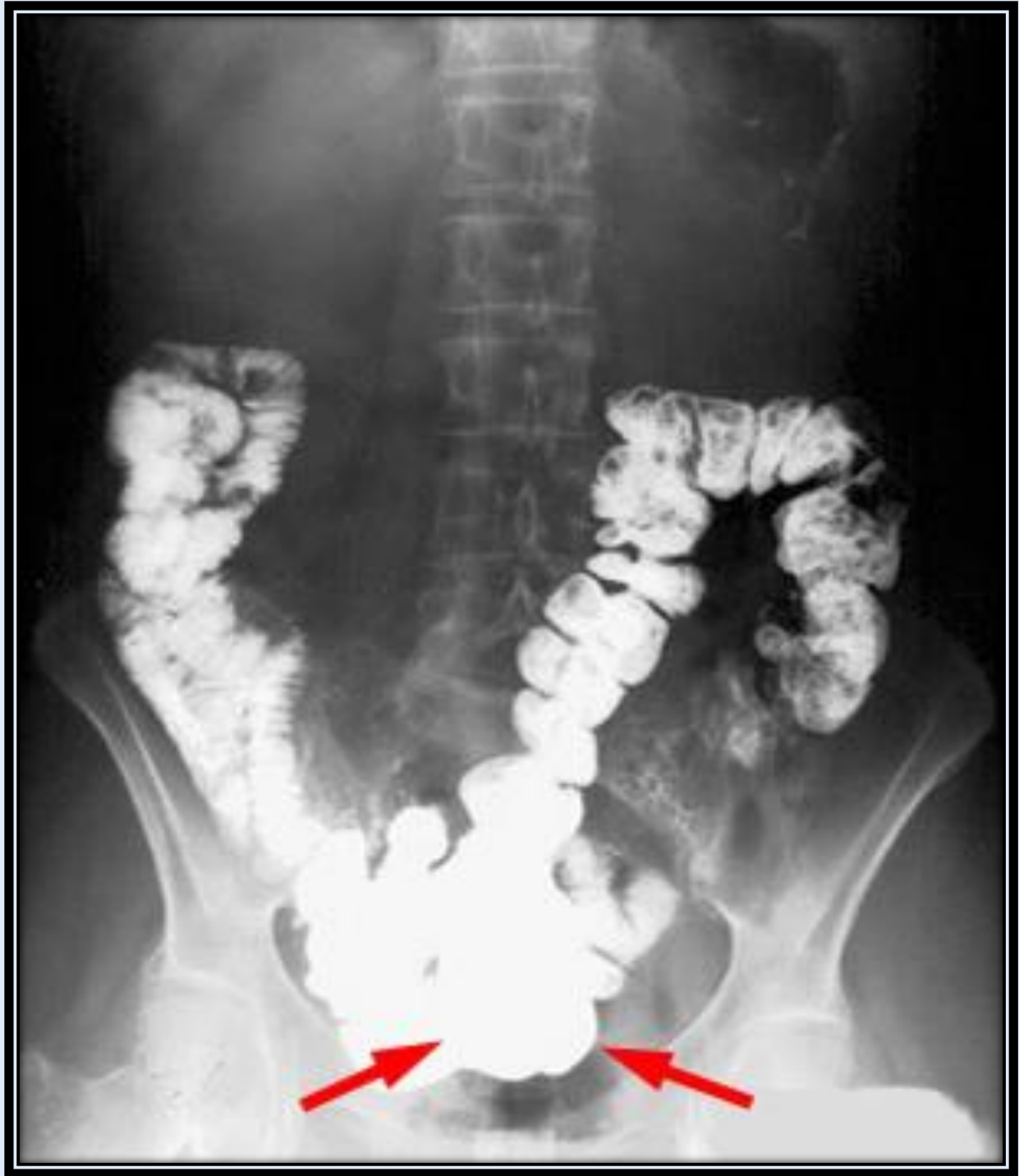


Rotation of the bowel



Normal position and malposition of the bowel

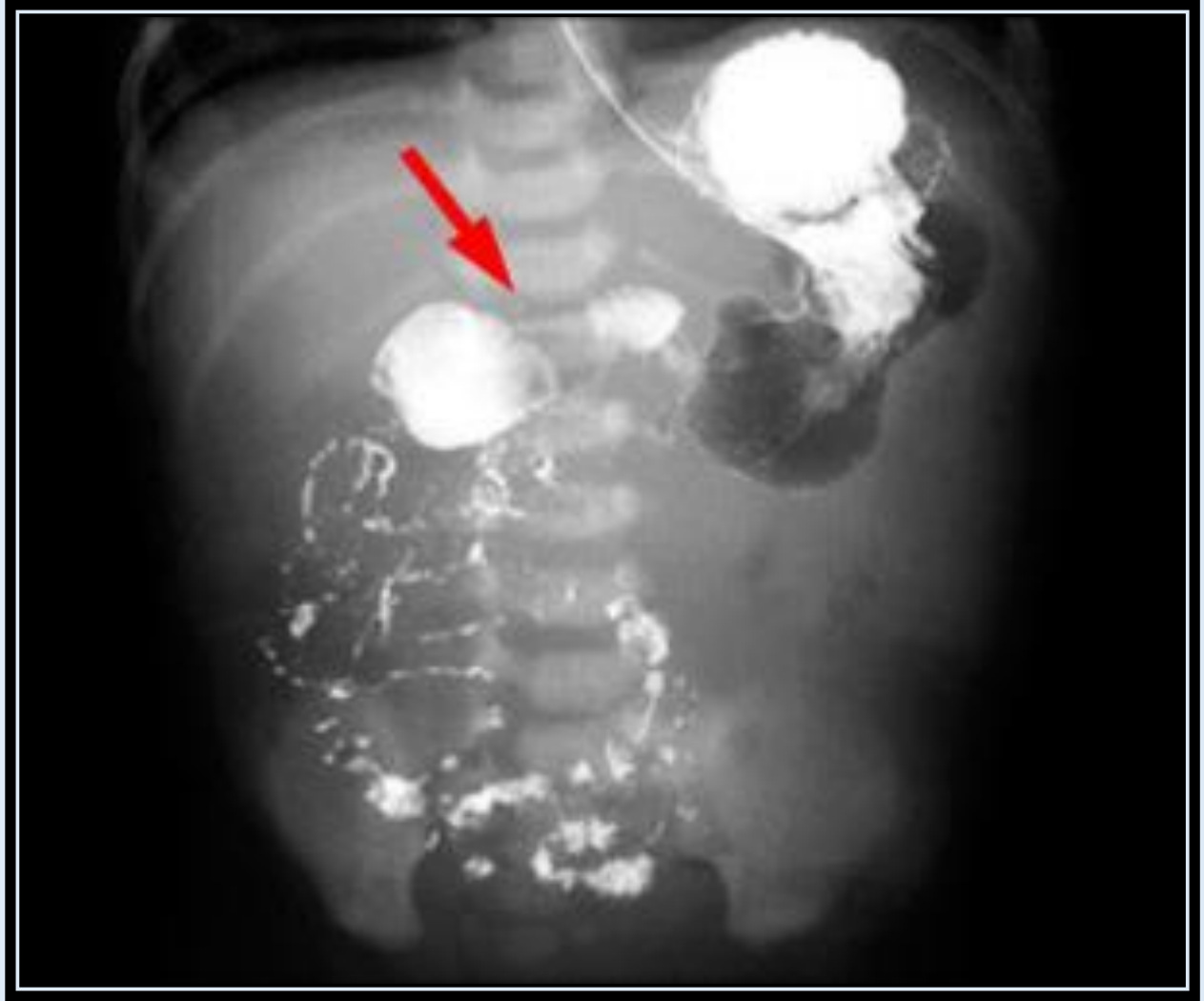
When suspecting malrotation, an upper GI series would best show the **abnormal position of the ligament of Treitz**.



Cecum is in an abnormal location in the mid pelvis



The duodenal-jejunal junction is to the right of the spine, and most of the small bowel is on the right side of the abdomen



This shows **Ladd Bands** resulting in a distended stomach with a small amount of distal gas.

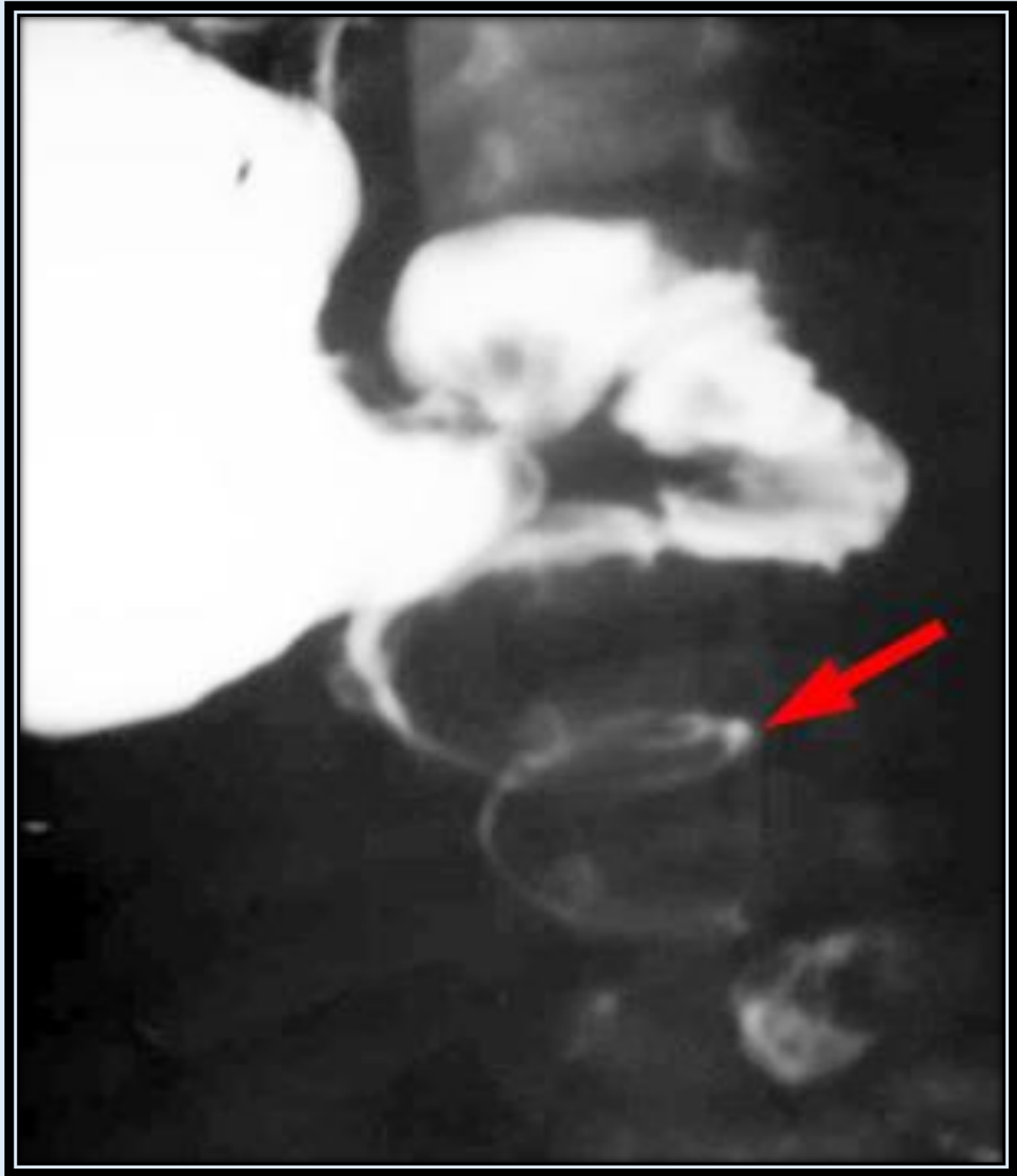
Midgut Volvulus

A midgut volvulus is a twisting of the small intestine around its vascular pedicle due to malrotation. The abnormal positioning of the duodenojejunal and ileocecal junctions results in a shortening of the normally broad based mesenteric attachment.

Patients usually present within the first month of life with bilious vomiting, abdominal distension, and shock. Associated disorders include duodenal atresia (20%), duodenal diaphragm, duodenal stenosis and annular pancreas. Complications include intestinal ischemia and necrosis in the distribution of the superior mesenteric artery. Therefore, malrotation with midgut volvulus is a surgical emergency.

Radiographic Features

- Dilated air-filled duodenal bubble
- **"Double bubble" sign:** double bubble with a little bit of distal gas
- Gas in bowel loops distal to obstructed duodenum
- Small bowel obstruction
- UGI:
 - duodenojejunal junction lower than duodenal bubble and to the right of expected position;
 - spiral course of midgut loops;
 - duodenal fold thickening;
 - malposition of cecum



Spiral course of small bowel

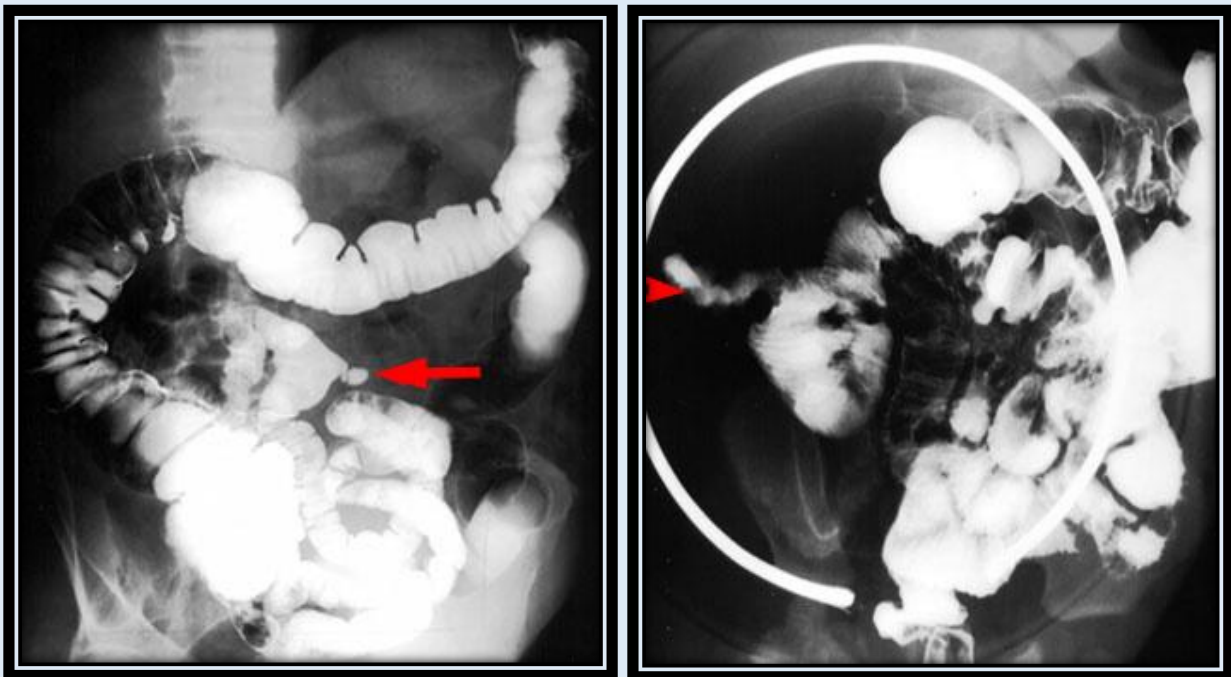
Meckel's Diverticulum

In a Meckel's diverticulum, there is a persistence of the omphalomesenteric duct. The incidence is 2-3% of the population, which makes it the most common anomaly of the gastrointestinal tract. The majority of patients will be under the age of ten, with a male to female ratio of 3:1. It is normally located within the last 6 feet of ileum with 94% of cases on the antimesenteric border.

Rule of 2's

- 1) 2% of the population
- 2) 2% of those with the diverticulum will become symptomatic
- 3) symptomatic usually before age 2
- 4) located within 2 feet of ileocecal valve
- 5) length of 2 inches

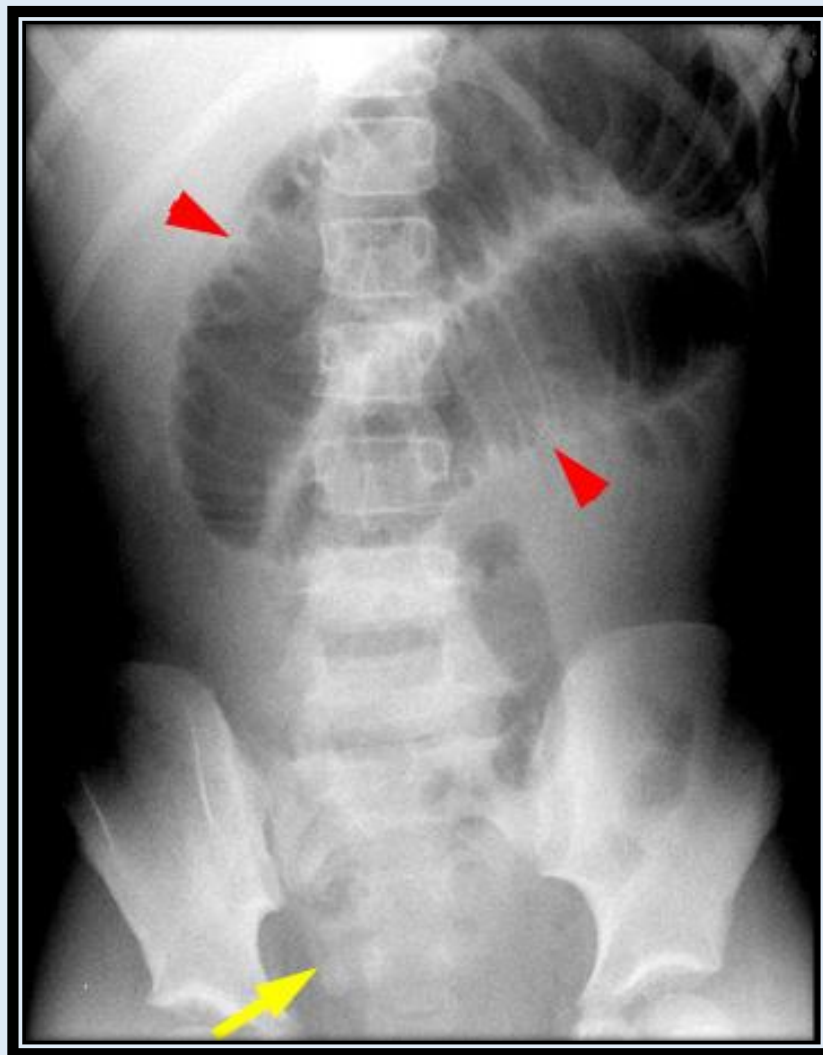
Patients present with bleeding because of ectopic gastric mucosa, focal inflammation, perforation, or intussusception. Nuclear scintigraphy is most often used for imaging.



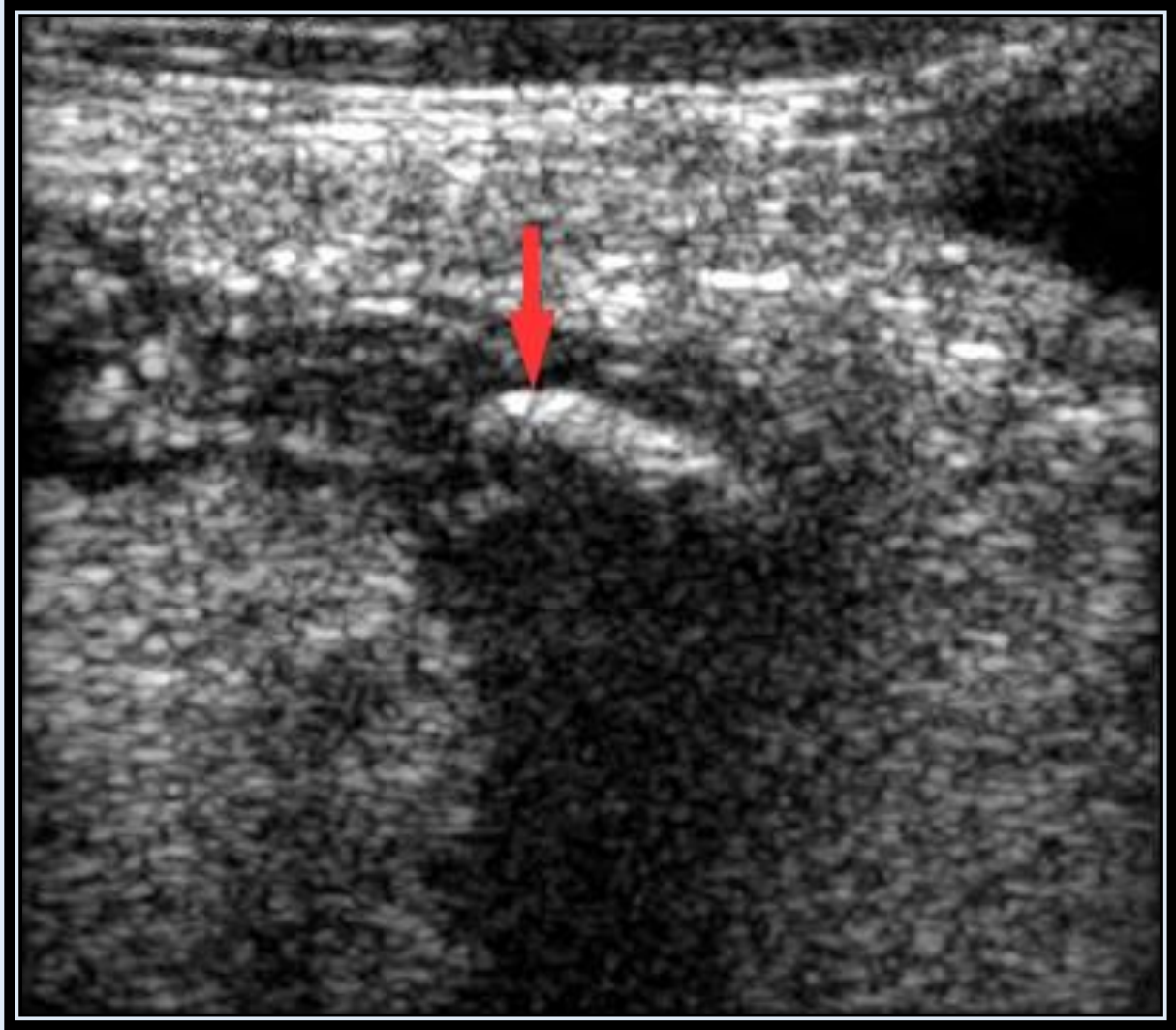
Appendicitis

Appendicitis is the obstruction of the appendiceal lumen resulting in distention of the appendix, superimposed infection, ischemia, and eventually perforation. The incidence is 7-12% of the Western world population, occurring in all ages. Symptoms include fever (56%), nausea and vomiting (40%), RLQ pain - **McBurney sign** (72%), and leukocytosis (88%). In 20-30% of patients, however, the classic signs and symptoms are not present. Perforation is a serious complication. Surgical removal of the appendix is the treatment.

Radiographic Features



Plain film XR demonstrates a **small bowel obstruction** with an **appendicolith** faintly visualized in the RLQ.



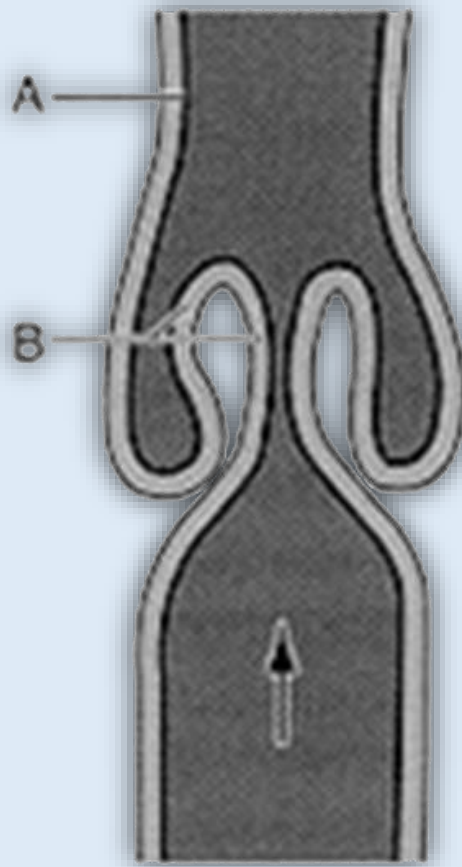
US confirms a **dilated appendix** with the **calcified appendicolith**



CT confirms the **calcified appendicolith** and findings of **appendicitis**

Intussusception

Intussusception is the telescoping of one portion of the bowel into another. For example, the terminal ileum could invaginate into the colon. Idiopathic incidences may be seen following viral illness with hypertrophy of Peyer's patches in the terminal ileum. Age of presentation is usually 3 months to 24 months. Pathologic intussusception is associated with a lead point such as a tumor, inspissated feces (cystic fibrosis) or lymphoma, often in older child greater than age 2. Symptoms include crampy abdominal pain, bloody stools, and vomiting. Treatment is fluoroscopically guided reduction with air or fluid enema or surgery if unreducible. At our institution an air enema is first performed followed by surgery if this method is unsuccessful.



Radiographic Features



Soft-tissue mass (intussusceptum outlined by barium in hepatic flexure)

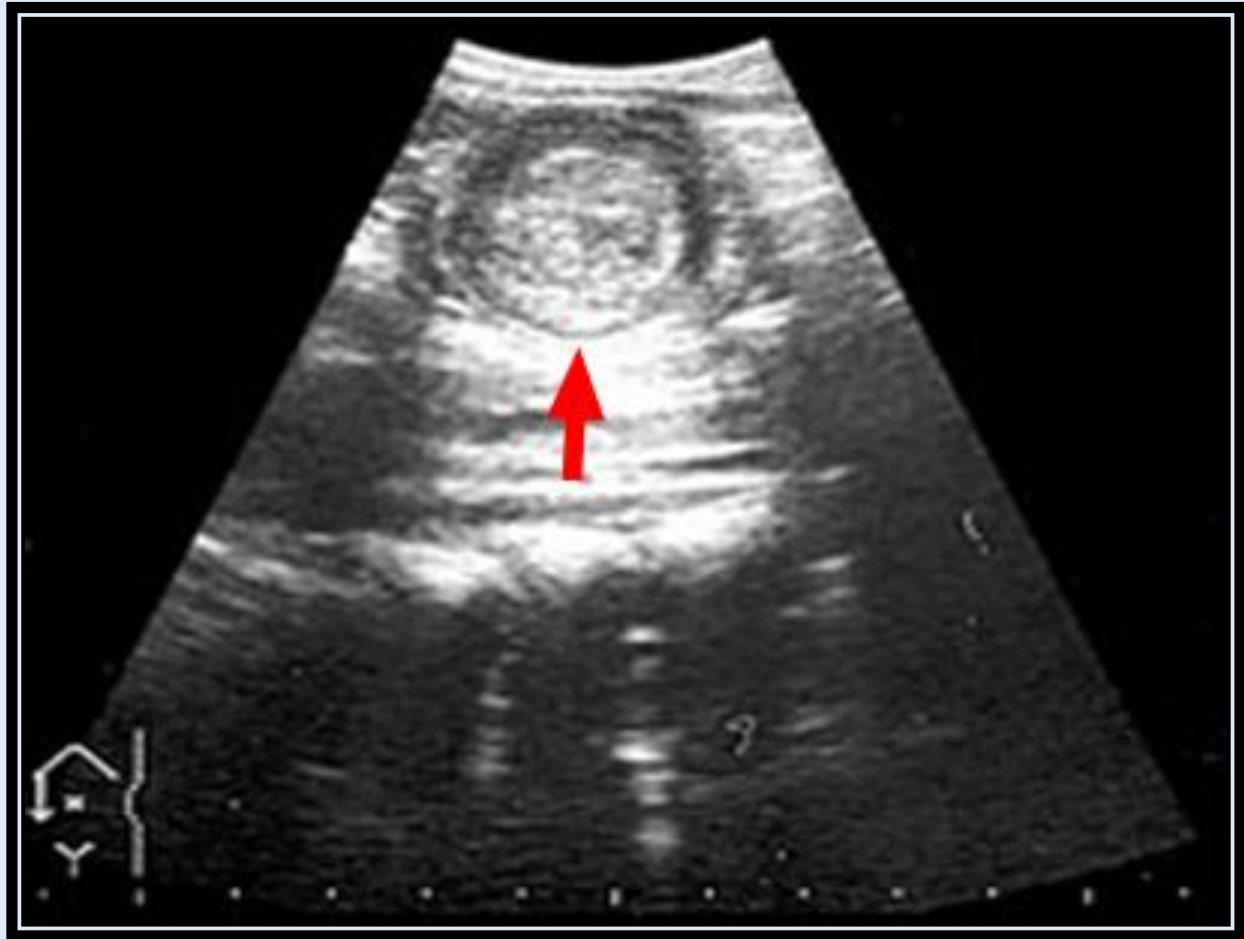


Soft-tissue mass (intussusceptum outlined by barium reduced to ileocecal valve)

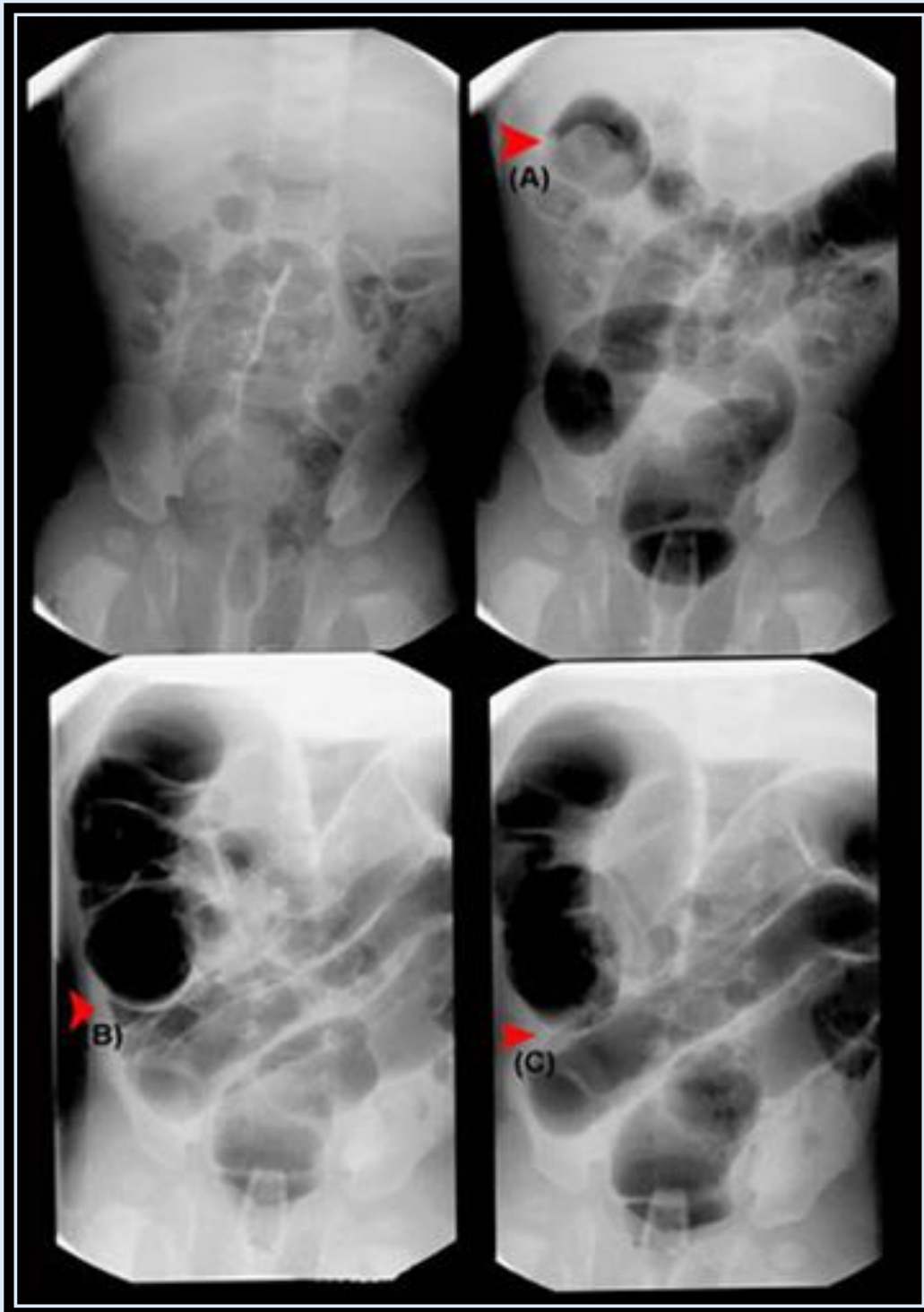


Complete reduction with reflux of contrast into distal small bowel

Ultrasound can be used to perform the initial study in children with suspected intussusception. One important radiographic finding is the "pseudo-kidney" sign. These alternating rings of hyper- and hypo-echogenicity indicate the telescoped bowel.



"Pseudo-Kidney" Sign



Air enema

- Pre-reduction scout film
- Demonstration of intussusception in hepatic flexure (A)
- Reduced to ileocecal valve (B)
- Completely reduced with air refluxed into small bowel (C)

Colonic Atresia

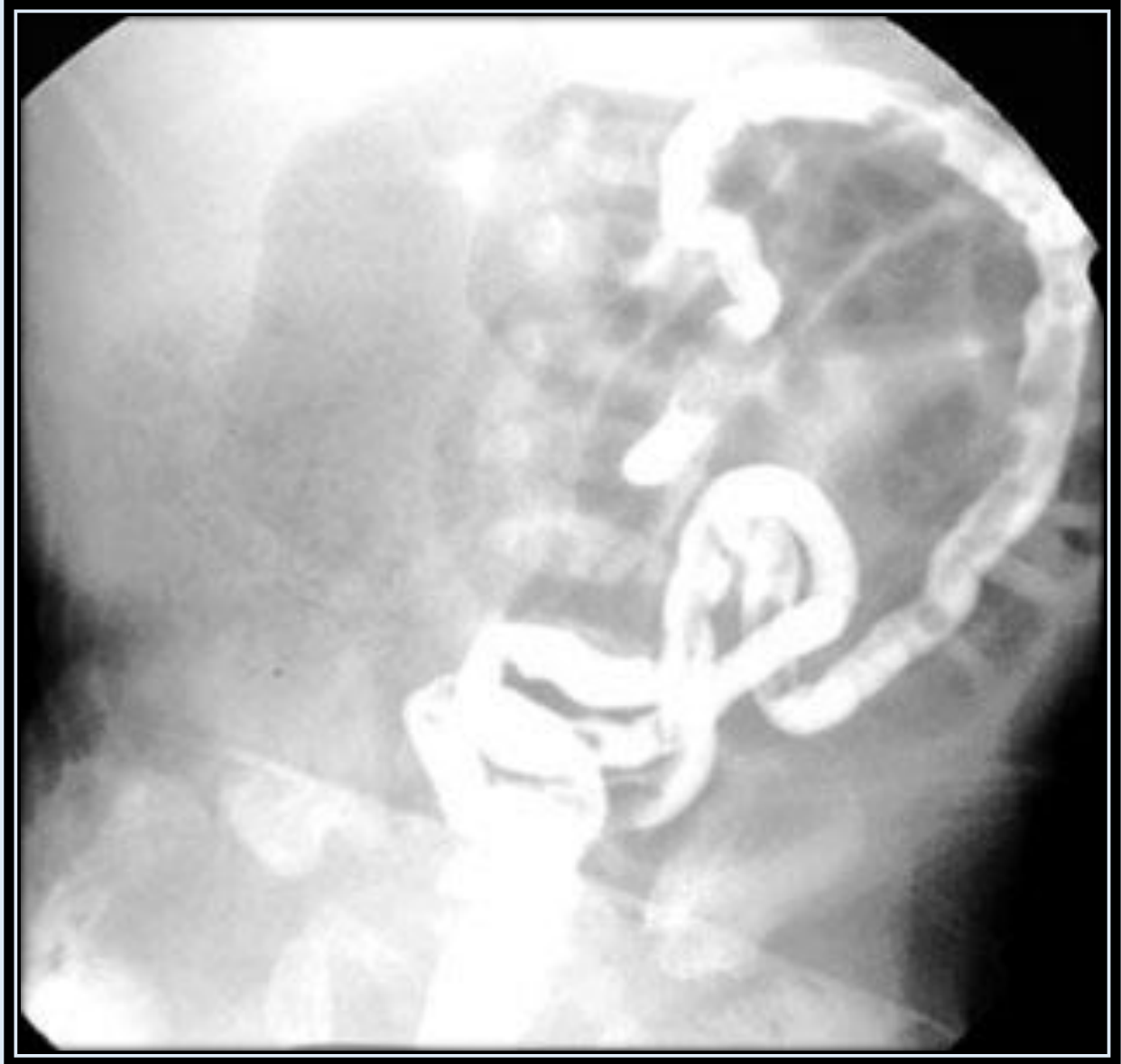
- Rare; likely secondary to in utero ischemic event
- Treatment: surgical

Radiographic features

- Abdominal film: distal obstruction often with "frothy" appearance of air mixed with meconium in RLQ
- Enema: small caliber distal unused colon; no filling proximal to atretic segment



Multiple dilated loops of bowel with frothy appearance in RLQ



Microcolon with abrupt cutoff in mid-transverse colon

Quiz - Lower GI

Q_1: Which of the following may lead to bowel necrosis?

- A. Midgut Volvulus
- B. Colonic Atresia
- C. Meckel's Diverticulum
- D. Hirschsprung's Disease

Q_2: Which of the following is NOT part of the Rule of 2's for Meckel's Diverticulum?

- A. Length of 2 inches
- B. 2 percent of the population
- C. Located within 2 feet of the ileocecal valve
- D. Usually symptomatic before the age of 2
- E. All of the above are part of the Rule of 2's

Q_3: An abdominal film may appear normal in a patient with intussusception.

- A. True
- B. False

Q_4: Appendicitis presents with which of the following?

- A. Laminated, calcified appendicolith in the RLQ
- B. Hypertrophy of Peyer's patches in the terminal ileum
- C. Small bowel obstruction pattern
- D. All of the above are correct

Answers

Q_1: Midgut Volvulus

Q_2: Located within 2 feet of the ileocecal valve

Q_3: True

Q_4: All of the above are correct

Biliary Atresia

- Congenital obstruction of biliary system, intrahepatic bile duct proliferation and focal/total absence of the extrahepatic bile ducts
- Complication: Cirrhosis (early onset) and Jaundice
- Associations: abdominal heterotaxia syndromes, polysplenia, trisomy 18
- Treatment: surgery before three months of age, Kasai Portoenterostomy

Radiographic Features

- Ultrasound: absence of gallbladder is suggestive; 20% of patients have a small or normal gallbladder. Normal hepatic parenchyma, normal intrahepatic bile ducts
 - Hepatobiliary scintigraphy: normal radiotracer uptake by liver, no excretion into GI tract
-

Neonatal Hepatitis

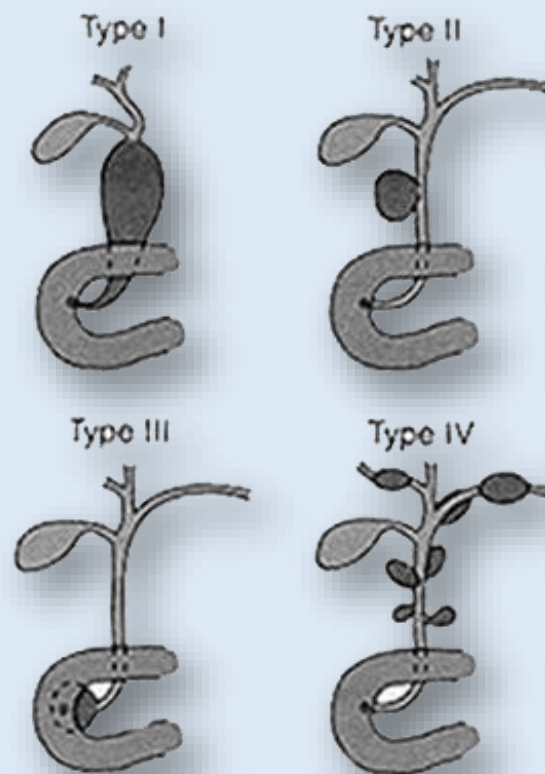
Inflammation of neonatal liver

Radiographic Features

- Normal/decreased hepatic tracer accumulation
- Prolonged clearance of tracer from blood pool
- Bowel activity faint/delayed usually by 24 hours
- Gallbladder may not be visualized

Choledochal Cyst

- Jaundice, RUQ pain, palpable mass
- Can present at any age; cause of prolonged jaundice in infancy
- Congenital malformation of biliary duct
- Aberrant insertion of pancreatic duct into the distal bile duct, reflux of pancreatic secretions damages forming bile duct
- Increased risk of malignancy
- Treatment: surgery

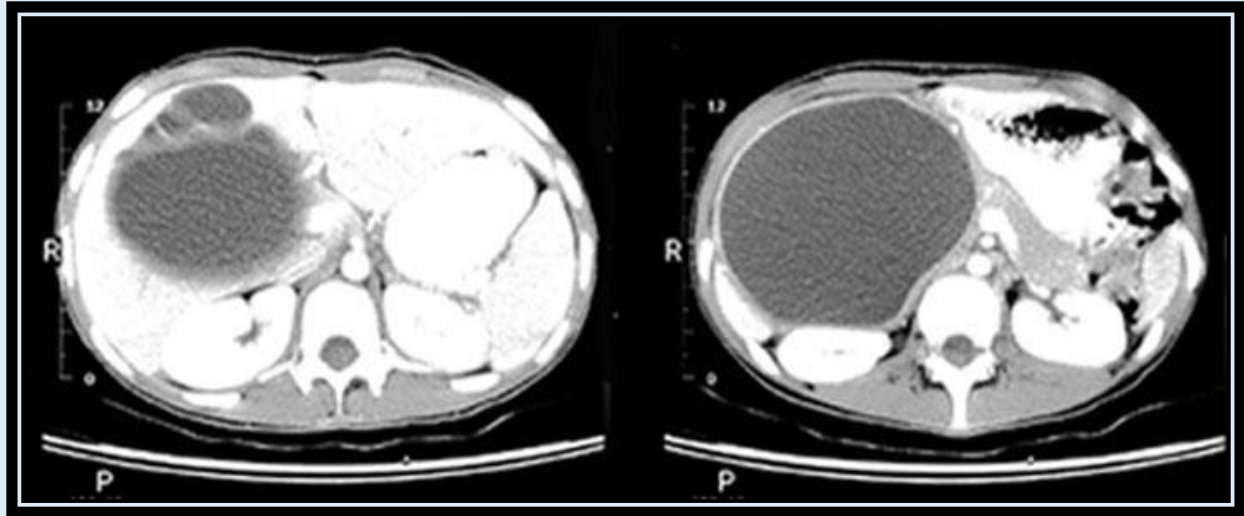


Type I: Dilatation of the extrahepatic duct (80% of cases)

Type II: Eccentric diverticulum

Type III (Choledochocele): Focal dilatation near the sphincter that extends into the duodenal wall

Type IV: Multiple dilatations



Large cystic lesion in location of common bile duct



Nuclear medicine hepatobiliary scan demonstrates cystic dilatation of the common bile duct and dilatation of the intrahepatic bile ducts secondary to obstruction

Quiz - Liver & Biliary

Q_1: Which of the following has prolonged clearance of tracer from the pool of blood?

- A. Choledochal Cyst
- B. Neonatal Hepatitis
- C. Biliary Atresia

Q_2: Choledochal cysts have an increased risk of malignancy.

- A. True
- B. False

Answers

Q_1: Neonatal Hepatitis

Q_2: True

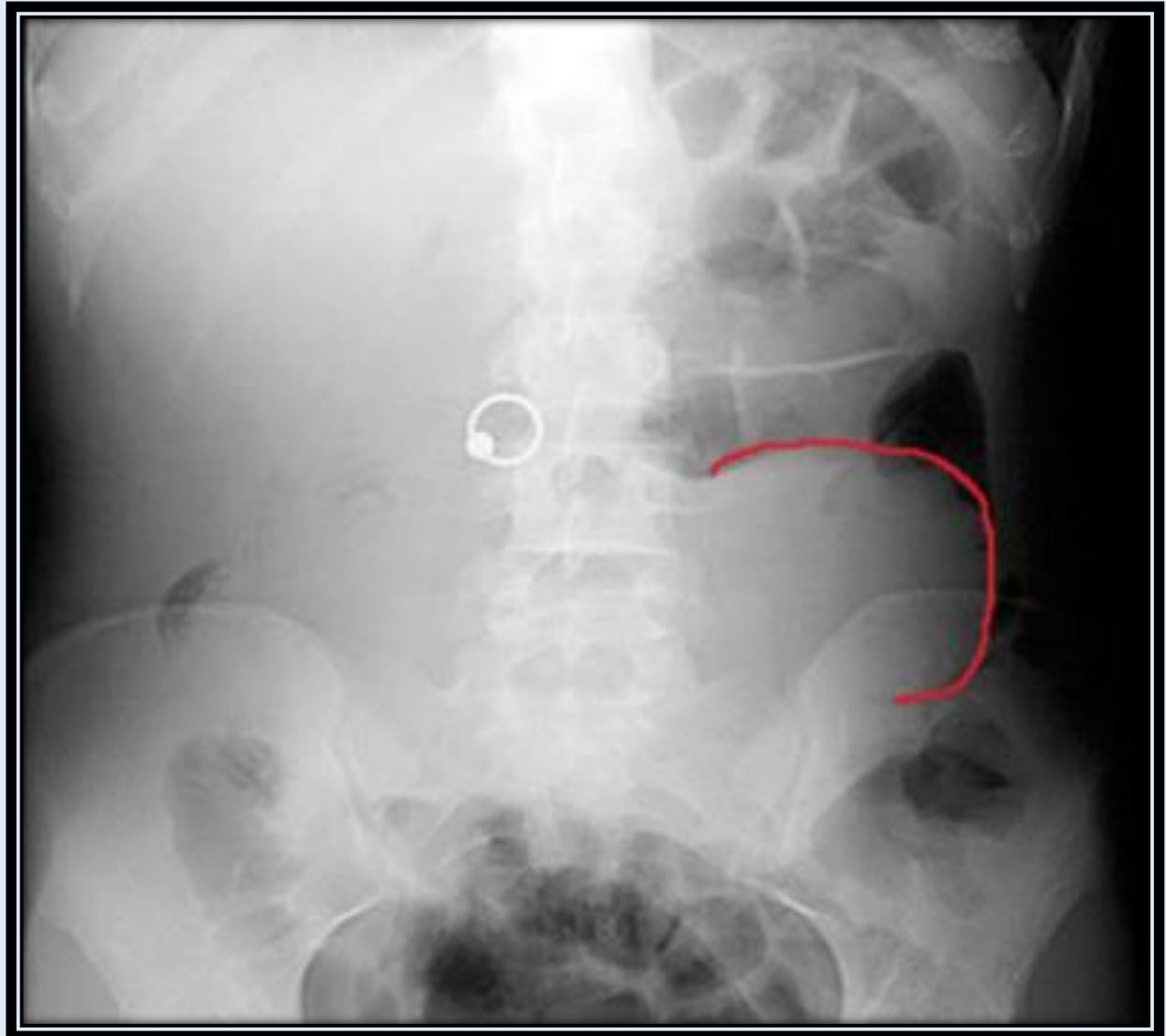
Pediatric Abdominal Radiology Quiz

Q_1: This patient presents with acute abdominal pain. What is the most likely diagnosis?

- A. Intussusception
- B. Appendicitis
- C. Small Bowel Obstruction
- D. Malrotation



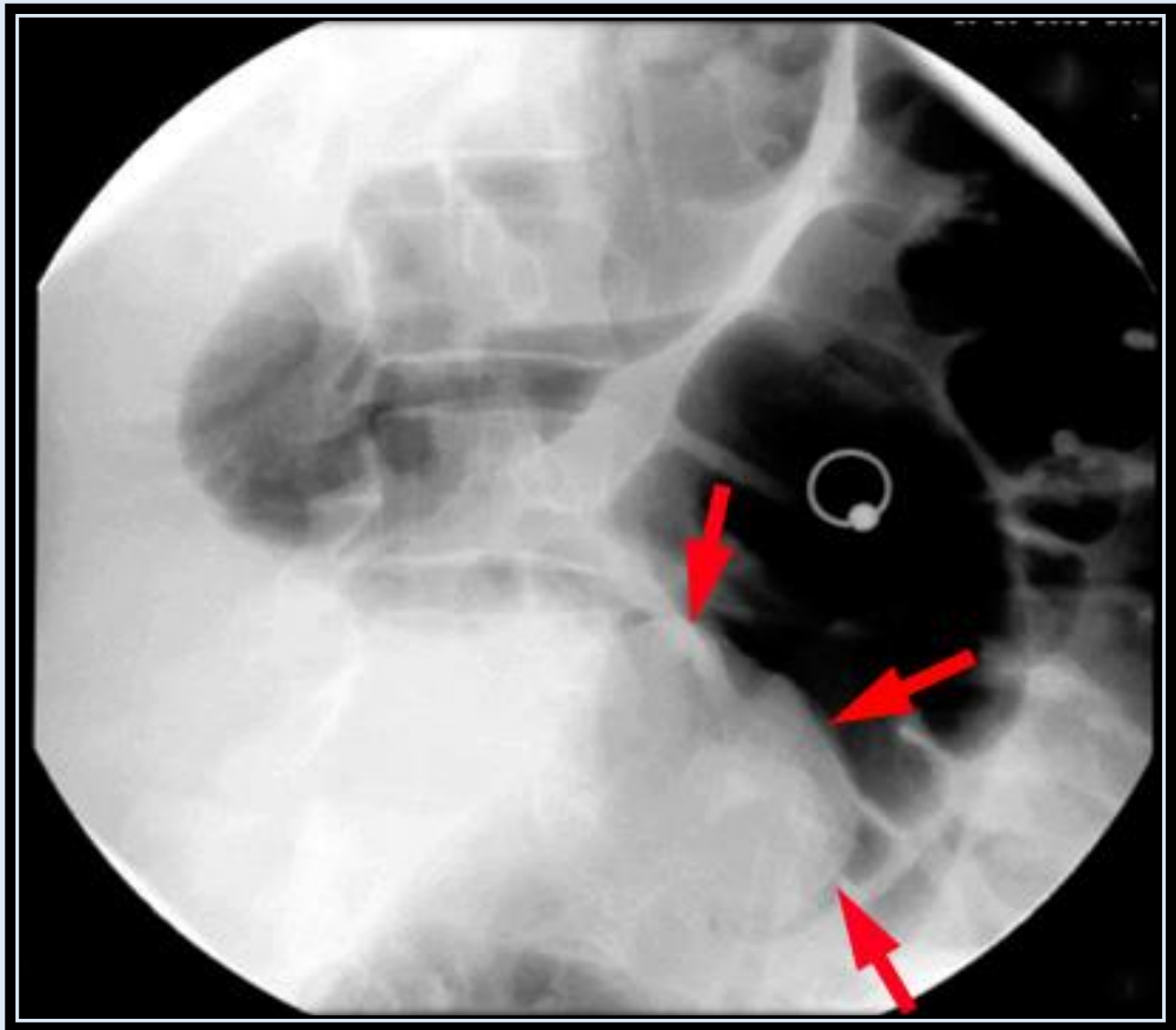
Answer



This patient is suffering from **intussusception**.
Note the intussusceptum, or soft tissue mass of proximal bowel, in the left abdomen

What procedure might be helpful in confirming this diagnosis?

Answer



An air reduction picture can confirm this diagnosis since the intussusceptum appears as a mass with air insufflation.

There are two categories of intussusception: idiopathic and pathologic.

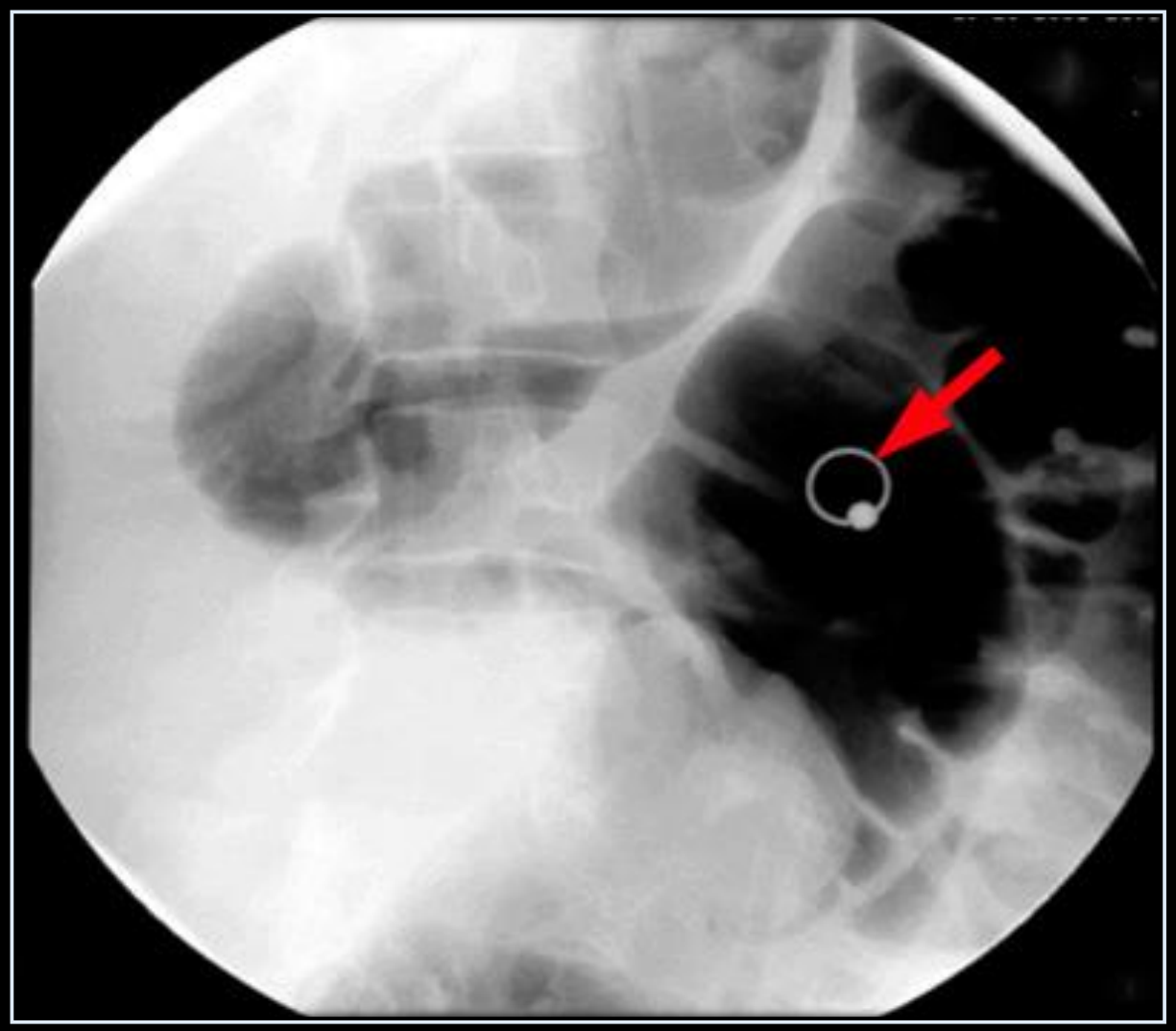
Approximately 90% of pediatric cases are idiopathic and typically occur in patients between 3 months to 1 year. Pathologic intussusception is the result of another disease state (e.g. Meckel diverticulum, Cystic Fibrosis, and Lymphoma), and the age of presentation is determined by the disease state.

Do you think this patient is suffering from idiopathic or pathologic intussusception?

- A. Idiopathic
- B. Pathologic

Answer

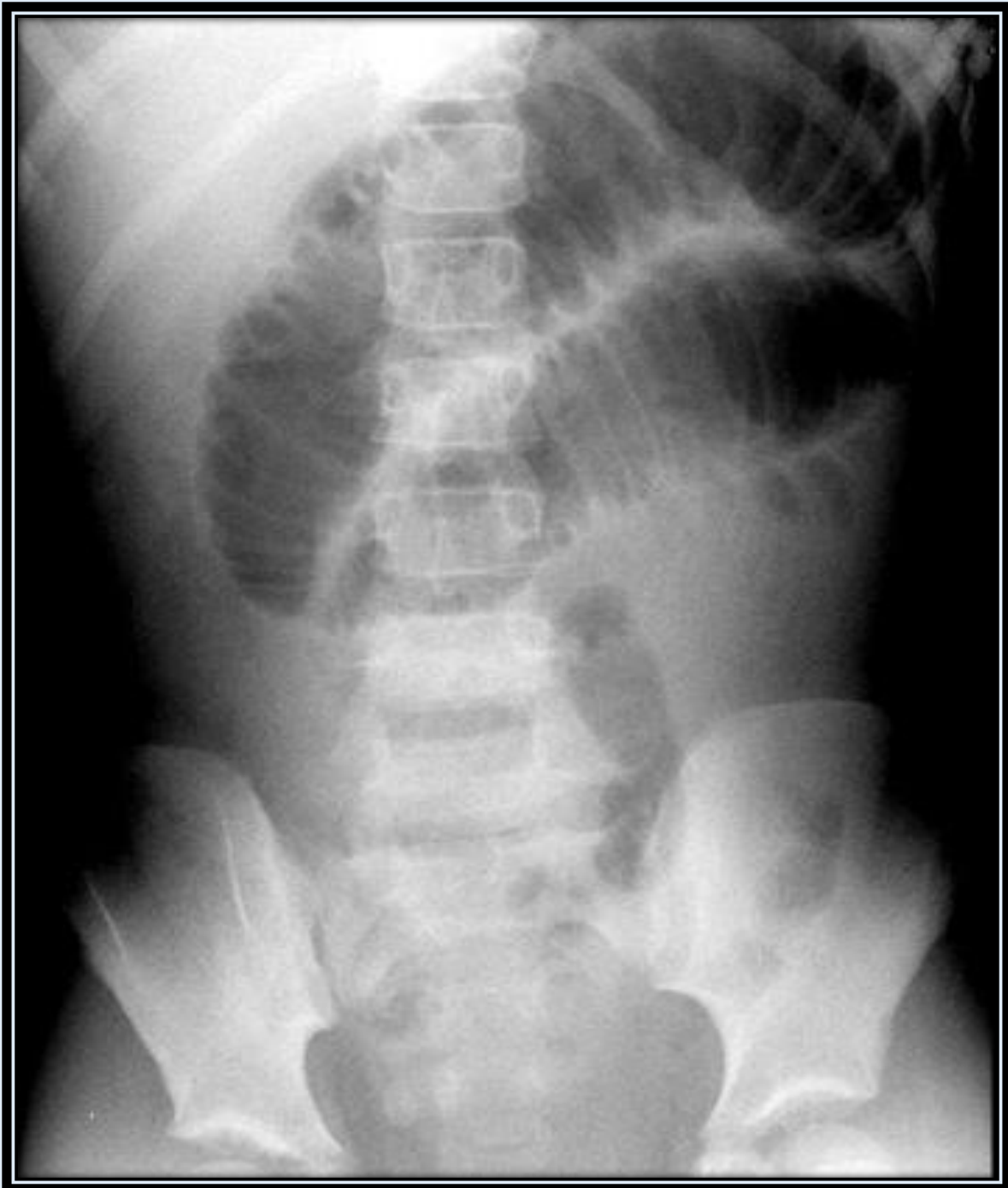
This patient has a pathologic intussusception as a result of Cystic Fibrosis.



One indication that this patient is older than most patients with intussusception is the presence of her belly piercing.

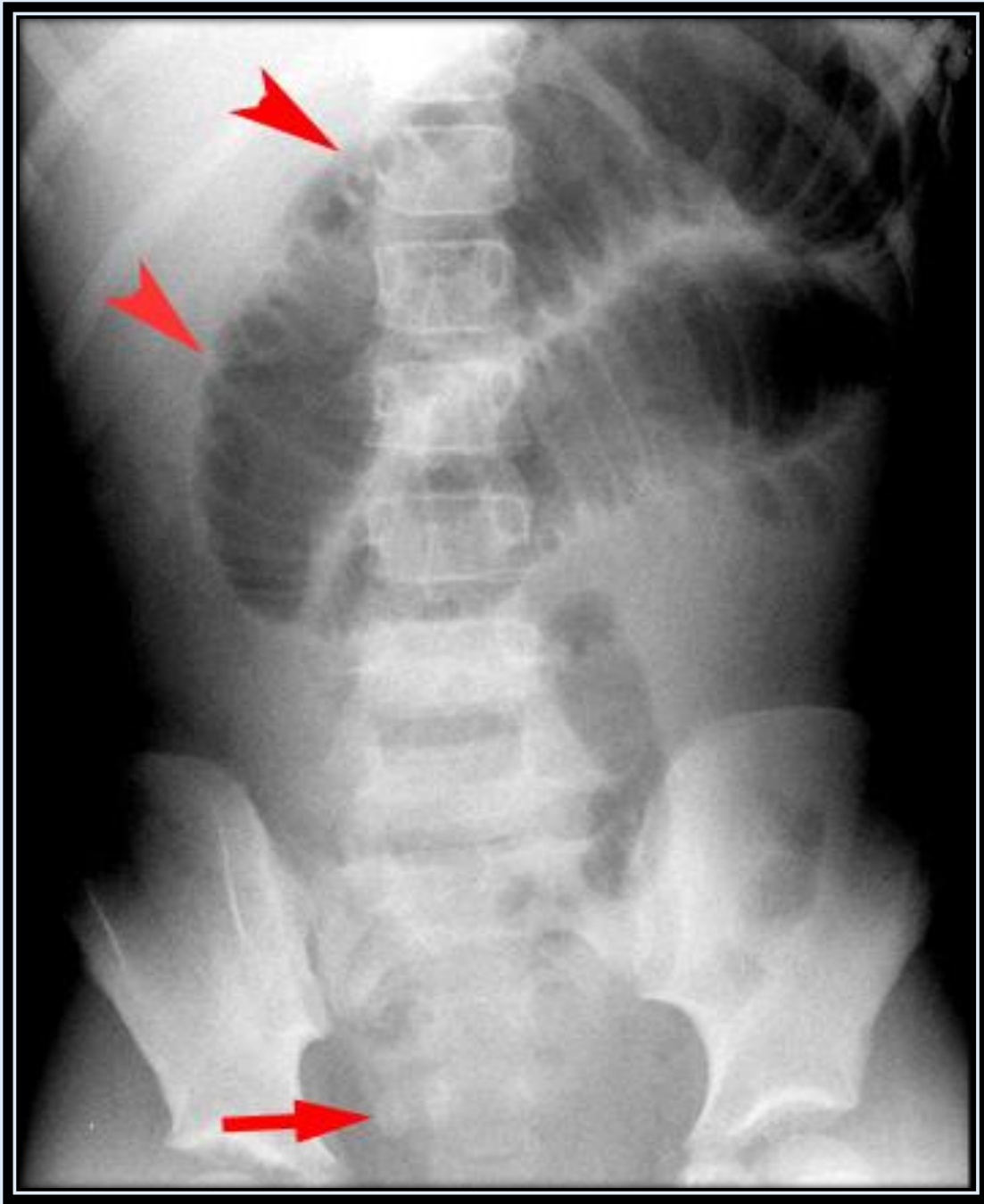
Q_2: What is the most likely diagnosis for this patient?

- A.** Intussusception
- B.** Appendicitis
- C.** Hernia
- D.** Malrotation



Answer

This patient is suffering from **appendicitis**. The supine exam demonstrates multiple dilated small bowel loops (arrowheads) which are consistent with small bowel obstruction. There is a differential for small bowel obstruction, but the etiology for this example can be determined by attention to the right lower quadrant.



What structure is indicated by the arrow?

Answer

The arrow is pointing to an **appendicolith**

The presence of this structure can be confirmed with other radiographic imaging:



Ultrasound showing an appendicolith in the RLQ



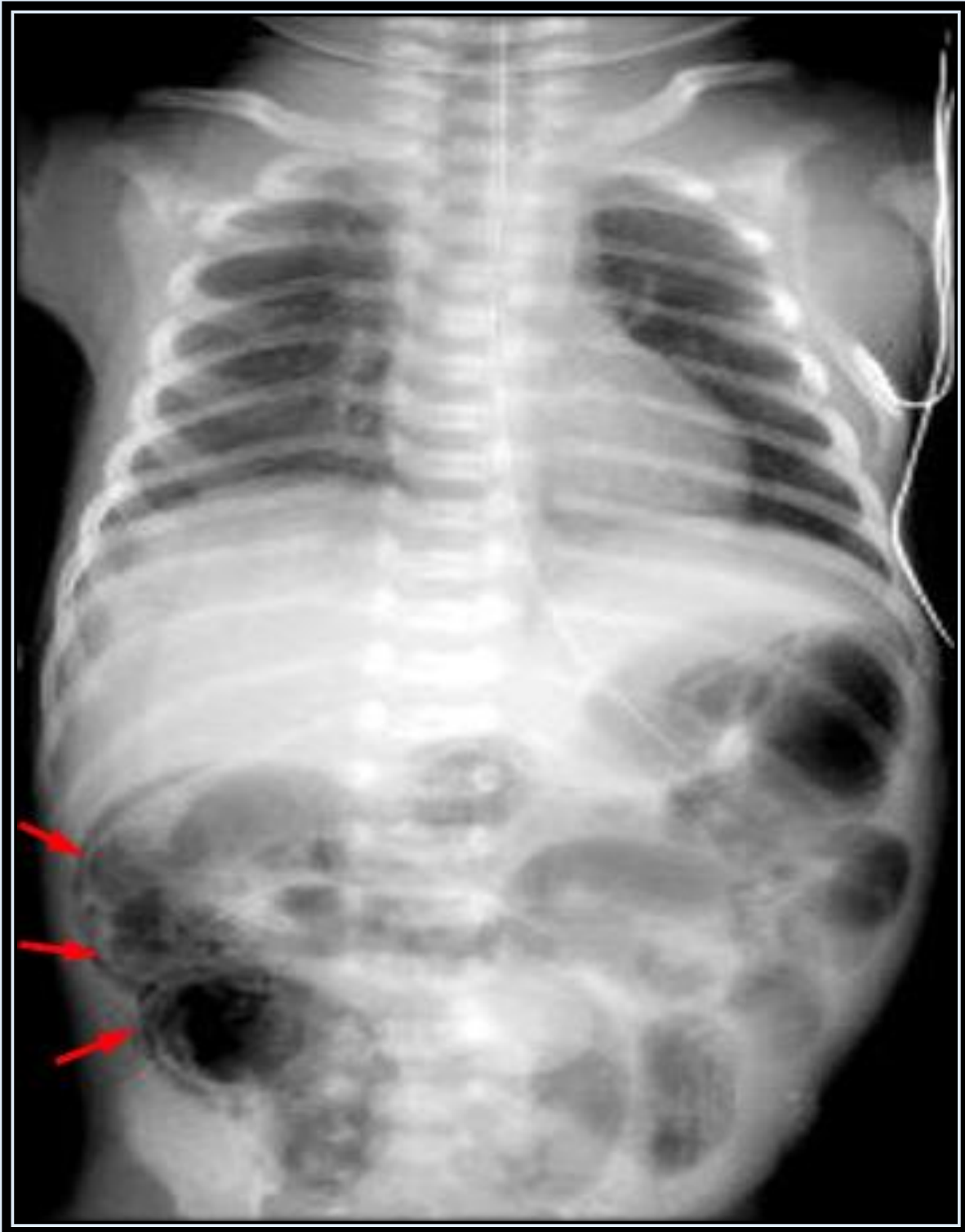
CT showing an appendicolith in the RLQ

Q_3: What is the most likely diagnosis?

- A.** Malrotation
- B.** Meconium Ileus
- C.** Hirschsprung Disease
- D.** Necrotizing Enterocolitis



Answer



This patient is suffering from **Necrotizing Enterocolitis (NEC)** . The presence of multiple bubble-like lucencies in the bowel wall indicates **pneumatosis**, which is diagnostic of NEC.

Which of the following is considered the only finding that is an absolute indication for surgery?

- A. Generalized Sepsis**
- B. Distended Abdomen**
- C. Free Intraperitoneal Air**
- D. Bilious Emesis**

Answer

Free intraperitoneal air generally requires surgical correction more often than does generalized sepsis, distended abdomen or bilious emesis.

Q_4: What is the most likely diagnosis?

- A. Proximal Obstruction
- B. Distal Obstruction
- C. Intussusception
- D. Necrotizing Enterocolitis



What should you do next for this patient with a distal obstruction?

- A. Upper GI
- B. Ultrasound
- C. Barium Enema
- D. CT

Answer

- **Distal Obstruction**
- **Barium Enema**

After looking at the results from the enema, what is your diagnosis?

- A.** Hirschsprung Disease
- B.** Meconium Ileus
- C.** Ileal Atresia
- D.** Small Left Colon Syndrome
- E.** Either Meconium Ileus or Ileal Atresia
- F.** Either Hirschsprung Disease or Small Left Colon Syndrome



Answer

Based on the enema, Meconium Ileus and Ileal Atresia are both in the differential diagnosis, and both are treated by surgery. Ileal atresia was found at surgery.

Pediatric Genitourinary Radiology

Pediatric Genitourinary Radiology

Comprehensive Outline for Pediatric Genitourinary Section

- **Voiding Cystourethrogram**
 - Vesicoureteral Reflux
 - Pathophysiology
 - Evaluation
 - Technique
 - Grading
 - Grading quiz
 - VCUG quiz
- **Cystic Renal Disease**
 - Autosomal recessive polycystic kidney disease
 - Autosomal dominant polycystic kidney disease
- **Congenital Urinary Tract Anomalies**
 - Examples
- **Hydronephrosis**
 - Introduction
 - Ureteropelvic junction obstruction
 - Posterior urethral valves
 - Primary megaureter
 - Ureterocele
 - Multicystic dysplastic kidney
- **Genitourinary tumors**
 - Mesoblastic nephroma
 - Wilms tumor
 - Wilms tumor imaging
 - Neuroblastoma
 - Neuroblastoma imaging
 - Mesoblastic nephroma versus Wilms
 - Wilms versus Neuroblastoma
 - Neonatal Adrenal Hemorrhage
- **Quiz**

Vesicoureteral Reflux

Vesicoureteral reflux is defined as the retrograde passage of urine from the urinary bladder into the ureter and in more severe cases into the proximal renal collecting system. It is a common pediatric genitourinary problem and has significant potential sequelae resulting from recurrent urinary tract infections and subsequent renal damage. Vesicoureteral reflux is present in 0.5 - 1% of asymptomatic children but will be present in 30 - 50% of children with urinary tract infections. Renal scarring is most common in children less than two years of age but new renal scarring is infrequent in children over the age of 5. There is a familial component with an incidence as high as 34% and therefore routine screening should be considered in all siblings. In children with vesicoureteral reflux, the etiology should be determined and appropriate prophylactic antibiotic therapy begun. Most mild cases will resolve by 5-6 years of age although more severe cases may require corrective surgery.

In conclusion, because of the significant risk of renal damage from recurrent UTI's, particularly in children less than 2 years of age, vesicoureteral reflux should be promptly diagnosed and treated effectively to avoid long term renal sequelae.

Pathophysiology:

Most cases of reflux are a primary abnormality due to incompetence of the ureterovesical junction. The ureterovesical junction (UVJ) normally acts as a passive valve mechanism because of the oblique course of the intramural portion of the ureter. There is also a more active component with peristalsis of the longitudinal muscles of the ureter. Reflux results from immaturity or developmental abnormality of the ureterovesical junction. The length of the intramural portion of the ureter may be too short or insert at an abnormal position into the bladder. The normal insertion of the ureter is one quarter of the distance from the bladder base to the bladder dome.

Evaluation

The voiding cystourethrogram (VCUG) is utilized in the detection and grading of vesicoureteral reflux. The VCUG is performed after the diagnosis of a urinary tract infection. Sedation is usually not necessary and can make the study more difficult by inhibiting the voiding reflex. The exam is performed in the radiology fluoroscopy suite, preferably with the ability to record the exam on videotape, as the reflux can be transitory.

A urinary bladder catheter should be placed under sterile conditions. A balloon should not be used as the balloon may inhibit visualization of ureterocele and may alter voiding. At our institution we use a 5 french pediatric feeding tube in the infant/ toddler population and an 8 french pediatric feeding tube in the older population.

Sterile urine collection or post void measurement may be requested by the referring urologist. Because of the radiation to the pelvic region, strict attention must be made to the fluoroscopic technique following the principle of "as low as reasonable" (ALAR) radiation exposure. Most uncomplicated exams should involve less than 10 seconds of fluoroscopy time. We use 30% hypaque, a dilute ionic contrast agent, to visualize the urinary tract. The bladder is filled by gravity at a height of approximately 2-3 feet above the table.

Bladder capacity can be estimated by:

$$(\text{Patient age} + 2) \times 30$$

This works out to be.

- Newborn: 15 cc
- One yr old: 90 cc
- Two yrs old: 120 cc
- Three yrs old: 150 cc
- Four yrs old: 180 cc
- Five yrs old: 210 cc

The standard normal VCUG should consist of **seven films**. A preliminary scout film should always be obtained to document any unusual densities or calcifications so not to confuse these with contrast which will have a similar density. Attention should also be drawn to the renal soft tissue outlines to detect any renal developmental anomalies. The spine should be examined for dysraphism.



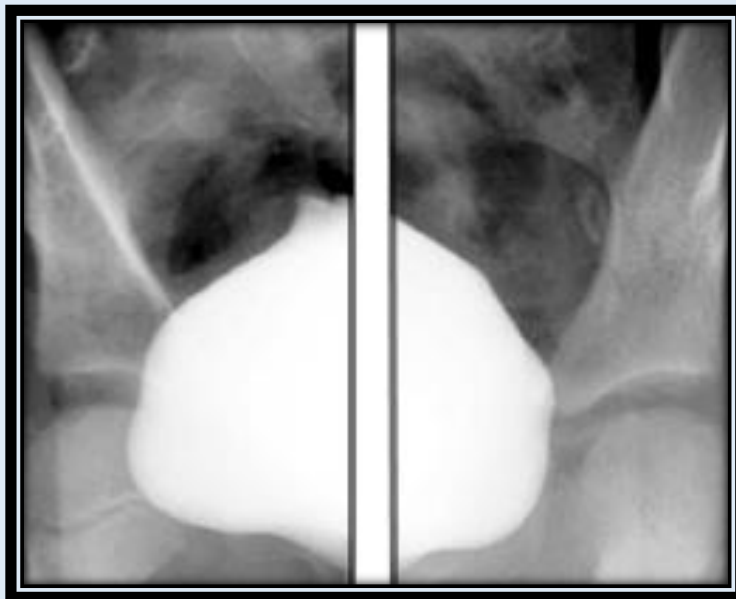
Preliminary Scout VCUG

An "early filling" film should be obtained with the bladder filled to $\frac{1}{3}$ - $\frac{1}{4}$ capacity. This film will allow visualization of a ureterocele which can otherwise be obscured with full distension of the bladder.



Early Filling

When the bladder is nearly filled to capacity, both thirty degree oblique views should be documented. These views allow visualization of the distal ureters as they enter the ureterovesicular junction which, because of their position posterior and lateral, will be obscured on the AP projection.



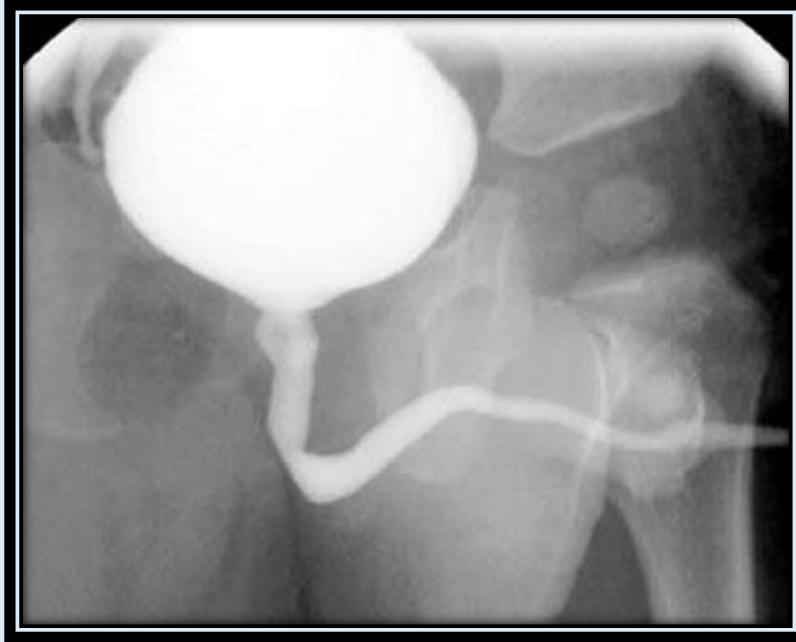
Right and Left Obliques

During the act of voiding the urethra should be documented. In the female this can be accomplished with an AP view to include the lower bladder. In the male the penis should be displaced to one side to allow for full visualization of the urethral anatomy.



Normal Female Bladder and Urethra

Finally, careful attention should be made for the presence of reflux during voiding. Reflux may only occur during the higher bladder pressures of active voiding. A film over the kidneys will allow documentation of the presence or absence of reflux and allow for grading of the severity of the reflux.

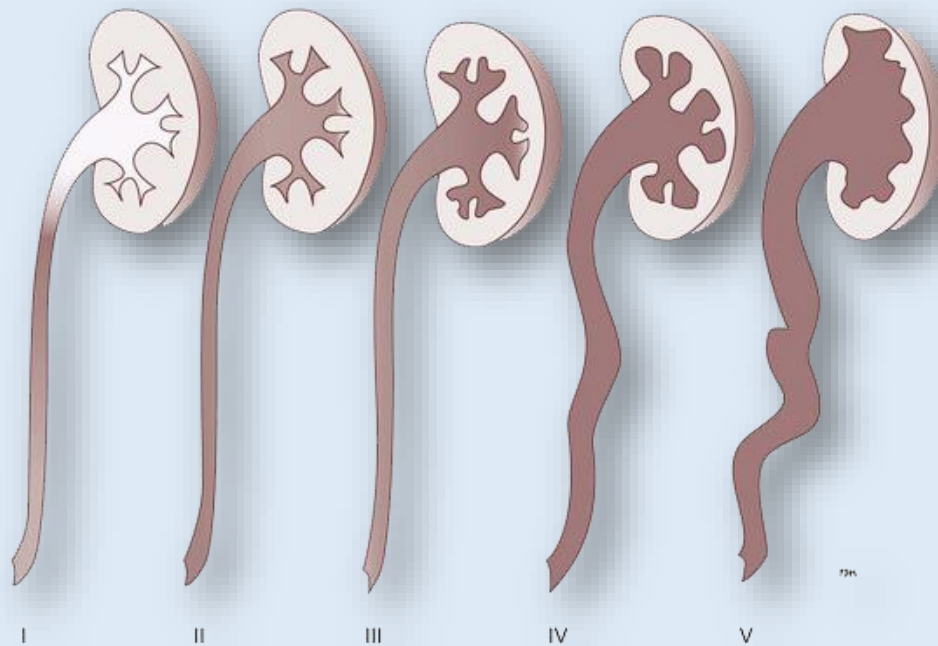


Normal Male Bladder and Urethra



Post void bladder film documenting the degree of post void residual volume

Grading of Vesicoureteral Reflux



Grade 1: reflux into the distal ureter

Grade 2: reflux into the proximal renal collecting system without dilatation

Grade 3: reflux into the renal calices with mild dilatation/tortuosity of the ureter, renal pelvis and calices.

Grade 4: reflux into the renal calices with moderate dilatation/tortuosity of the ureter, renal pelvis and calices with obliteration of the fornices but maintenance of the papillary impressions.

Grade 5: reflux into the renal calices with gross dilatation/tortuosity of the ureter, renal pelvis and calices. The papillary impressions will be lost in the majority of the calices. This type is typically treated with surgery.

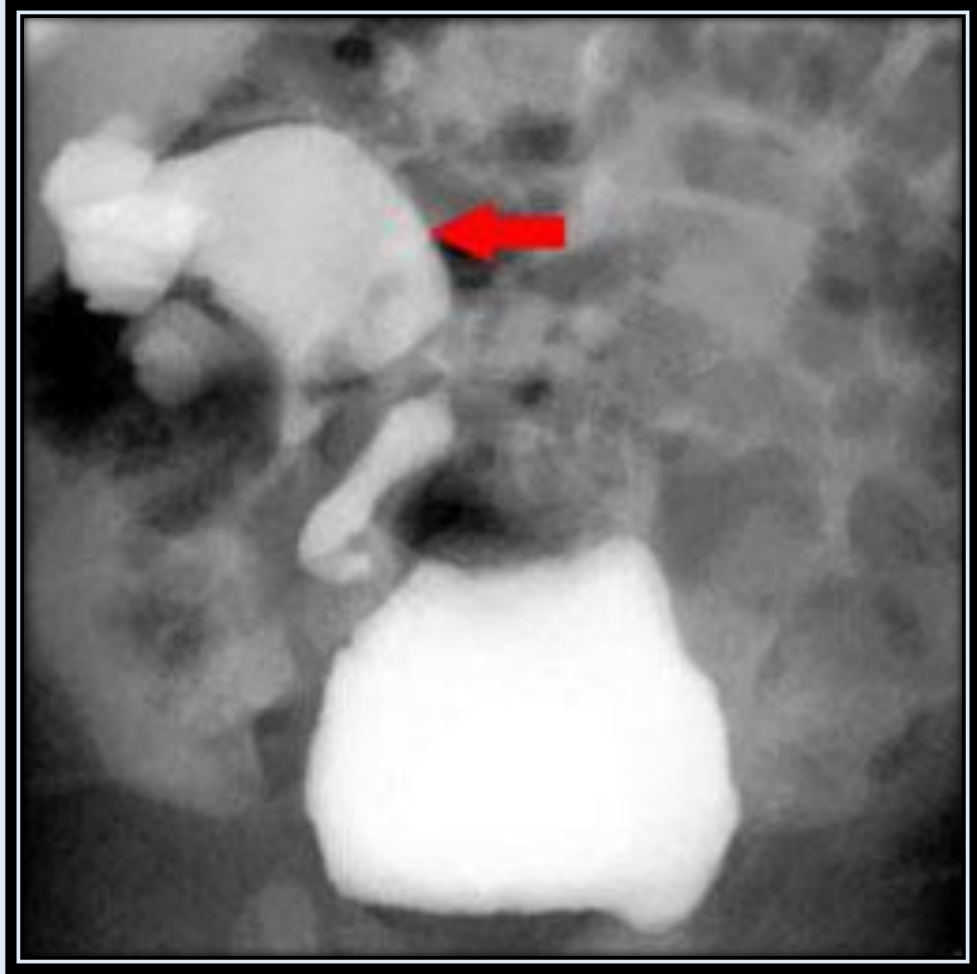
What grade is this?



Grade 1 Reflux.



Grade 3 Reflux.



Grade 5 Reflux.

Vesicoureteral Reflux Quiz

Q_1: Which grade of reflux is typically treated with surgery?

- A. Grade 1
- B. Grade 2
- C. Grade 3
- D. Grade 5

Q_2: What type of contrast is used in performing the VCUG?

- A. Barium
- B. Dilute Hypaque
- C. Gastrografin
- D. Gadolinium

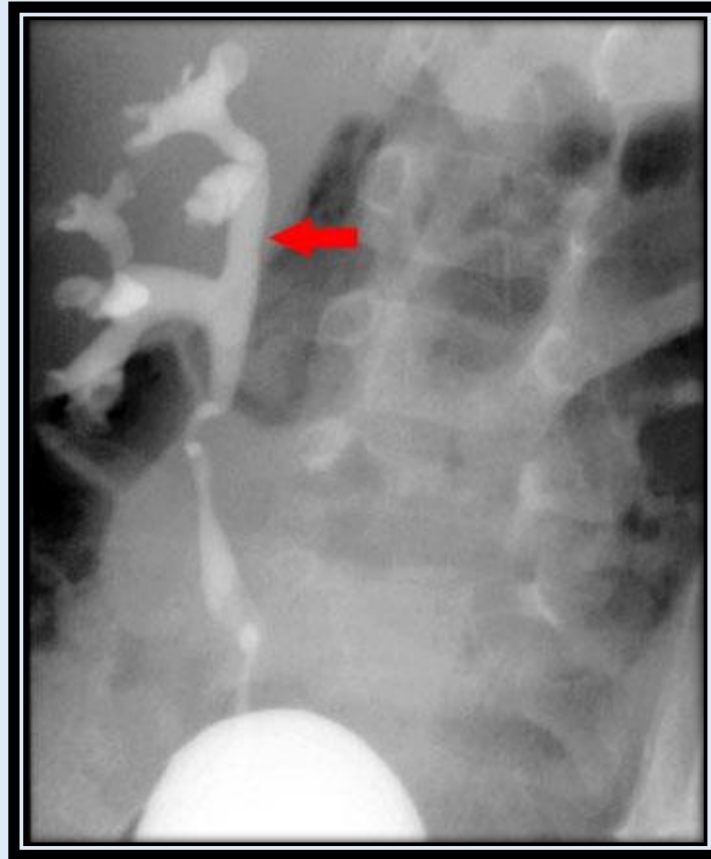
Q_3: What percentage of children with a urinary tract infection will also have vesicoureteral reflux?

- A. 10%
- B. 40%
- C. 80%
- D. 100%

Q_4: The expected bladder capacity of a two year old is:

- A. 20cc
- B. 90cc
- C. 120cc
- D. 150cc

Q_5: This exam demonstrates what grade of reflux?



- A. Grade 1
- B. Grade 2
- C. Grade 3
- D. Grade 5

Question 6: The standard normal voiding cystourethrogram consists of how many spot films?

- A. Two
- B. Five
- C. Seven
- D. Ten

Question 7: Most children will require sedation for the voiding cystourethrogram.

- A. True
- B. False

Question 8: What grade of reflux is demonstrated with contrast refluxing into the proximal renal collecting system without dilatation?

- A. Grade 2
- B. Grade 3
- C. Grade 4
- D. Grade 5

Question 9: A preliminary KUB film is not necessary in the VCUG exam because it results in unnecessary radiation.

- A. True
- B. False

Question 10: Reflux is typically seen during early filling of the bladder.

- A. True
- B. False

Answers

Question 1: Which grade of reflux is typically treated with surgery?

Grade 5

Question 2: What type of contrast is used in performing the VCUG?

Dilute Hypaque

Question 3: What percentage of children with a urinary tract infection will also have vesicoureteral reflux?

40%

Question 4: The expected bladder capacity of a two year old is:

120cc (Hint: $[(2+2) \times 30 = 120]$)

Question 5: This exam demonstrates what grade of reflux?



Grade 2 (Hint: see question 8)

Question 6: The standard normal voiding cystourethrogram consists of how many spot films?

Seven

Question 7: Most children will require sedation for the voiding cystourethrogram.

False

Question 8: What grade of reflux is demonstrated with contrast refluxing into the proximal renal collecting system without dilatation?

Grade 2 (Hint: see question 5)

Question 9: A preliminary KUB film is not necessary in the VCUG exam because it results in unnecessary radiation.

False

Question 10: Reflux is typically seen during early filling of the bladder.

False

Autosomal Dominant Polycystic Kidney Disease

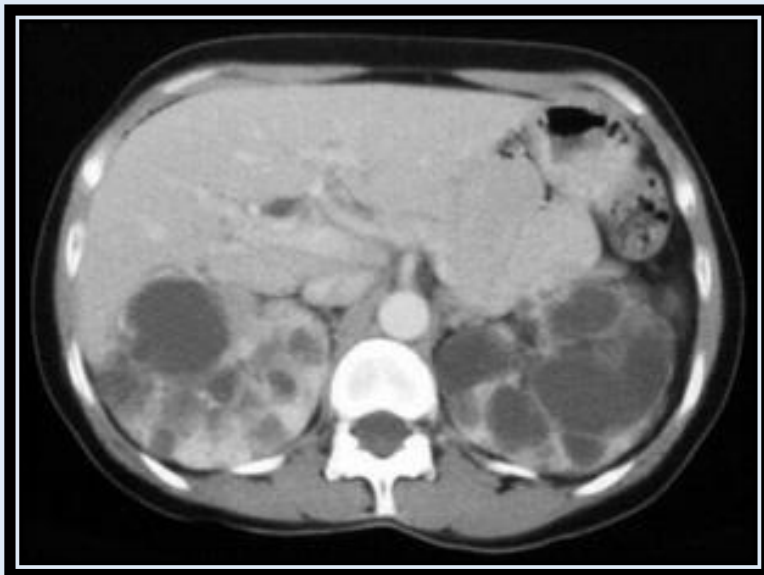
Autosomal dominant polycystic kidney disease (ADPKD) is inherited in a dominant trait with variable expression. ADPKD presents in late childhood or early adulthood. US appearance may look similar to autosomal RECESSIVE polycystic kidney disease (ARPKD) initially. Macroscopic cysts will develop during the second decade and be identified by US exam. Hepatic cysts are seen in one third of cases. Cysts can also be seen in multiple other organs. There is an association with intracranial aneurysms in approximately 20% of cases.



Enlarged bilateral polycystic kidneys on an IVP



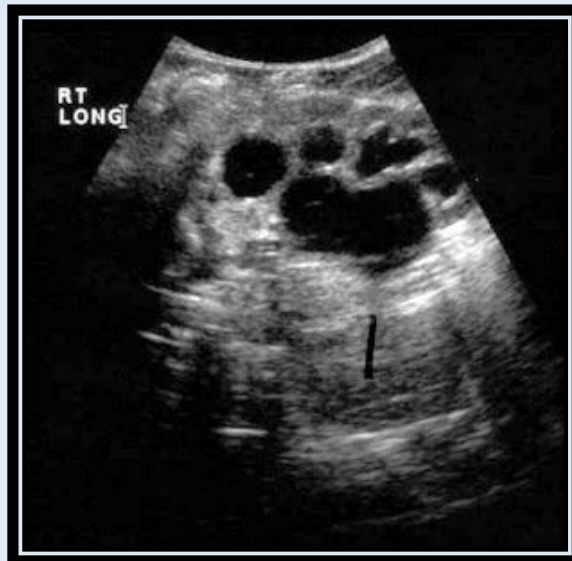
Enlarged bilateral polycystic kidneys on an IVP



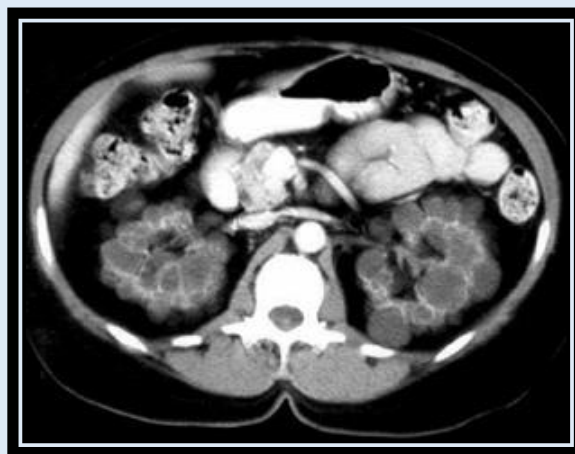
CT showing multiple cysts bilaterally



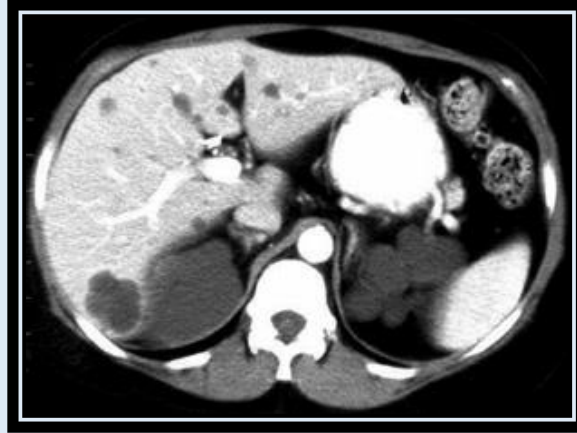
CT showing multiple cysts bilaterally



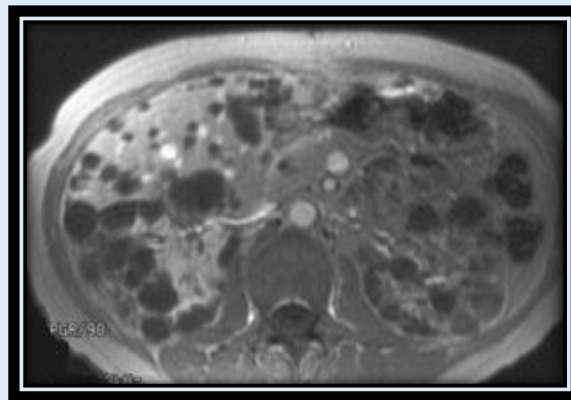
Longitudinal view of a polycystic kidney



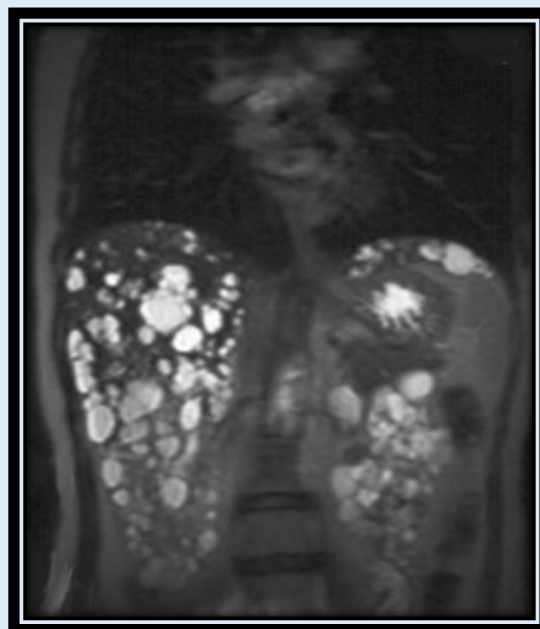
Bilateral polycystic kidneys with renal scarring



CT showing hepatic cysts in ADPKD



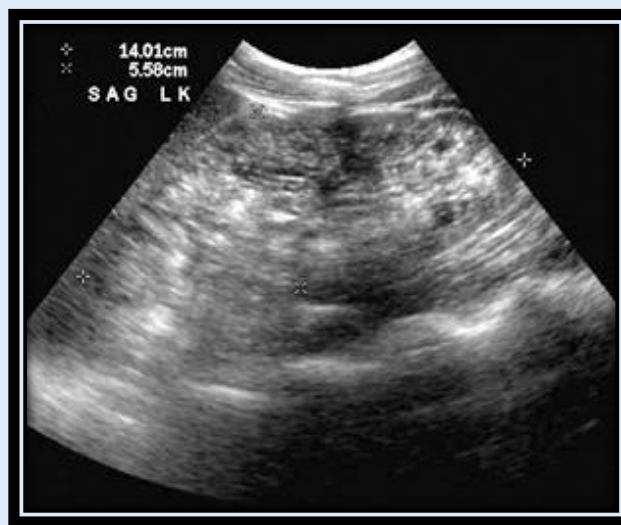
Hepatic and splenic cysts in ADPKD



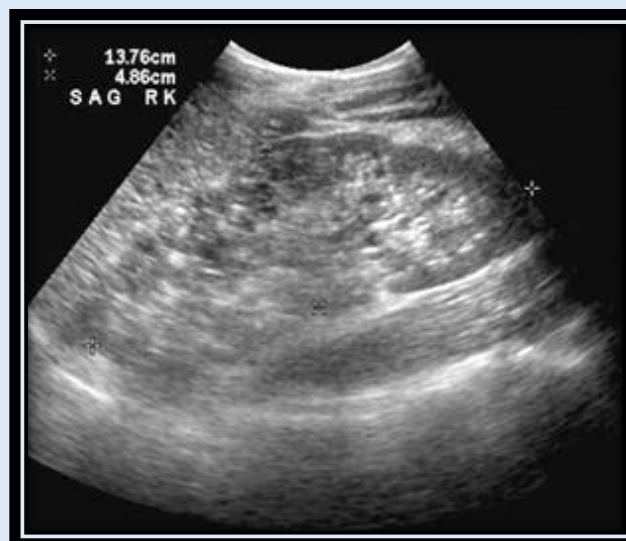
Enlarged bilateral polycystic kidneys on coronal T2 MRI

Autosomal Recessive Polycystic Kidney Disease

Autosomal recessive polycystic kidney (ARPKD) disease is inherited in a recessive fashion with varying degrees of clinical presentations. There is medullary ductal ectasia and loss of renal function. Most children will die shortly after birth. US demonstrates renal enlargement and increased renal echogenicity. No macroscopic cysts are seen, in contradistinction to autosomal dominant polycystic disease. ARPKD is also associated with periportal fibrosis. The degree of periportal fibrosis is inversely proportional to the degree of renal involvement. ARPKD can be classified into perinatal, neonatal, infantile, and juvenile forms.



Renal enlargement and increased renal echogenicity



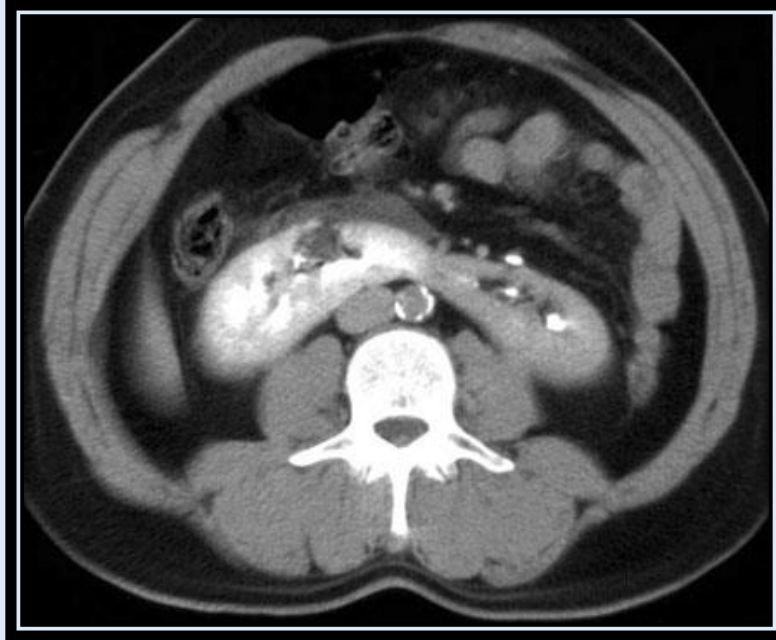
Renal enlargement and increased renal echogenicity

Congenital Urinary Tract Anomalies

Bilateral renal agenesis is present in 1 in 8000 births and is not compatible with a normal life. Unilateral renal agenesis is more common, present in 1 in 500 births. The ipsilateral adrenal gland is usually present and the contralateral kidney will demonstrate compensatory hypertrophy. If a normal kidney is not identified and renal agenesis is suspected a careful search will need to be made for a malpositioned kidney. Renal ectopia describes an abnormal position of the kidney. The kidney may migrate too far superiorly (thoracic kidney) or may not ascend completely (pelvic kidney). One or both kidneys may be on the contralateral side of the abdomen. This is seen with crossed fused ectopia where in most cases the kidneys are fused. The kidneys may also fuse across midline resulting in a horseshoe kidney. Horseshoe kidneys are more susceptible to trauma and are thought to be more prone to developing renal neoplasms.



Example of **crossed fused ectopia** on an IVP



Example of a **horseshoe kidney** on CT

Other congenital urinary tract anomalies include the following:



Duplicate lower tracts



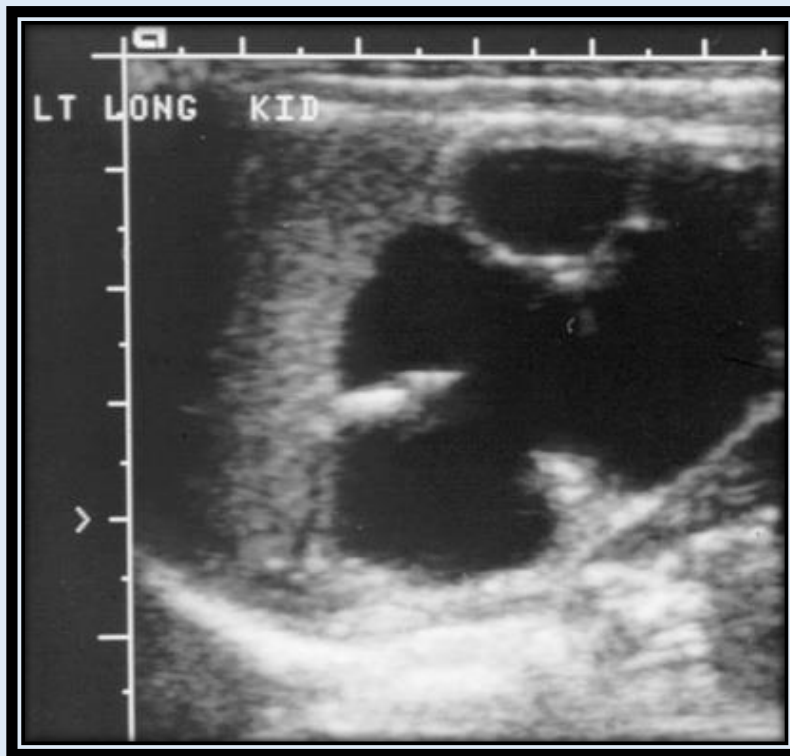
Duplicate upper tracts

Hydronephrosis

Hydronephrosis is the most common cause of an abdominal mass in the neonate. Hydronephrosis is dilatation of the urinary tract collecting system. This may be due to obstructive causes, reflux or prune belly syndrome. Hydronephrosis is frequently diagnosed on an OB ultrasound. Nearly all of these cases will resolve postnatally. This should be demonstrated with an ultrasound exam. If the hydronephrosis persists greater than 3 months, then further workup should include a nuclear medicine renal scan to evaluate for obstruction and a VCUG to evaluate for reflux.

Ureteropelvic junction obstruction

Ureteropelvic junction obstruction (UPJ) is the most common anomaly of the GU tract. UPJ obstruction may be due to intrinsic causes from a defect in the musculature of the ureter or less commonly from extrinsic causes like a crossing renal vessel. UPJ is more common on the left but is frequently bilateral (20%). UPJ is evaluated with a nuclear medicine renal scan. If the renal function is severely impaired, the UPJ may be surgically repaired.



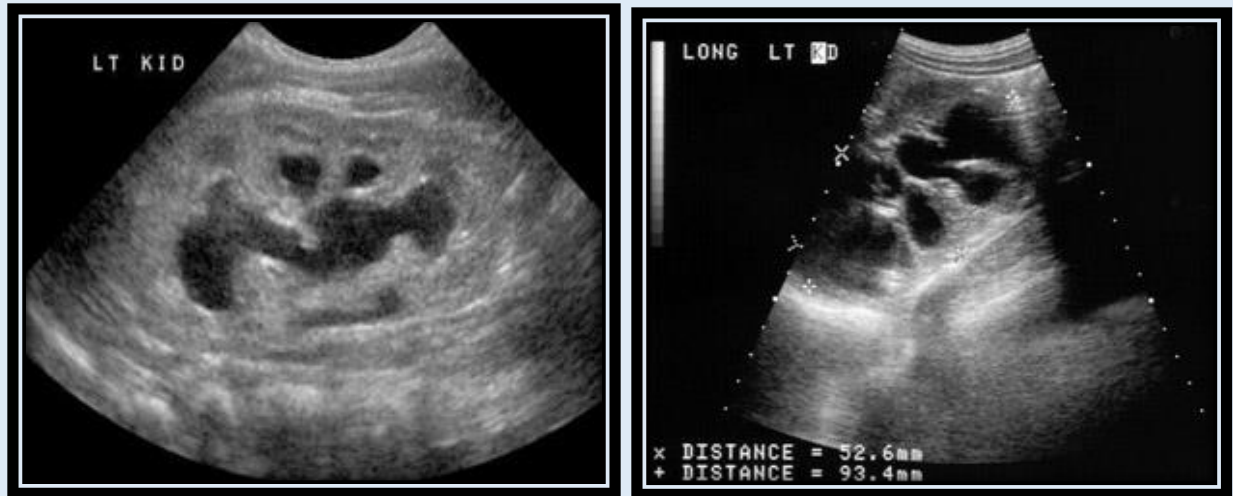
UPJ obstruction resulting in severe **hydronephrosis** as demonstrated on ultrasound.

Posterior Urethral Valves

Bilateral hydronephrosis can be caused by posterior urethral valves (PUV). Posterior urethral valves are abnormal folds in the posterior urethra resulting in a functional obstruction. PUV are best demonstrated with a VCUG. The VCUG shows dilatation and elongation of the posterior urethra with a normal anterior urethra. The valves can be seen as transverse filling defects. The bladder will be heavily trabeculated secondary to the obstruction.



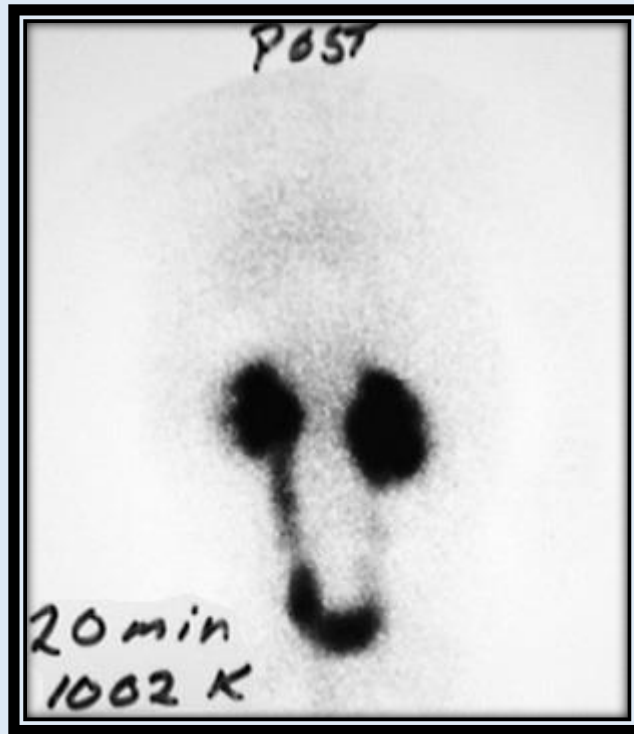
VCUG of posterior ureteral valves



US of hydronephrosis caused by PUV

Primary Megaureter

Primary megaureter is demonstrated by a straightened dilated ureter which is not tortuous. Primary megaureter is secondary to a short aperistaltic distal segment of the ureter, resulting in a functional obstruction. The degree of obstruction can be quantified with a nuclear medicine scan or an intravenous urogram. Primary megaureter is more common on the left but can be bilateral.



Scintigraphy



Enlarged right ureter



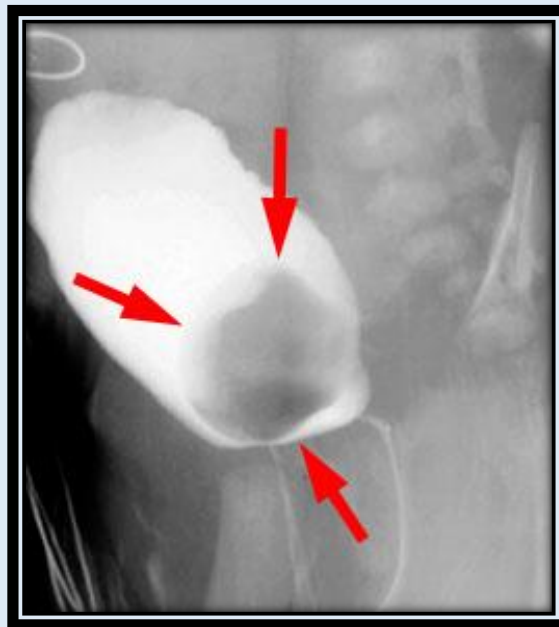
US of hydronephrosis caused by a megaureter



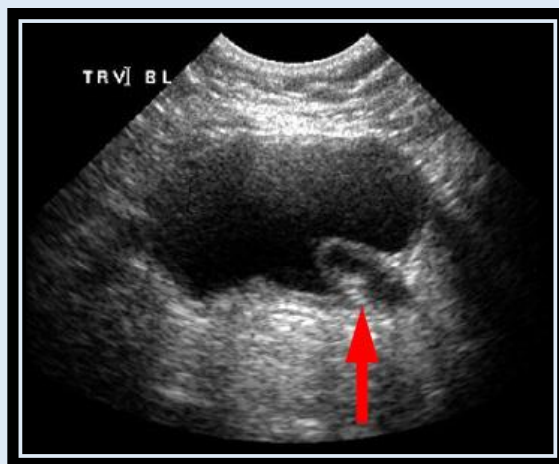
Left megaureter

Ureterocele

Ureterocele is an abnormal dilatation of the intramural portion of the ureter within the bladder. Ureteroceles may be simple or ectopic. Simple ureteroceles are in an otherwise normally positioned ureter. Simple ureteroceles are usually seen in adults. Ectopic ureteroceles are associated with the upper moiety of a duplicated collecting system which inserts ectopically into the bladder. The ectopic ureterocele results in obstruction of the upper pole moiety and can contribute to reflux of the lower pole moiety by mass effect. Ureteroceles are best demonstrated during the early filling phase of the VCUG. Ureteroceles can also be demonstrated on ultrasound.



VCUG of ureterocele

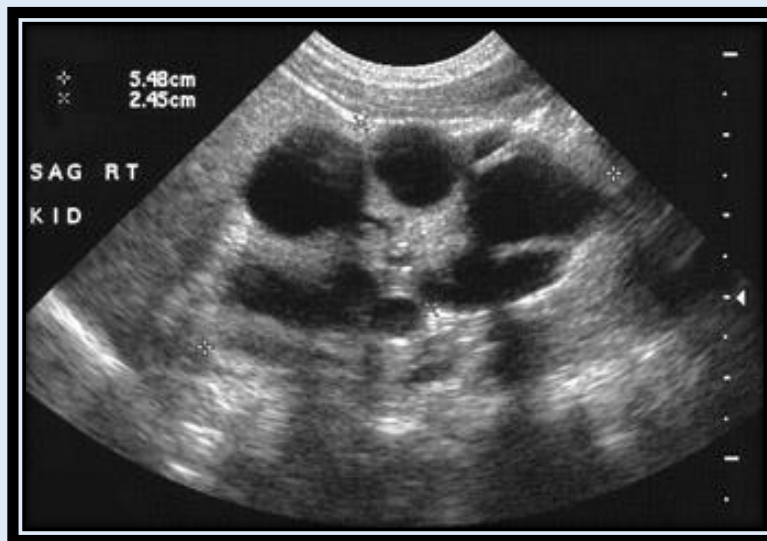


US of ureterocele

Multicystic Dysplastic Kidney

Multicystic dysplastic kidney (MCDK) results from a severe ureteropelvic junction (UPJ) obstruction. The kidney is comprised of large, noncommunicating cysts. It is important to differentiate this from hydronephrosis. In hydronephrosis the cystic spaces are seen to communicate. In difficult cases renal scintigraphy can be useful. MCDK will show no excretory function. The kidney usually gets smaller over time. MCDK may be associated with other abnormalities in the contralateral kidney, most commonly UPJ obstruction.

Which of the following shows a multicystic dysplastic kidney? (The other is hydronephrosis.)



Remember that the multicystic dysplastic kidney has large, noncommunicating cysts whereas in hydronephrosis, the cystic spaces communicate.

Mesoblastic Nephroma

Mesoblastic nephroma is a benign hamartoma of mesenchymal connective tissue. It is the most common solid renal mass in the neonate (Wilms tumor is unusual in the neonate). The mean age of presentation is 3 months with a palpable abdominal mass. Ultrasound demonstrates a large mixed echogenic intrarenal mass. CT demonstrates a large solid renal mass with variable degrees of enhancement. A small percentage of mesoblastic nephromas will be atypical and have malignant characteristics. Because imaging cannot absolutely distinguish a mesoblastic nephroma from a rare early Wilms tumor, surgical excision is necessary.



Mesoblastic nephroma

Wilms Tumor

Wilms tumor is a malignant embryonal neoplasm, arising from metanephric blastema. The majority of cases involve children less than five years old with 50% less than two years of age. 5 - 10% of Wilms will be bilateral.

The clinical presentation is a large palpable abdominal mass. 50% of cases will present with hypertension from excess renin production. The mass can also fracture due to minimal trauma, resulting in internal bleeding.

Wilms tumor is associated with sporadic aniridia, hemihypertrophy, Beckwith-Wiedemann syndrome (macroglossia, omphalocele, and visceromegaly) and Drash syndrome (pseudohermaphroditism, glomerulonephritis, and Wilms tumor).

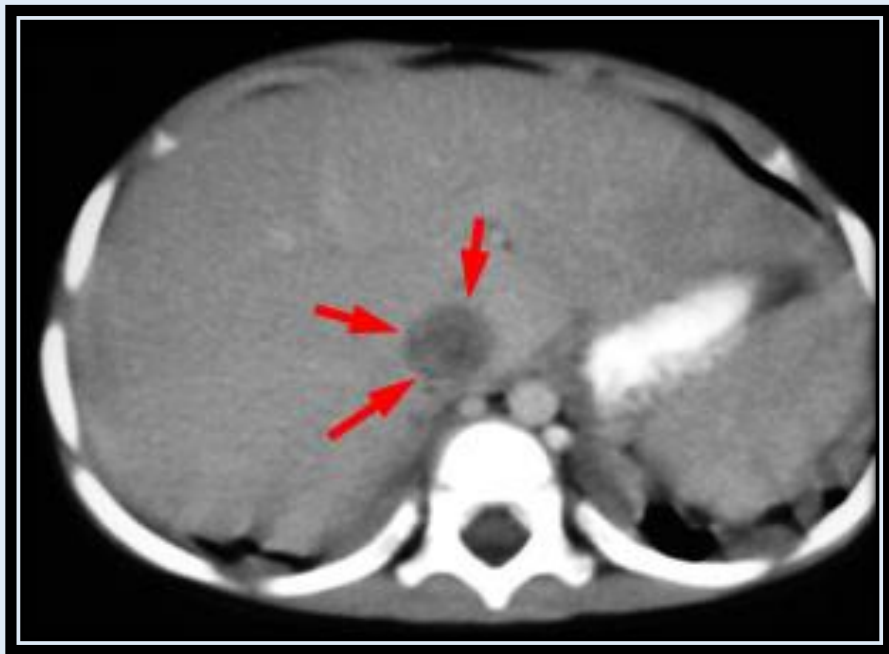
Staging of Wilms	
Stage 1	confined to kidney and totally resectable
Stage 2	extends beyond kidney but remains totally resectable
Stage 3	residual tumor after surgery but hematogenous spread
Stage 4	hematogenous metastasis
Stage 5	bilateral synchronous tumors

Imaging of Wilms Tumor

Wilms tumor presents as a large mass with a mean diameter of 12 cm arising from the cortex of the kidney. Ultrasound is the first imaging modality used to evaluate an abdominal mass, although CT is frequently utilized. The "claw sign" will indicate the mass is arising from the kidney. In addition there will be intrinsic displacement of the renal collecting system. The mass will be hyperechoic on ultrasound with areas of heterogeneity. On CT Wilms tumor is a predominately solid enhancing renal mass. On both imaging studies there will be areas of heterogeneity due to hemorrhage and necrosis. Calcifications are uncommon, seen in less than 15%. On both imaging studies, it is important to look for invasion of the renal vein, IVC and right atrium. Pulmonary metastasis are relatively common (20%).



Contrast enhanced CT of large mass arising from the kidney as evidenced by the claw sign and intrinsically displacing the renal collecting system. Note the absence of calcifications.



Contrast enhanced CT demonstrating tumor involvement of the IVC.

Neuroblastoma

Neuroblastoma is the second most common solid childhood neoplasm. Brain neoplasms are the most common. The tumor arises from primitive neuroblasts in the neural crest of the sympathetic chain. Neuroblastomas can arise anywhere along the course of the sympathetic chain, but the majority will be in the abdominal cavity, and the majority of these will arise from the adrenal gland.

Most patients will be less than 4 years old at presentation. Most neuroblastomas present between 2 months and 2 years. This is a slightly younger age group than Wilms. However there is considerable overlap. The clinical presentation, similar to Wilms, is with an incidental abdominal mass.

Treatment involves surgical resection and chemotherapy. The prognosis depends on the number of copies of the n-myc oncogene. Age at presentation is also an important factor. Presentation before one year of age has a significantly better prognosis.

Staging of Neuroblastoma	
Stage 1	tumor confined to organ of origin with complete resection
Stage 2	tumor extends beyond the organ of origin without crossing midline
Stage 3	tumor crosses midline
Stage 4	distant metastases
Stage 4s	metastases confined to liver, skin and bone marrow

Imaging of Neuroblastoma

Conventional radiographs will demonstrate an upper quadrant mass. Dystrophic calcifications will be present in 85% of cases. An excretory urogram will show displacement but not distortion of the collecting system. US, CT and MRI all have a role in imaging of neuroblastoma. Imaging is used to characterize the mass and define the extent of disease. The mass is most commonly suprarenal with displacement but no involvement of the kidney. Neuroblastoma will encase the vessels without any invasion or displacement.



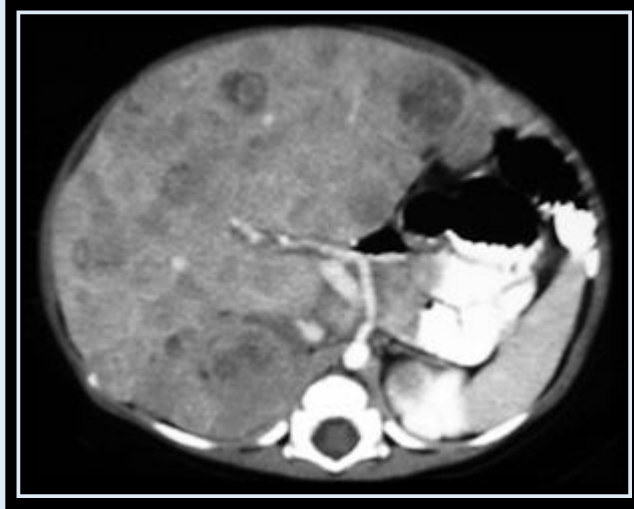
Neuroblastoma with disease crossing midline



Neuroblastoma with calcifications



Neuroblastoma encasing vessels



With liver metastasis

Mesoblastic Nephroma versus Wilms

- Mesoblastic nephroma and Wilms tumor look very similar on imaging as both present as large solid renal masses.
- Mesoblastic nephroma occurs in the neonate whereas Wilms tumor is very rare in the newborn.
- Both are treated with surgical excision and the final distinction is made with pathology.



Mesoblastic nephroma



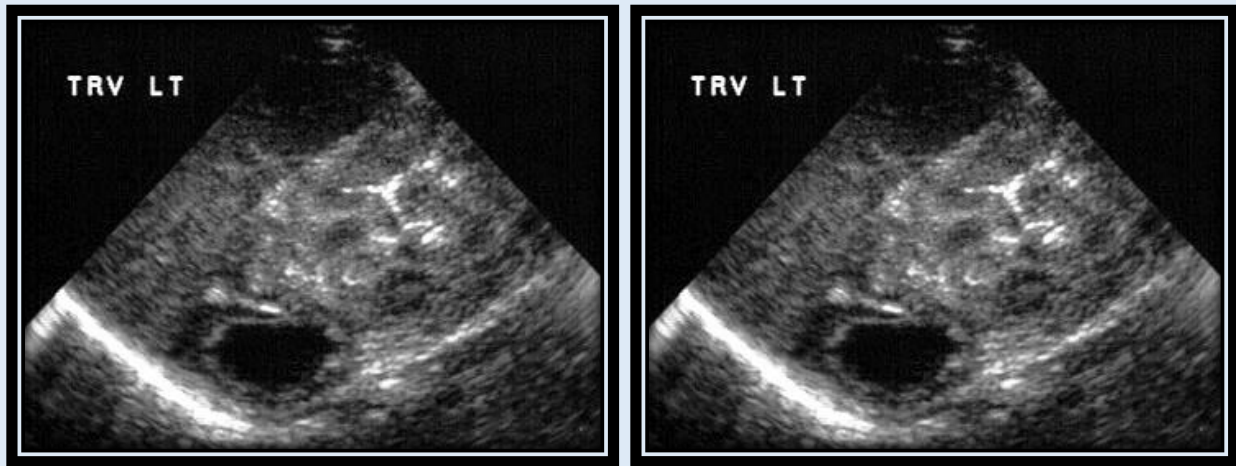
Wilms tumor

Wilms versus Neuroblastoma

	Wilms	Neuroblastoma
Age	Slightly older 1-5 years	Slightly younger 2 months - 2 years
Organ of origin	Kidney Intrinsic mass effect on collecting system	Adrenal Extrinsic mass effect on collecting system
Calcifications	15%	85%
Vascular Involvement	Invades renal vein, IVC; displaces vessels	Encases but does not invade or displace vessels
Distant Spread	Pulmonary, liver No skeletal	Bone involvement

Neonatal Adrenal Hemorrhage

Adrenal hemorrhage can occur secondary to birth trauma or stress. It is more common on the right (70%) but can be bilateral (10%). As it is usually asymptomatic, its importance lies in differentiating it from neuroblastoma. Adrenal hemorrhage usually is anechoic and avascular whereas neuroblastoma is an echogenic mass with evidence of vascularity. Serial ultrasound exams may be helpful to show the resolution of the hemorrhage. MRI may also be useful in problematic cases to show the hemorrhage.



Pediatric Genitourinary Quiz

What is this image depicting?



3:



4:





5:



6:



7:

Answers



Wilms tumor or Mesoblastic nephroma



Autosomal dominant polycystic kidney disease



3

Horseshoe kidney



4

Multicystic dysplastic kidney



Posterior ureteral valves



Megaureter



7

Crossed fused ectopia

Pediatric Musculoskeletal Radiology

Pediatric Musculoskeletal Radiology

Comprehensive Outline for Pediatric Musculoskeletal Section

- **Trauma**
 - General Principles
 - Salter-Harris Fractures
 - Anatomic Locations of Fractures
 - Stress Injury
 - Avulsion Injury
 - Non-accidental Trauma
- **The Pediatric Hip**
 - Developmental Dysplasia of the Hip (DDH)
 - Proximal Femoral Focal Deficiency
 - Septic Arthritis and Toxic Synovitis
 - Legg-Calve-Perthes Disease
 - Slipped Capital Femoral Epiphysis
- **The Pediatric Lower Extremity**
 - Osgood-Schlatter Disease
 - Clubfoot
 - Tarsal Coalition
- **Benign Lesions**
 - Distal Femoral Metaphyseal Irregularity
 - Benign Cortical Defect
 - Osteoid Osteoma
 - Osteochondroma
 - Enchondroma
 - Fibrous Dysplasia
- **Aggressive Lesions**
 - Osteomyelitis
 - Newborn Periosteal Reaction
 - Langerhans Cell Histiocytosis
 - Ewing Sarcoma
 - Osteosarcoma
 - Metastatic disease

- **Constitutional Disorders of Bone**

- Achondroplasia
- Mucopolysaccharidoses
- Osteogenesis Imperfecta
- Osteopetrosis
- Neurofibromatosis
- Blount Disease

- **Metabolic Disorders**

- Rickets
- Lead Poisoning
- Juvenile Rheumatoid Arthritis
- Hemophilia
- Sickle Cell and Thalassemia

- **Quiz**

General Principles of Pediatric Trauma

A multitude of factors help to explain why children respond differently than adults to trauma. First, children have immature bone with open growth plates and cartilaginous epiphyses. They possess a thick, tough periosteum with incomplete mineralization of underlying bone which results in greater elasticity and a greater propensity to deform prior to breaking. As a result, complete fractures are far less common in children, whereas bending, bowing and partial fractures are much more common. Moreover, with malleable bones and open epiphyseal plates, children are far less likely to sustain ligamentous damage as a result of trauma than are adults.

Common types of bone injuries in children:

- Elastic deformation: a momentary, non-permanent deformation
- Bowing deformation: a deformity of bone that may or may not be completely resolved with bone remodeling
- Torus (Buckle) Fracture: involves the buckling of one cortex
- Greenstick fracture: an incomplete transverse fracture with fracture and periosteal rupture on the convex side
- Salter-Harris fracture: involves epiphyseal plate
- Stress Injury: a fracture caused by repetitive trauma
- Avulsion Injury: a bony structural defect at a tendinous or aponeurotic insertion resulting from excess stress



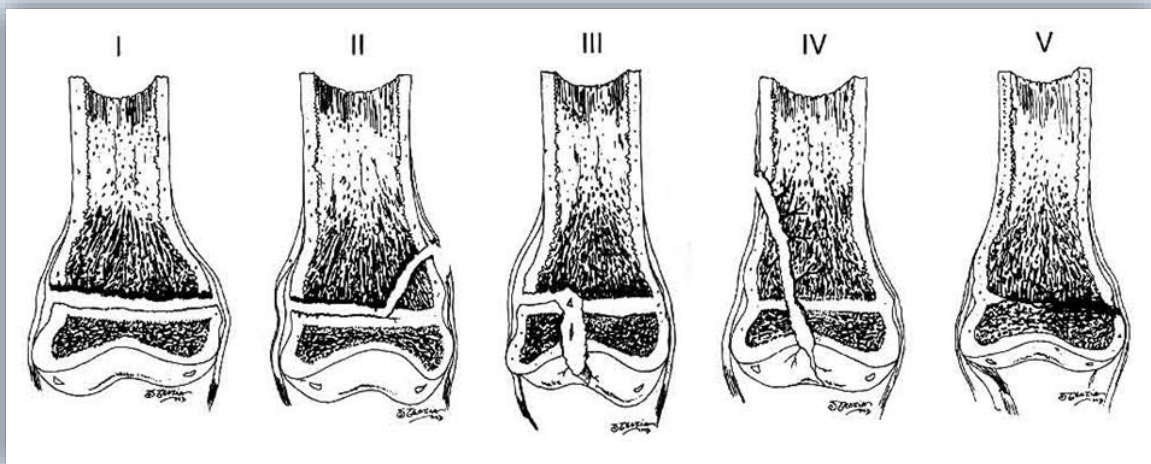
Right tibial fracture with associated bowing fracture of fibula in a 5-year-old male. AP radiograph shows a complete fracture through the mid-shaft of the tibia. Note the valgus deformity. There is marked bowing of the fibula both medially and posteriorly (seen best on lateral view).

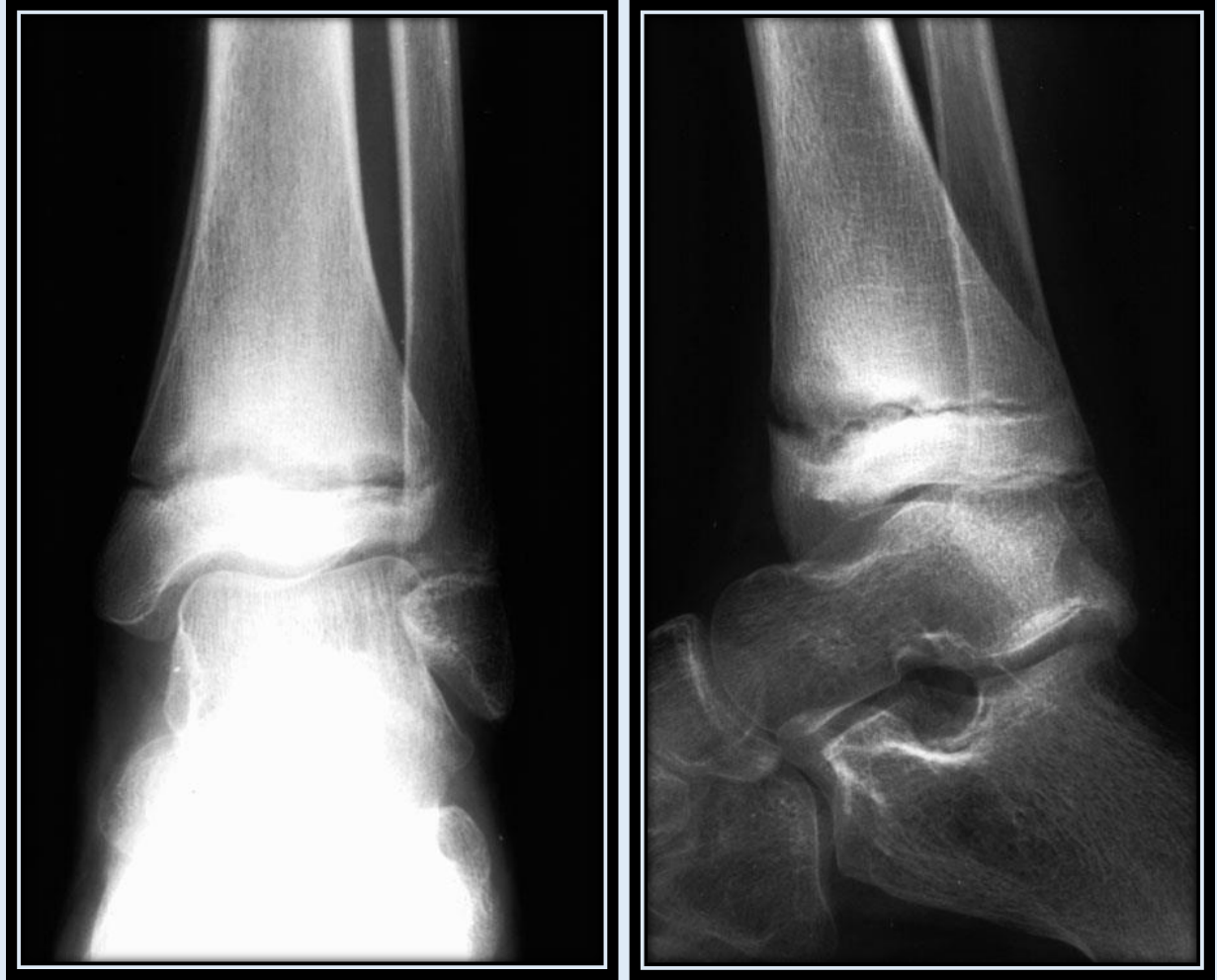
Salter-Harris Fractures

The physal plate is often involved in traumatic pediatric injuries. Up to one-third of all pediatric fractures involving the long bones will involve the physis. These fractures carry added significance because involvement of the "growth plate" may lead to arrested development of the affected limb. The more severe the injury, the higher the likelihood of requiring surgery with internal fixation.

The standard classification for physal fractures was set forth by Salter and Harris. This classification divides fractures into five types based on whether the metaphysis, physis or epiphysis is involved as demonstrated radiographically.

Salter-Harris Fracture Classification	Description
Type I	fracture through the physal plate (often not detected radiographically)
Type II	fracture through the metaphysis and physis (most common; up to 75% of all physal fractures)
Type III	fracture through the epiphysis and physis
Type IV	fracture through the metaphysis, physis and epiphysis
Type V	crush injury involving part or all of the physis



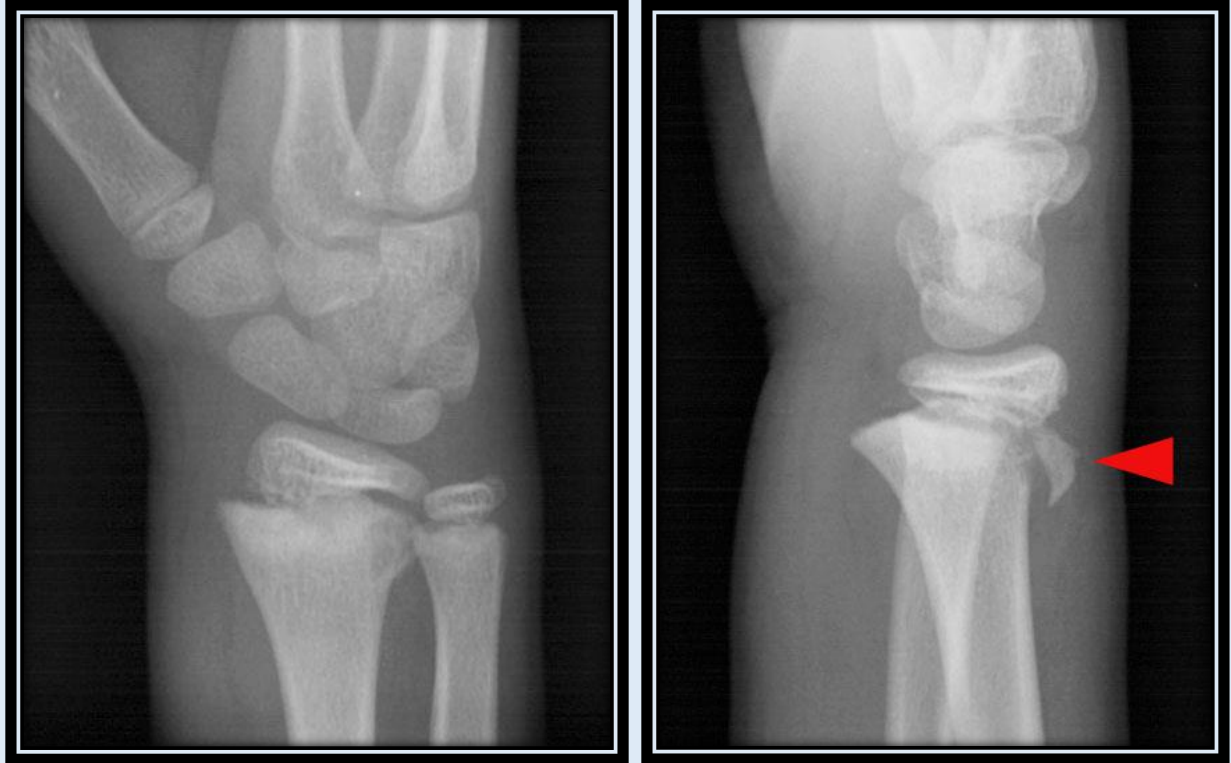


Salter-Harris Type I fracture of tibial physis in a 10-year-old girl.

AP (left) and lateral (right) radiographs of right ankle demonstrate a widened tibial physis. On the AP view, note the periosteal reaction on the medial aspect of the distal tibial metaphysis.



Salter-Harris Type II fracture of the left distal tibia. AP radiograph of tibia shows a fracture-dislocation of the tibial physis with a fracture through the metaphysis.
Note the associated comminuted fracture of the distal fibula.



Salter-Harris Type II Fracture of distal radius.

Oblique (left) and lateral (right) radiographs demonstrate a fracture of the radial physis with involvement of the metaphysis. Note the fracture fragment (arrowhead) which is displaced dorsally on the lateral image.



Salter-Harris III fracture of distal tibial epiphysis in an 11-year-old boy.
There is a vertical fracture through the medial portion of the distal tibial epiphysis.



Salter-Harris IV fracture of the thumb.

Two views of the left thumb reveal a fracture at the base of the proximal phalanx (arrows), involving the metaphysis, physis, and epiphysis.

Anatomical Locations of Common Fractures

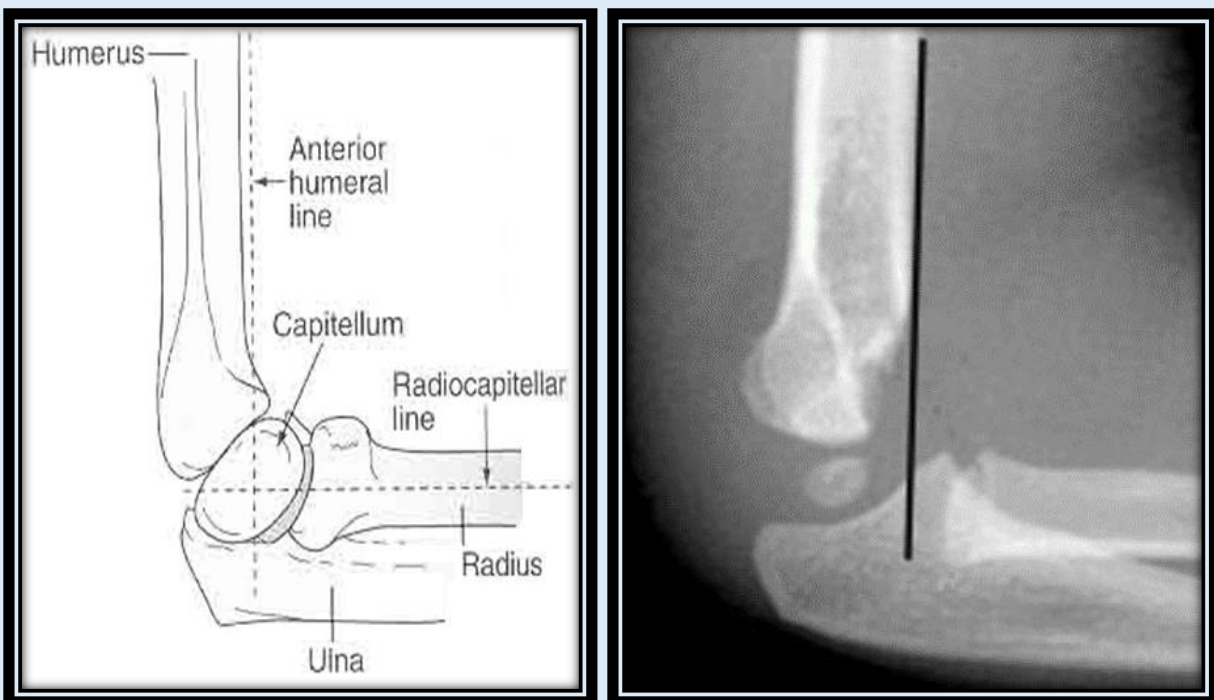
The most commonly encountered locations for pediatric fractures include the wrist and elbow. With regards to the wrist, the most common scenario involves a buckle or transverse fracture of the distal radial metaphysis with or without involvement of the distal ulnar metaphysis. Note that roughly 25-30% of all physeal fractures occur in the wrist. The pronator fat pad (seen on a lateral view of the forearm as a thin line of fat with a mild convex border) is often displaced or obliterated if a fracture is present.



Buckle fracture of the distal radius.

The AP view (left) demonstrates a cortical defect on the medial aspect of the distal radius.
The lateral view (right) reveals the indentation or buckling of the cortex.

Injuries involving the elbow are often secondary to hyperextension sustained from falling on an outstretched hand. In adults, this mechanism of injury would result in a fracture of the radial neck, whereas supracondylar fractures are more prevalent in the pediatric population. Radiographs of supracondylar fractures demonstrate posterior displacement of the distal fragment such that the *anterior humeral line* does not bisect the middle third of the capitellum (see figure below). Fracture lines are often seen through the anterior cortices on lateral views. Joint effusions are also typically present as evidenced by displacement of the posterior fat pad. Normally, this fat pad lies within the olecranon fossa and is not seen on the lateral view. A joint effusion may also elevate the anterior fat pad. This fat pad is often normally visualized, but with an effusion, it may become more prominent.

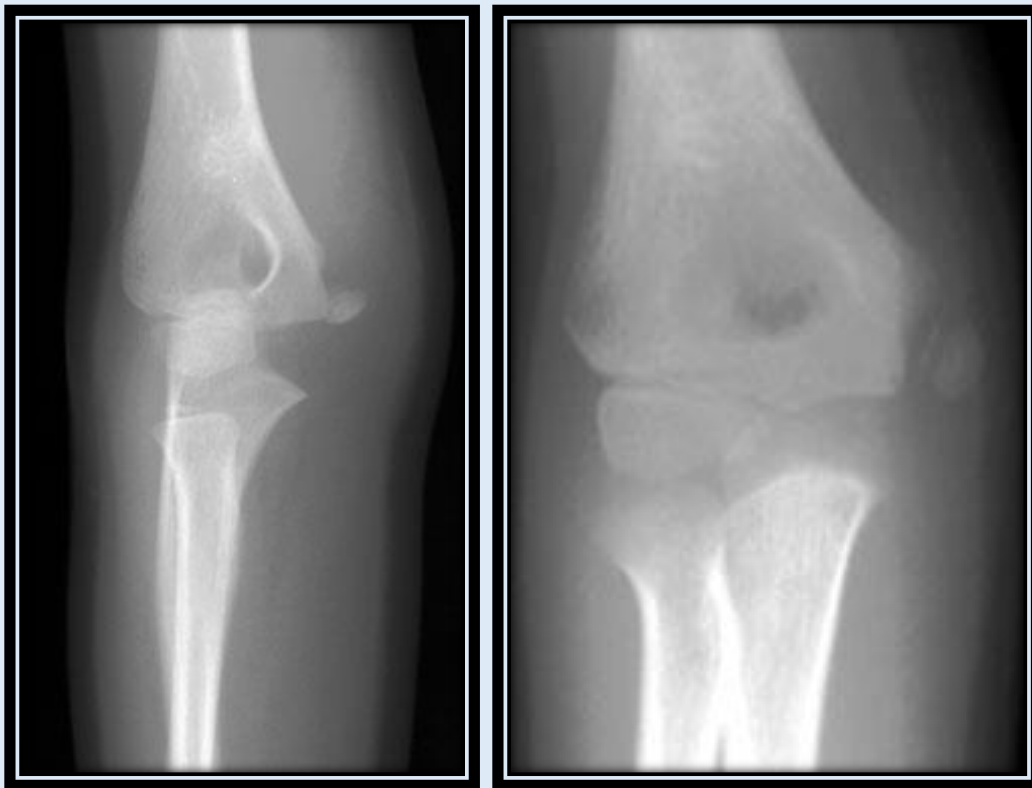


Supracondylar fracture. Lateral radiograph shows disruption of the anterior cortex with posterior displacement of the capitellum in relation to the anterior humeral line (dark line).

Other prevalent elbow injuries include fractures of the lateral epicondyle and avulsion injuries of the medial epicondyle ("little league elbow"). With avulsion injuries, which comprise roughly 10% of all elbow injuries, there may be some displacement. It is necessary to know the sequence of ossification of the elbow to avoid mistaking a displaced apophysis for one of the ossicles of the elbow.

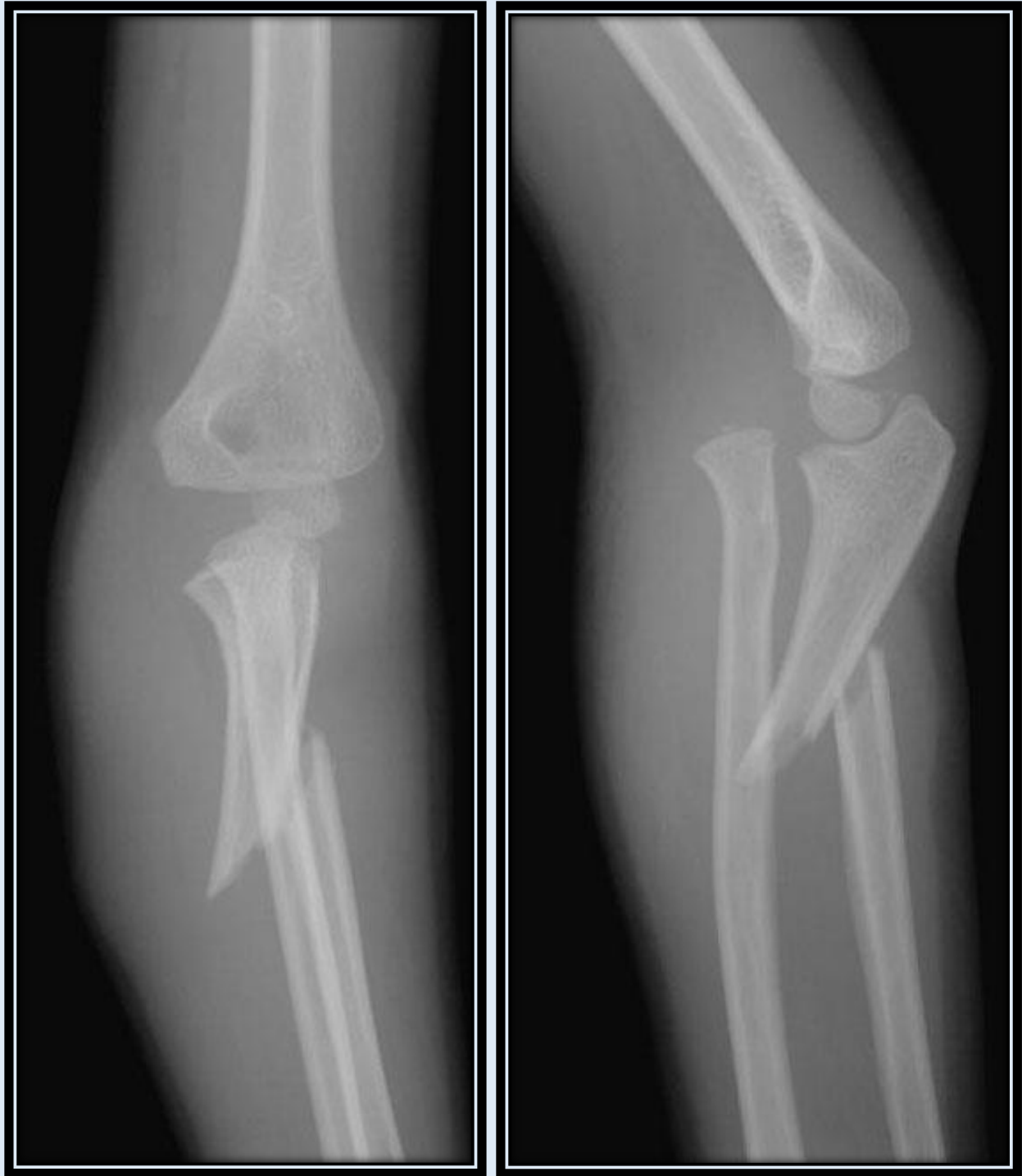
The predictable order of elbow ossification is:

- capitellum - 1 year
- radial head - 5 years
- medial epicondyle - 7 years
- trochlea - 10 years
- olecranon - 10 years
- lateral epicondyle - 11 years



Avulsion of the medial epicondyle in an 8-year-old girl.

First radiograph shows inferior and medial displacement of the medial epicondyle.
Second radiograph, taken three weeks, later reveals continued medial displacement with evidence of calcification abutting the avulsed fragment.



Monteggia Fracture of the left upper extremity.

Note the fracture of the proximal ulna with accompanying radial head dislocation (seen best on the lateral view, right).

Toddler's fractures are non-displaced oblique or spiral fractures of the midshaft of the tibia. They are found in children who have just recently begun to walk. Most children present refusing to bear weight or walk on the involved extremity. These fractures are often best viewed on oblique images.



Toddler's Fracture in a young patient who recently became ambulatory.
AP radiograph shows a non-displaced spiral fracture of the tibial shaft

Stress Reactions

Stress fractures are injuries caused by repetitive trauma. Stress injuries usually manifest themselves when a new or intense activity is started.

Most common locations: tibia > fibula > metatarsals > calcaneus.

Radiographic appearances include a) periosteal new bone formation, b) transverse or oblique band of sclerosis, or c) a lucent line surrounded by sclerosis. Often new periosteal bone will be the only finding.



Stress reaction involving the tibia.

Lateral radiograph (left) of a 13-year-old boy shows marked cortical thickening and sclerosis surrounding a horizontal lucency through the anterior cortex of the tibia.

AP radiograph (right) of a 6-year-old boy demonstrates periosteal reaction (arrow) on the medial aspect of the proximal tibia

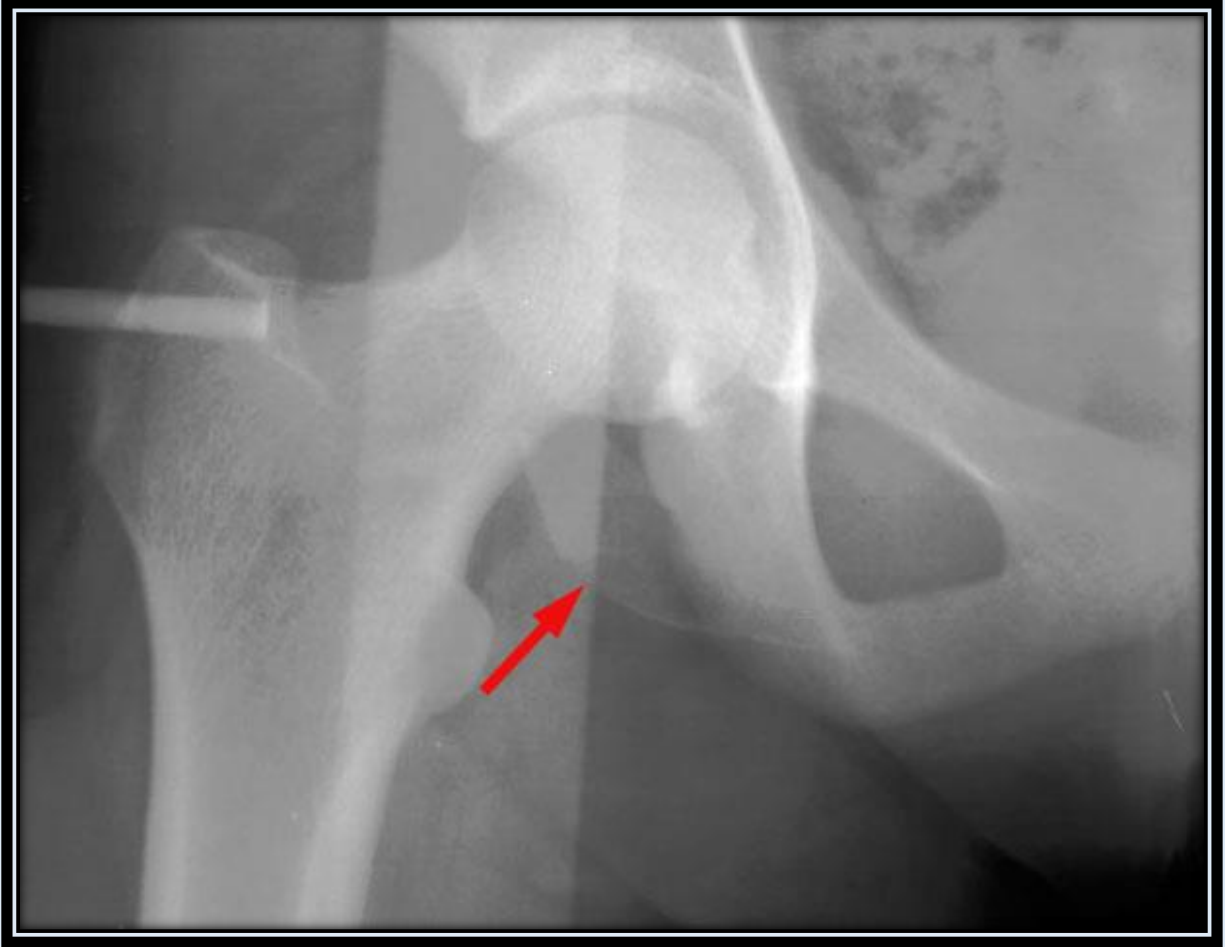
Avulsion Fractures

Avulsion fractures occur most commonly in adolescent athletes as a result of abnormal stress placed on the tendinous attachments of muscles. Prior to fusion of the ossification centers, the growing apophysis is more likely to become injured than the adjoining tendons. The most common sites of avulsion occur in the pelvis where the muscles with the greatest strength are attached.

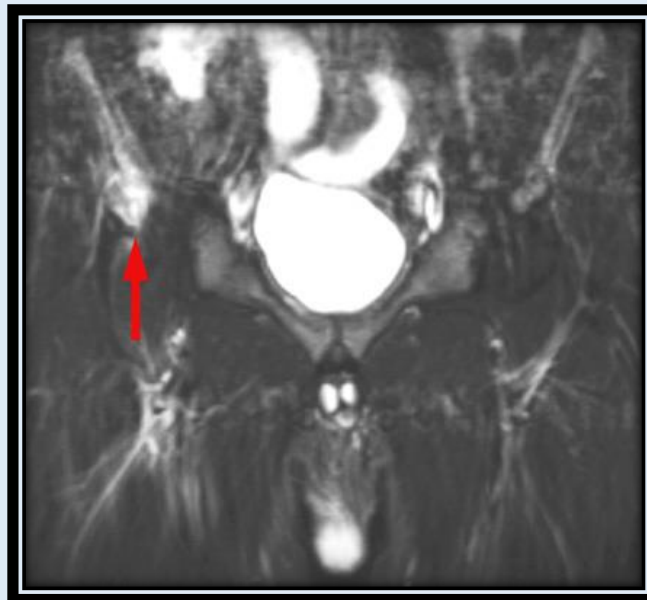


The most common locations:

- iliac crest: transversalis, internal oblique and external oblique muscles
- anterior superior iliac spine: sartorius muscle
- anterior inferior iliac spine: rectus femoris muscle
- ischial tuberosity: hamstring muscles (biceps femoris, gracilis, semimembranosus and semitendinosus)
- lesser trochanter: iliopsoas muscle



Avulsion injury of the right ischial tuberosity in a 14-year-old boy. Radiograph shows lateral displacement of a right ischial tuberosity fragment (arrow) likely secondary to an avulsion fracture involving the biceps femoris



Avulsion type fracture of right anterior inferior iliac spine in a 14-year-old male sprinter.

AP view of right hip reveals bony fragmentation inferior to the iliac spine and lateral to the femoral head.

Coronal MR through pelvis shows increased signal in the right anterior inferior iliac spine at the site of insertion of the rectus femoris muscle, consistent with an avulsion fracture.

Non-Accidental Trauma

Child abuse, or non-accidental trauma, is an all-too-common entity. Estimates have suggested that over one million children (most under one year of age) are seriously injured and up to 5000 children killed each year in the United States secondary to physical abuse. When suspicions of potential abuse are raised due to either clinical or radiographic findings, a skeletal survey must be obtained.

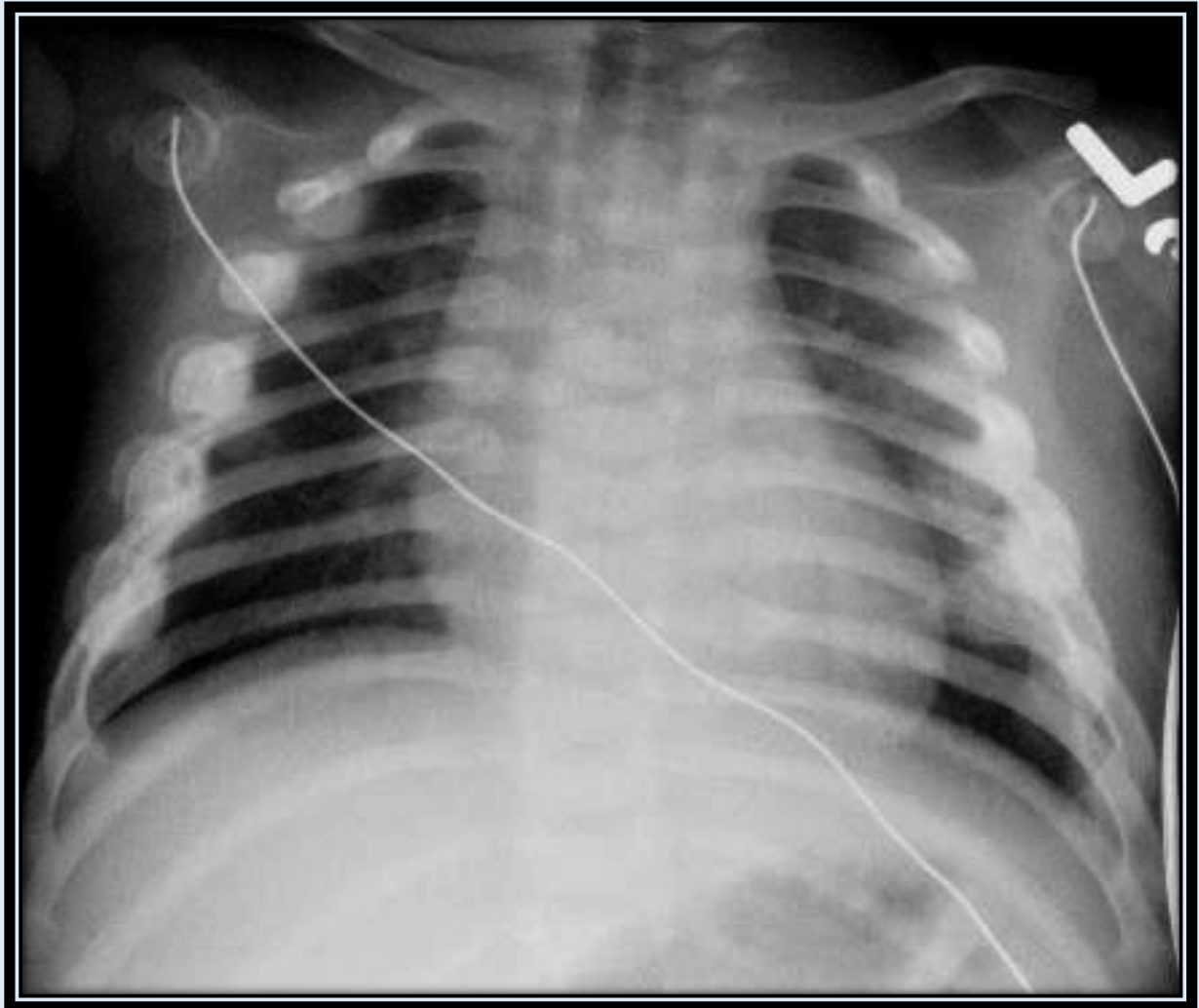
A skeletal survey consists of:

- two views of the skull
- lateral thoracic and lumbar spine
- AP views of both upper and both lower extremities
- AP views of both hands and both feet
- AP view of the Pelvis
- *may* require CT scan of head
- *may* require repeat skeletal survey in two weeks to look for healing injuries not seen on initial survey

Specific Radiographic findings suggestive of abuse:

- posterior rib fractures near costovertebral joints: highly specific for abuse; likely mechanism involves excessive squeezing force applied to infant's thorax
- metaphyseal corner fractures: likely secondary to forceful pulling of an extremity
- spiral fractures of long bones in non-ambulatory infants
- multiple fractures in different areas of the body and at different ages of healing

Skeletal survey performed on a 10-month-old male demonstrates multiple findings of abuse.



AP chest radiograph reveals multiple broken ribs as evidenced by the **callus formation** seen on both the lateral and posteromedial aspects of the right ribs #2-6 and on the lateral aspect of the left rib #5



Axial CT image (right) shows **subdural hemorrhages** in the frontal and occipital lobes and along the falx



Radiograph of left knee (center) reveals corner fractures (arrows) of the medial and lateral aspects of the distal femoral metaphyses. Note the periosteal reaction on the medial aspect of the tibial shaft.

The Pediatric Hip

There are a host of abnormalities that can be seen when radiographically evaluating the pediatric hip. This section will cover Developmental Dysplasia of the Hip (DDH), Proximal Femoral Focal Deficiency, Septic Arthritis, Toxic Synovitis, Legg-Calve-Perthes disease and Slipped Capital Femoral Epiphysis.

Developmental Dysplasia of the Hip

Developmental Dysplasia of the hip (DDH), also known as congenital hip dislocation, is recurrent subluxation or dislocation of the hip secondary to acetabular dysplasia, abnormal ligamentous laxity, or both. The acetabular dysplasia yields an increased acetabular angle and a shallow acetabular fossa. Early diagnosis of DDH is important because chronic dislocation of the femoral head can lead to growth deformity of the acetabular fossa.

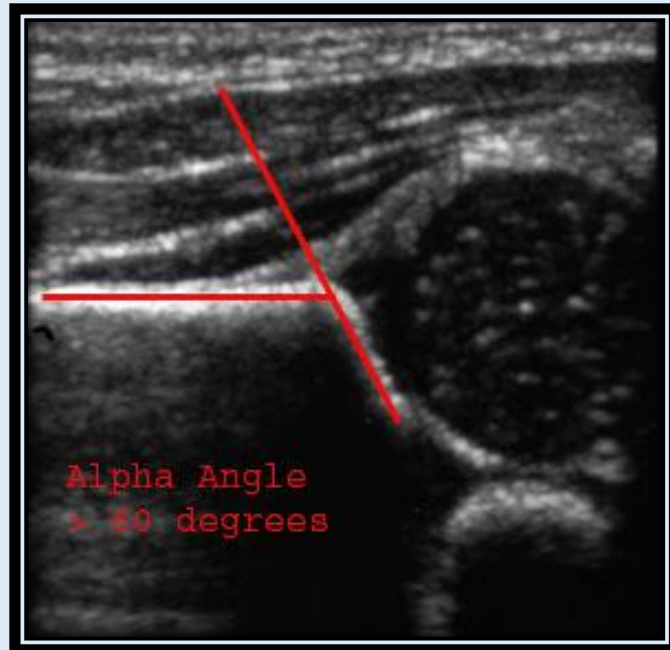
DDH is much more prevalent in females than males (9:1). It also is predisposed to affect the left hip > right hip (approximately 70-75% of the time). DDH is seen bilaterally in 5% of patients.

Clinical findings of DDH include a shortened leg with decreased range of abduction when flexed, asymmetry of the gluteal folds, and positive "clicks" with dislocation (Barlow maneuver) and relocation (Ortolani maneuver).

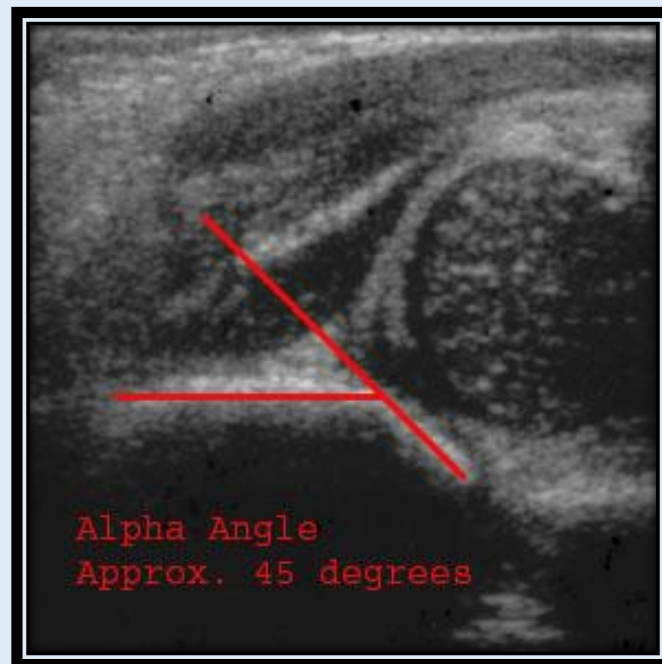
Ultrasound is the study of choice at most centers when clinical suspicion of DDH is present. It allows the hip to be evaluated for both abnormal mobility and dysmorphic acetabular features. Ultrasound is not generally performed in the first two weeks of life due to physiologic ligamentous laxity likely from maternal estrogen effects. Ultrasound is also not generally performed after 6 months of age due to increasing ossification of the femoral head.

Plain film radiography has a very limited role in evaluation of DDH in children under 6 months of age due to the lack of ossification of the femoral head. In particular, radiographs are unreliable in children 6-12 months of age because of a lack of skeletal ossification. When radiography is used, AP views are most helpful as frogleg views are likely to reduce a subluxed or dislocated hip.

Coronal Ultrasound. This view mimics the anatomy seen on an AP view of the pelvis. The iliac bone forms an echogenic line on the horizontal which should bisect the femoral head. The *alpha angle* is formed by lines drawn through the roof of the acetabulum and the straight portion of the iliac bone. A normal alpha angle measures > 60 degrees (55 degrees in newborns).



Coronal ultrasound of a normal right hip. Note how the echogenic iliac bone bisects the femoral head. The alpha angle in this study is measured to be > 60 degrees.



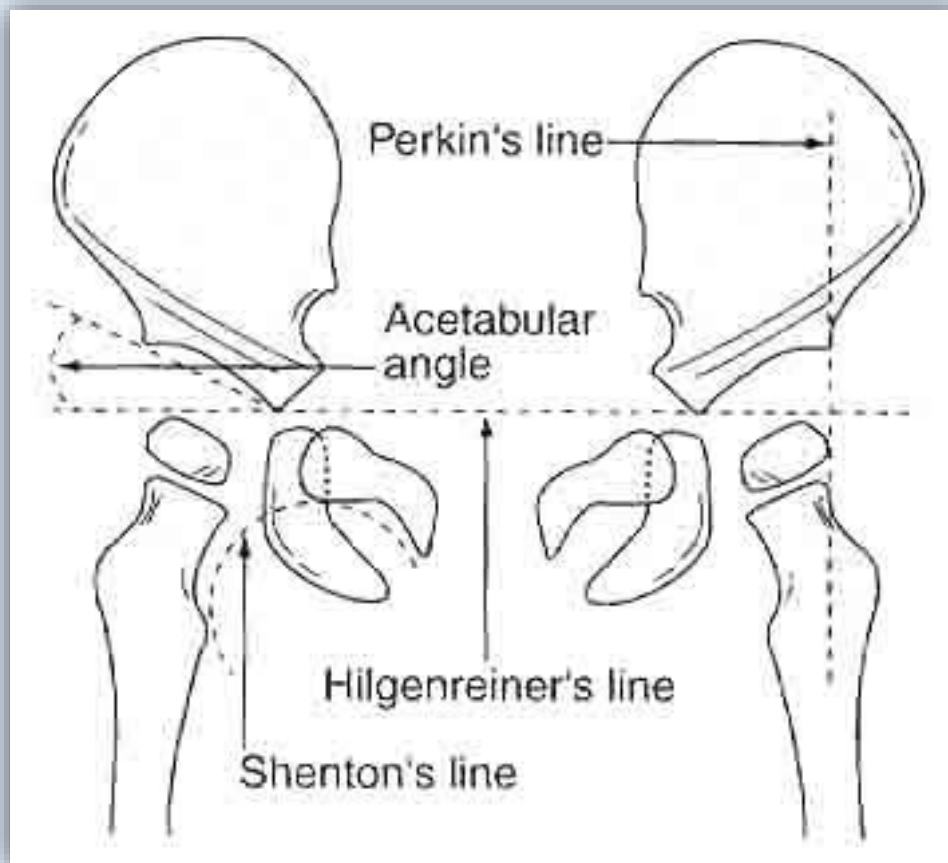
Coronal ultrasound demonstrating mild left hip dysplasia. Note the superior and lateral displacement of the femoral head. The line through the iliac bone barely transects the femoral head. The measured alpha angle is approximately 45 degrees.

Radiographic features of DDH:

- shallow acetabulum
- acetabular angle greater than 30 degrees (same as alpha angle less than 60 degrees)
- small capital femoral epiphysis
- delayed ossification of the femoral head
- acetabular sclerosis
- loss of *Shenton's curve*
- femoral head lateral to *Perkin's line*
- femoral head superior to *Hilgenreiner's line*



AP pelvic radiograph of a 2-year-old girl with developmental dysplasia of the left hip. The femoral heads are partially ossified. There is a dysplastic left acetabulum (shallow left acetabulum), and a small left femoral epiphysis when compared to the right. The left proximal femoral metaphysis is displaced superiorly and laterally. Note the fraying of the proximal femoral metaphyses (this patient was also diagnosed with rickets).



Shenton's curve: smooth, curved line connecting medial border of femoral metaphysis with the superior border of the obturator foramen

Hilgenreiner's line: a horizontal line through the triradiate cartilage of the acetabulum

Perkin's line: a vertical line (perpendicular to Hilgenreiner's line) from the lateral margin of the ossified acetabular roof that is normally tangential to the lateral margin of the ossification center of the femoral head

Acetabular angle: angle that the acetabular line makes with Hilgenreiner's line

Proximal Femoral Focal Deficiency

Proximal Femoral Focal Deficiency (PFFD) is a congenital disorder consisting of variable degrees of hypoplasia or absence of proximal portions of the femur. In its most devastating forms, the proximal femur as well as the femoral head and acetabulum may be absent. The patients will often present with a varus deformity in addition to the shortened limb. Associated findings in patients with PFFD include ipsilateral fibular hemimelia (absent fibula) and deformity of the foot.



Proximal focal femoral deficiency of the left femur. AP radiograph of an infant boy shows a markedly shortened left femur. The left femoral metaphysis and epiphysis are undergoing delayed formation when compared with the normal contralateral side. Note the absence of the fibula in the left lower extremity.

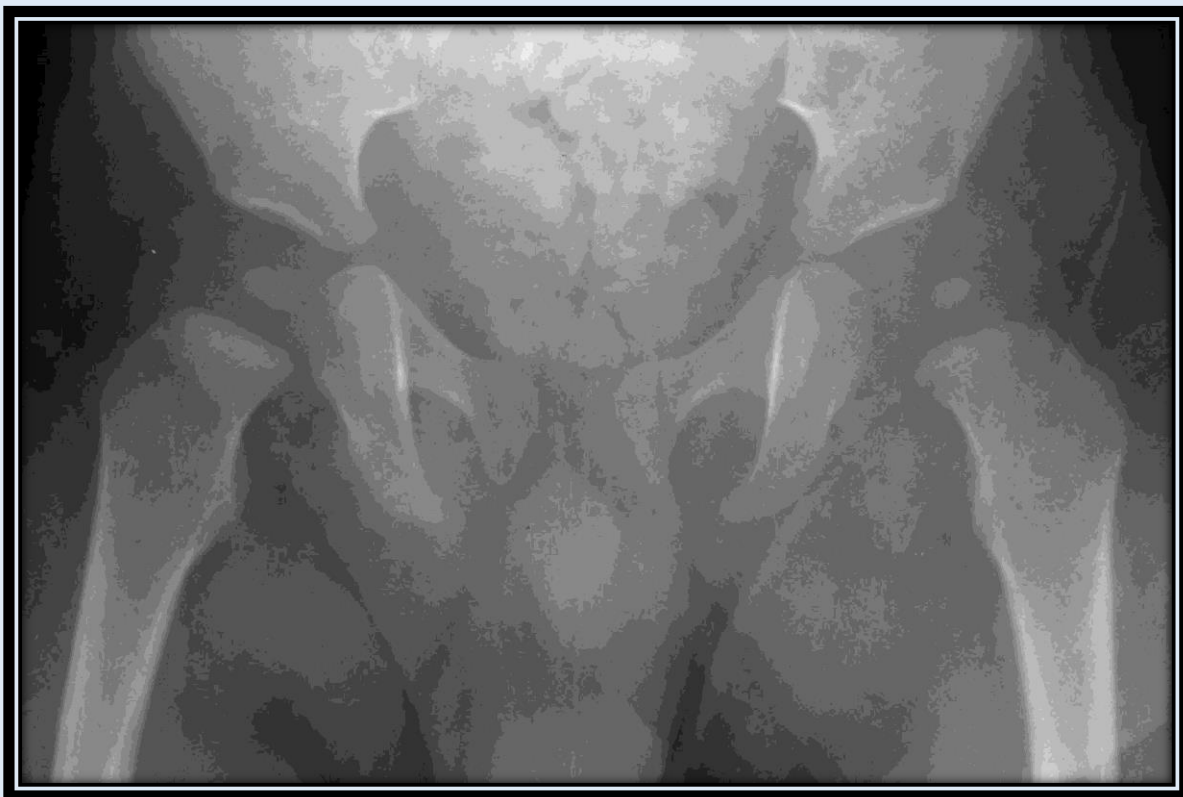
Septic Arthritis and Toxic Synovitis

Septic arthritis can present at any age but is most common in infants and teenagers. It is extremely important to exclude septic arthritis when confronted with a painful hip because failure to properly diagnose this entity can result in joint destruction. In the pediatric population, septic arthritis most commonly occurs from infectious extension from the adjacent metaphysis. Bacterial organisms (*Staphylococcus aureus* > Group A *Streptococci*) are the most common etiologic agents of septic arthritis. Most cases are monocular and involve large joints (hip > knee).

Radiographic findings of septic arthritis include asymmetric widening of the hip joint spaces by > 2mm (the distance is measured between the teardrop of the acetabulum and the medial cortex of the femoral metaphysis). Other findings include displacement or obliteration of the fat pads surrounding the hip (obturator internus, iliopsoas and gluteus). Unfortunately, these findings are not sensitive for the presence of a joint effusion. A normal appearing plain film by no means excludes the diagnosis of septic arthritis.

Toxic Synovitis is a diagnosis of exclusion. It occurs most commonly in children under the age of 10 who present with no limping and no pain on palpation. These patients have a positive joint effusion that is negative for organisms on aspiration and that resolves with rest. The effusion is likely due to a viral infection.

Condition Causing Hip Pain	Typical Presenting Age
Septic Arthritis	any (infants and teenagers most common)
Toxic Synovitis	< 10
Osteomyelitis	< 5
Legg-Calve-Perthes disease	5-8
Slipped Capital Femoral Epiphysis	12-15
Langerhans Cell Histiocytosis	any, pelvic involvement usually < 5
Juvenile Rheumatoid Arthritis	Second Decade
Osteoid Osteoma	10-20
Ewing Sarcoma	10-20



Septic arthritis of the left hip in a 2-year-old child with fever and a limp.
 AP Radiograph shows marked asymmetry of the hip joint spaces, with the left being greater than the right.

Legg-Calve-Perthes Disease

Legg-Calve-Perthes disease is idiopathic avascular necrosis of the femoral head. It occurs most commonly in children between the ages of 5-8 who present with knee or hip pain or a limp. Boys are more commonly affected than girls (5:1). The disease is bilateral in approximately 15% of cases. A good prognostic indicator in Legg-Calve-Perthes disease is the age of onset because if it occurs by age six, then restoration of the spherical femoral head is likely and degenerative osteoarthritis can be avoided.

Early radiographic findings:

- widening of the joint space: secondary to effusion or hypertrophic synovium
- *crescent sign*: subchondral linear lucency representing a fracture through necrotic bone (best seen on frogleg view)
- MRI: high-signal marrow edema on T2WI
- bone scan: decreased activity in the capital femoral epiphysis early and increased activity during healing

Chronic findings:

- fragmentation and/or collapse of the femoral epiphysis with areas of increased sclerosis and lucency
- coxa magna = broad overgrown femoral head
- coxa plana = flat femoral head
- short femoral neck
- arrest of physeal growth



Legg-Calve-Perthes disease in a 6-year-old boy.

AP pelvic radiograph shows irregularity in contour of the right femoral head and widening of the right joint space as compared with the normal findings on the left.



Legg-Calve-Perthes disease in a 6-year-old boy.

Coned-down frogleg view of the right hip shows a crescentic subchondral lucency consistent with a fracture through necrotic bone.



Legg-Calve-Perthes disease in a 6-year-old boy.

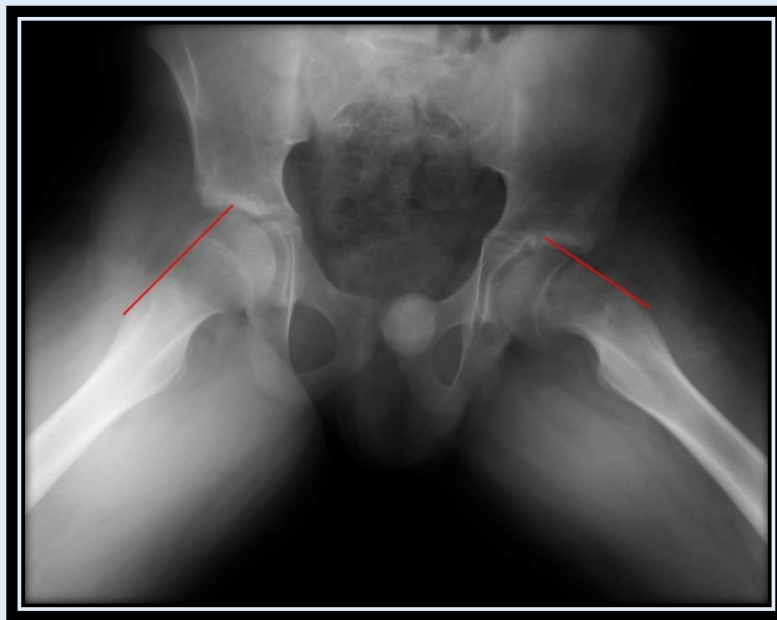
Coned-down AP view of the right hip demonstrates the progression of this disease. Note how the femoral head has become markedly flattened (coxa plana) and enlarged (coxa magna).

Slipped Capital Femoral Epiphysis

Slipped Capital Femoral Epiphysis (SCFE) is a Salter-Harris Type I fracture through the physal plate of the proximal femur resulting in displacement. It should be suspected in any adolescent who complains of hip or knee pain. It is twice as common in males (12-15 years) than females (10-13 years). Predisposed risk factors include obesity, renal osteodystrophy, and endocrine disorders including hypothyroidism and hypopituitarism. Bilateral involvement of the hips can be seen in 20-30% of patients, but it is unusual to present at the same time.

Displacement of the femoral head is posteromedial and often difficult to see on a standard AP film. Findings on AP film can include asymmetric physal widening and/or an indistinct metaphyseal border at the level of the physis. Frogleg lateral views are often essential for diagnosis as minimal slippage can be better appreciated. Here, one can appreciate the posterior displacement of the epiphysis in relation to the metaphysis. On frogleg views, a line drawn tangential to the lateral cortex of the metaphysis should bisect a portion of the ossified epiphysis. If the epiphysis is medial to this tangential line, SCFE is the diagnosis.

SCFE is typically treated surgically with pin fixation (done at current location) to prevent further slippage. Potential complications include avascular necrosis and chondrolysis.



Slipped Capital Femoral Epiphysis in a 13-year-old male.

AP and frogleg views demonstrate widening of the left proximal femoral physis. There is medial and dorsal displacement of the capital femoral epiphysis.

On the frogleg view, the line drawn tangential to the lateral cortex of the left metaphysis does not bisect any portion of the ossified left epiphysis (compare with a similar tangential line on the contralateral side).

Note the assymetric appearance of the left acetabulum and the irregularity of the femoral neck adjacent to the physis.

The Pediatric Lower Extremity

In this section, we will briefly discuss three entities which are commonly found upon examination of the lower extremity.

Knee disorder:

- Osgood-Schlatter disease

Foot disorders:

- clubfoot
- tarsal coalition

Osgood-Schlatter Disease

Osgood-Schlatter disease is an avulsive injury of the patellar tendon at its distal attachment to the tibial tuberosity which results in a painful tibial tuberosity. The condition is most prevalent in pre-adolescent boys (5:1 boys > girls).

The radiologic findings of Osgood -Schlatter disease include:

- soft tissue swelling about the patellar tendon
- thickened patellar tendon
- loss of infrapatellar fat pad
- irregularity of the tibial tuberosity



Osgood-Schlatter disease in a 13-year-old girl.

A lateral view of the left knee shows fragmentation of the tibial tubercle with displacement of the tibial tubercle fragments. Also note the soft tissue swelling inferior to the patellar ligament.

Clubfoot

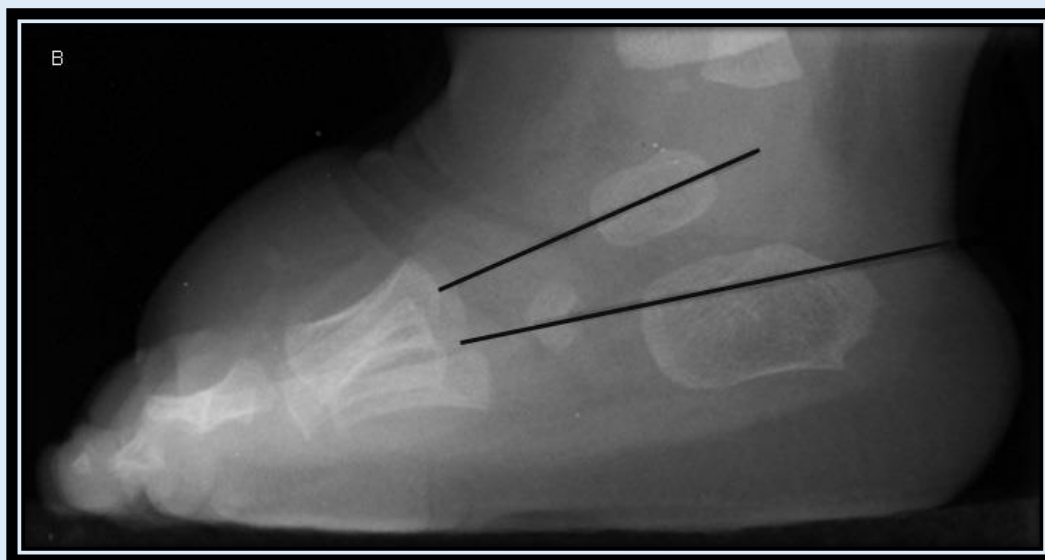
Clubfoot, or talipes equinovarus, is a relatively common congenital abnormality with a frequency of roughly 1:1000. Males are affected twice as often as females. It is bilateral in about half of the cases. Clinically the foot is plantar flexed, the forefoot is medial and the sole faces inwards. Standard radiographs include AP and lateral weight-bearing films. These XR's are utilized in surgical planning.

The four main components of clubfoot are:

1. hindfoot varus (calcaneus is too far medial)
2. equinus heel (fixed plantar flexion of the heel)
3. metatarsus adductus (adduction of the metatarsals with forefoot varus)
4. talonavicular subluxation

Radiographic characteristics include:

- hindfoot varus - decreased AP talocalcaneal angle, < 20 degrees
- equinus heel - decreased lateral talocalcaneal angle, < 35 degrees (the talus and calcaneus are nearly parallel); increased lateral tibio-calcaneal angle, > 90 degrees
- metatarsus adductus - medial displacement of the first metatarsal relative to the long axis of the talus
- talonavicular subluxation - medial subluxation of the navicular with respect to the talus



Talipes Equinovarus in a 2-year-old male.

A: Frontal view of the right foot shows hindfoot varus with a decreased AP talocalcaneal angle of 17 degrees. There is also forefoot varus - the line through the long axis of the talus lies lateral to the first metatarsal and actually bisects the third metatarsal shaft.

B: Lateral view shows a decreased lateral talocalcaneal angle of 11 degrees - the talus and calcaneus are nearly parallel. Equinus heel is also present with the hindfoot plantarflexed in relation to the tibia.

Tarsal Coalition

Tarsal coalition is a congenital fusion of two of the tarsal bones of the foot. This union can be either a complete or partial bony fusion, or a cartilaginous/fibrous fusion. Tarsal coalition will often manifest itself as chronic foot pain, and most patients will present during adolescence.

The two most common forms of tarsal coalition are:

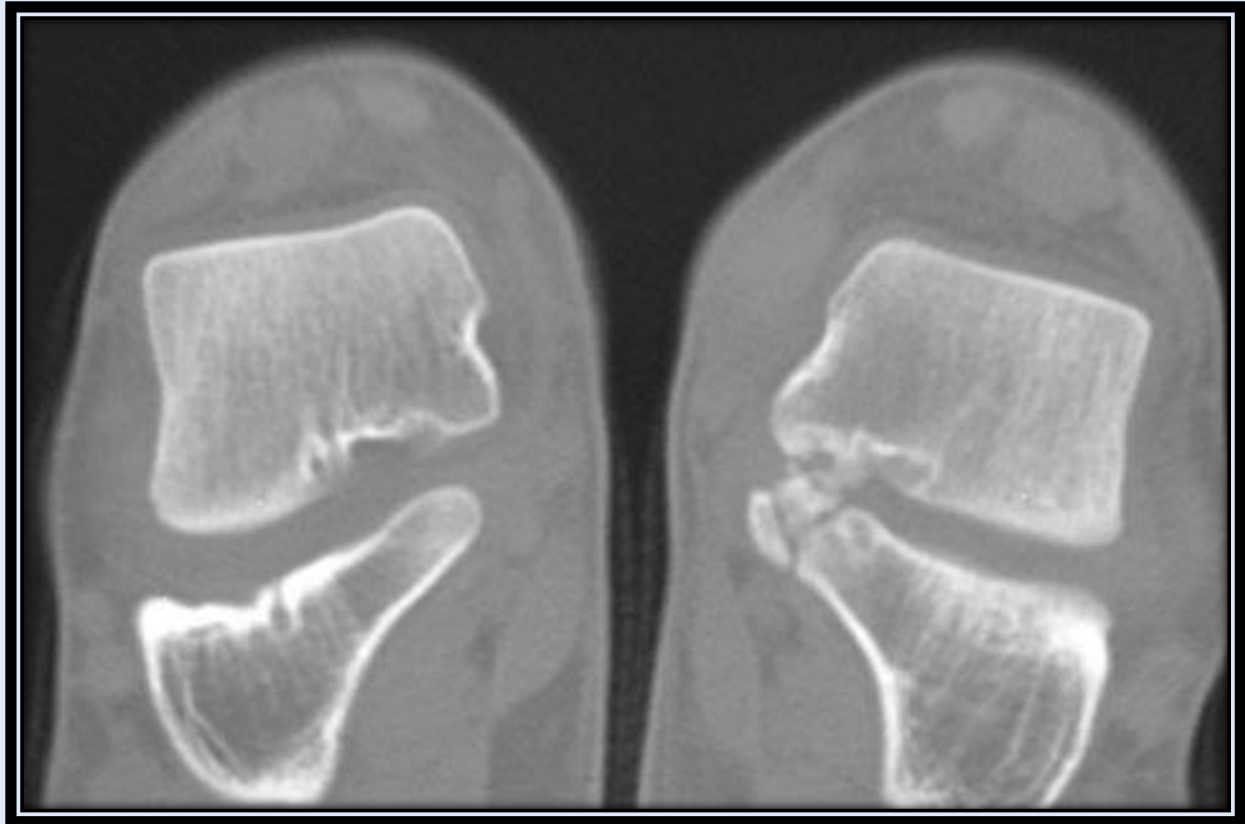
1. ***calcaneonavicular*** (most common) - best seen on oblique view => either a direct connection (bony coalition) or close proximity with irregular joint margins (fibrous coalition) can be seen between the calcaneus and the navicular bones; on lateral view => anterosuperior aspect of calcaneus appears to extend further than normal ("beaking") towards the navicular bone.
2. ***talocalcaneal*** - more subtle on plain films - CT is often necessary to make the diagnosis; plain film (lateral) findings include talar beaking, poor visualization of talocalcaneal joint, and a C-shaped band of overlapping bone noted over the calcaneus; coronal CT views will show evidence of bony or fibrous fusion between the middle facet of the talus and the sustentaculum tali of the calcaneus.

Treatment may include surgical repair/division of the coalition.



Calcaneonavicular coalition in an 11-year old male.

Top, Lateral radiograph shows the superior calcaneus to be elongated. Bottom, Oblique radiograph demonstrates fibrous coalition with close proximity and irregularity of the margins of the calcaneonavicular joint.



Talocalcaneal Coalition in an 11-year-old male.

Coronal CT demonstrates an ossified coalition at the sustentacular articulation of the calcaneus with the talus.

Benign Lesions

The benign lesions covered in this section include:

- distal femoral metaphyseal irregularity
- benign cortical defect
- osteoid osteoma
- osteochondroma
- enchondroma
- fibrous dysplasia

Distal Femoral Metaphyseal Irregularity

Distal femoral metaphyseal irregularity (*cortical desmoid*) is an irregular cortical margin with an associated lucency found in the posteromedial aspect of the distal femoral metaphysis. It is thought to be an avulsion off the medial supracondylar ridge of the distal femur. These lesions may or may not be associated with pain. They are primarily found in young boys > young girls (found in up to 10% of boys aged 10-15 years). The lesions are often bilateral.

Radiographic findings:

- cortical irregularity along the posteromedial cortex of the distal femoral metaphysis
- associated lucency on frontal view (often)
- periosteal new bone (often)

Familiarity with the appearance and location of the lesion as well as the patient's age are helpful in differentiating this benign process from an aggressive malignancy. Obtaining plain films of the contralateral knee to look for bilateral lesions can also aid in determining the benign nature of these lesions, as can a CT. *Biopsy should **not** be performed on these lesions.*



Distal femoral metaphyseal irregularity in a 7-year-old female.

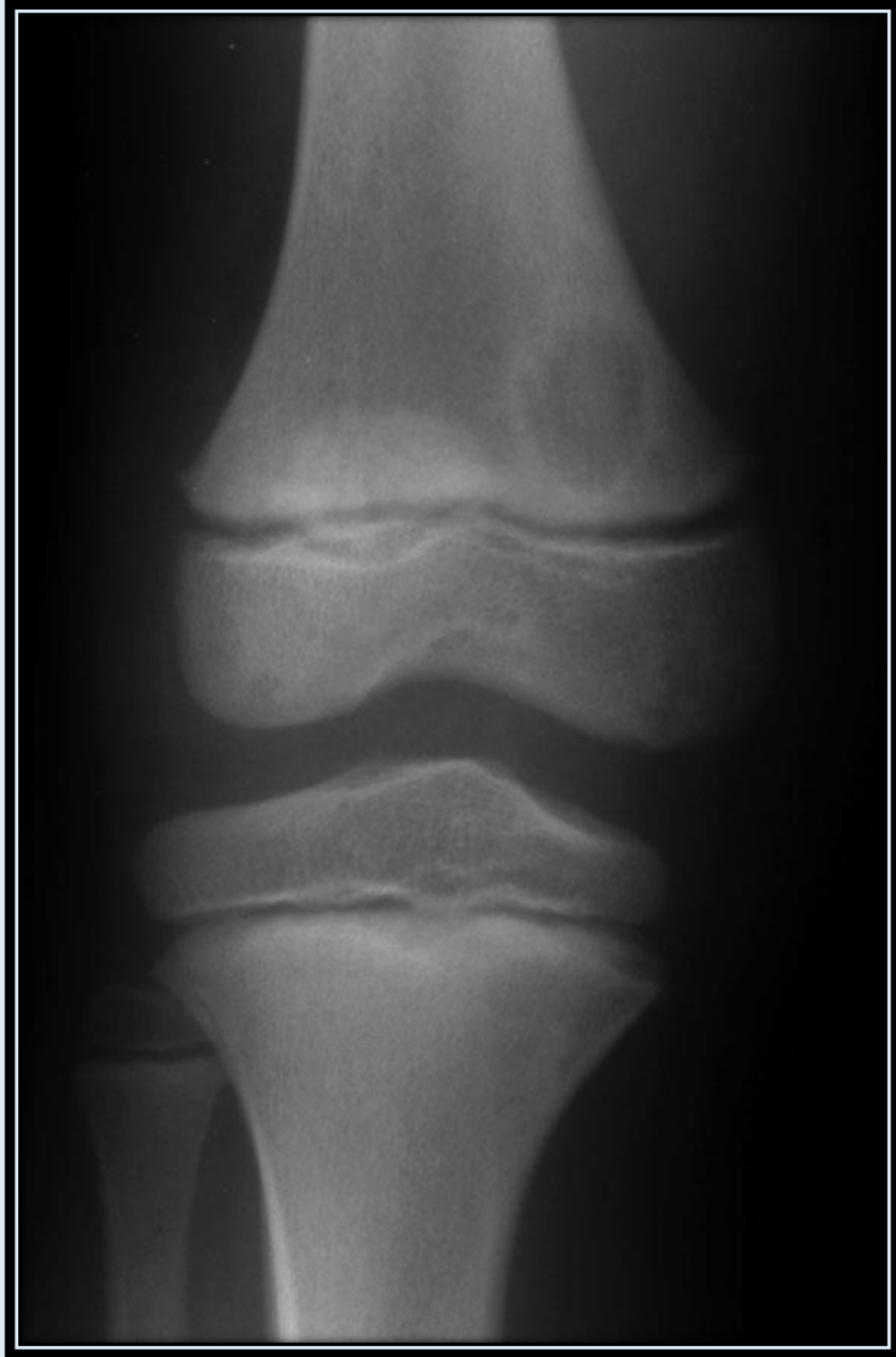
A, Frontal radiograph shows a well-defined, eccentric lucency (arrow) of the distal medial right femoral metaphysis. **B**, Lateral radiograph demonstrates a focal cortical irregularity (arrow) in the posterior aspect of the distal femoral metaphysis with adjacent periostitis. **C**, Axial MRI shows posteromedial cortical irregularity with associated periosteal reaction. **D**, Sagittal MRI localizes the defect to the femoral origin of the gastrocnemius muscle (medial head).

Benign Cortical Defect

Benign cortical defects are seen in up to 40% of all children at some time in their development. They are most prevalent in children between ages 4-6. The term *non-ossifying fibroma* is used for lesions >2 cm. They are found emanating from the cortex of long bone metaphyses. The most common location is the distal femur.

Radiographically, these lesions appear as lucent, eccentric, well-defined lesions with a thin, sclerotic border. They are typically round or oval in shape.

These lesions are not painful, do not exhibit periostitis, and they usually spontaneously regress over time.



Benign Cortical Defect in a 7-year-old male.

AP view of the right knee shows a radiolucent defect in the distal femoral metaphysis measuring 2cm X 1cm. Note the slight sclerotic margin surrounding the lucency.



Non-ossifying fibroma in an asymptomatic 8-year old male. AP radiograph of the right knee demonstrates a multilocular, expansile, well-defined lytic lesion in the medial supracondylar ridge of the femur.

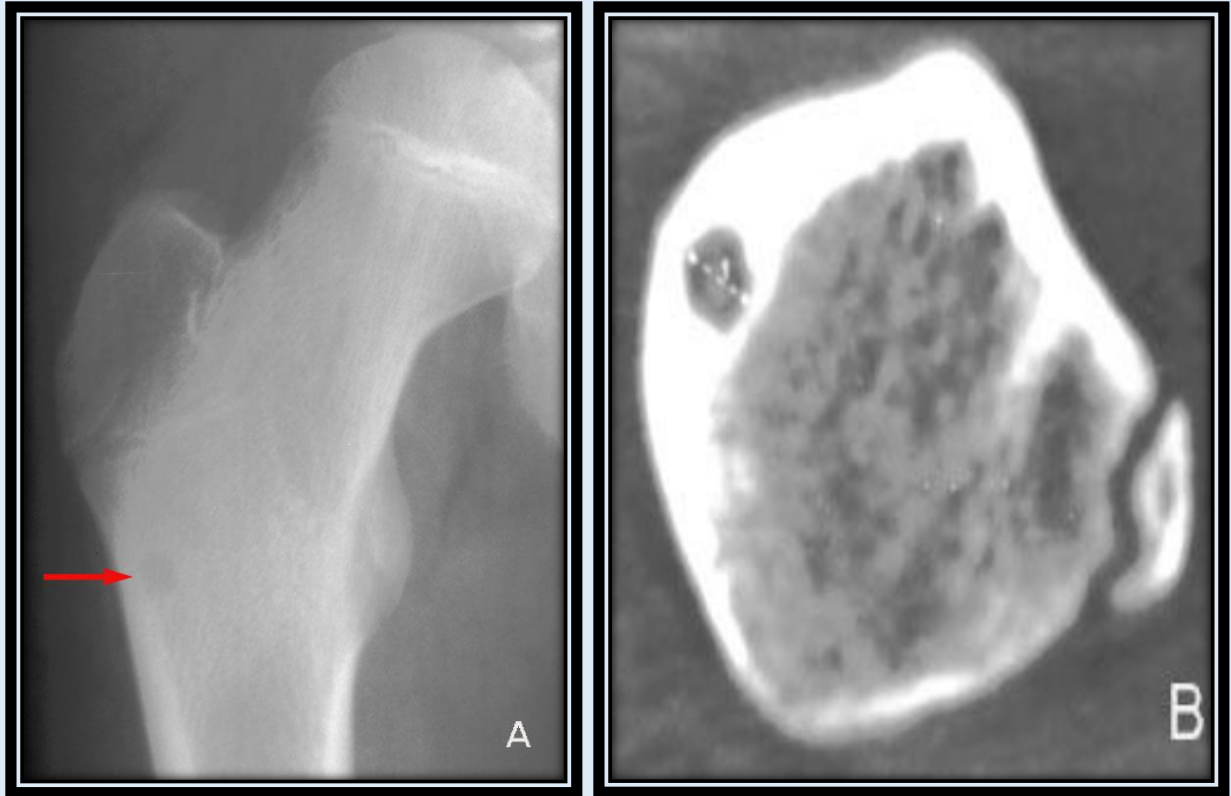
Osteoid Osteoma

Osteoid osteoma is a benign osteogenic tumor that usually manifests itself in patients during their second decade of life (boys > girls). The patients usually present with pain, which is worse at night and is relieved by aspirin. It is most commonly found intracortically within the metadiaphyses or diaphyses of the long bones of the lower extremity (femur > tibia). It can also present in the hands and feet.

Radiographic findings:

- plain film - lucent cortical nidus (typically < 1.5 cm) with surrounding area of sclerosis; the classic punctate radiodensity within the area of lucency is often difficult to visualize due to associated sclerosis.
- CT - better visualization of the central nidus (used for detailing exact location)
- MRI - extensive reactive bone marrow
- bone scan - "double density sign" of abnormally increased uptake by the surrounding sclerotic bone with an even more intense increased uptake by the central nidus.

Treatment: surgical excision or CT-guided percutaneous ablation.



Osteoid Osteoma in a 14-year-old male with hip pain.

A, AP radiograph of the right hip reveals a 1cm round, well-defined lytic lesion (arrow) just inferior to the greater trochanter. Note the associated sclerosis in the intertrochanteric region.

B, CT demonstrates a calcified central nidus within the lytic lesion. Again, appreciate the sclerotic cortical margin.

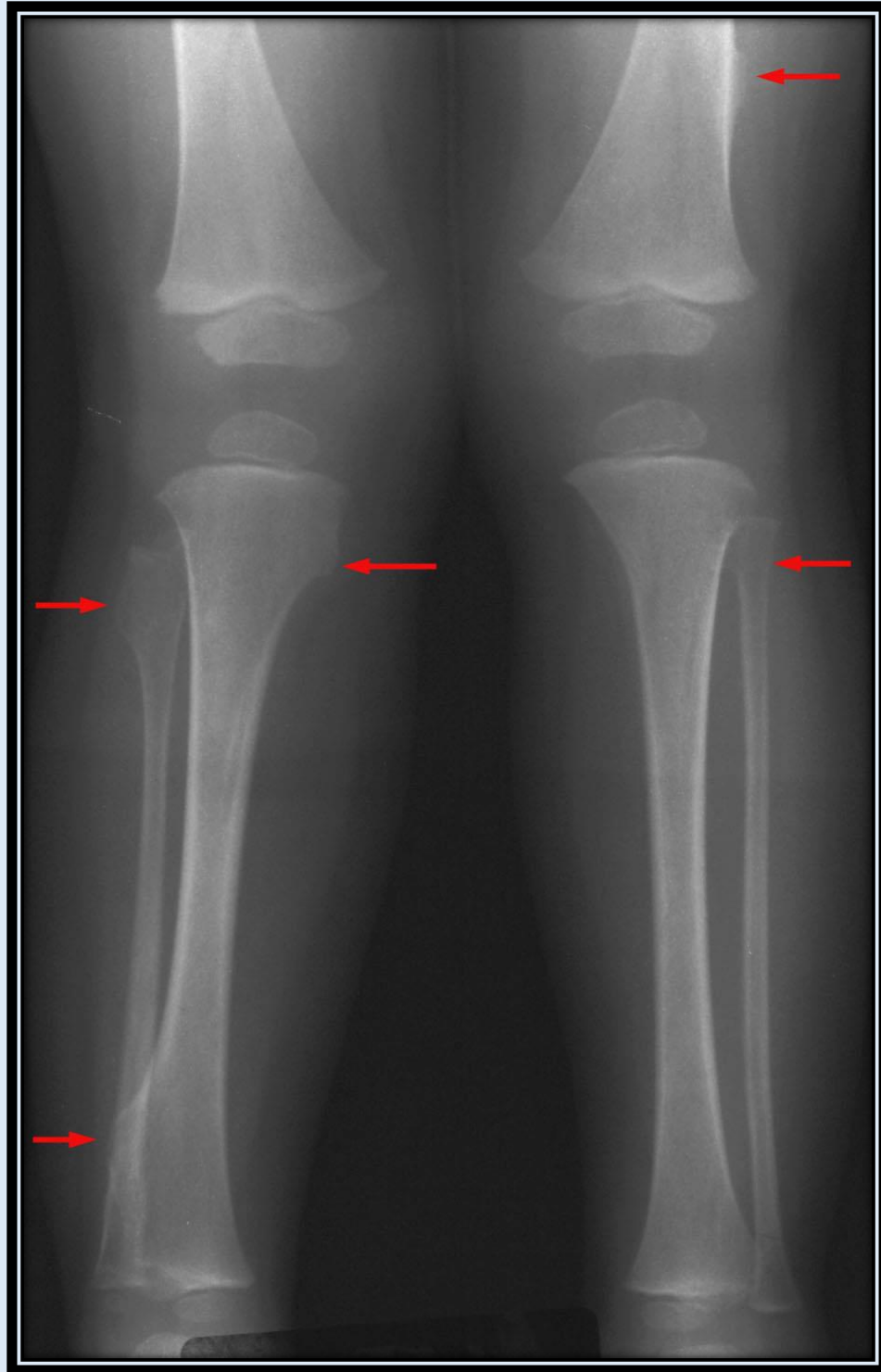
Osteochondroma

Osteochondroma is a painless, slow growing osteocartilaginous exostosis (cartilage-capped bony projection). Boys are affected twice as often as females. Growth arises from the metaphyses and the cortex of the lesion is continuous with the adjacent bone. Growth continues until the growth plate closes. These lesions are typically located on the tibia, femur and humerus and often will grow away from the joint.

Multiple hereditary exostoses (osteochondromatosis) is an autosomal dominant disease characterized by multiple, usually sessile, osteochondromas. The knee, ankle and shoulder are simultaneously affected.

Complications:

- severe growth abnormalities including bowing and other deformities as well as leg-length discrepancy (limb shortening)
- compression of adjacent vessels or nerves
- malignant transformation to chondrosarcoma (in as many as 20%)



Hereditary multiple exostoses in a 2-year-old female with multiple hard painless "lumps" near multiple joints. AP radiograph of the bilateral lower extremities shows exostoses (arrows) in the distal left femur, proximal left fibula, proximal right tibia and fibula, and distal right tibia.

Note how these lesions tend to point away from the nearest joint.

Enchondroma

Enchondromas are benign cartilaginous growths of the medullary cavity. Patients are typically 10-30 years old. Enchondromas are the most common benign cystic lesion to involve the phalanges, but they can appear in any bone formed from cartilage.

Radiographic findings:

- oval lucency, usually metaphyseal
- chondroid calcification (except in the phalanges)
- no periostitis

Ollier disease (enchondromatosis) is a non-hereditary condition in which patients have multiple enchondromas. The lesions can be unilateral or bilateral. With growth, these lesions may appear as "flame-shaped" linear configurations that are perpendicular to the physis. Patients often have hand and foot deformities, and are at an increased risk for malignant degeneration to chondrosarcoma.

Maffucci disease is a non-hereditary multiple enchondromatosis associated with multiple soft-tissue hemangiomas (phleboliths may be seen in soft-tissue masses on plain film). Patients with this condition have a higher rate of transformation to chondrosarcoma than patients with Ollier disease. Moreover, they are at an increased risk for malignancies of the abdomen and CNS.



Enchondromatosis (Ollier disease) shown as multiple lucent lesions.

AP radiograph of the left tibia and fibula demonstrates multiple enchondromas in the proximal and distal metaphyses. These lesions have a flame-shaped appearance that run perpendicular to the physes.



Enchondromatosis (Ollier disease) shown as multiple lucent lesions.

Radiograph of the left hand shows multiple enchondromas involving the phalanges of the first and second digits as well as the metacarpal of the first digit.

Fibrous Dysplasia

Fibrous dysplasia is a developmental disorder in which medullary bone is replaced by fibrous tissue and abnormal bone. It typically occurs in children between the ages of 5 and 20 and is often associated with endocrine disorders like hyperthyroidism and hyperparathyroidism. This disorder is associated with a very low risk of malignant transformation.

There are two types of fibrous dysplasia:

1. *Monostotic fibrous dysplasia* (85%) - predilection for ribs, femur and skull
2. *Polyostotic fibrous dysplasia* (15%) - typically in younger children (mean age = 8 years); likely to involve pelvis with concurrent involvement of ipsilateral proximal femur; also found in proximal femur (without pelvic involvement) and in tibia.

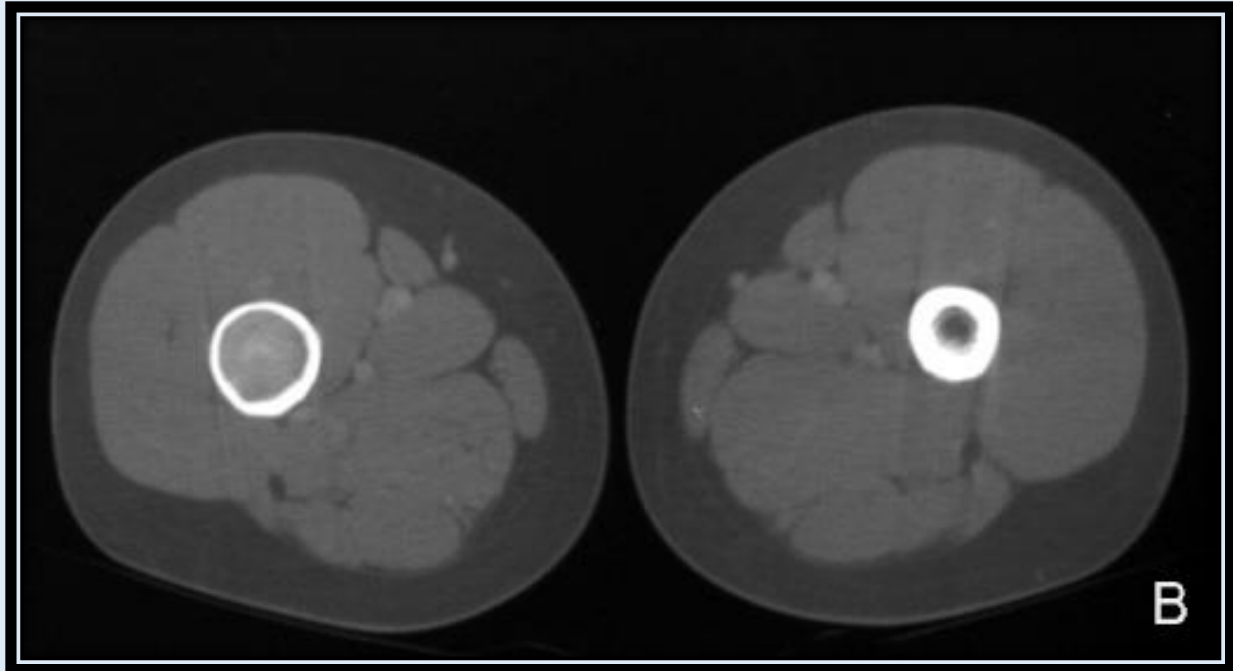
McCune-Albright Syndrome - triad of features include:

- polyostotic, usually unilateral, fibrous dysplasia
- endocrine abnormalities (precocious puberty, hyperthyroidism)
- cafe au lait spots



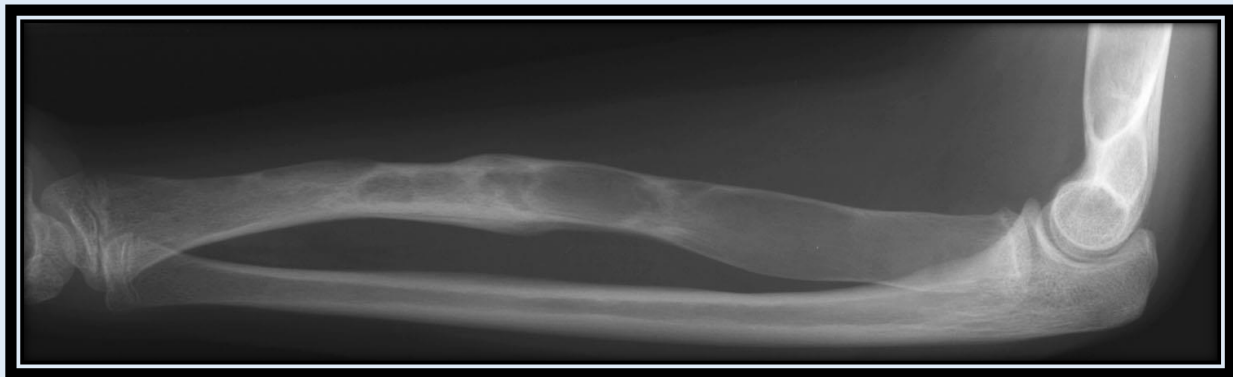
Fibrous Dysplasia of femoral metaphysis in an 8-year-old girl.

A, AP view shows an expansile lesion in the metaphysis of the right femur. This lesion exhibits some scalloping of the intracortical margin with a ground-glass appearance. A pathologic fracture is seen across the distal femoral neck.



Fibrous Dysplasia of femoral metaphysis in an 8-year-old girl.

B, CT through bilateral femurs shows thinning of the cortex and abnormal increased density within the medullary cavity. CT numbers measured 150 Hounsfield units in the right medullary cavity versus 23 (normal) on the left.



Polyostotic fibrous dysplasia in an 11-year-old female with precocious puberty (McCune-Albright syndrome).

Plain film of left forearm shows a "ground glass" geographic lesion in the radius consistent with fibrous dysplasia. Note the healing pathologic fracture in the mid-shaft. A similar ground glass lesion was noted in the patient's left humerus, the distal aspect of which can be seen on this film.

Aggressive Lesions

Aggressive lesions that are discussed in this section include:

- Osteomyelitis
- Newborn Periosteal reaction
- Langerhans Cell Histiocytosis
- Ewing Sarcoma
- Osteosarcoma
- Metastatic Disease

Osteomyelitis

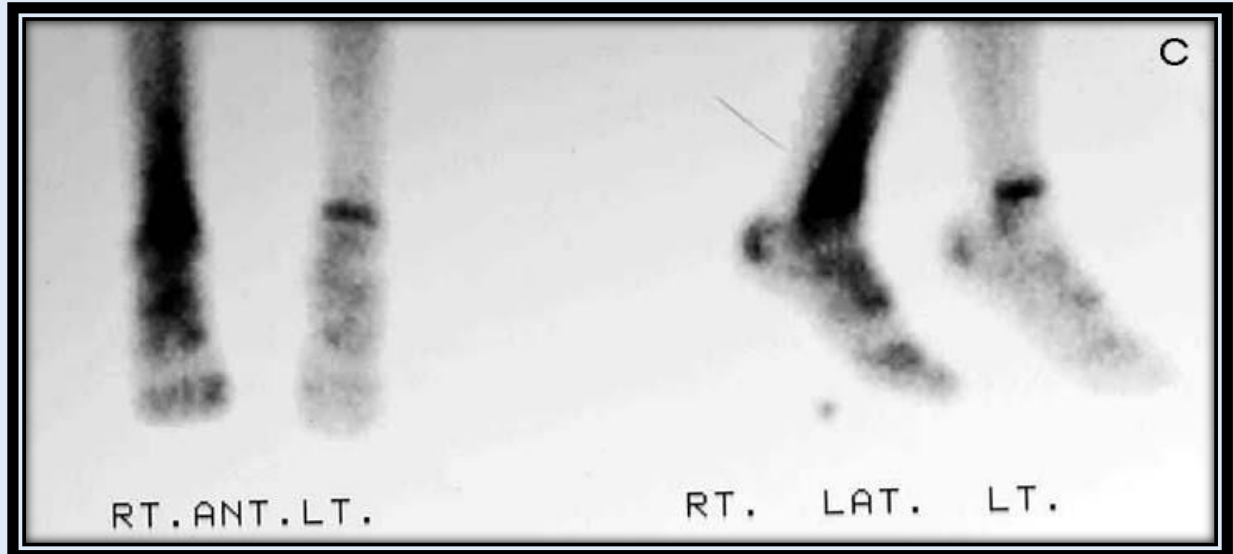
Osteomyelitis is a bacterial infection of bone that primarily affects infants and young children. 1/2 of all cases occur before 5 years of age with 1/3 of these cases occurring before age 2. Patients may present clinically with pain, fever, and elevated WBC and/or ESR. Many patients will have a history positive for a recent respiratory tract infection or otitis media (most cases of osteomyelitis in the pediatric population have a hematogenous etiology).

Osteomyelitis usually occurs in the metaphyses or metaphyseal equivalents in children. Roughly 75% of all infections will involve the long bones (femur > tibia > humerus), while the remaining 25% will involve the flat bones, in particular the hip.

Radiographic findings of osteomyelitis:

- *plain films*: deep soft-tissue swelling => displacement or obliteration of the the fat planes adjacent to the metaphysis (early finding); initial bony changes (i.e. loss of cortical white line with poorly-defined lucencies of the metaphysis) are not apparent until 7-10 days after the onset of symptoms; evidence of periosteal reaction becomes evident at about ten days; subacute and chronic changes include mixed bone lysis and sclerosis.
- *MRI* (most specific): cortical destruction of the metaphysis with bone marrow edema (high signal on T2WI) as well as surrounding soft tissue edema.
- *bone scan*: focal area of increased uptake in all three phases (angiographic/blood flow, soft tissue/blood pool, and skeletal phases); differs from cellulitis where there is increased activity in the blood flow and blood pool phases but a normal late phase.

* Evidence of osteomyelitis is seen on MRI and bone scans early after the onset of symptoms.



Osteomyelitis involving the tibia of a 10-year-old male with foot pain, fever, and elevated ESR. A, AP radiograph of the right leg demonstrates focal demineralization with sclerosis of the distal tibia. **B,** Sagittal T2WI reveals marrow edema in the distal tibia which crosses the physis to invade the epiphysis. **C,** Bone scan reveals increased tracer uptake in the right tibia compared with normal uptake on the contralateral side.

Newborn Periosteal Reaction

Newborn periosteal reaction can result from a host of underlying entities, which are included in the following table:

Etiologies for Periosteal Reaction in the Newborn
Physiologic growth
Prostaglandin therapy
TORCH infections
Non-accidental trauma
Caffey disease (<i>infantile cortical hyperostosis</i>)
Metastatic Neuroblastoma

Physiological periosteal new bone formation is seen in up to 1/3 of infants during the first few months of life. This type of periosteal reaction is benign in appearance and usually symmetric, involving the long bones (femur, tibia, and humerus). Radiographs demonstrate one or more dense lines of periosteal reaction along the diaphyses.

Prostaglandins are often used to maintain the patency of the ductus arteriosus in patients with congenital heart disease. Prominent periosteal reaction may be a sequelae from extended use of these therapeutic agents.

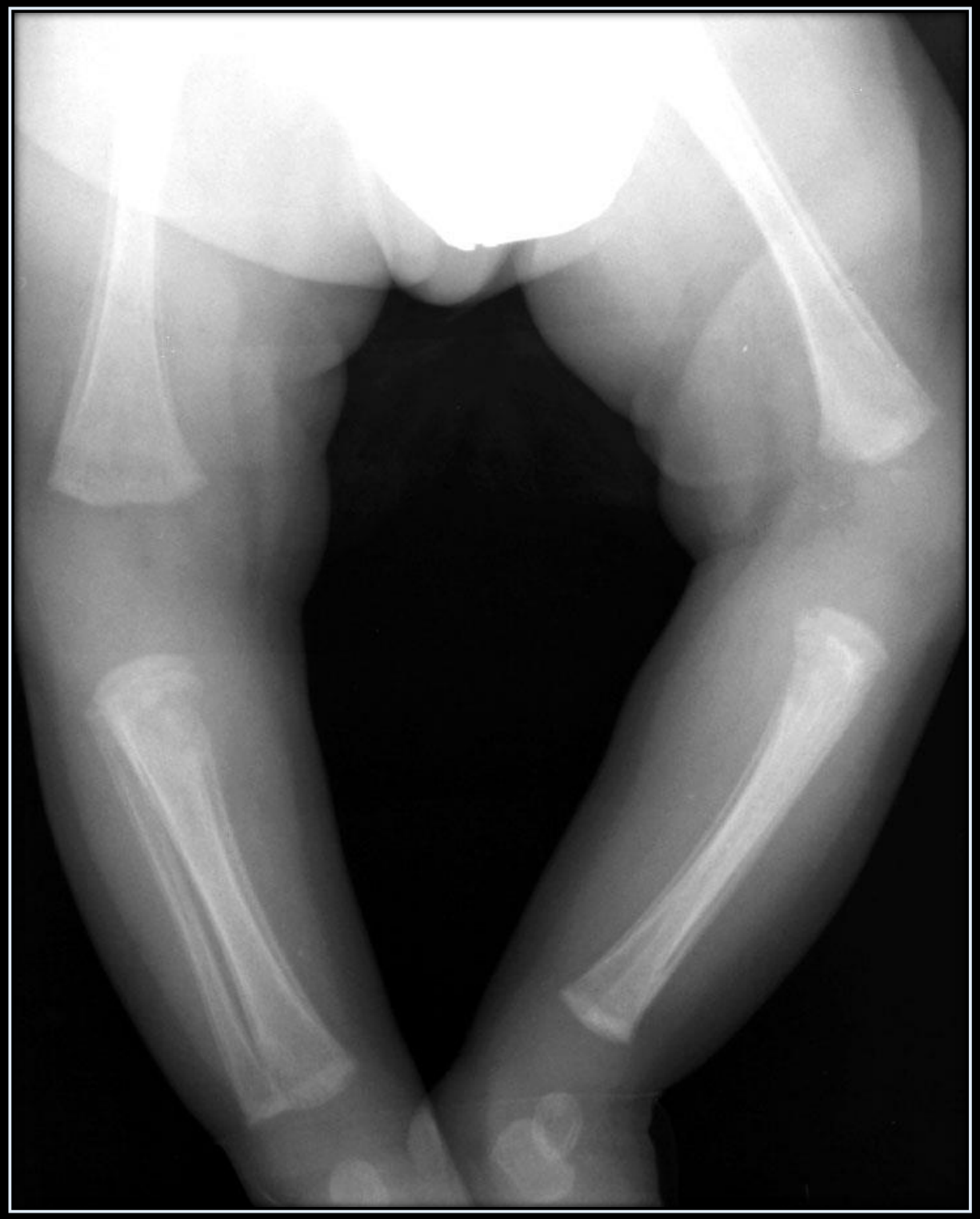
The TORCH infections are acquired either transplacentally or at birth. The mnemonic TORCH stands for:

- **T**oxoplasmosis
- **O**ther diseases (HIV, Syphilis)
- **R**ubella
- **C**ytomegalovirus (CMV)
- **H**erpes Simplex Virus (HSV)

Congenital rubella, acquired transplacentally, has musculoskeletal manifestations in about half of all cases. Radiographic findings include irregular, frayed long bone metaphyses with alternating longitudinal light and dark bands of density (the general appearance is said to resemble a "celery stalk").

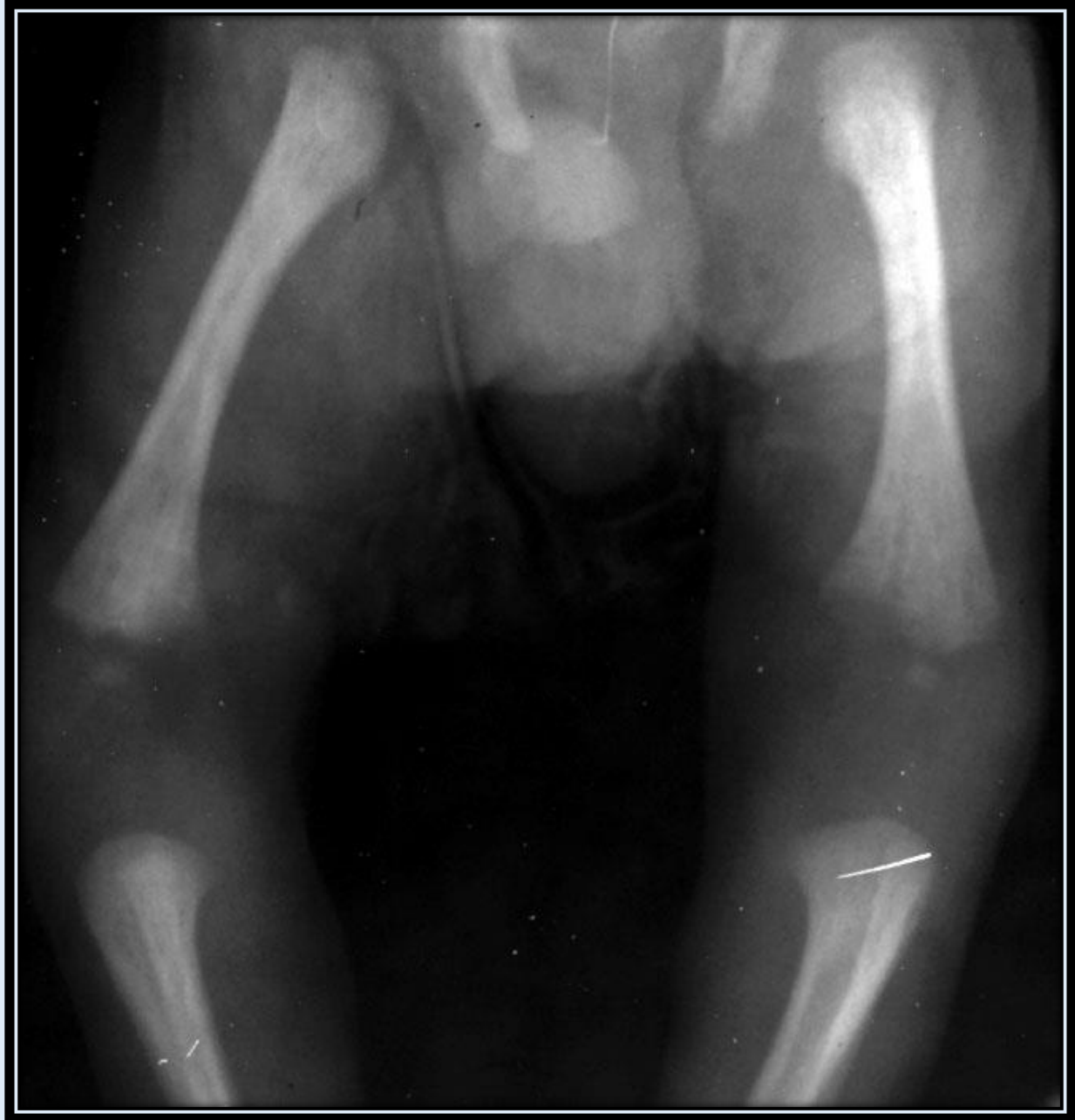
Congenital syphilis is also acquired transplacentally (during the 2nd or 3rd trimesters) but musculoskeletal involvement is much more common, roughly 95% of the time. Radiographic evidence of this condition include non-specific metaphyseal lucent bands with periosteal reaction involving multiple long bones. The *Wimberger corner sign*, thought to be specific to syphilis, is an area of irregular lucency resulting from destruction of the proximal medial tibial metaphysis.

Caffey disease (Infantile Cortical Hyperostosis) is an idiopathic condition manifested by periosteal reaction commonly involving the mandible, clavicles, ribs, humerus, ulna, femur, scapula, and radius. This syndrome usually occurs in the first few months of life and is self-limited. Radiographic findings include periosteal new bone formation, sclerosis, and adjacent soft tissue swelling.



Congenital syphilis in a 2-month old female.

AP radiograph of the bilateral lower extremities demonstrates marked periosteal reaction with destruction of the proximal medial tibial metaphyses (*Wimberger corner sign*).



Congenital rubella in a newborn male.

AP view of the lower extremities demonstrates metaphyseal fraying and longitudinal alternating radiolucent and radiodense stripes ("celery stalking")



Periosteal reaction from prostaglandin therapy in a 1-month old male.

AP radiograph of the distal right lower extremity shows diffuse periosteal reaction involving the tibia and fibula. This patient had a congenital heart disorder that required a patent ductus arteriosus for survival. Prostaglandin E1 was used for patency until surgical correction was performed.

Langerhans Cell Histiocytosis

Langerhans Cell Histiocytosis (LCH), previously known as histiocytosis X, is an idiopathic disease characterized by abnormal proliferation of Langerhans cells. The disease can exist along a spectrum from localized to systemic manifestations. The disease is more common in males > females (2:1), and more prevalent amongst the caucasian population.

Radiographic findings are highly variable; bony lesions may be sclerotic or lucent, have a sclerotic or poorly-defined border, and be permeative or geographic in appearance. The most common sites with radiographic findings are: skull > ribs > femur > pelvis > spine > mandible.

Classification is controversial but the 3 main clinical subtypes of LCH are:

Unifocal, previously known as *Eosinophilic Granuloma* - most common form with best prognosis; disease isolated to bone or lung; usually presents between 5 and 15 years of age

- punched-out lytic skull lesions
- vertebra plana (vertebral destruction with vertebral collapse)
- lytic lesions in other bones (e.g. mandible - destruction of alveolar bone causes the "floating teeth" appearance)

Multisystem, previously known as *Letterer-Sewe disease* - acute, diffuse, and often fatal; worst prognosis; usually presents before age 2

- rash
- hepatosplenomegaly
- lymphadenopathy
- pulmonary involvement
- marrow failure

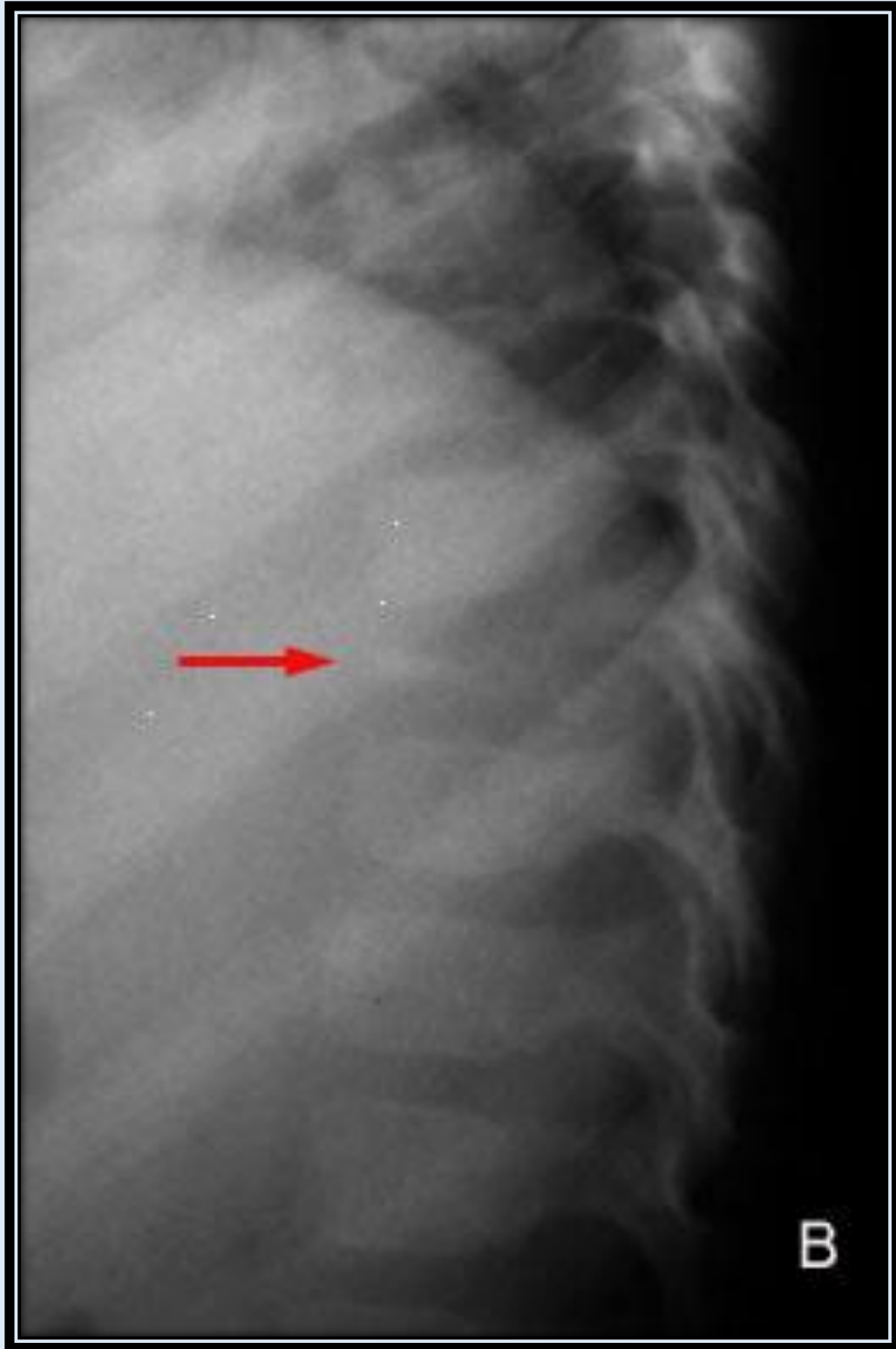
Multifocal, previously known as *Hand-Schuller-Christian disease* - chronic and diffuse with high morbidity; fatal in about 15% of patients; usually presents before age 5

- predilection for skull defects
- exophthalmos (from mass effect of orbital bone disease)
- diabetes insipidus (from basilar skull disease or infiltration of posterior pituitary)
- hepatosplenomegaly
- growth retardation



Langerhans Cell Histiocytosis in a 1-year-old male.

A, Lateral radiograph of the skull shows multiple well-defined lytic lesions "geographic skull"



Langerhans Cell Histiocytosis in a 1-year-old male.

B, Lateral radiograph of the thoracic spine demonstrates *vertebra plana* (vertebral destruction with vertebral collapse, arrow)



Langerhans Cell Histiocytosis in a 1-year-old male.

C, AP radiograph of the left distal extremity reveals a lytic lesion in the mid-shaft of the fibula.



Langerhans Cell Histiocytosis in a 4-year-old male.

A, AP view of the skull demonstrates multiple well-defined lytic lesions. Note the involvement of the right mandible as well.



Langerhans Cell Histiocytosis in a 4-year-old male.

B, AP radiograph of the pelvis shows lytic lesions (arrows) involving the iliac regions and the proximal femurs bilaterally.



A classic example of "floating teeth" in a child with Eosinophilic Granuloma.
Note the bilateral lytic lesions involving the mandible on this panorex view.

Ewing Sarcoma

Ewing sarcoma is a malignant tumor from undifferentiated mesenchymal bone cells. It is the second most common primary bone malignancy in children. It generally occurs in the second decade of life (mean age is 11 years). Males are affected twice as often as females. Patients will present with symptoms including pain, swelling, elevated WBC, elevated ESR, and occasionally fever.

Most common bone distribution: femur > pelvis > tibia > humerus > ribs

Radiographic findings include:

- "moth-eaten" appearance
- distribution in the long and flat bones
- lytic lesions with poorly defined margins and permeative pattern (these tumors can appear predominantly sclerotic in 15% of cases)
- "onion skin" periosteum (non-specific)
- large soft-tissue component

Most Ewing tumors are very radiosensitive; radiation therapy is the treatment of choice.

At the time of presentation, approximately one-third of patients will already have metastases to the lung, other bones, or lymph nodes. 5-year survival is 70% for localized disease and 30% for metastatic disease.



Ewing Sarcoma in a 15-year old male with recent onset of pain in the left leg.

AP radiograph of the left distal femur demonstrates widening with sclerosis. Note the elevation of the periosteum with laying down of calcification forming an "onion skin" appearance.

Osteosarcoma

Osteosarcoma (*osteogenic sarcoma*) is the most common primary bone malignancy in the pediatric population. It is more common in males, and patients most commonly present between the ages of 10 and 25. Osteosarcomas can arise from either the medullary cavity or the bony cortex (the periosteal and parosteal forms). The most common sites are the metaphyses of long bones, particularly around the knee (roughly 2/3 of all cases of osteosarcoma arise in the distal femur or proximal tibia).

Radiographic findings include:

- large, aggressive, eccentric lesion (can be either sclerotic, lucent, or both)
- lesions usually do not cross the physis
- **"moth-eaten"** appearance with **"sunburst"** periosteal reaction or classic *Codman triangle*
- pathologic fractures at time of presentation
- large soft tissue component

Plain films accurately depict the nature of the tumor, but MRI and CT are often used to determine the precise anatomic location and soft tissue extension.

Treatment includes surgical removal in conjunction with chemotherapy. Five-year survival is between 75-80%.

Osteosarcomas typically metastasize hematogenously to the lungs and other bones.



Osteosarcoma of the femur in a 13-year-old male.

AP radiograph of the right distal femur demonstrates a permeative destructive pattern in the distal femoral metaphysis. There is a soft tissue mass with non-specific ossification noted.



Osteosarcoma of the femur in a 14-year-old female.

Left, AP radiograph shows a permeative sclerotic lesion in the mid-diaphysis of the right femur. There is significant new bone formation and periosteal reaction. Note the *Codman triangle* (arrow). **Right,** Lateral radiograph demonstrating the overall extent of the lesion.

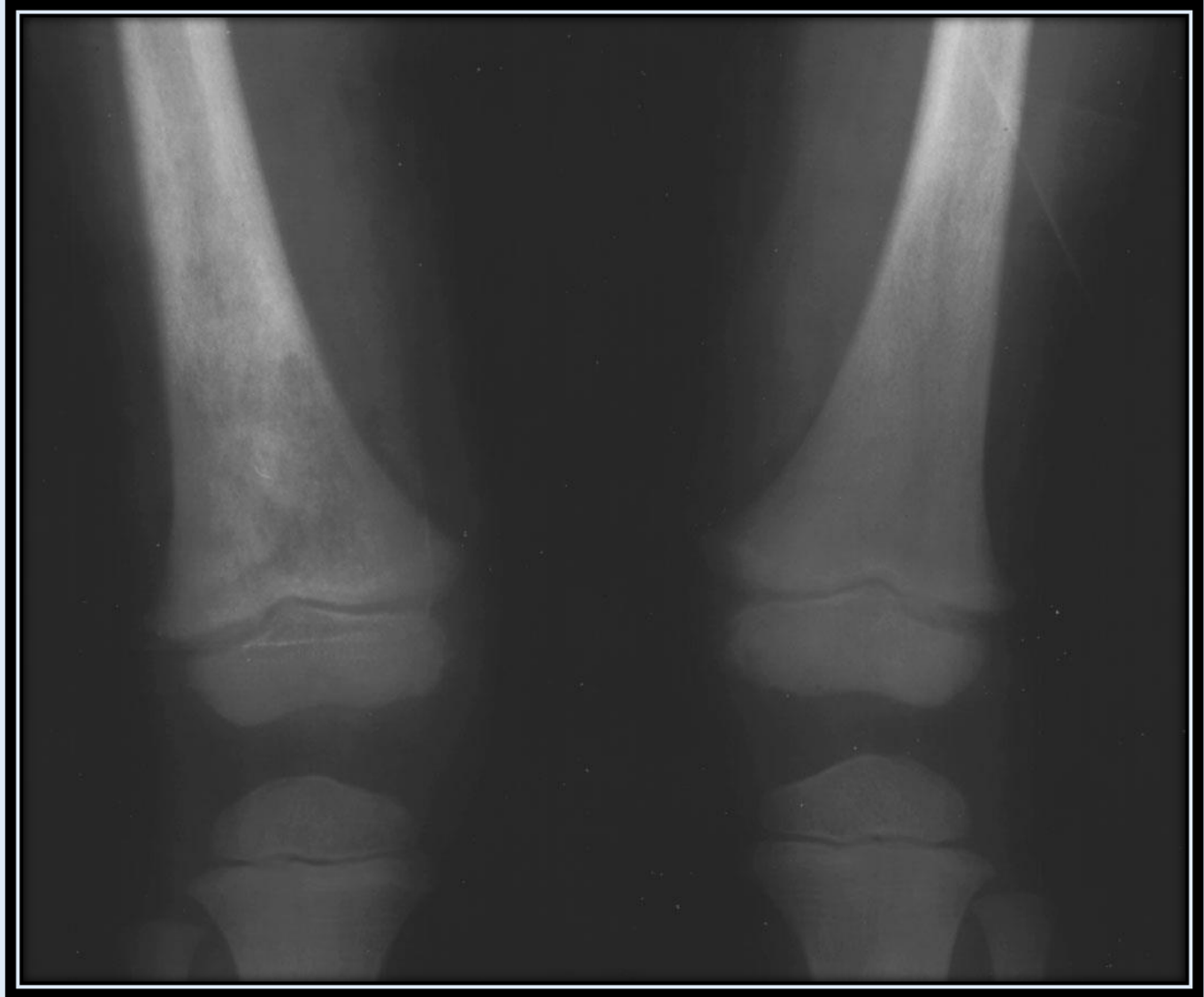
Metastatic Disease

In children, the most common primary malignancies to metastasize to bone include neuroblastoma and leukemia or lymphoma. Metastatic neuroblastoma should be at the top of the differential in a child < 5 years of age who presents with a neoplastic bony lesion (it is far more common than a primary bone lesion in this age group).

Leukemia and metastatic lymphoma have a predilection for the metaphyseal regions of long bones where they can cause bony destruction. Both will often present radiographically as lucent metaphyseal bands, which have been termed "leukemic lines."

Acute Lymphocytic Leukemia is the leading cause of cancer in the pediatric population. Radiographically detectable lesions are seen in up to one-half of all childhood leukemic cases. These lesions are not deemed metastases, but rather primary bone involvement from neoplastic proliferation of marrow elements.

Primary bone lymphoma is rare in children.



Metastatic neuroblastoma in a 2-year-old female who complained of pain in the right knee.
AP radiograph shows an asymmetric permeative lucency within the right distal femur.



Metastatic neuroblastoma in a 2-year-old female who complained of pain in the right knee.
Lateral view of the right knee shows the permeative process.



Acute Lymphocytic Leukemia in a 15-month-old male.
AP view of the left hip shows a lucent band in the proximal metaphysis.



Acute Lymphocytic Leukemia in a 4-year-old female.

AP view of the left knee shows a lucent band in the metaphysis with a sclerotic margin just proximal to the lucent band. Also note the irregularity of the metaphysis.

Constitutional Disorders of Bone

A *constitutional disorder of bone* is a developmental abnormality of bone which results in diffuse bony abnormalities. Germane to the discussion of constitutional bony disorders, the following are addressed in this section:

- skeletal dysplasias (achondroplasia)
- mucopolysaccharidoses
- osteogenesis imperfecta
- osteopetrosis
- neurofibromatosis
- Blount disease

Achondroplasia

There are a host of disorders that fall within the category of skeletal dysplasias. These dysplasias are usually categorized by comparing the relative shortening of the proximal versus the distal long bones (e.g. femur versus tibia or humerus versus radius). The various types of skeletal dysplasias include:

- *rhizomelia* - shortening of the proximal limb (humerus, femur) relative to the distal limb
- *mesomelia* - shortening of the middle limb (radius-ulna, tibia-fibula)
- *acromelia* - shortening of the distal limb (hands, feet) relative to the proximal limb
- *micromelia* - shortening of both the proximal and distal limbs

Achondroplasia, the most common of the skeletal dysplasias, is a rhizomelic growth deformity that results from abnormal bone formation at the growth plate. Achondroplasia is an autosomal dominant disorder with a lethal homozygous form and a heterozygous form that demonstrates the multiple clinical manifestations of the disease.

Radiographic imaging findings include:

- rhizomelic limb shortening
- craniofacial disproportion with large calvarium, diminutive skull base, small foramen magnum (may compress brainstem) and small jugular foramina
- shortened spinal pedicles distally with a decreased interpedicular distance (on AP films) in the inferior lumbar spine compared with the superior lumbar spine
- spinal stenosis (secondary to above)
- rounded iliac wings with decreased acetabular angles providing a "tombstone" appearance



Achondroplasia in a 10-year-old male.

A, AP radiograph of the pelvis demonstrates rounded iliac wings with decreased acetabular angles ("tombstone" appearance).



Achondroplasia in a 10-year-old male.

B, AP view of the spine shows a decrease in the interpedicular distance from the upper (L1) to the lower (L5) lumbar spine.



Achondroplasia in a 10-year-old male.

C, Lateral radiograph of the skull reveals a large calvarium with a diminutive skull base.



Achondroplasia in a 10-year-old male.

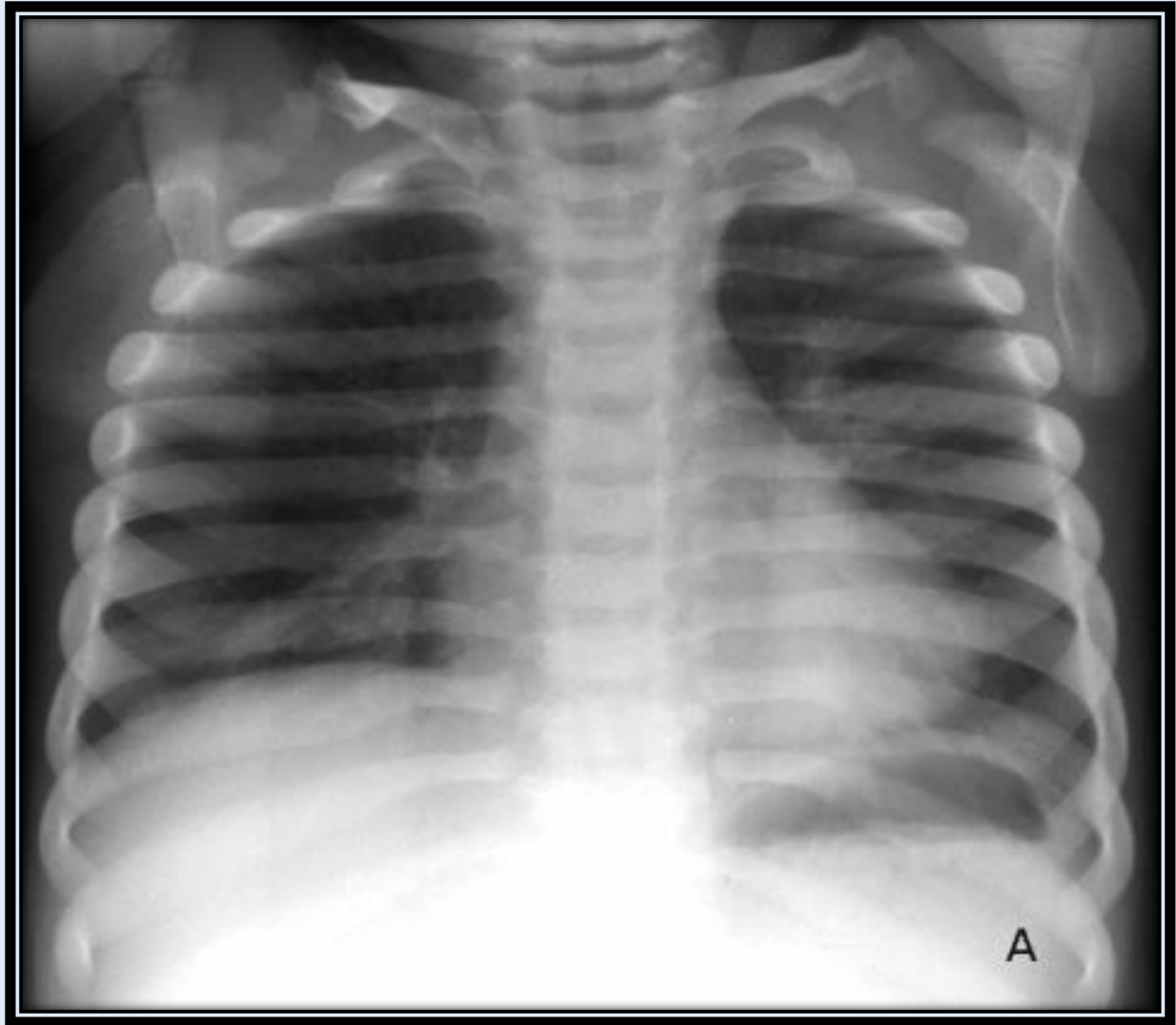
D, Radiograph of the right hand shows short, broad tubular bones.

Mucopolysaccharidoses (MPS)

The mucopolysaccharidoses are a group of lysosomal storage diseases characterized by the accumulation of excess glycosaminoglycans (GAGs). Included in this group of disorders are Hunter, Hurler, Morquio, and Sanfilippo syndromes. Associated skeletal deformities are similar throughout this group of diseases, and are collectively referred to as *dysostosis multiplex*. These deformities likely occur secondary to the accrual of GAGs in the chondrocytes, resulting in abnormal ossification.

Radiographic features of the mucopolysaccharidoses include:

- osteopenia
- thickened calvarium, particularly at the base
- vertebral body deformities - often oval-shaped with beaking of the anterior cortex (most prominent in lumbar region) - beak at midportion of vertebrae with Morquio syndrome but located more inferiorly with Hurler syndrome; posterior vertebral body scalloping may exist.
- thickened clavicles and ribs (ribs become narrower posteromedially => "canoe paddle" appearance)
- scoliosis
- lordosis
- pelvis has tall, flared iliac wings and increased acetabular angles (the opposite of achondroplasia)
- femoral epiphyseal dysplasia => coxa valga
- hands with proximal tapering of metacarpals and short, stubby phalanges



Radiologic manifestations in MPS found in a 2-year-old female with Hurler syndrome.

A, AP chest radiograph demonstrates thickened short clavicles, wide oar-shaped ribs, and elevation of the right hemidiaphragm likely secondary to recurrent atelectasis.

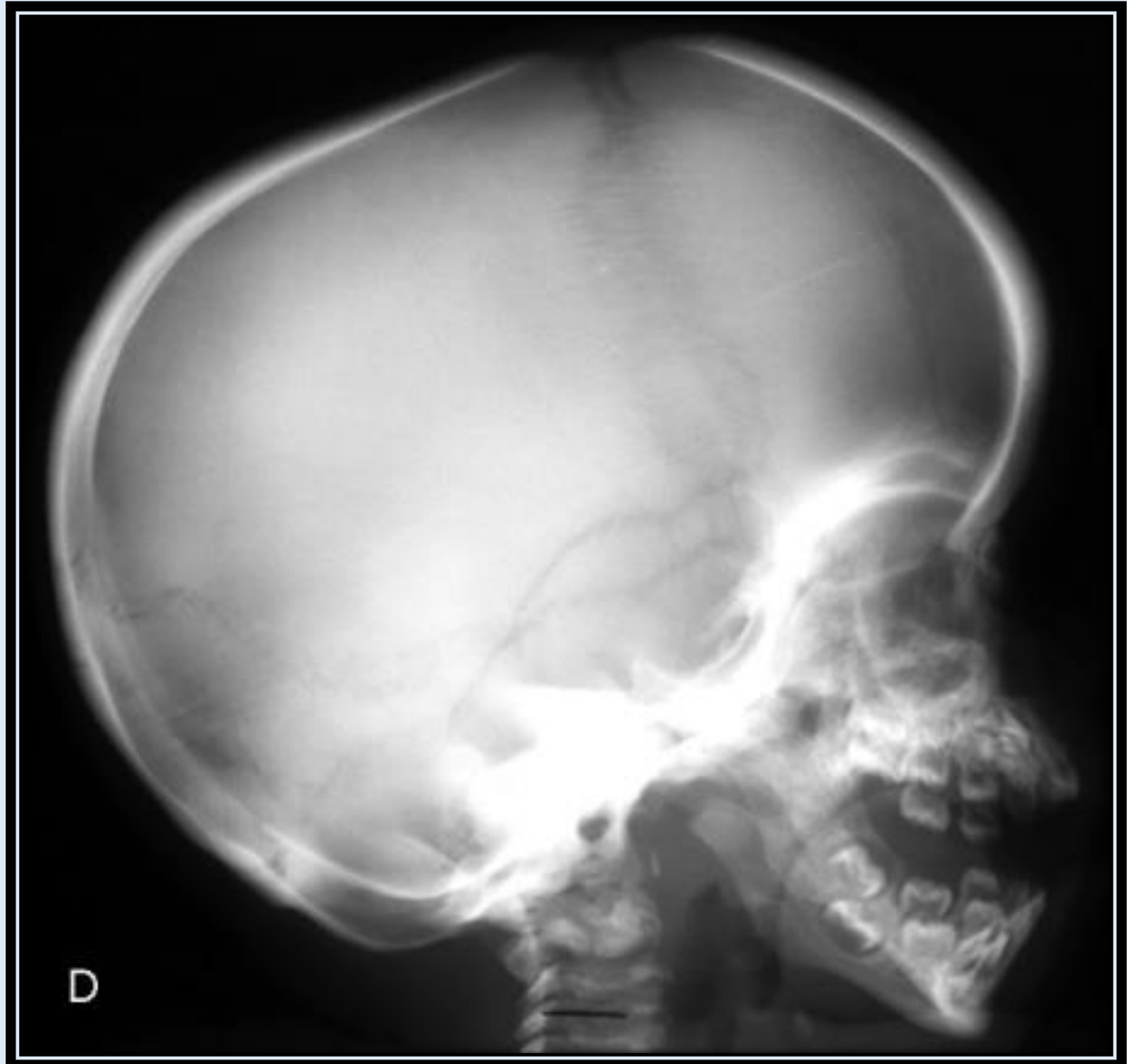


Radiologic manifestations in MPS found in a 2-year-old female with Hurler syndrome.
B, Lateral radiograph of the spine shows oval-shaped vertebrae with anteroinferior beaking.



Radiologic manifestations in MPS found in a 2-year-old female with Hurler syndrome.

C, Radiograph of the right hand reveals diaphyseal widening of the metacarpals, proximal phalanges, and middle phalanges; note the tapered ends of the proximal second through fifth metacarpals.



Radiologic manifestations in MPS found in a 2-year-old female with Hurler syndrome.
D, Lateral skull radiograph shows a thick calvarium, particularly at the base, with an enlarged J-shaped sella turcica.



Radiologic manifestations in MPS found in a 2-year-old female with Hurler syndrome.
E, AP radiograph of the pelvis demonstrates small, flared iliac wings with increased acetabular angles.

Osteogenesis Imperfecta

Osteogenesis Imperfecta (OI) is a group of hereditary disorders of type I collagen synthesis characterized by extremely fragile bones with a propensity to fracture. Often patients will present with multiple fractures at various stages of healing, which can be confused with non-accidental trauma. The underlying osteopenia and the fact that OI fractures tend to involve the diaphysis rather than the metaphyseal corners can help to distinguish the two entities.

Two major types:

1. Congenita (develops at or before birth) - autosomal recessive with frequency of 1:60,000
2. Tarda (develops later, less severe) - autosomal dominant with frequency of 1:30,000

Radiographic characteristics of OI:

- demineralization of the diaphyses of long bones with deformity/bowing and multiple fractures
- wormian bones of the skull
- vertebral bodies that are shallow, radiolucent, and bi-concave



Osteogenesis Imperfecta, congenital form.

Radiograph of the left upper extremity in a child reveals a pathologic fracture with healing resulting in a thick tubular bone.



Osteogenesis Imperfecta Tarda in a 15-year-old male.

Lateral radiograph of the right knee demonstrates marked cortical thinning with undertubulation of the long bones (gracile bones).

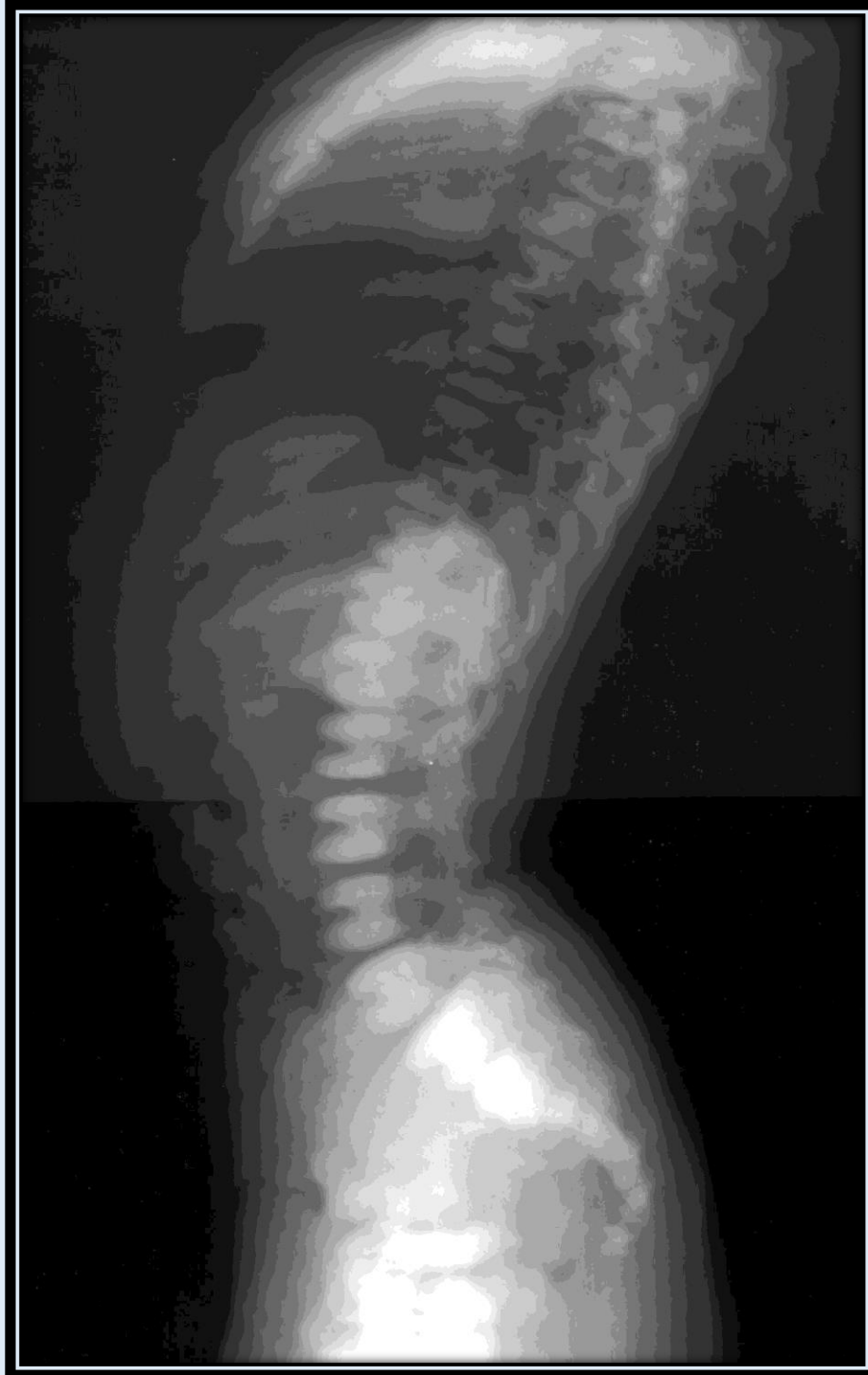
Osteopetrosis

Osteopetrosis is a rare inherited disorder of defective osteoclastic activity. The osteoclasts are ineffective at resorbing and remodeling bone. That is, as more bone is laid down, the calcified cartilage begins to encroach upon the marrow cavity and dense bony sclerosis develops. As a result of reduced marrow space, these patients often suffer from pancytopenia and develop hepatosplenomegaly and lymphadenopathy. The autosomal recessive form of the disorder is usually lethal whereas the autosomal dominant form is more compatible with life.

Despite their increased density, the bones are abnormally brittle and pathologic fractures are common in osteopetrosis. All bones may be affected. Thick lines of increased density are first seen in the metaphysis, which eventually extend throughout the bony shaft. It is thought that the disease process ceases from time to time during development, resulting in the classic "bone-within-bone" appearance.

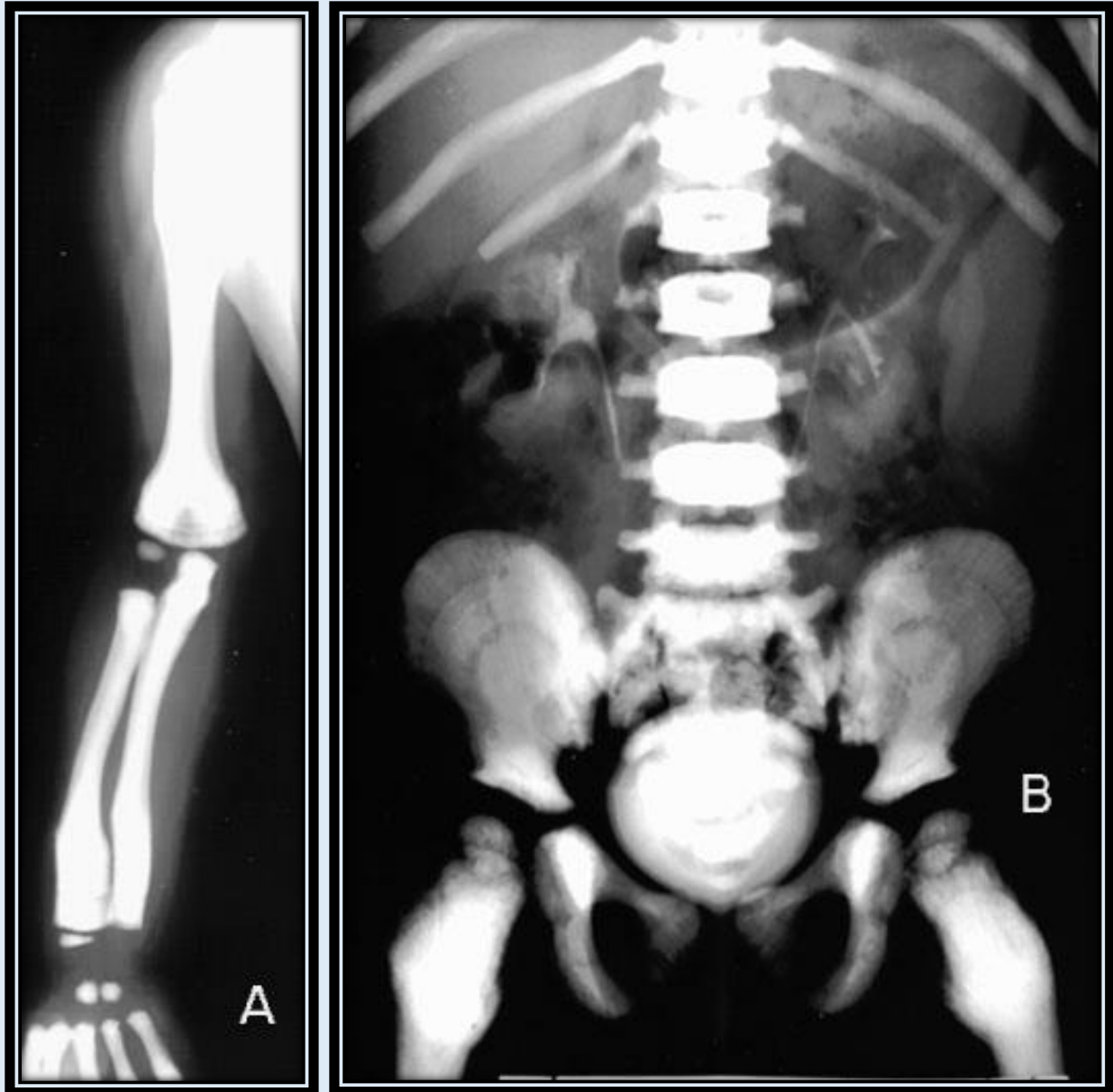
Radiographic findings:

- short, block-like radiodense bone
- widening of the epiphyses and metaphyses of long bones
- multiple fractures
- alternating sclerotic, osteopenic-appearing metaphyseal lines



Osteopetrosis in a 7-year-old female who presented with scoliosis.

Lateral radiograph of the spine reveals diffuse bony sclerosis involving the entire spine. The vertebral bodies show an asymmetry in the amount of increased bony density with the upper and lower end plates appearing more dense (like a sandwich).



Osteopetrosis in a 22-month-old male.

A, Radiograph of the right upper extremity demonstrates diffuse intense sclerosis of the long bones with obliteration of the marrow cavity. Note the short, block-like nature of these bones and the widened metaphyses (*Erlenmeyer flask* deformity).

B, AP radiograph of the pelvis again shows diffuse sclerosis throughout the spine, pelvis, and femurs. There is a characteristic "bone-within-bone" appearance, seen best in the iliac crest.

Neurofibromatosis

Neurofibromatosis is the most common neurocutaneous syndrome. This disorder is subdivided into multiple categories, the most prevalent of which are Type 1 (NF1 or Von Recklinghausen disease) and Type II (NF2). NF1 is an autosomal dominant disorder characterized by cafe-au-lait spots, axillary or inguinal freckling, optic gliomas, and plexiform neurofibromas. Musculoskeletal abnormalities include bony overgrowth, bowing, sclerotic changes, and cortical defects.

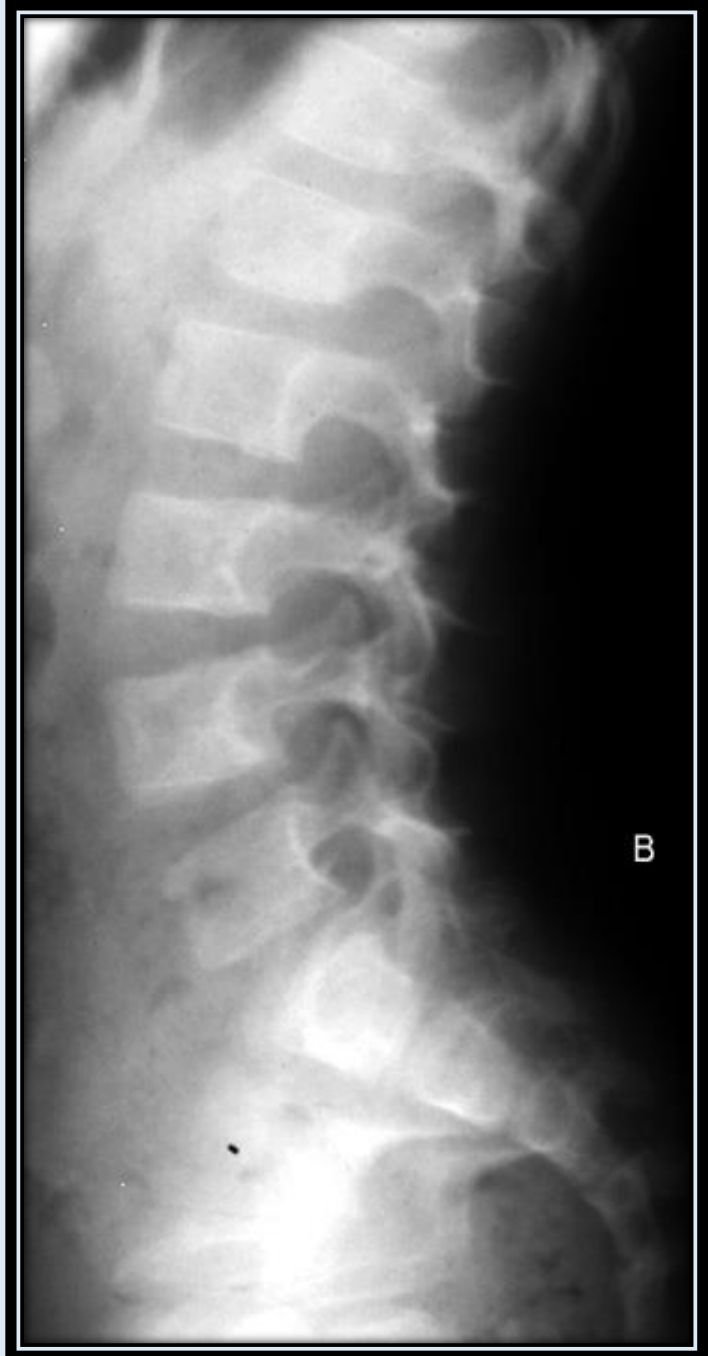
Characteristic findings include:

- pseudarthrosis formation (especially of the tibia)
- **"ribbon-like"** ribs
- posterior scalloping of the vertebral bodies
- kyphoscoliosis



Neurofibromatosis in a 3-year-old female.

Lateral radiograph shows anterior bowing of the tibia. There are sclerotic changes with thinning of the medullary canal in the tibial diaphysis. Also note the lucency at the proximal end of the tibial shaft.



Neurofibromatosis in a 5-year-old female.

A, Lateral radiograph shows the progression of this disease with the development of pseudarthrosis of the tibia and fibula.

B, Lateral radiograph of the spine demonstrates posterior scalloping of the vertebral bodies.

Blount Disease

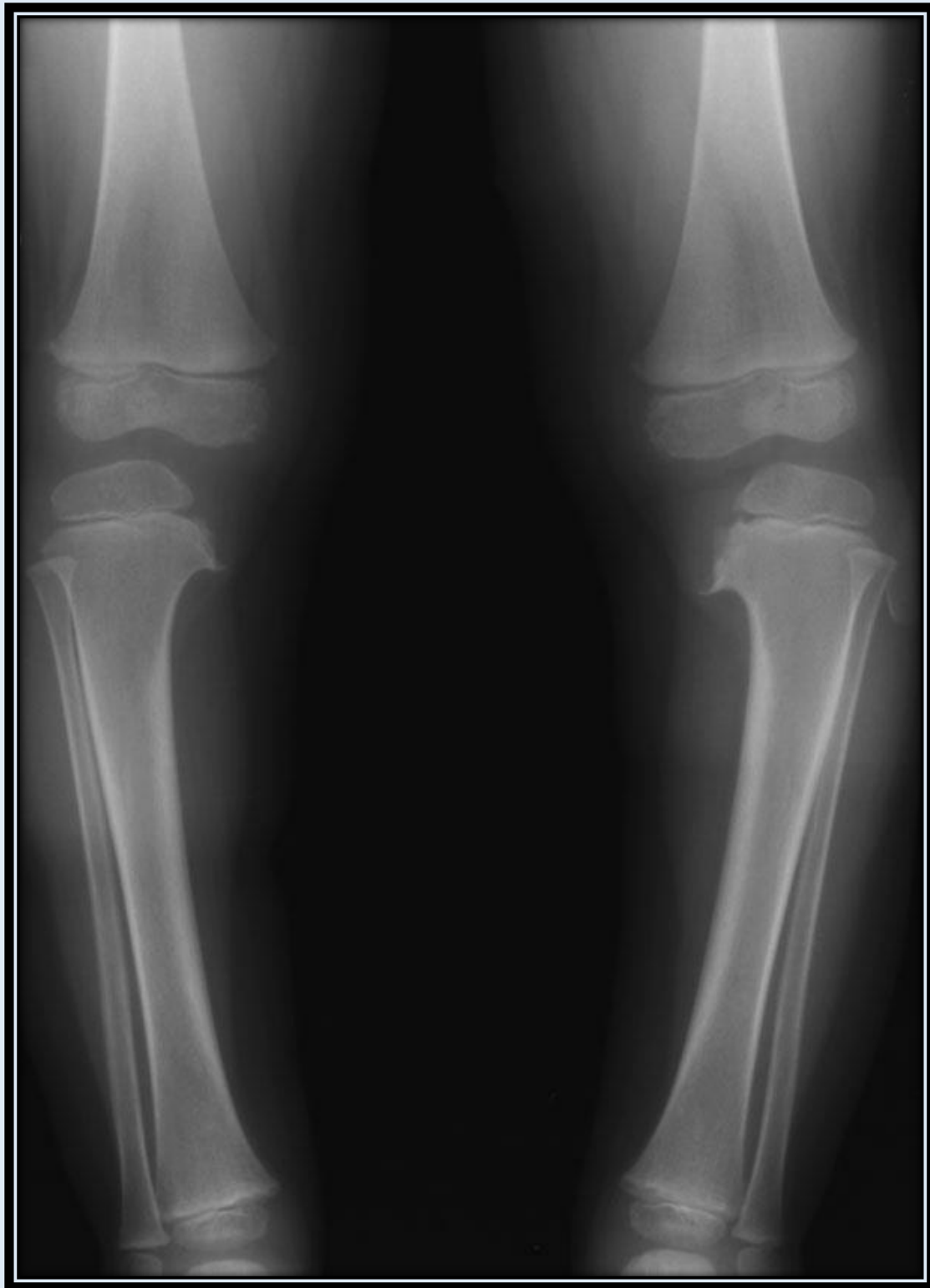
Blount disease is a growth deformity of the medial proximal tibia resulting in excessive medial bowing of the lower extremities (*tibia vara*). It is an idiopathic condition but may occur secondary to abnormal enchondral ossification from excess stress and compression. It is more common in obese children. The disease can be unilateral or bilateral. There are two types: 1) infantile form (presents at 1-3 years of age) and 2) juvenile form (presents at 6-13 years of age).

Radiographic findings:

- irregularity of the proximal medial tibia (fragmentation and beaking of the medial tibial metaphysis)
- varus deformity (tibiofemoral angle > 15 degrees)

This condition can be distinguished from physiologic bowing of the tibia by the severity of the bowing as well as the degree of irregularity of the medial tibial metaphysis.

Severe cases may require tibial osteotomies for treatment.



Blount Disease in a 2-year-old female.

AP radiograph (standing) demonstrates deformity of both lower extremities, left worse than right. Also note the beaking, irregularity and fragmentation of the medial tibial metaphyses.



Blount disease in a 4-year-old female.

AP radiograph shows depression, beaking, and irregularity of the medial tibial metaphyses. Note that this patient is s/p bilateral osteotomies to correct the resultant tibial and fibular bowing.

Metabolic Diseases

The metabolic diseases with musculoskeletal manifestations affecting the pediatric population include:

- rickets
- lead poisoning
- juvenile rheumatoid arthritis
- hemophilia
- sickle cell disease and thalassemia

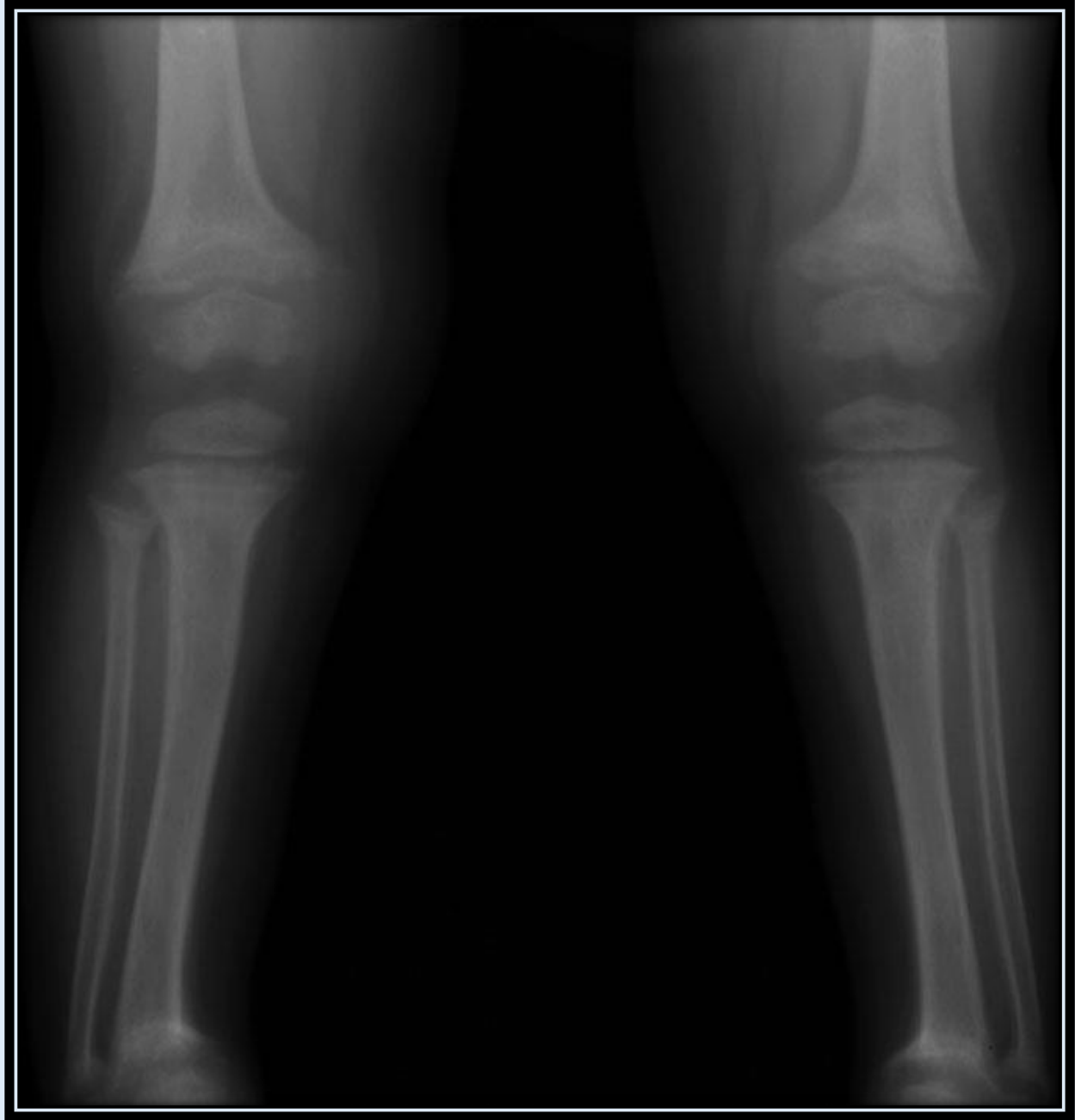
Rickets

Rickets is a metabolic abnormality in which a deficiency of Vitamin D leads to failure of normal bone mineralization. This disease is manifested earliest at the sites of rapid growth, namely the knees and wrists. Common causes of rickets include: 1) nutritional (dietary insufficiency), 2) malabsorption, 3) renal disease, or 4) increased requirement for vitamin D.

Radiographic findings:

- demineralization with coarsening of the trabecular pattern
- widening of the physis
- metaphyseal fraying, cupping and irregularity at the physeal margin
- deformity (i.e. bowing)
- flared anterior ribs

Patients may be susceptible to slipped capital femoral epiphyses as well as pathologic fractures.



Rickets in a 2-year-old female.

AP radiograph of the knees demonstrates widened growth plates and frayed metaphyses. Also note the bowing of the long bones (tibia and fibula bilaterally).

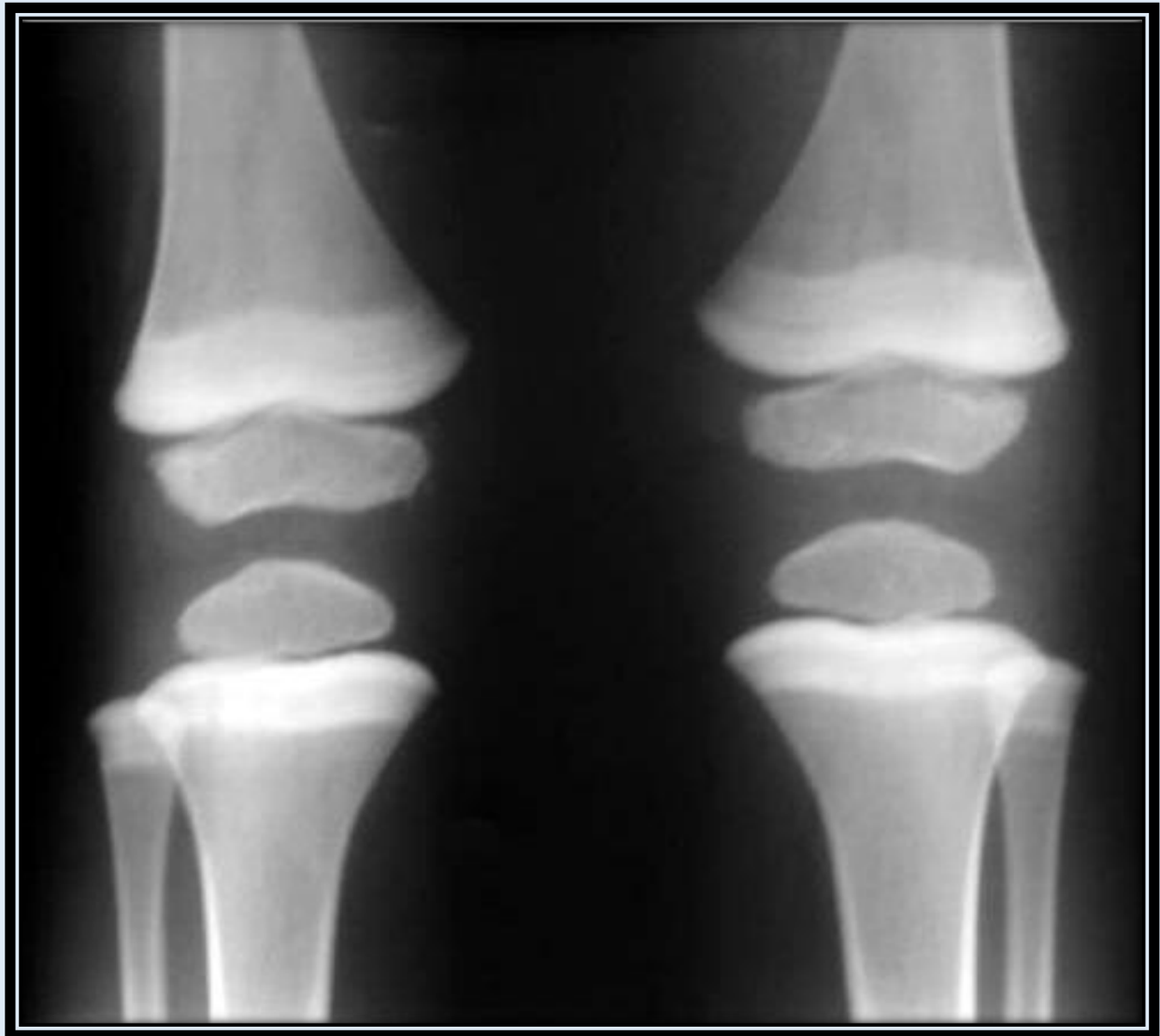


Rickets in a 5-year female.

Radiograph of the left wrist reveals widened physes. The distal ulnar and radial metaphyses appear cupped and frayed.

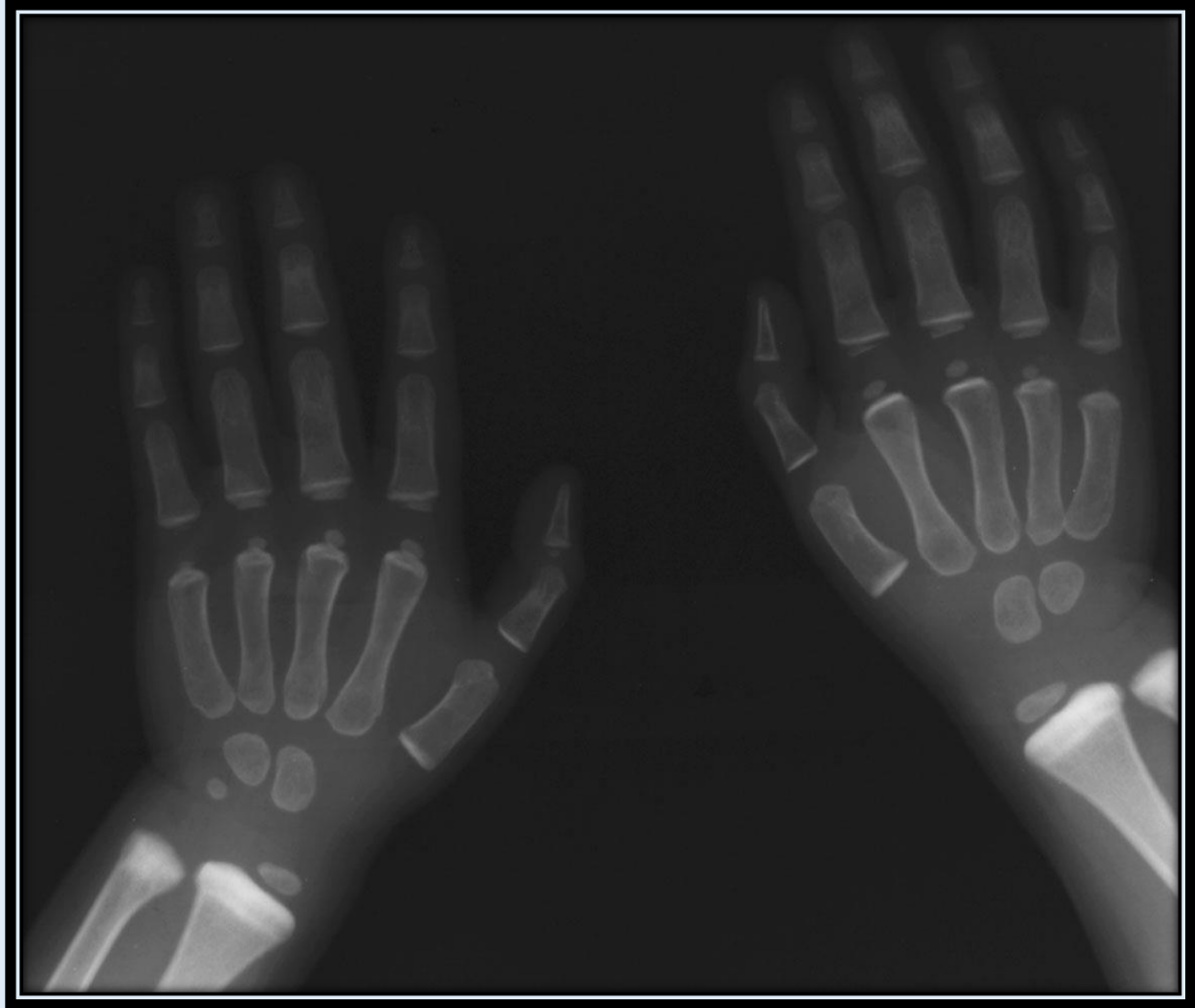
Lead Poisoning

Lead poisoning occurs most commonly in children less than two years of age. The underlying etiology is often consumption of lead-containing substances including old paint chips. Radiographically, affected patients may have broad sclerotic metaphyseal bands (**lead lines**) best shown in areas of rapid growth including the knees and wrists. Normal variants can also possess dense metaphyseal bands, but these tend to not involve the proximal fibula. In cases of lead poisoning, all metaphyses are involved including the fibula.



Lead poisoning in a 3-year-old male.

Classic radiographic evidence of lead poisoning with sclerotic metaphyseal bands involving the knees bilaterally. Note the involvement of both proximal fibulas.



Lead poisoning in a 3-year-old male.

Classic radiographic evidence of lead poisoning with sclerotic metaphyseal bands involving the wrists bilaterally.

Juvenile Rheumatoid Arthritis

Juvenile Rheumatoid Arthritis (JRA) is a form of rheumatoid arthritis with onset before 16 years of age. JRA differs from the adult form of rheumatoid arthritis in many respects. First, 70% of patients are seronegative. Second, large joints are more commonly involved as opposed to the adult disease in which small joint involvement predominates. The most commonly involved joints in JRA are: knee (epiphyseal overgrowth with widening of the intracondylar notch) > ankle > wrist (small, square carpal bones) > hand > elbow > hip. Joint involvement is most often pauciarticular (between 2 and 4 joints) with JRA.

Radiographic features of JRA:

- soft tissue swelling
- periostitis
- epiphyseal overgrowth secondary to hyperemia
- premature closure of physis with associated growth retardation
- ankylosis/fusion of spine articulation (predominantly cervical spine ankylosis of the apophyseal joints)

Still's disease is an acute form of JRA that is associated with fever, rash, hepatosplenomegaly, and lymphadenopathy. Musculoskeletal involvement is rare in this JRA variant.



Juvenile Rheumatoid Arthritis in a 10-year-old male.

A, AP radiograph of the knees demonstrates bilateral epiphyseal overgrowth with widening of the intracondylar notch.



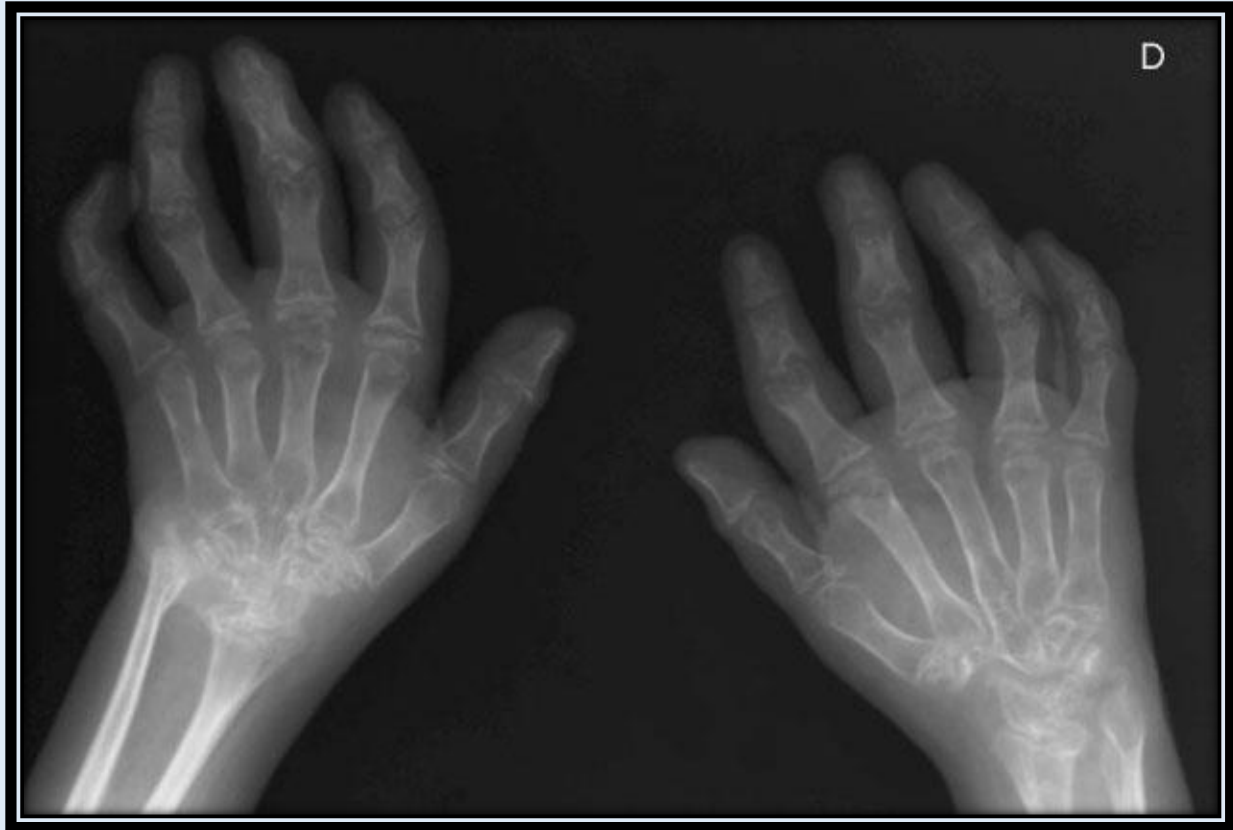
Juvenile Rheumatoid Arthritis in a 10-year-old male.

B, AP radiograph of the pelvis shows marked destruction of both hip joints.



Juvenile Rheumatoid Arthritis in a 10-year-old male.

C, Lateral cervical spine radiograph details ankylosis of the apophyseal joints.



Juvenile Rheumatoid Arthritis in a 10-year-old male.

D, Radiograph of the hands reveals joint space narrowing and erosions of the intercarpal joints, right worse than left.

Hemophilia

Hemophilia is a bleeding disorder which can have profound musculoskeletal sequelae. Roughly 90% of patients with hemophilia suffer from spontaneous hemarthroses, many of which are recurrent. Typically, these hemarthroses are monoarticular and occur most frequently in the knee > elbow > ankle. Hemosiderin is deposited within the synovium of the affected joint leading to synovial hypertrophy, which in turn can lead to destruction of the underlying articular cartilage.

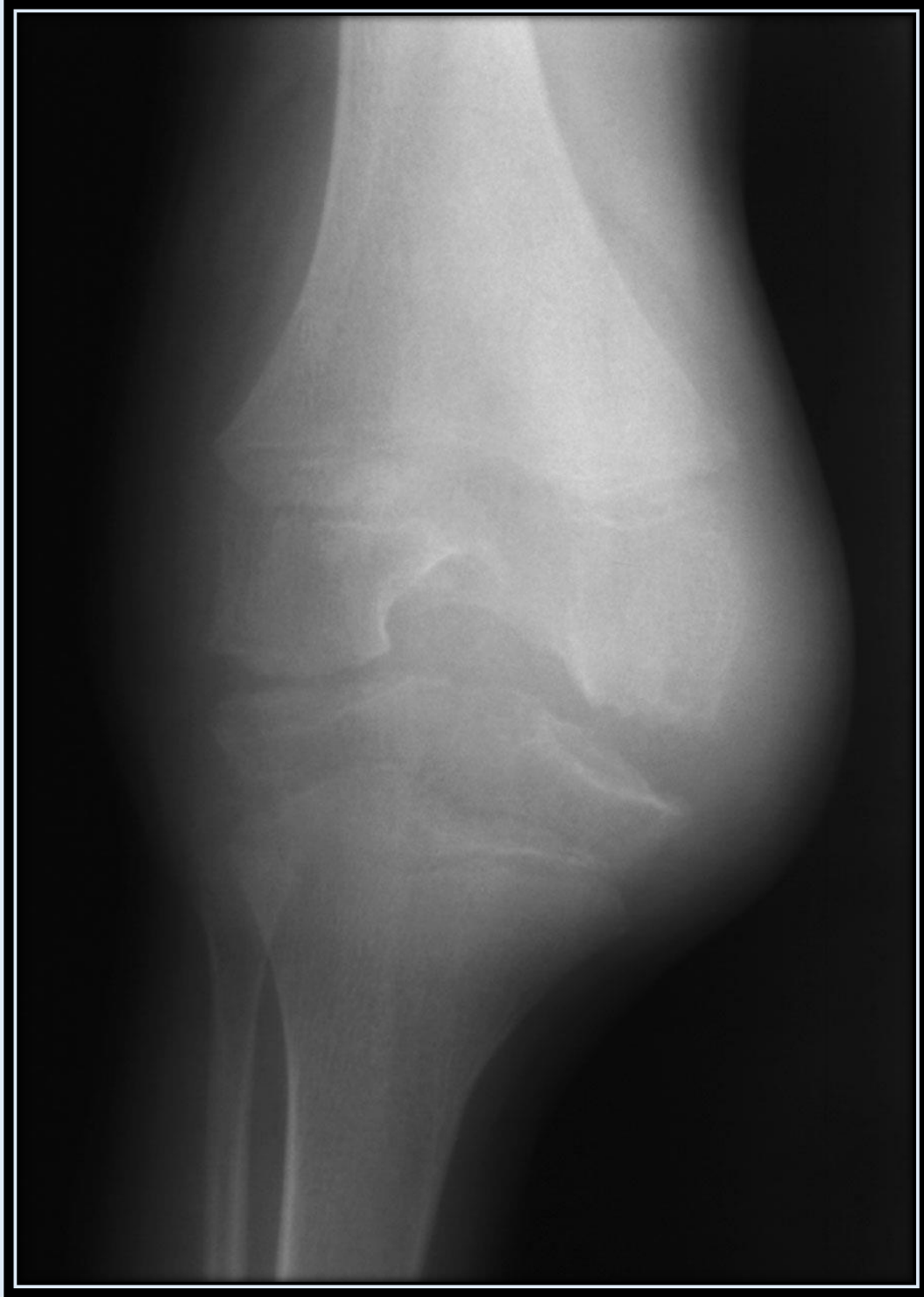
Radiographic appearance:

Acute findings

- joint effusion
- periarticular osteopenia

Chronic findings

- epiphyseal overgrowth (e.g. widening of intracondylar notch in the knee) - may mimic findings of JRA
- *pseudotumor formation* (hematoma with thick fibrous capsule) - usually in the soft tissues but may compress adjacent bone
- osteoarthritic changes



Hemophilic arthropathy in a 7-year old male.

AP radiographs of the right knee demonstrate joint irregularity and an effusion. There is widening of the intracondylar notch. Also note the squaring and epiphyseal overgrowth involving the tibia and femur.



Hemophilic arthropathy in a 7-year old male.

Lateral radiographs of the right knee demonstrate joint irregularity and an effusion. There is widening of the intracondylar notch. Also note the squaring and epiphyseal overgrowth involving the tibia and femur.

Sickle cell disease is a hemoglobinopathy in which polymerization of the prevalent HbS occurs, causing deoxygenated erythrocytes to lose their normal biconcave shape and become "sickle-shaped." Clinical manifestations of this disease include hemolytic anemia, infections, chest and abdominal pain, and skeletal pain (resulting from infarcts and osteomyelitis).

Radiographic findings in sickle cell disease:

- osteopenia
 - osteonecrosis (hips and shoulders in particular)
 - "H-shaped" vertebrae
 - bone infarcts (may appear as sclerotic or lucent areas)
 - osteomyelitis (*Salmonella* is prevalent in this population but *Staphylococcus Aureus* is still more common)
 - dactylitis (painful enlargement of a digit)
-

Thalassemia is a hereditary disorder resulting in decreased production of either alpha or beta globin chains.

Radiographic findings in thalassemia:

- expanded marrow space (marrow hyperplasia)
- widened diploic space in the skull with "hair-on-end" appearance
- "Erlenmeyer flask" deformity of the long bones
- paravertebral masses
- premature growth plate closure
- diffuse bony sclerosis
- "H-shaped" vertebrae



Sickle Cell "hand-foot syndrome" in an 8-month-old African American male with two week history of swollen hands and feet.

AP radiograph of the right hand shows periostitis with subperiosteal new bone formation involving the 3rd-5th metacarpals. There are areas of lytic destruction (most noticeable involving the distal third metacarpal) possibly indicating an infarct.



Chronic findings of "hand-foot syndrome" in a 12-year-old male with sickle cell disease. Left, Shortening of the 5th metacarpal of the left hand. Right, Shortening of the 1st metatarsal of the left foot. These findings are secondary to infarcts during bony growth.



Sickle cell disease manifested in the spine of an adolescent female.

Lateral thoracic spine film demonstrates "**H-shaped**" **vertebral bodies**. These findings represent compression infarcts of the end plates resulting from osteonecrosis of the vertebrae.



Thalassemia in a pre-adolescent male.

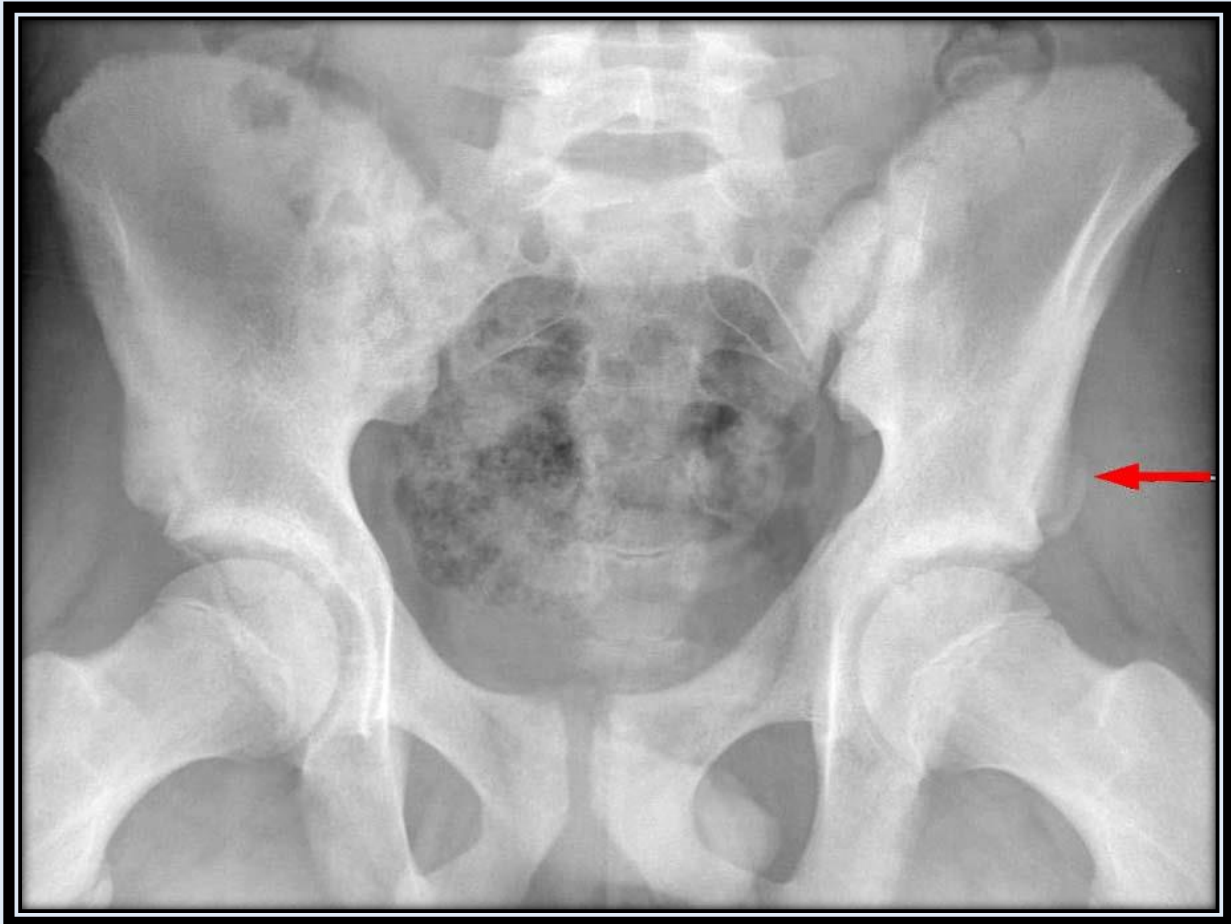
Lateral skull radiograph shows a widened diploic space, especially in the frontal region. Also note the radiating spicules of bone extending at right angles to the inner-island tables, providing the **"hair-on-end"** appearance common in this and other forms of anemia.

Pediatric Musculoskeletal Quiz - Part I

Q_1: What type of fracture are these images depicting?



Q_2: What type of fracture is this image depicting?



Q_3: What type of Salter-Harris fracture is depicted in this image?



Q_4: What type of Salter-Harris fracture is depicted in this image?



Q_5: What type of Salter-Harris fracture is depicted in this image?



Q_6: What is this image depicting?



Q_7: What type of fracture is noted in this patient who just recently became ambulatory?

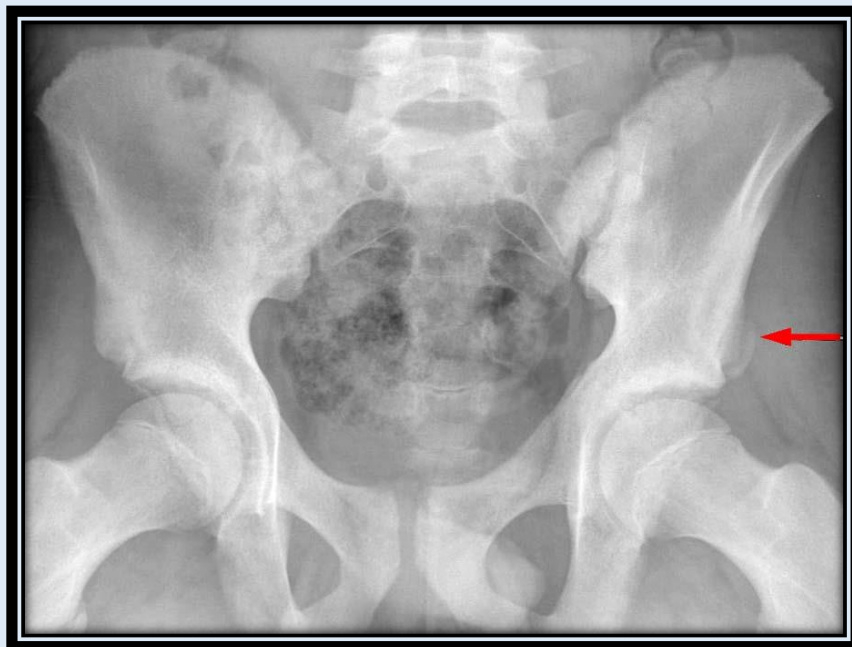


Answers

Q_1: Buckle (or Torus) fracture of the distal radius



Q_2: Avulsion fracture of the anterior inferior iliac spine



Q_3: Type I Salter-Harris fracture of the distal radius



Q_4: Type II Salter-Harris fracture of the distal tibia



Q_5: Type IV Salter-Harris fracture of the proximal phalanx of the thumb



Q_6: Stress fracture of the tibia



Q_7: Toddler's fracture of the tibia



Pediatric Musculoskeletal Quiz Part II

Q_1: A supracondylar fracture of the humerus is likely if there is:

- A. Anterior displacement of the distal fragment such that the anterior humeral line does not bisect the middle third of the capitellum.
- B. Posterior displacement of the distal fragment such that the anterior humeral line does not bisect the middle third of the capitellum.

Q_2: Each of the following is true of Developmental Dysplasia of the Hip (DDH) except.

- A. Early diagnosis of DDH is important because chronic dislocation of the femoral head can lead to growth deformity of the acetabular fossa.
- B. DDH is more prevalent in males than females.
- C. Clinical findings of DDH may include positive "clicks" with dislocation (Barlow maneuver) and relocation (Ortolani maneuver) of the hip.
- D. DDH more commonly involves the left hip.

Q_3: Early radiographic findings in Legg-Calve-Perthes disease include a bone scan which reveals increased activity in the femoral epiphysis.

- A. True
- B. False

Q_4: Imaging findings seen in Clubfoot (or Talipes Equinovarus) include all of the following except.

- A. Decreased talocalcaneal angle.
- B. Medial displacement of the first metatarsal relative to the long axis of the talus.
- C. Equinus heel (fixed plantar flexion of the heel).
- D. Hindfoot valgus.
- E. Talonavicular subluxation.

Q_5: Patients with Ollier disease have a higher rate of transformation to chondrosarcoma than do patients with Maffucci syndrome.

- A. True
- B. False

Q_6: Osteomyelitis in the pediatric population most often:

- A. Shows a focal area of increased uptake in all three phases of a bone scan.
- B. Involves the flat bones as opposed to the long bones.
- C. Can be detected on plain films within 2-3 days of the onset of symptoms.
- D. Found in children between the ages of 6 and 10.

Q_7: Classic radiographic findings in Langerhans Cell Histiocytosis include all of the following except.

- A. Geographic Skull.
- B. Floating Teeth.
- C. Vertebra Plana.
- D. Paddle-shaped ribs.

Q_8: Radiographic findings in Achondroplasia include each of the following except.

- A. A pelvis with tall, flared iliac wings and increased acetabular angles.
- B. Shortened spinal pedicles distally with a decreased interpedicular distance.
- C. Rhizomelic limb shortening.
- D. Craniofacial disproportion with large calvarium, diminutive skull base, small foramen magnum and small jugular foramina.

Q_9: The sclerotic metaphyseal bands (seen in cases of high lead exposure) are best shown in areas of rapid growth including the knees and wrists.

- A. True
- B. False

Q_10: Hemophilic Arthropathy can be distinguished from Juvenile Rheumatoid Arthritis by the presence of epiphyseal overgrowth and widening of the intracondylar notch in the knee.

- A. True
- B. False

Answers

Q_1: A supracondylar fracture of the humerus is likely if there is:

posterior displacement of the distal fragment such that the *anterior humeral line* does not bisect the middle third of the capitellum.

Q_2: Each of the following is true of Developmental Dysplasia of the Hip (DDH) except:

DDH is more prevalent in males than females.

Q_3: Early radiographic findings in Legg-Calve-Perthes disease include a bone scan which reveals increased activity in the femoral epiphysis.

False

Q_4: Imaging findings seen in Clubfoot (or Talipes Equinovarus) include all of the following except:

Hindfoot valgus.

Q_5: Patients with Ollier disease have a higher rate of transformation to chondrosarcoma than do patients with Maffucci syndrome.

False

Q_6: Osteomyelitis in the pediatric population most often:

Shows a focal area of increased uptake in all three phases of a bone scan.

Q_7: Classic radiographic findings in Langerhans Cell Histiocytosis include all of the following except:

Paddle-shaped ribs.

Q_8: Radiographic findings in Achondroplasia include each of the following except:

A pelvis with tall, flared iliac wings and increased acetabular angless.

Q_9: The sclerotic metaphyseal bands (seen in cases of high lead exposure) are best shown in areas of rapid growth including the knees and wrists.

True

Q_10: Hemophilic Arthropathy can be distinguished from Juvenile Rheumatoid Arthritis by the presence of epiphyseal overgrowth and widening of the intracondylar notch in the knee.

False

Pediatric Neurological Radiology

Pediatric Neurological Radiology

Comprehensive Outline for Pediatric Neurology Section

- **Head Ultrasound**

- Normal
- Germinal Matrix Hemorrhage Grade I
- Germinal Matrix Hemorrhage Grade II
- Germinal Matrix Hemorrhage Grade III
- Germinal Matrix Hemorrhage Grade IV
- Periventricular Leukomalacia

- **Developmental Abnormalities**

- Introduction
- Chiari I
- Chiari II
- Holoprosencephaly
 - Alobar
 - Semilobar
 - Lobar
- Abnormal Neuronal Migration
 - Heterotopias
 - Schizencephaly
 - Porencephaly and encephalomalacia
 - Lissencephaly
- Corpus Callosum Dysgenesis
- Hydranencephaly
- Cephaloceles
- Vein of Galen Malformation
- Posterior Fossa Cystic Malformation
- Myelination Abnormalities
 - Introduction
 - White Matter Age
 - Abnormal Myelination
 - Genetic Diseases

- **Neurocutaneous Syndromes**

- Introduction
- Neurofibromatosis
- Tuberous Sclerosis
- Sturge-Weber syndrome

- **Infection**

- TORCH
- Encephalitis
- Subacute sclerosing panencephalitis
- Acute disseminated encephalomyelitis
- Meningitis
- Cysticercosis

- **Posterior Fossa Tumors**

- Introduction
- Cerebellar Astrocytoma
- Medulloblastoma
- Brainstem Glioma
- Ependymoma

- **Supratentorial Tumors**

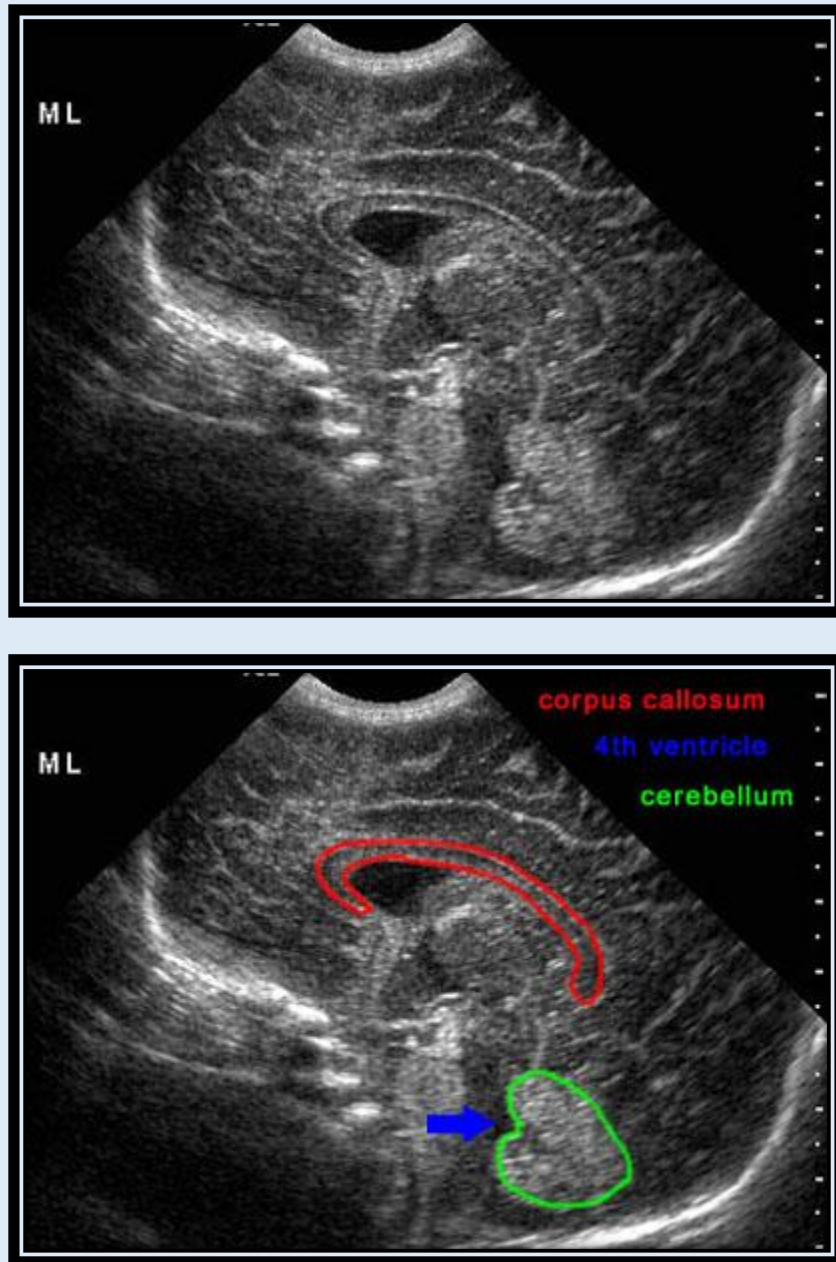
- Parasellar
 - Craniopharyngioma
 - Suprasellar astrocytoma
 - Hypothalamic hamartoma
 - Germ cell tumors
- Pineal
 - Pineocytoma and pineoblastoma
 - Germinoma
 - Tectal glioma
- Intraventricular
- Hemispheric

- **Quiz Part 1**

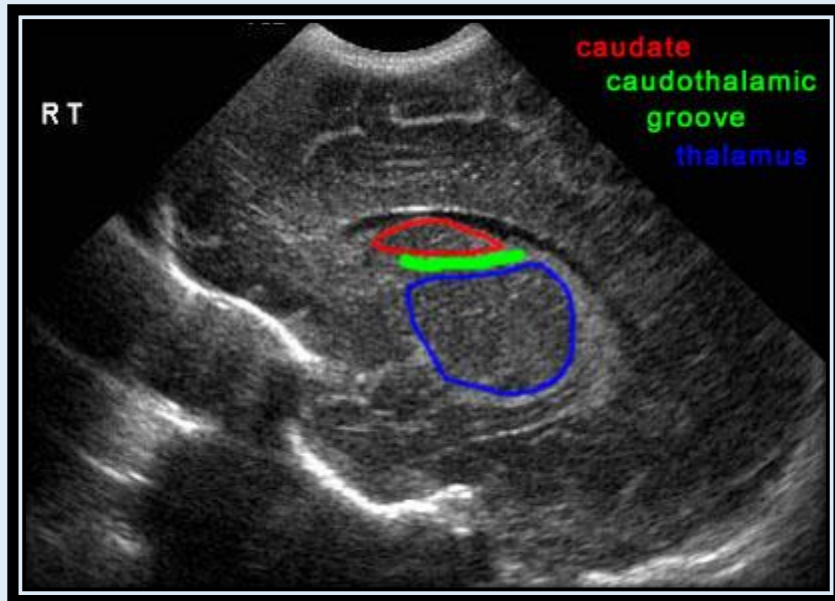
- **Quiz Part 2**

Head Ultrasound

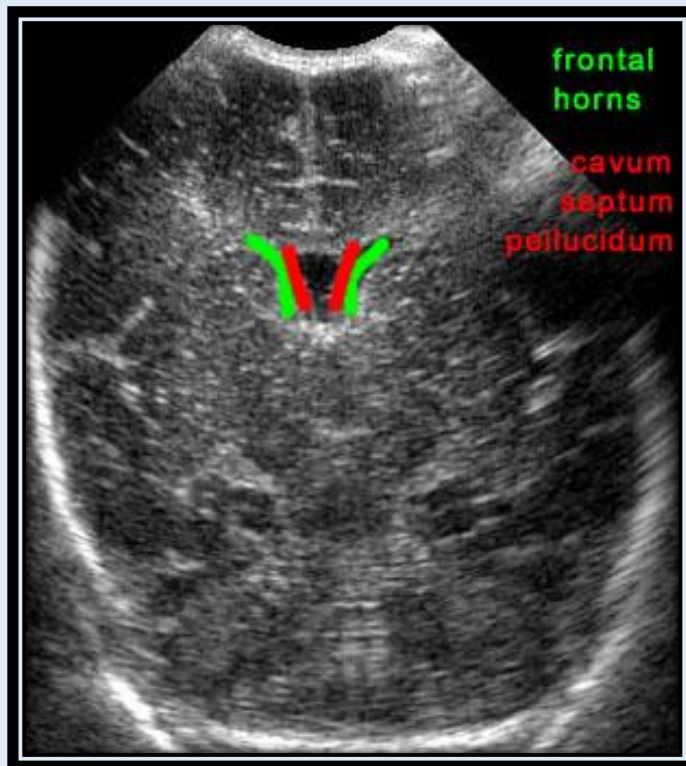
Ultrasound is used to diagnose and follow complications of prematurity and screen for congenital abnormalities or hydrocephalus. The most common complications are germinal matrix hemorrhages and periventricular leukomalacia. Head ultrasound is performed in the neonate or infant through the open anterior fontanelle. Images are obtained in the sagittal and coronal planes.



Sagittal midline image



Parasagittal image through caudothalamic groove



Coronal image through frontal horns and cavum septum pellucidum

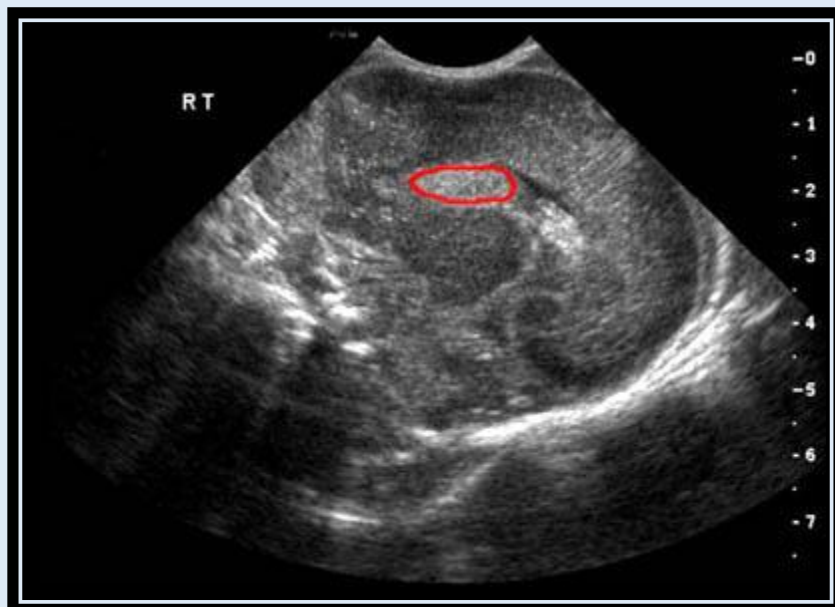
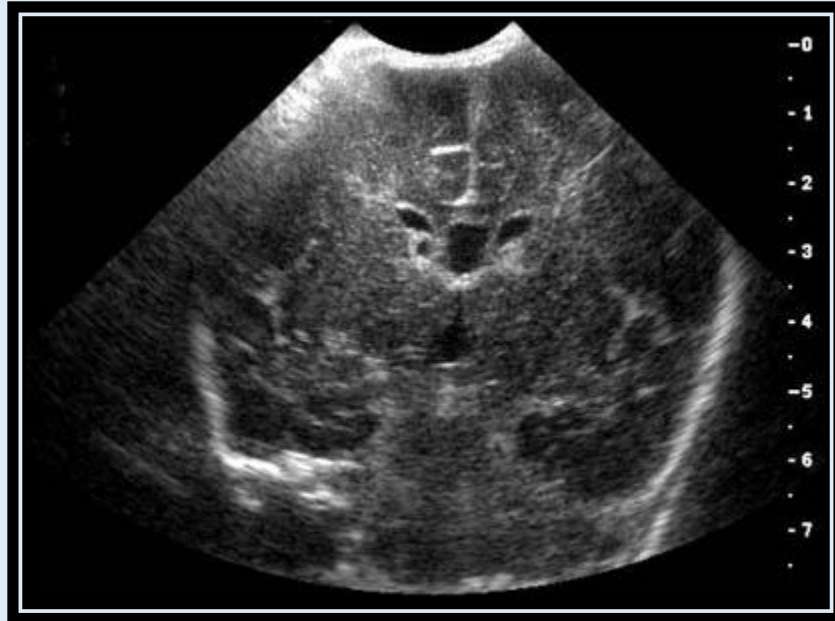
Germinal Matrix Hemorrhage Grade 1

The germinal matrix is the stem source for neuroblasts and is a fetal structure only. It typically involutes by term but is still present in premature infants. The germinal matrix is very vascular and is prone to hemorrhage. It lies within the caudothalamic groove, which is the space between the caudate nucleus head and the thalamus. Hemorrhage is seen as echogenic material within the caudothalamic groove. Choroid plexus is also echogenic and care should be made not to misinterpret choroid for hemorrhage; normal choroid plexus does not extend anterior to the caudothalamic groove on the parasagittal views. Germinal matrix hemorrhage is classified into four grades, I-IV. Grade IV hemorrhage is thought to be a venous infarction hemorrhage rather than direct extension from the germinal matrix.

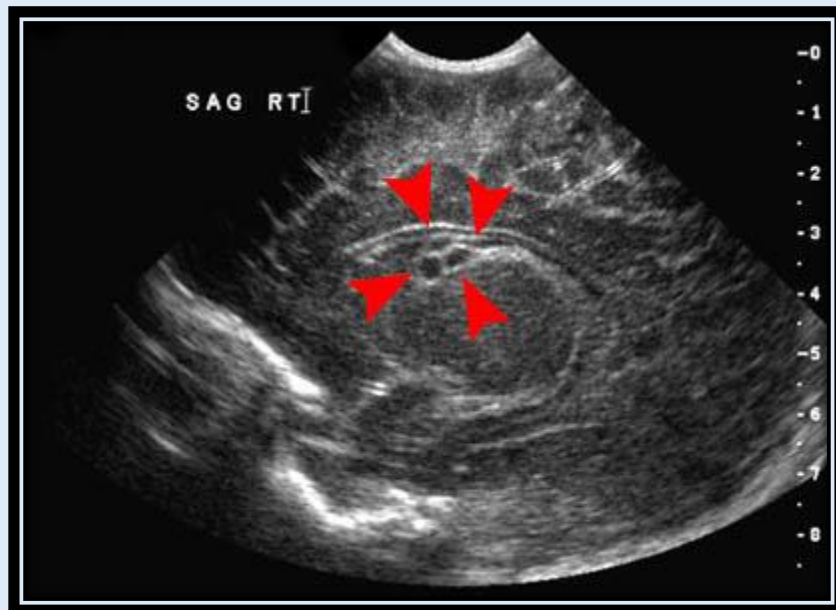
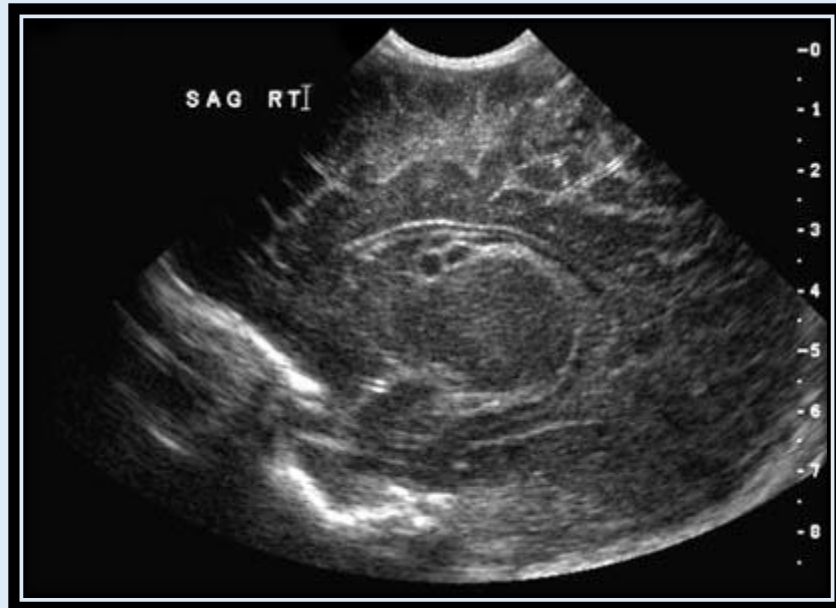
Grade I	Hemorrhage confined to germinal matrix
Grade II	Intraventricular hemorrhage without ventricular dilatation
Grade III	Intraventricular hemorrhage with ventricular dilatation
Grade IV	Intraparenchymal hemorrhage



Coronal, Grade I with hyperechoic hemorrhage in caudothalamic groove



Sagittal, Hyperechoic hemorrhage in caudothalamic groove



Sagittal, Grade I hemorrhage showing evolution to cystic changes

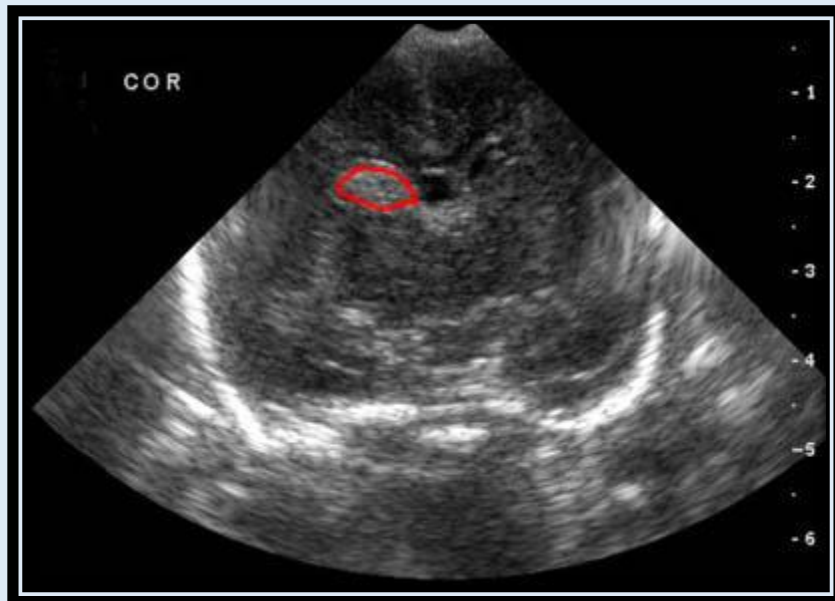
Germinal Matrix Hemorrhage Grade 2

Grade I Hemorrhage confined to germinal matrix

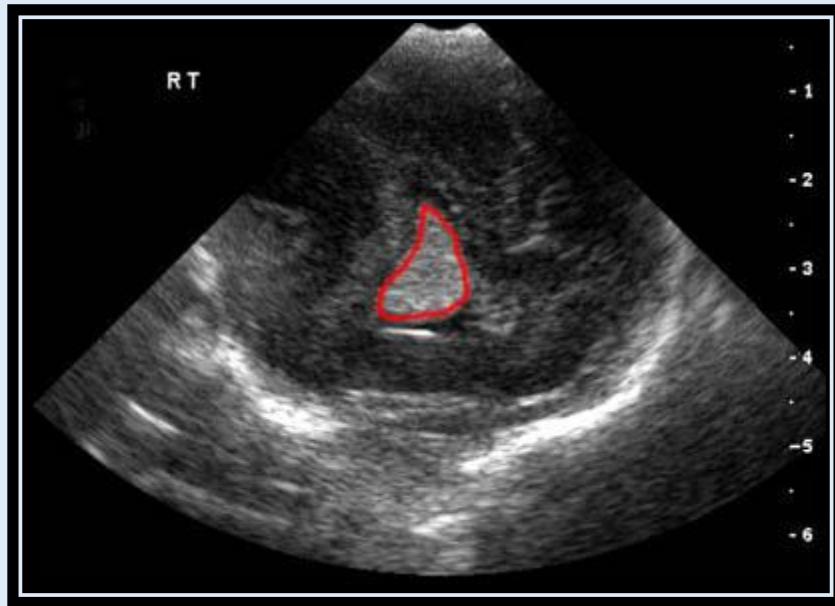
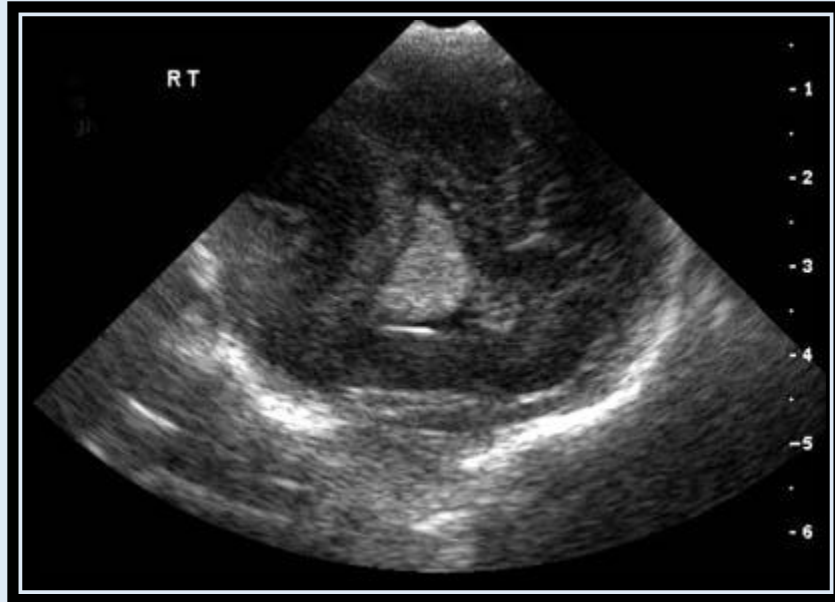
Grade II Intraventricular hemorrhage without ventricular dilatation

Grade III Intraventricular hemorrhage with ventricular dilatation

Grade IV Intraparenchymal hemorrhage



Coronal, Grade II with hyperechoic hemorrhage in the frontal horn of the right lateral ventricle



Sagittal, Grade II with hyperechoic hemorrhage in the occipital horn

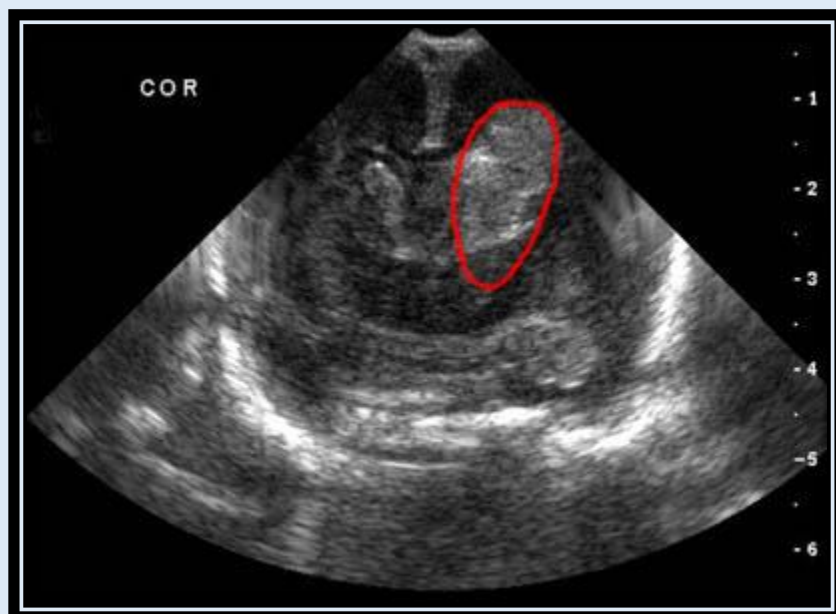
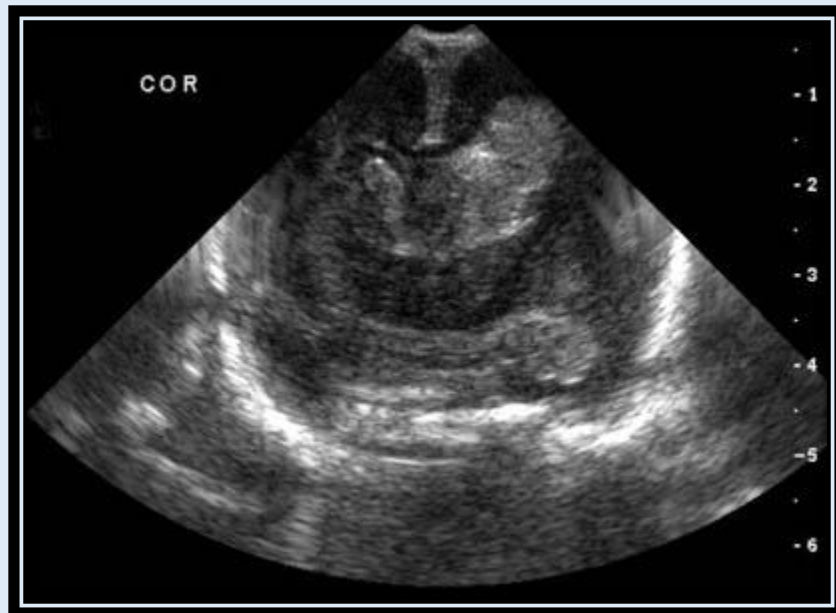
Germinal Matrix Hemorrhage Grade III

Grade I Hemorrhage confined to germinal matrix

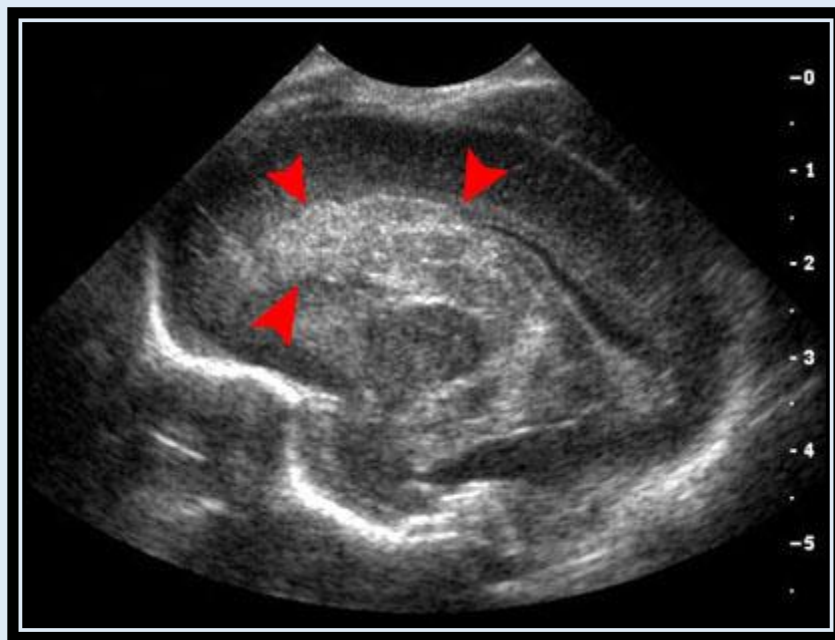
Grade II Intraventricular hemorrhage without ventricular dilatation

Grade III Intraventricular hemorrhage with ventricular dilatation

Grade IV Intraparenchymal hemorrhage



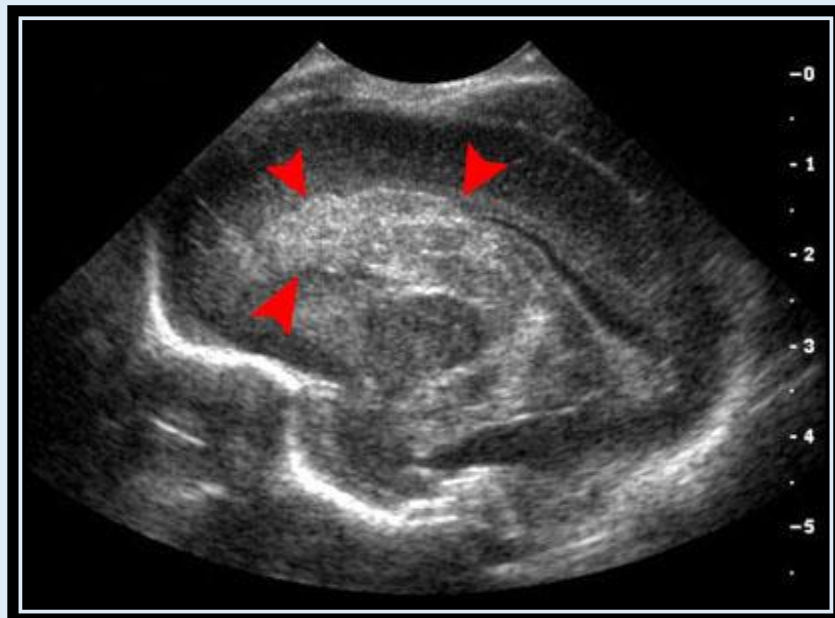
Grade III



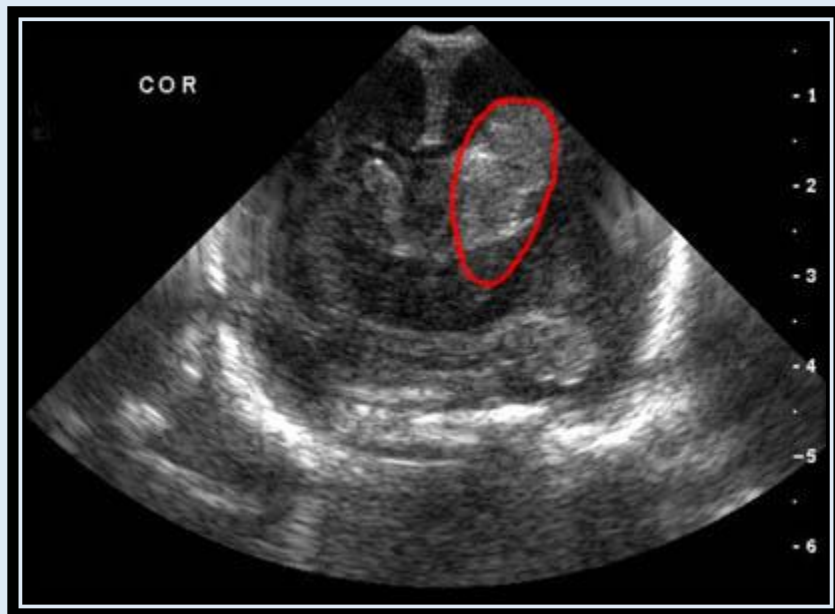
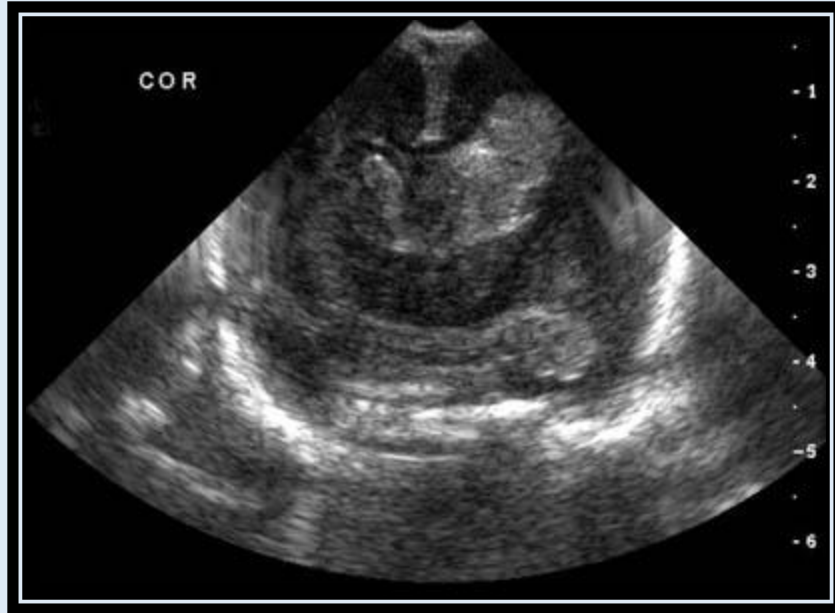
Grade III

Germinal Matrix Hemorrhage Grade IV

- Grade I Hemorrhage confined to germinal matrix
- Grade II Intraventricular hemorrhage without ventricular dilatation
- Grade III Intraventricular hemorrhage with ventricular dilatation
- Grade IV Intraparenchymal hemorrhage**



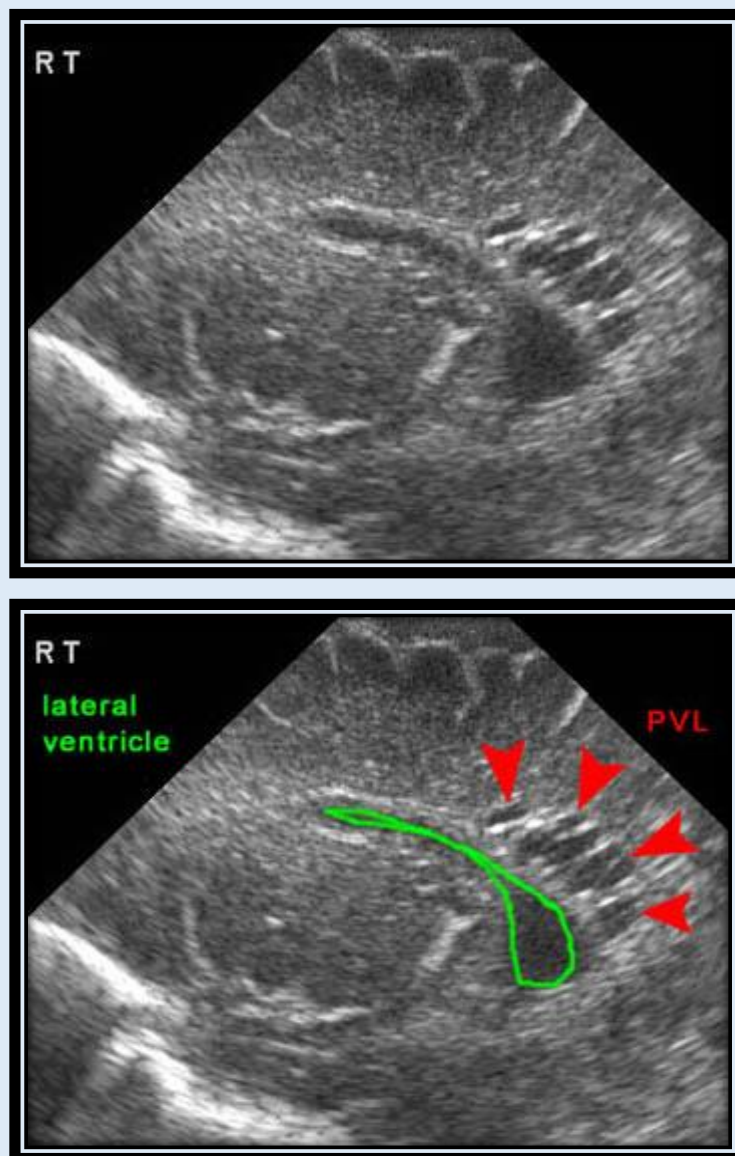
Sagittal, Hyperechoic hemorrhage within the brain parenchyma



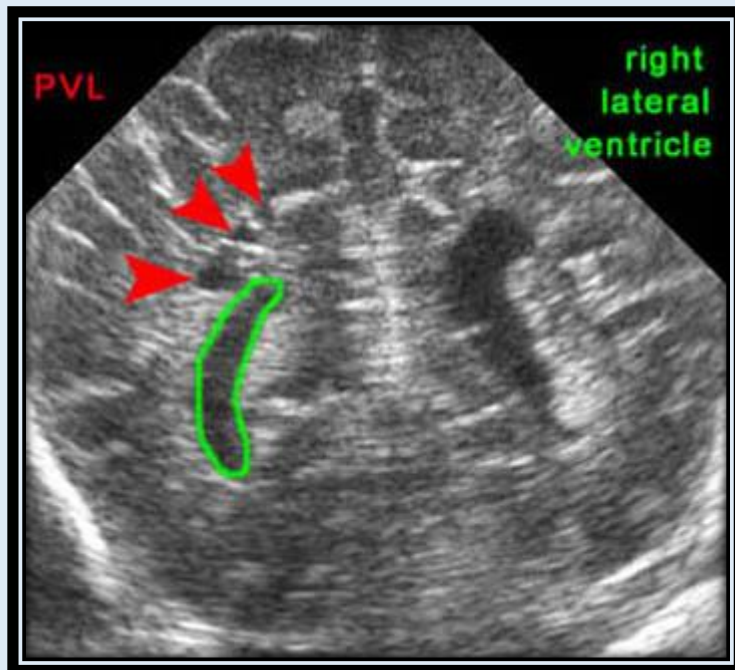
Coronal, Hyperechoic hemorrhage within the brain parenchyma

Periventricular Leukomalacia

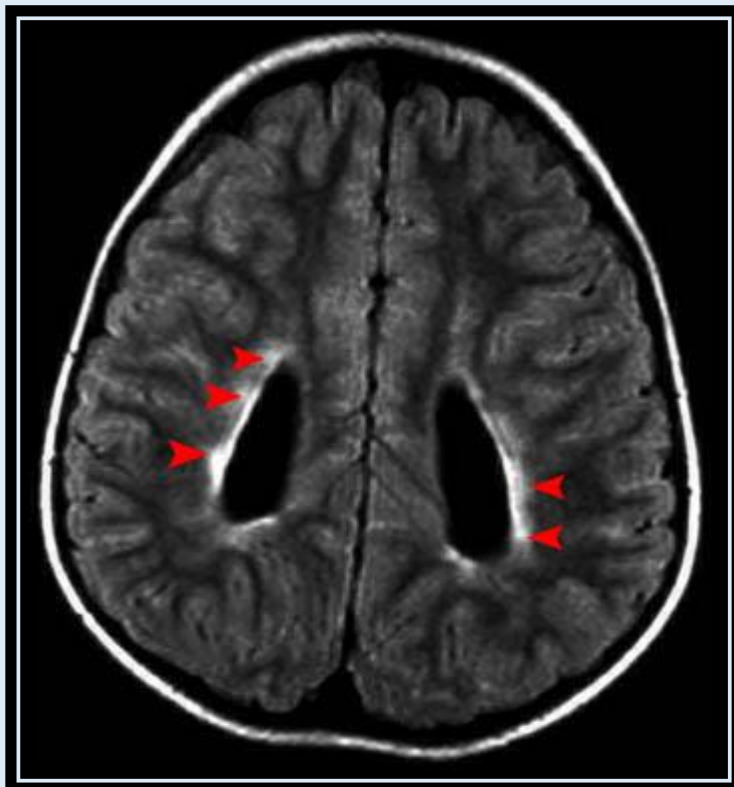
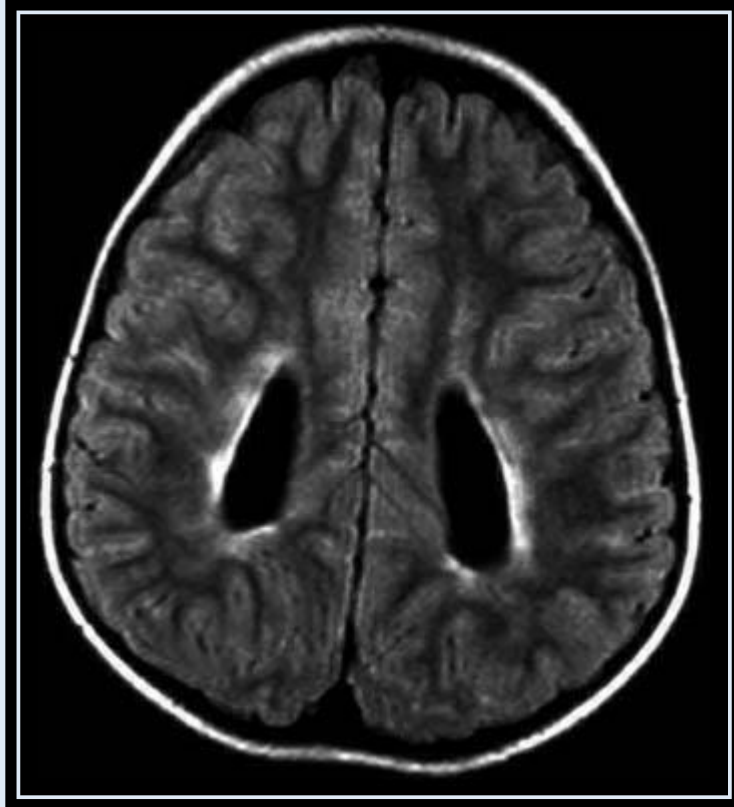
The watershed zone of the premature infant is the periventricular white matter, and perinatal partial asphyxia can result in ischemic damage. Periventricular leukomalacia (PVL) most commonly affects the white matter adjacent to the atria and the frontal horns of the lateral ventricles. PVL is associated with neurologic sequelae such as movement disorders, seizures, and spasticity. Heterogeneous echogenicity is seen within the periventricular white matter and may appear cystic in severe cases. The chronic changes of PVL are best demonstrated with MRI as white matter loss with relative sparing of the overlying cortex.



Sagittal head US showing cystic PVL along the right ventricle



Coronal head US showing cystic PVL along the right ventricle



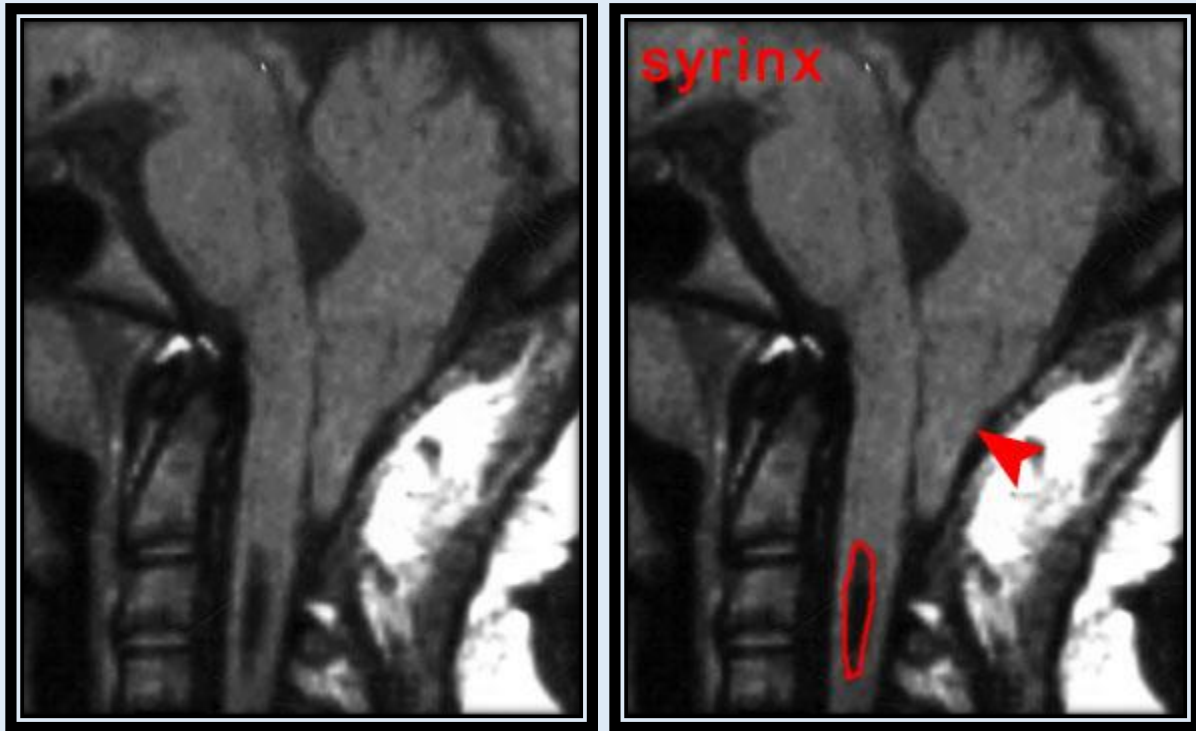
Increased periventricular T2 signal on FLAIR image indicating PVL

Developmental Abnormalities

Development abnormalities can be secondary to embryologic events that fail to progress normally or may result from destruction of already formed structures. Embryologic events include abnormalities of dorsal induction, ventral induction, migration and cortical organization, neuronal proliferation and differentiation, and myelination. Often multiple distinct developmental abnormalities are present simultaneously.

Chiari I

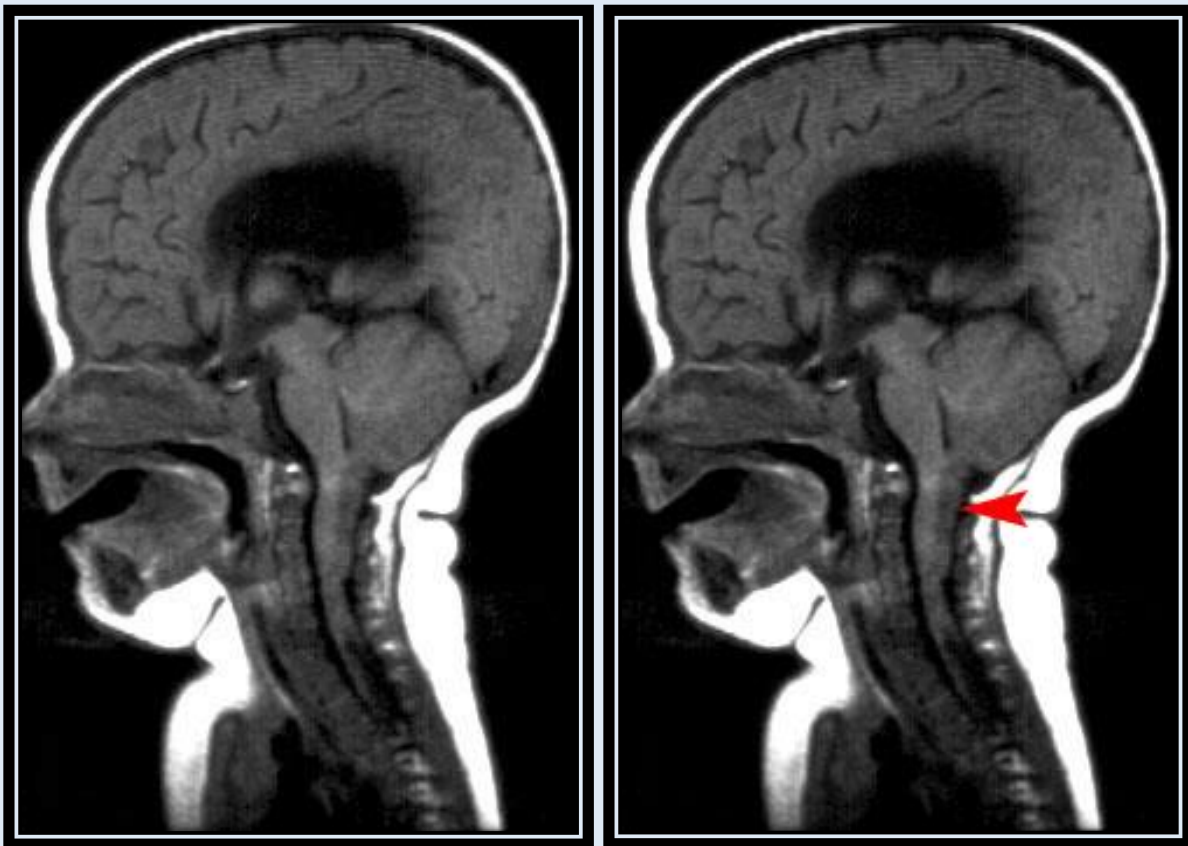
Chiari I malformation is the abnormal inferior location of the cerebellar tonsils below the foramen magnum. The medulla and fourth ventricle are typically normal. It is best visualized on sagittal MRI images. Complications include hydrocephalus and hydrosyringomyelia/syrinx.



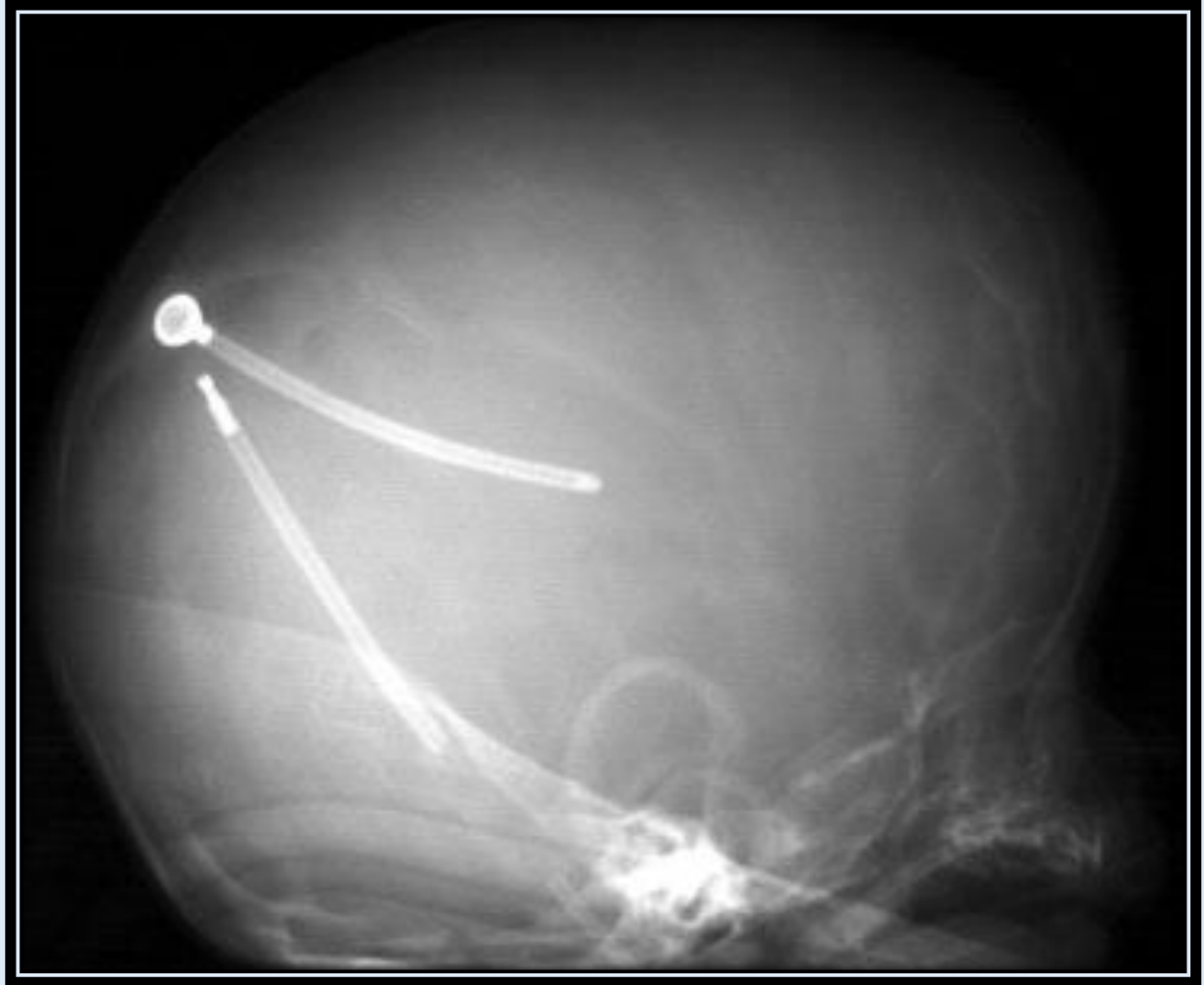
Chiari I

Chiari II

Type II Chiari malformations are almost always associated with myelomeningoceles, and almost all patients with myelomeningocele have Chiari II. There is typically hydrocephalus. The posterior fossa is small with inferior displacement of the cerebellum, medulla, and fourth ventricle into the upper cervical canal. Other imaging findings are a kinked medulla, colpocephaly (enlargement of the posterior body of the lateral ventricles), enlarged massa intermedia, inferior pointing of the lateral ventricles, and tectal beaking.



A lacunar skull is often present in the first year of life representing a dysplasia of bone that disappears by the end of the first year of life with or without the treatment of the hydrocephalus. The skull appears scalloped representing bony septations of the dysplasia.



AP and lateral views of a lacunar skull

Holoprosencephaly

The lack of cleavage of the brain into two hemispheres is called holoprosencephaly. There is a close embryologic association with facial anomalies, and the severity of the brain abnormality is reflected in the severity of the midline facial abnormality. The abnormality is subdivided into alobar, semilobar, and lobar holoprosencephaly.

Alobar Holoprosencephaly

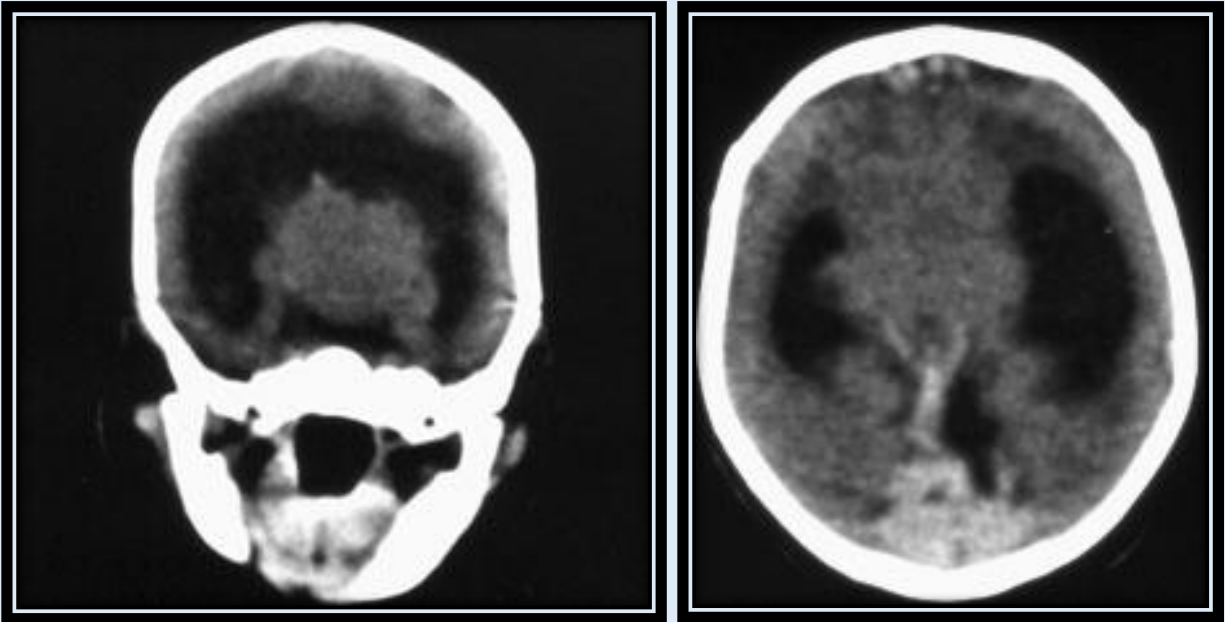
Alobar is the most severe form as there is no attempt at cleavage of the cerebral hemispheres. It is characterized by a monoventricle, fusion of the thalami, absence of the falx cerebri and corpus callosum, and a single anterior cerebral artery.



Alobar holoprosencephaly with a monoventricle

Semilobar Holoprosencephaly

Semilobar is the intermediate form where the cerebral hemispheres are partially cleaved or there is partial separation of the thalami. Midline structures such as the corpus callosum and falx cerebri may be present.

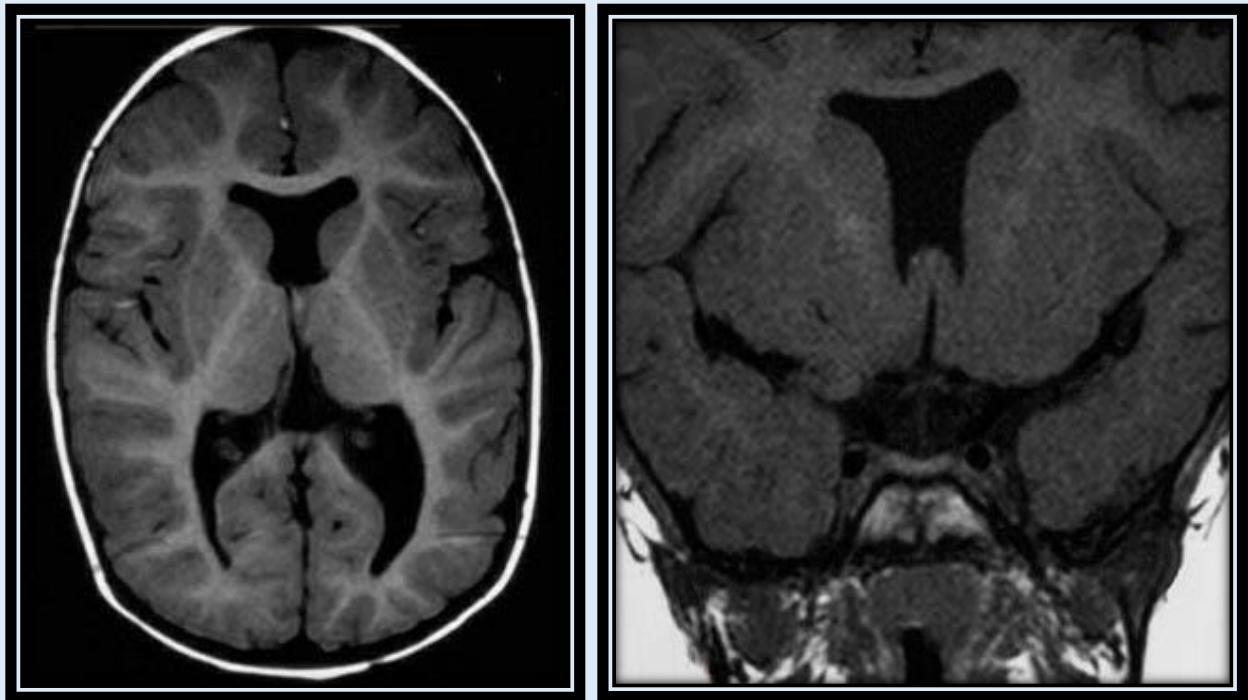


Semilobar holoprosencephaly

Lobar Holoprosencephaly

Lobar holoprosencephaly is the least severe form where the occipital and temporal horns are well formed but the cerebral hemispheres frontally are not completely cleaved. The septum pellucidum is absent, and the corpus callosum may be absent or dysplastic.

Septo-optic dysplasia is analogous to mild holoprosencephaly and is characterized by absence of the septum pellucidum and hypoplasia of the optic nerves. The frontal horns of the lateral ventricles have a squared appearance and point inferiorly on coronal imaging.



Lobar holoprosencephaly with absence of the septum pellucidum

Abnormal Neuronal Migration

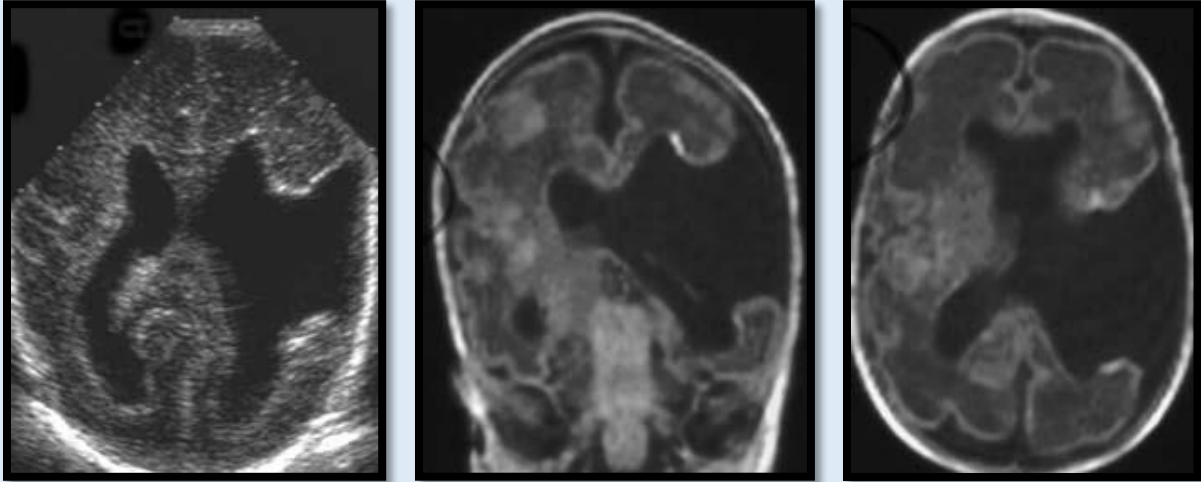
Heterotopias are an abnormality of neuronal migration characterized by arrest in migration of the neurons from the subependymal area to the cortex. Typically, heterotopias are associated with other migrational disorders such as schizencephaly, lissencephaly, or polymicrogyria. Patients typically present with focal seizures. The lesions image as gray matter in abnormal locations within the white matter.



Gray matter heterotopia associated with colpocephaly from agenesis of the corpus callosum.

Schizencephaly

Schizencephaly is another migrational disorder that refers to a gray matter lined cleft in the cerebral hemisphere that typically extends from the lateral ventricle to the surface of the brain. In most cases, there is associated agenesis of the corpus callosum. The presence of gray matter lining the entire cleft is the diagnostic feature that differentiates it from other causes of clefts such as porencephaly, which is lined by both gray and white matter.



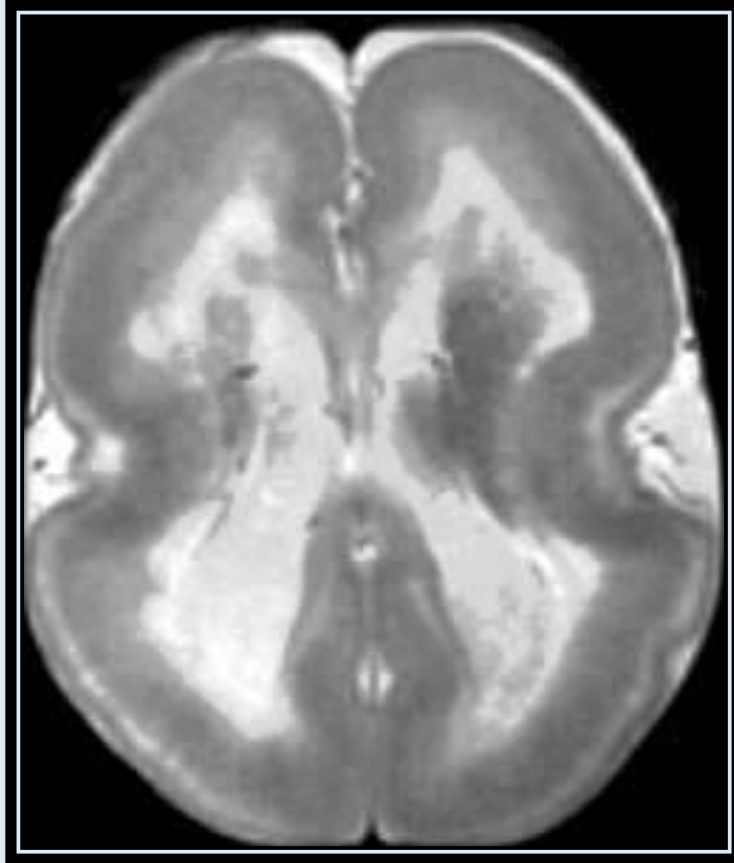
Schizencephaly on ultrasound (left) and MRI (center and right)

Porencephaly and Encephalomalacia

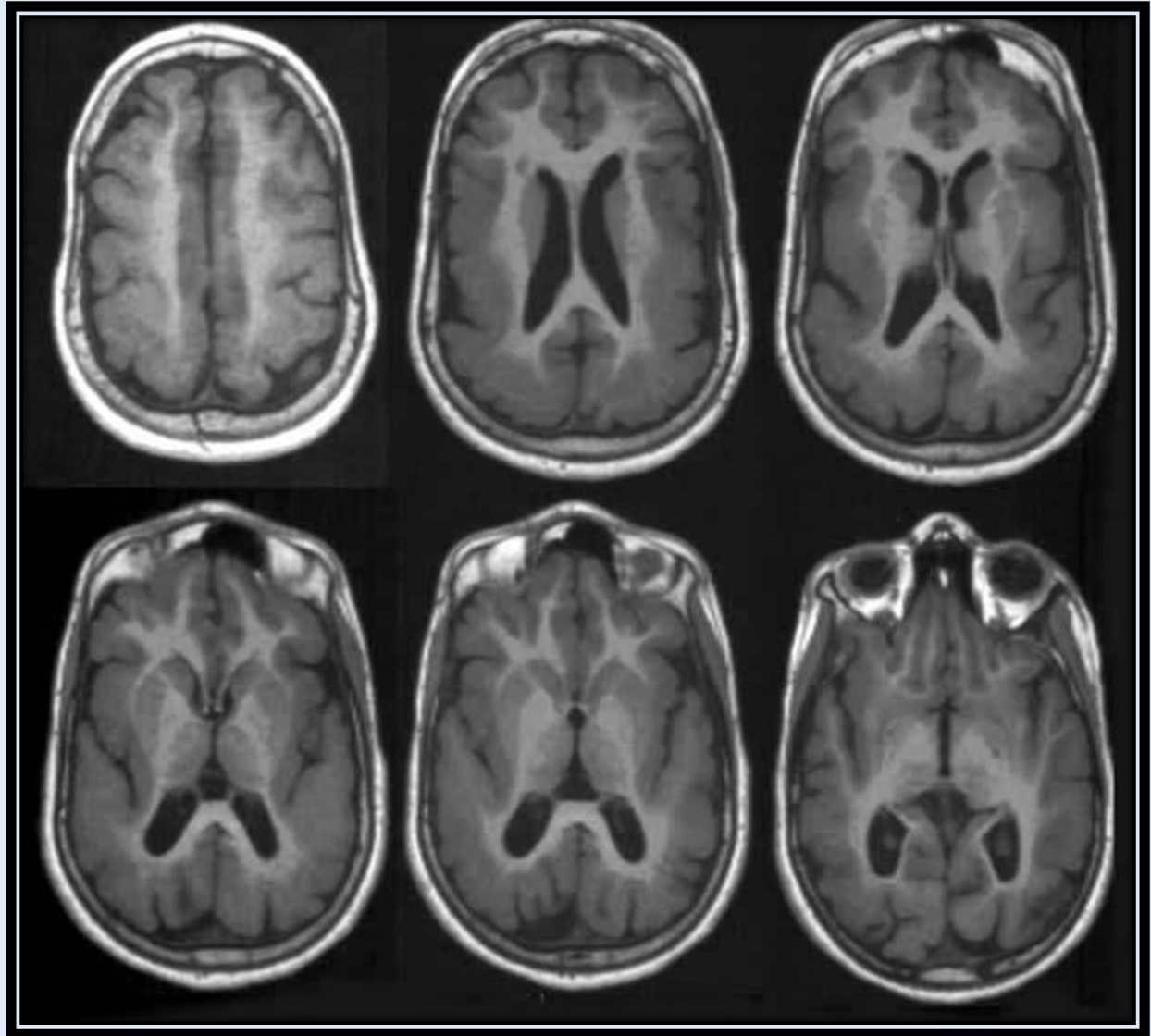
Porencephaly and encephalomalacia may appear similar to schizencephaly but are the result of parenchymal injury to previously developed structures. Before the end of the second trimester, glial scar formation does not occur and focal injury results in the development of a fluid filled space, porencephaly that would not be lined by only gray matter. During the third trimester, parenchymal injury incites glial scar, encephalomalacia, which appears as high T2 signal in the region of injury.

Lissencephaly

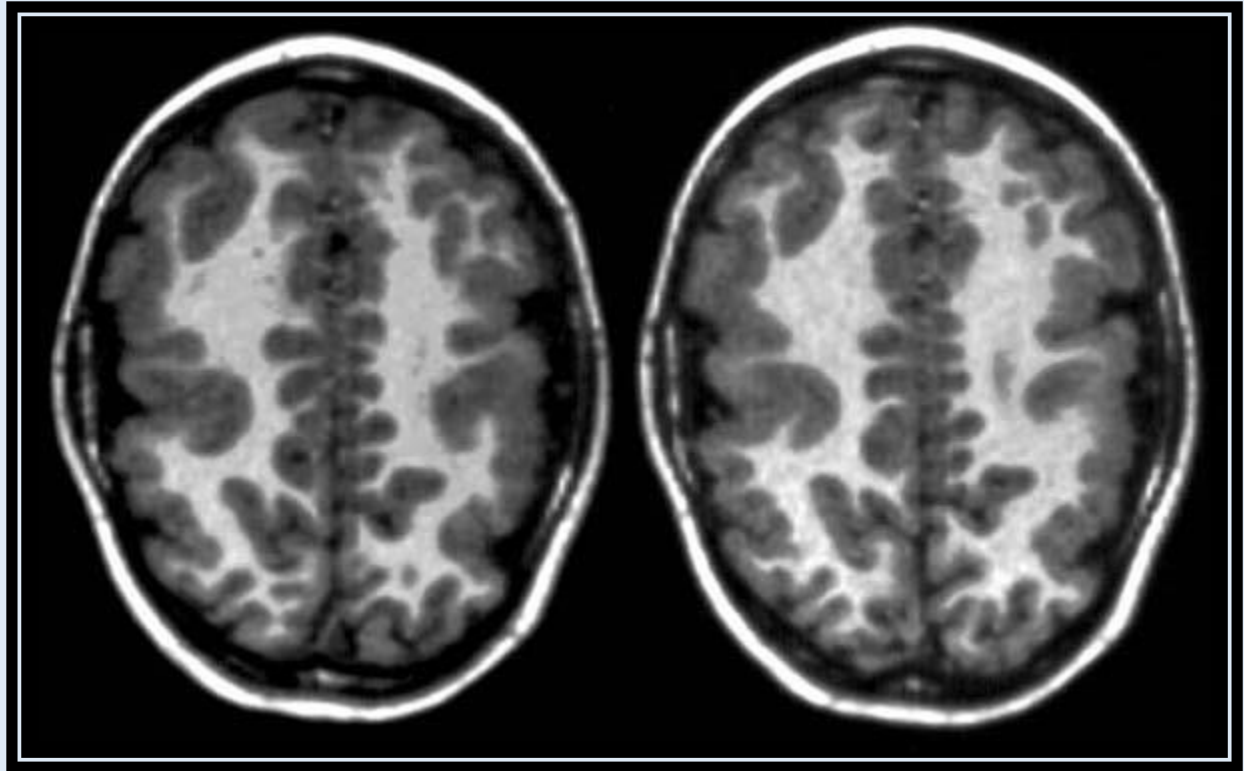
Lissencephaly is the arrest of neuronal migration causing either developmental failure of sulci and gyri (agyria) or development of abnormal broad and flat gyri with abnormal shallow sulci (pachygyria). Lesions typically do not appear in isolation. Polymicrogyria is a similar disorder that results in small, disorganized gyri. It is unknown whether this is due to abnormal neuronal migration or cortical dysplasia.



Agyria



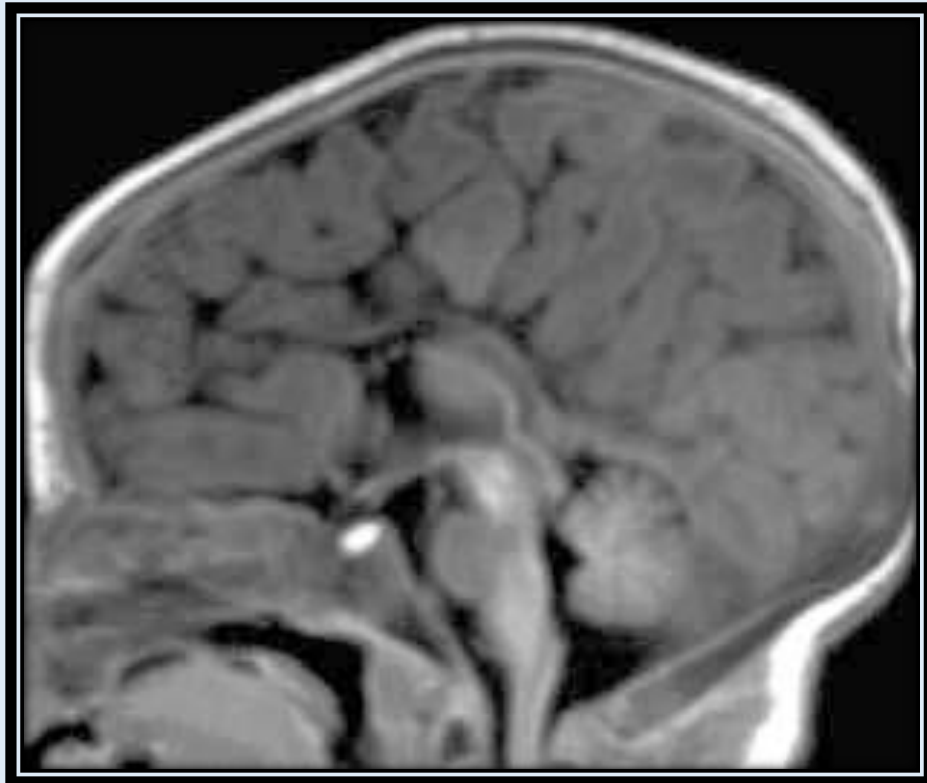
Pachygyria



Polymicrogyria in the bilateral parietal lobes.

Dysgenesis of the Corpus Callosum

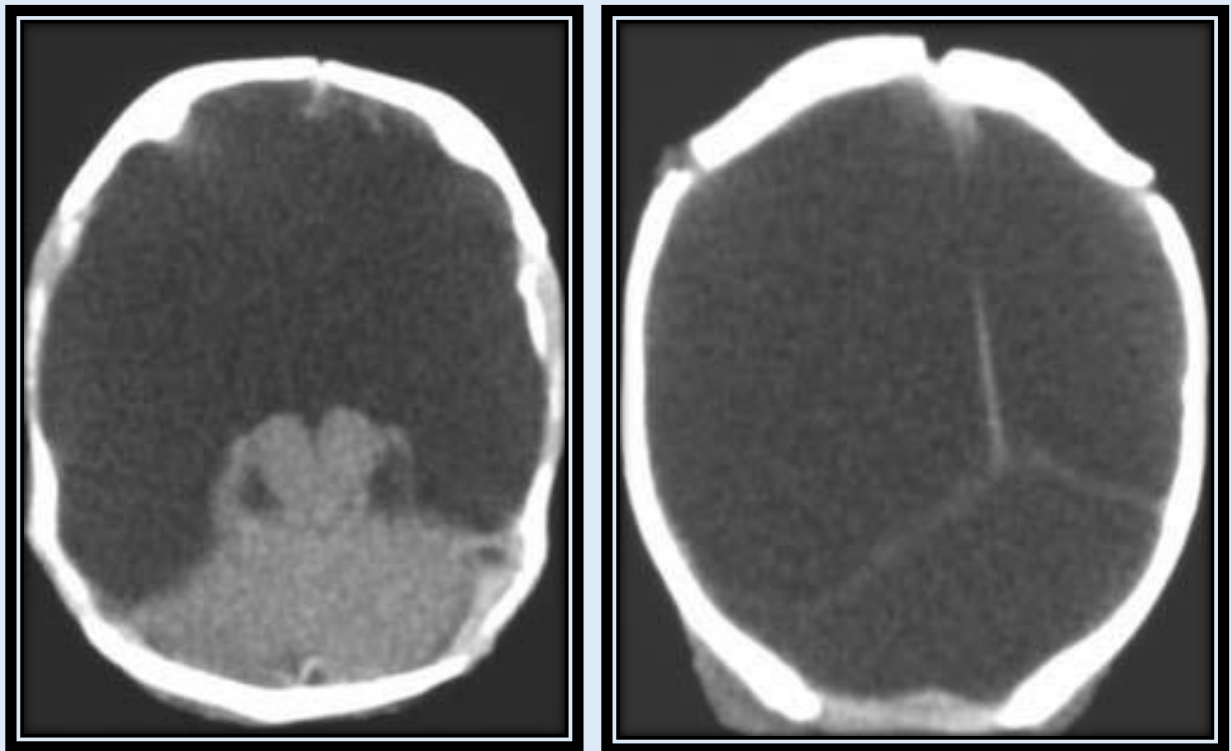
The corpus callosum normally develops from an anterior to posterior direction. Dysgenesis of the corpus callosum includes both complete and partial absence. Absence can occur as an isolated lesion or in conjunction with many other development abnormalities. In partial absence, the more anterior part of the corpus callosum is present.



Midline Sagittal MRI demonstrates absence of the corpus callosum

Hydranencephaly

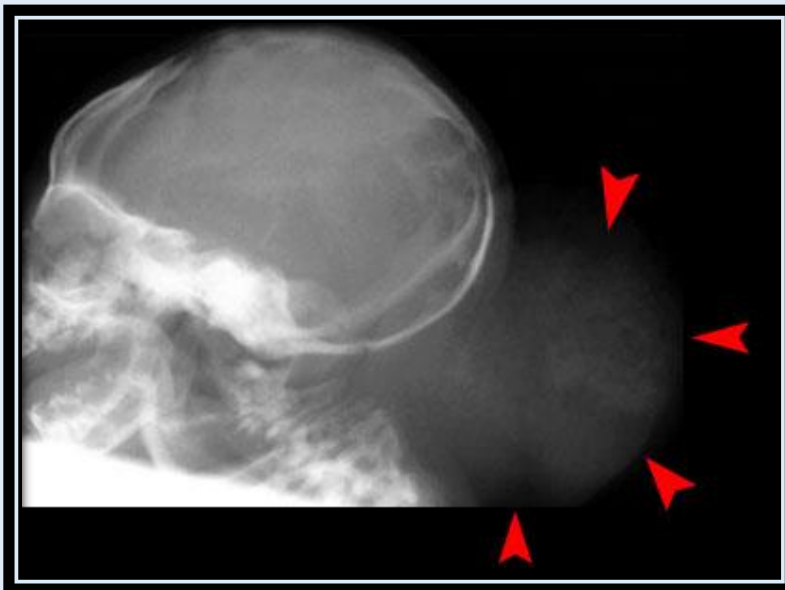
Other congenital abnormalities arise from destruction of already developed structures. Hydranencephaly refers to destruction of the majority of the cerebral hemispheres secondary to a massive ischemic event thought to be bilateral internal carotid artery occlusion. Thin walled cystic structures replace the cerebral parenchyma. Posterior circulation structures are typically intact because they are supplied by the vertebrobasilar system. The presence of a falx cerebri and separation of the thalami differentiates hydranencephaly from severe alobar holoprosencephaly. It is sometimes however impossible to differentiate it from severe hydrocephalus.



Hydranencephaly on head CT

Cephaloceles

Cephalocele refers to an extracranial extension or protrusion of intracranial structures through a congenital defect in the skull and dura mater. Cephaloceles are classified by their contents and by the location of the cranial defect through which the herniation occurs. The herniating neural tissues found within the external skin covered sac may include meninges, brain parenchyma and/or ventricles with choroid plexus, and vascular structures. Occipital encephaloceles are most frequent among white populations in Europe and North America.



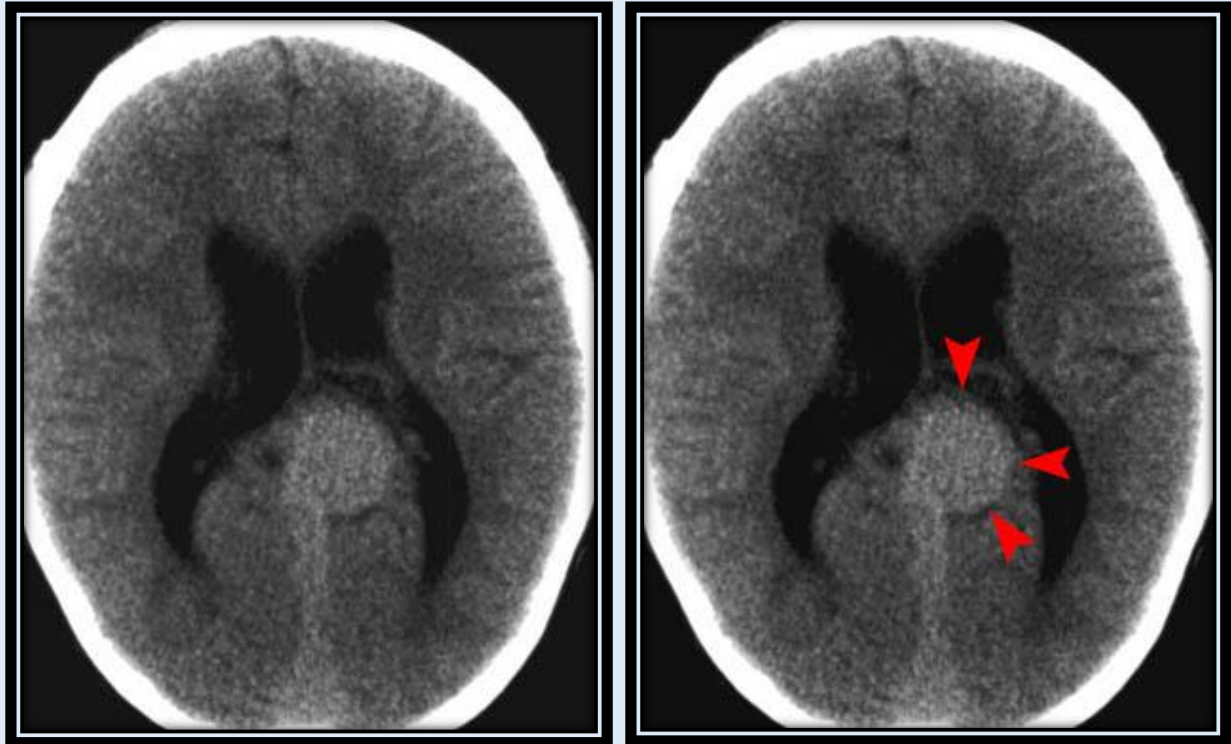
Lacunar skull with soft tissue occipital mass.



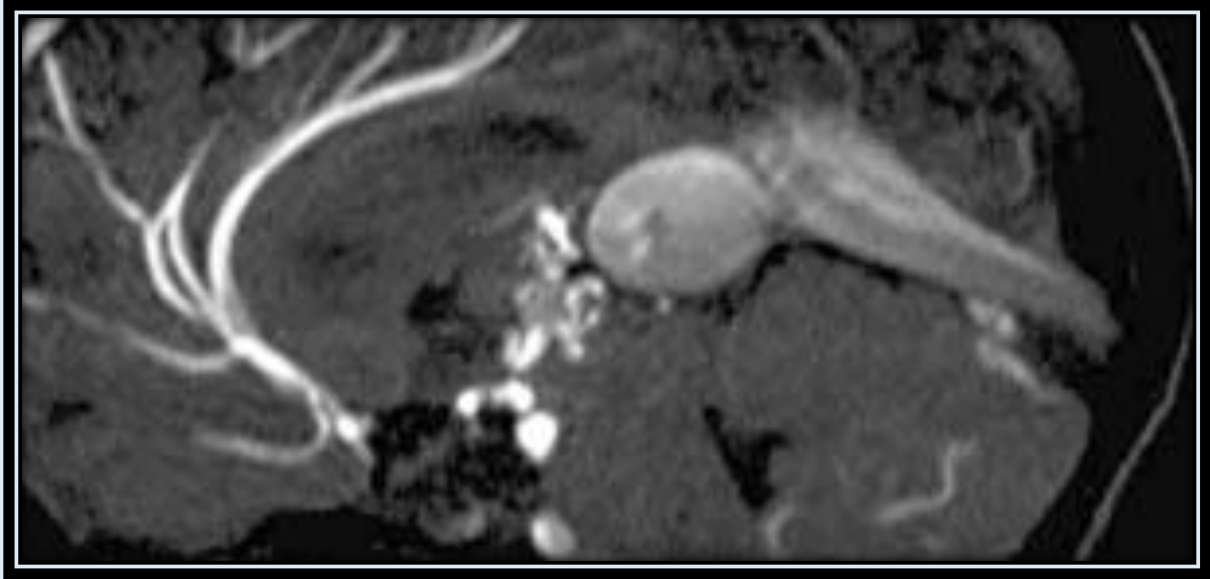
MRI demonstrating occipital encephalocele.

Vein of Galen Malformation

A vein of Galen malformation is an arteriovenous fistula connecting one or more cerebral arteries and the vein of Galen. Typical patient presentation is high output congestive heart failure. Imaging demonstrates a large mass in the region of the posterior third ventricle that displays vascular characteristics. There is often associated hydrocephalus. Treatment is typically arterial embolization.



Head CT



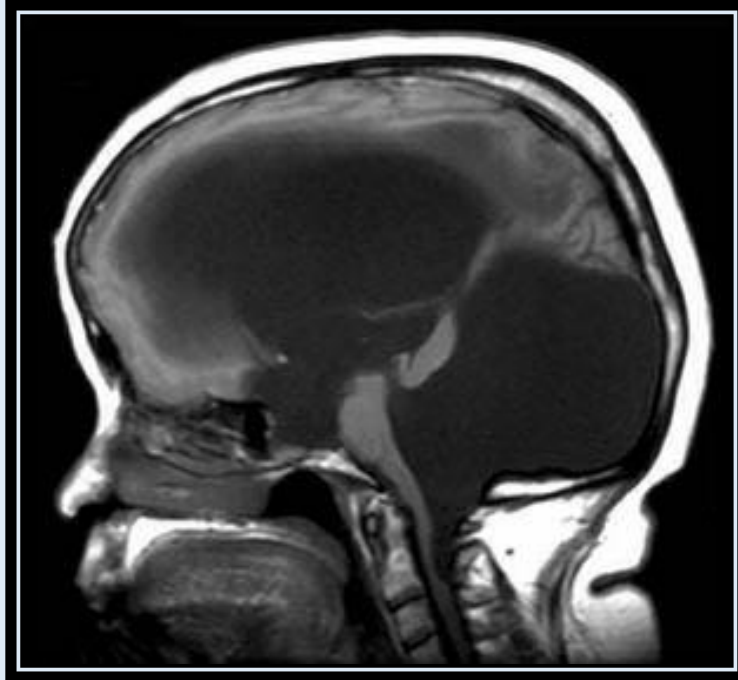
MRA and MRV

Posterior fossa cystic malformations

There are four defined posterior fossa malformations: Dandy Walker malformation, Dandy Walker variant, mega cisterna magna, and arachnoid cyst. Dandy Walker malformation is an enlarged posterior fossa with complete or partial agenesis of the cerebellar vermis in conjunction with the presence of a posterior fossa cyst that communicates with the fourth ventricle. Hydrocephalus is common and there are often supratentorial abnormalities. Dandy Walker variant is considered present when not all the criteria for the classic malformation are present. Most commonly, the cerebellar vermis is hypoplastic but present and the posterior fossa is not enlarged.

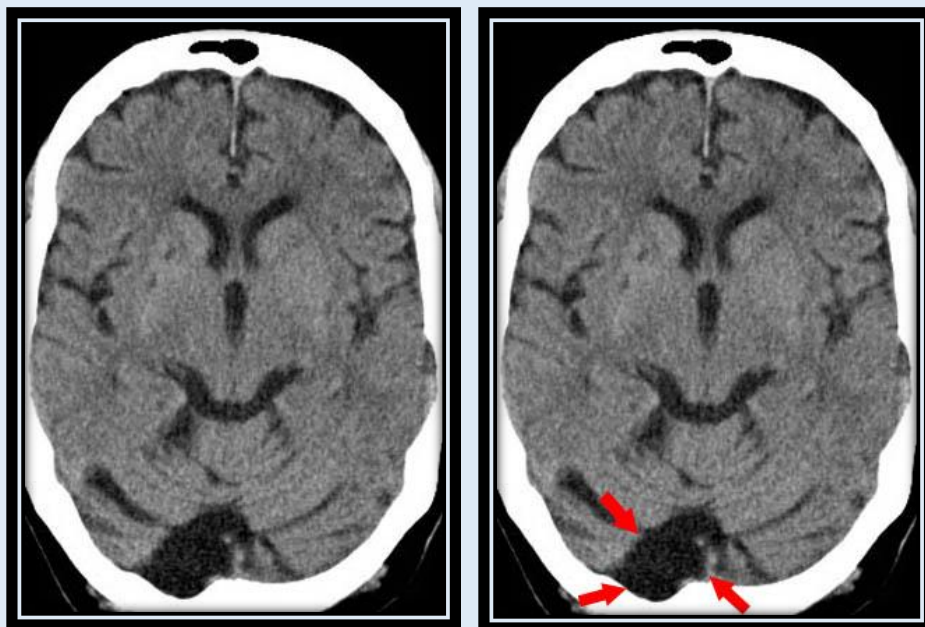


Dandy Walker cyst on axial head CT



Dandy Walker cyst on sagittal MRI

When an enlarged posterior fossa CSF cyst is present in the presence of a fully developed cerebellar vermis, a mega cisterna magna or arachnoid cyst are the two possibilities. If there is no mass effect on the cerebellum then it is considered a mega cisterna magna, whereas mass effect is considered to be from an arachnoid cyst.



Posterior arachnoid cyst with mild mass effect on the right cerebellum.

Myelination Abnormalities

During the first two years of life, there are great changes of myelination in the brain. Before myelination, white matter is hydrophilic and appears high in signal on T2 imaging and low signal on T1. With myelination, white matter becomes hydrophobic and becomes lower signal on T2 and higher on T1. The adult pattern of myelination is complete by 18 to 24 months and progresses in an expected pattern. It is interesting to note that brain maturation occurs at different rates and times on T1 and T2 weighted images. The exact reason is not understood. Myelination progresses from a caudal to cranial direction. Typically, before age 6 months, T1 weighted images are used to determine brain maturation. After 6 months of age, T2 weighted images are used.

Ages when changes on myelination appear on MRI		
Anatomic Region	T1 weighted image	T2 weighted image
Middle cerebellar peduncle	Birth	Birth - 2 months
Cerebral white matter	Birth - 4 months	3-5 months
Anterior portion of posterior limb of internal capsule	2-3 months	4-7 months
Posterior portion of posterior limb of internal capsule	4-6 months	Birth - 2 months
Anterior limb of internal capsule	2-3 months	7-11 months
Genu corpus callosum	4-6 months	5-8 months
Splenium corpus callosum	3-4 months	4-6 months
Central occipital white matter	3-5 months	9-14 months
Peripheral occipital white matter	4-7 months	11-15 months
Central frontal white matter	3-6 months	11-16 months
Peripheral frontal white matter	7-11 months	14-18 months
Centrum semiovale	2-6 months	7-11 months

White Matter Age

Flow Chart for myelination to determine white matter age (WMA)

Chronologic age <6 months use T1 weighted images

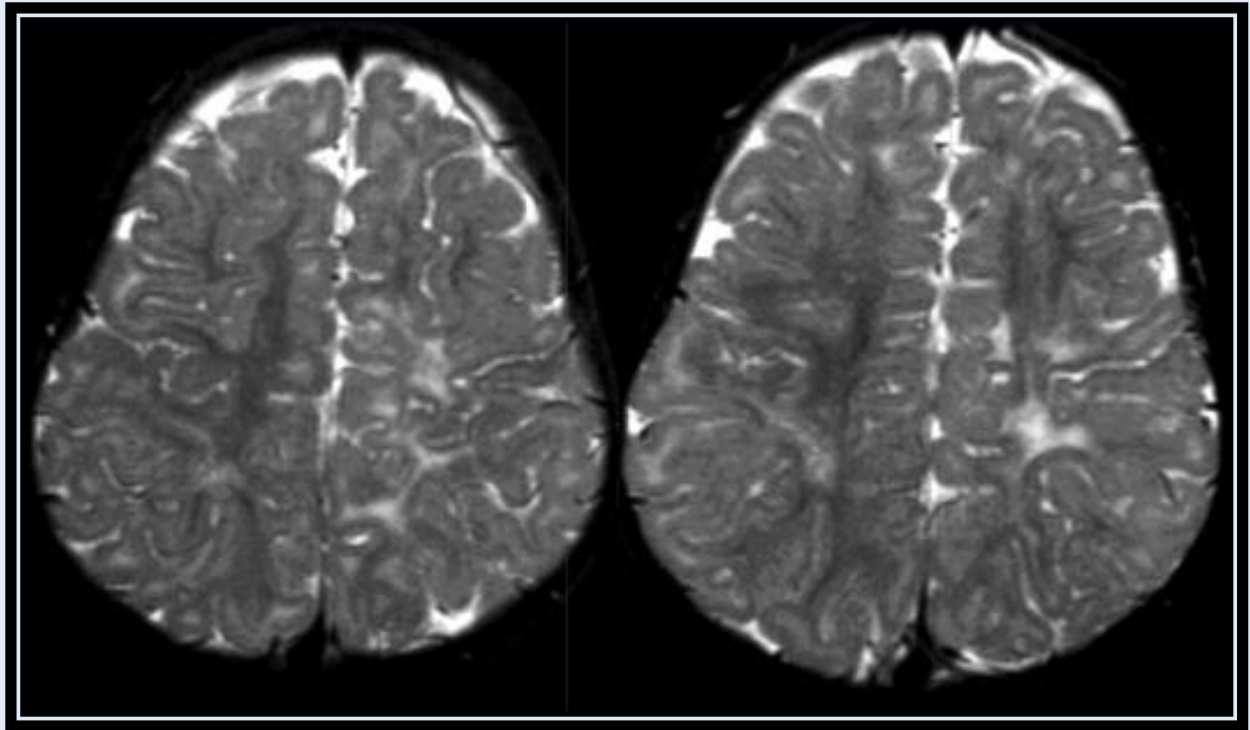
- | | | |
|--------------------------------|----------------|-------------------------------|
| 1. Cerebellum | Not myelinated | WMA <3 months |
| 2. Splenium of corpus callosum | Not myelinated | WMA 3-4 months |
| 3. Genu of corpus callosum | Not myelinated | WMA 4-6 months |
| | Myelinated | Proceed to T2 weighted images |

Chronologic age >6 months use T2 weighted images

- | | | |
|---|----------------|----------------------|
| 1. Splenium of corpus callosum | Not myelinated | WMA <6 months |
| 2. Genu of corpus callosum | Not myelinated | WMA 6-8 months |
| 3. Anterior limb of internal capsule | Not myelinated | WMA 8-11 months |
| 4. Frontal white matter | Not myelinated | WMA 11-14 months |
| 5. Peripheral extension/fine arborization | Not myelinated | WMA 14-18 months |
| | Myelinated | Adult WMA > 18months |

Abnormal Myelination

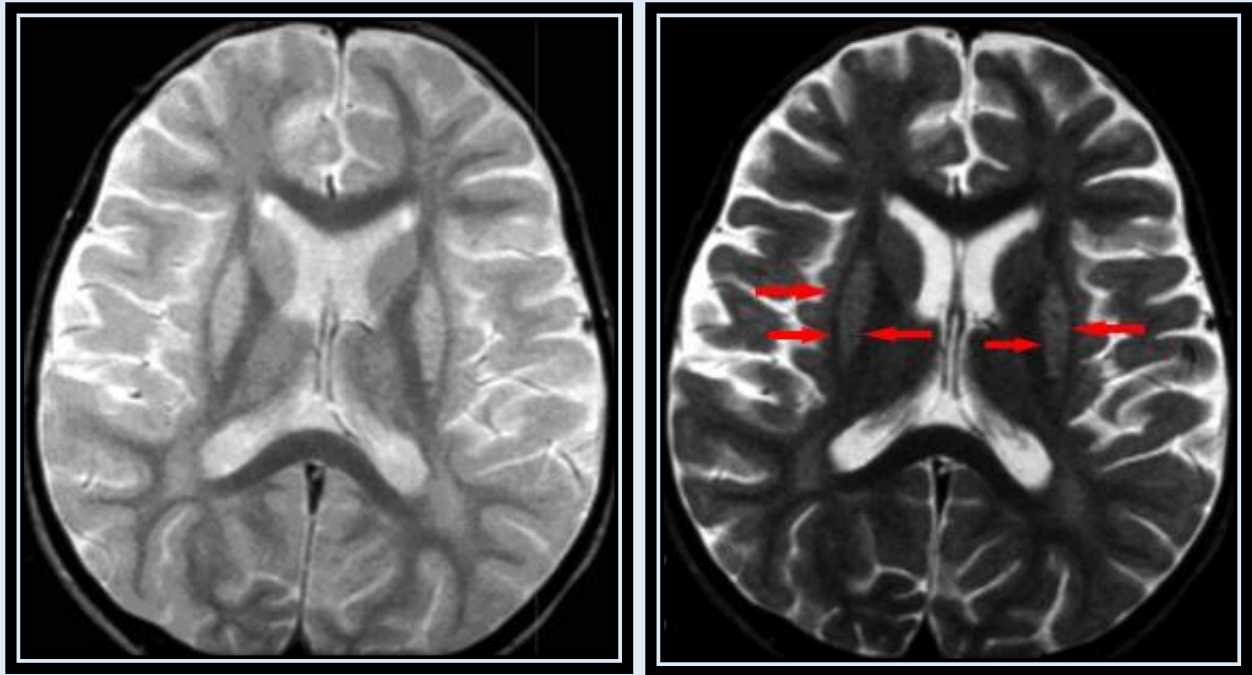
Abnormal myelination is a nonspecific finding and can be caused by metabolic diseases, infection, trauma, hypoxia-ischemia, and malformation syndromes. On a single examination, the pathologic process cannot be determined to be delayed myelination or an arrest of myelination. Two points in time are required to make that determination.



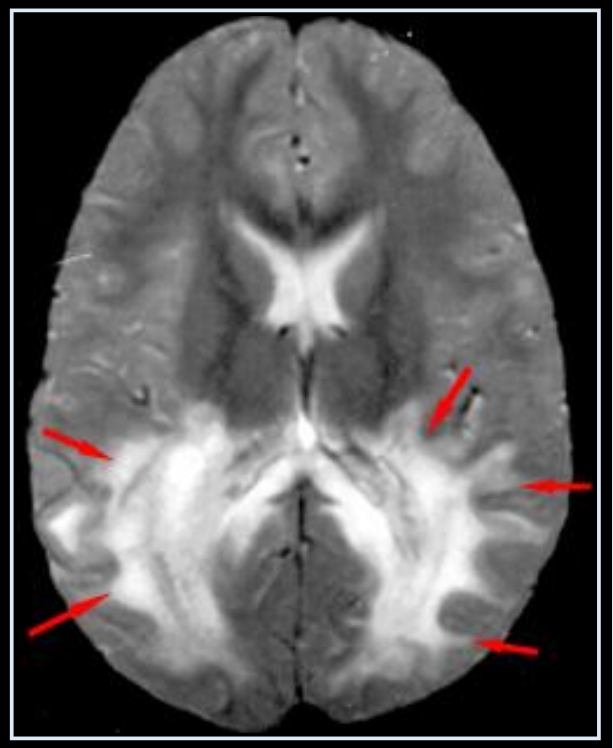
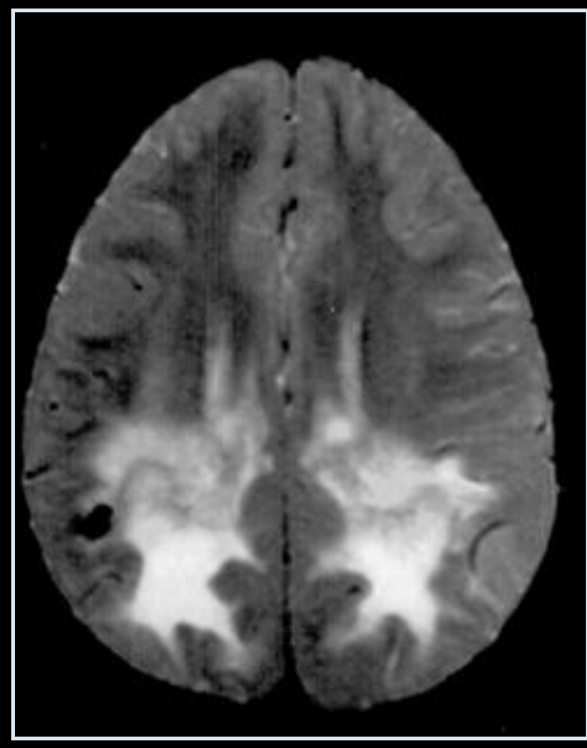
Abnormal myelination in an 18 month old on T2W images - the peripheral white matter is still high signal, more notable on the left.

Genetic Diseases

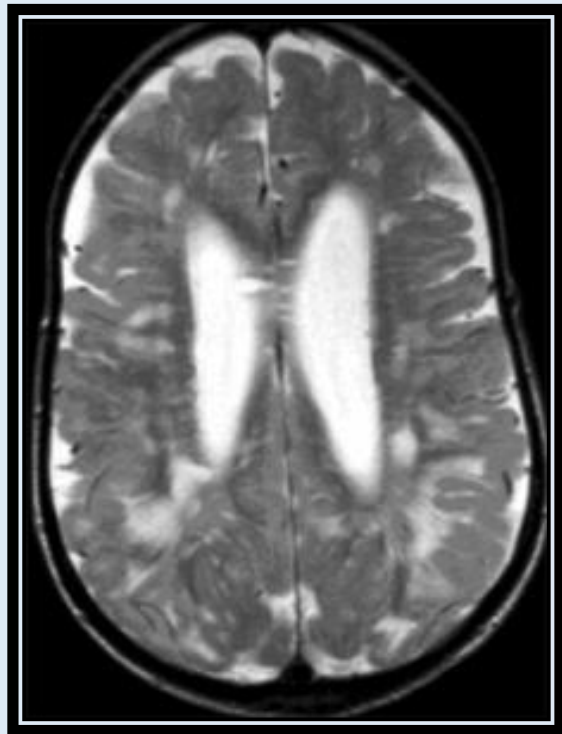
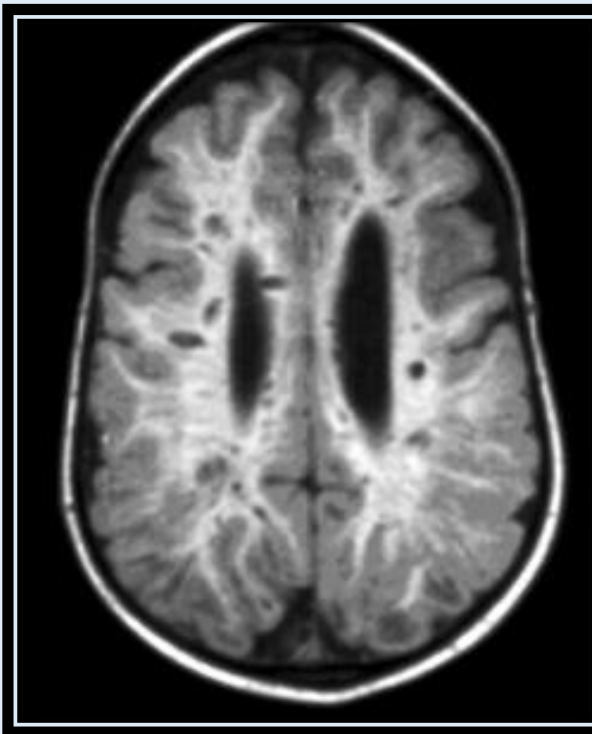
There are a large number of metabolic, degenerative, and toxic disorders that can result in abnormal myelination patterns. Typically there is abnormally increased T2 signal involving portions of white matter or gray matter, or a combination. The distribution of signal abnormality may help narrow the differential diagnosis.



Leigh disease, a disorder of mitochondria, characterized by abnormal T2 signal in the putamen.



Adrenoleukodystrophy, a peroxisomal disorder, characterized by central white matter T2 abnormality posteriorly.



Mucopolysaccharidoses Type IV, a lysosomal storage disease, characterized by expanded Virchow-Robin spaces and increased T2 signal in the white matter

Neurocutaneous Syndromes

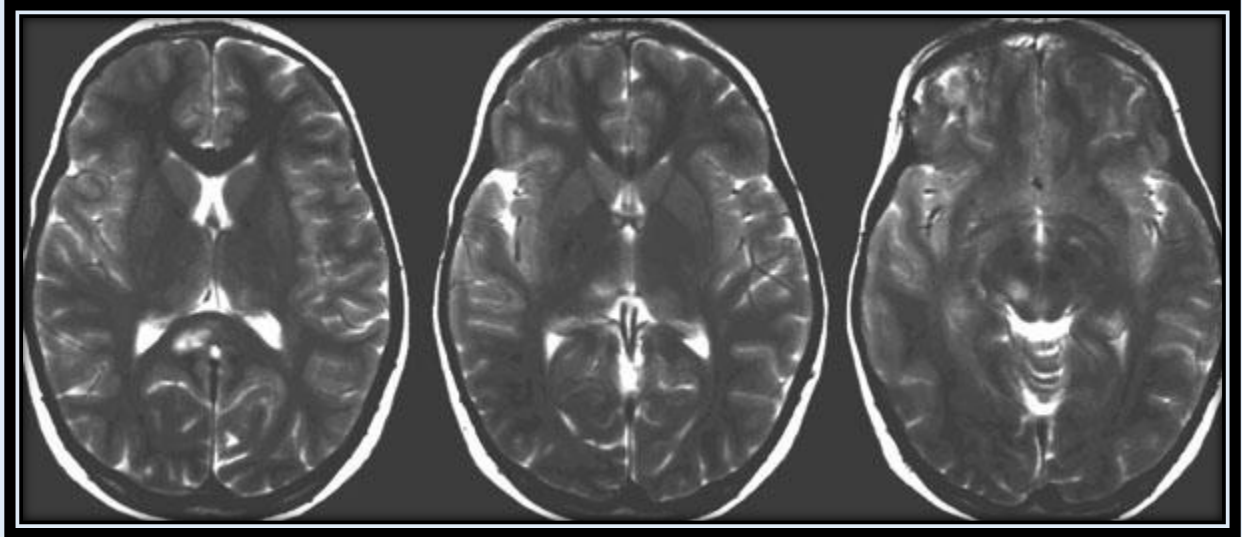
The neurocutaneous syndromes or phakomatoses are a group of related diseases that affect tissues of ectodermal origin, primarily the skin and nervous system. The most common phakomatoses to present in childhood are Neurofibromatosis, Tuberous Sclerosis, and Sturge-Weber syndrome.

Neurofibromatosis

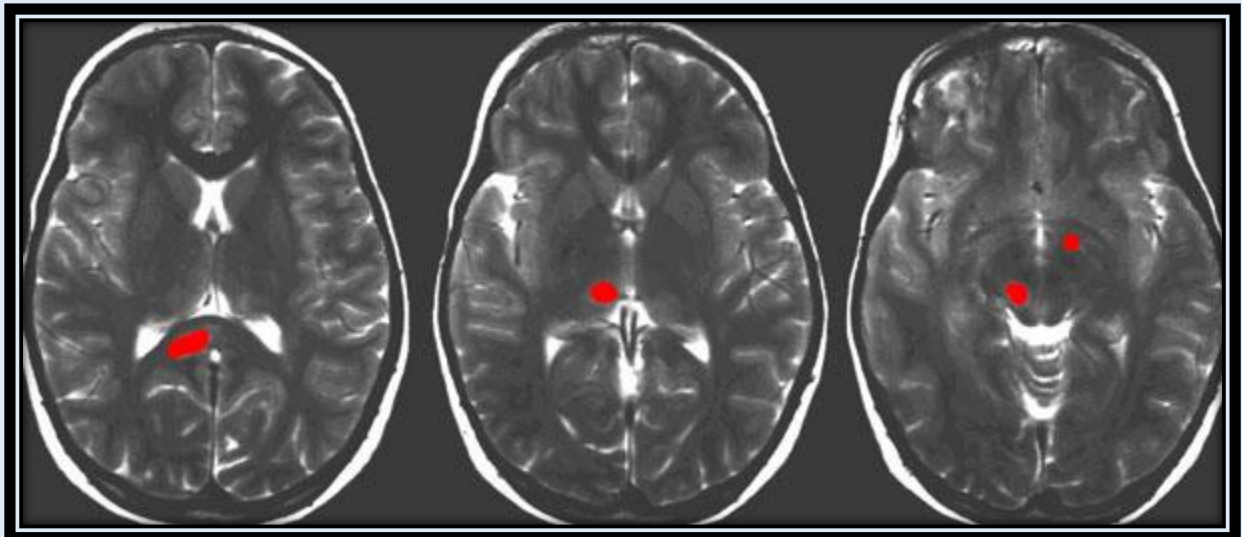
The most common phakomatoses are divided into a number of subcategories, of which neurofibromatosis 1 (NF1) and 2 (NF2) are the most common. NF1 is an autosomal dominant disorder. The diagnostic criteria for NF1 include two or more of the following:

1. Six or more café-au-lait macules
2. Two or more neurofibromas or one plexiform neurofibroma
3. Axillary or inguinal freckles
4. Bilateral optic nerve gliomas
5. Two hamartomas of the iris (Lisch nodules)
6. Parent, sibling, or child with NF1

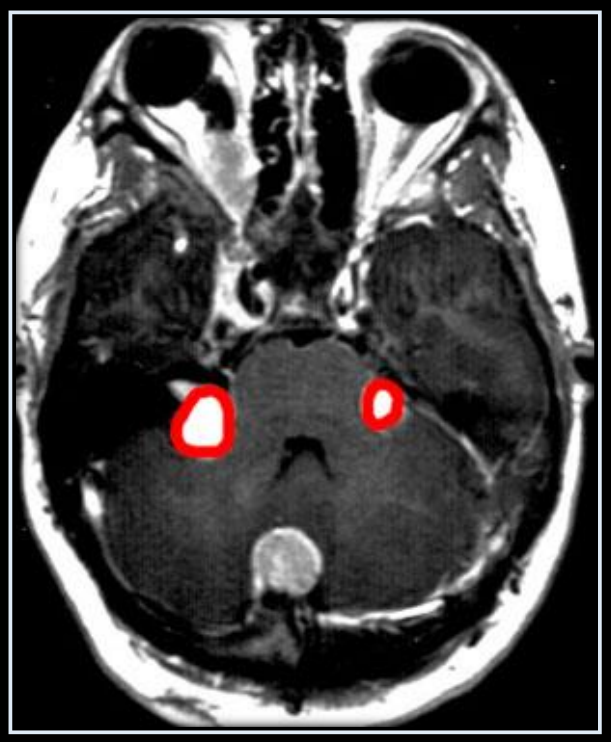
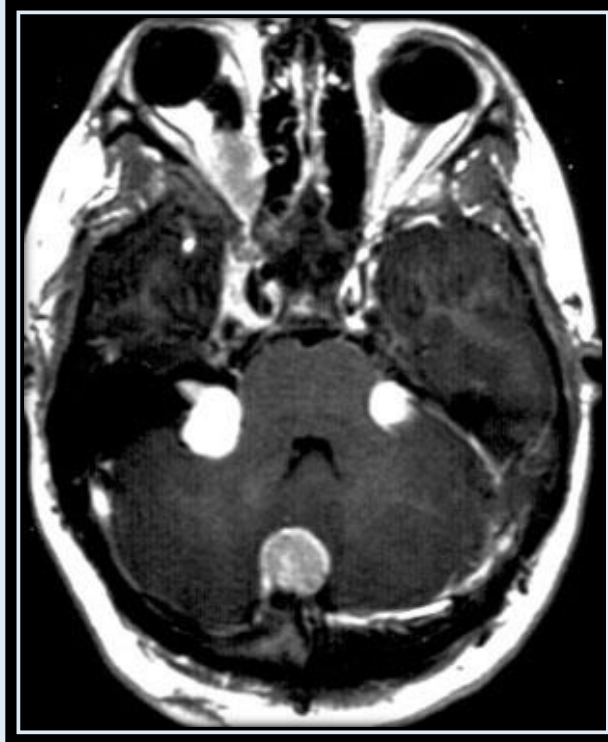
The most common CNS lesions are the NF1 spots that are high signal intensity lesions in the globus pallidus, cerebellum, brainstem, internal capsule, splenium, and thalami. The lesions arise at 3 years and typically regress after 12.



The pictures below show where the lesions are in the above MRI images



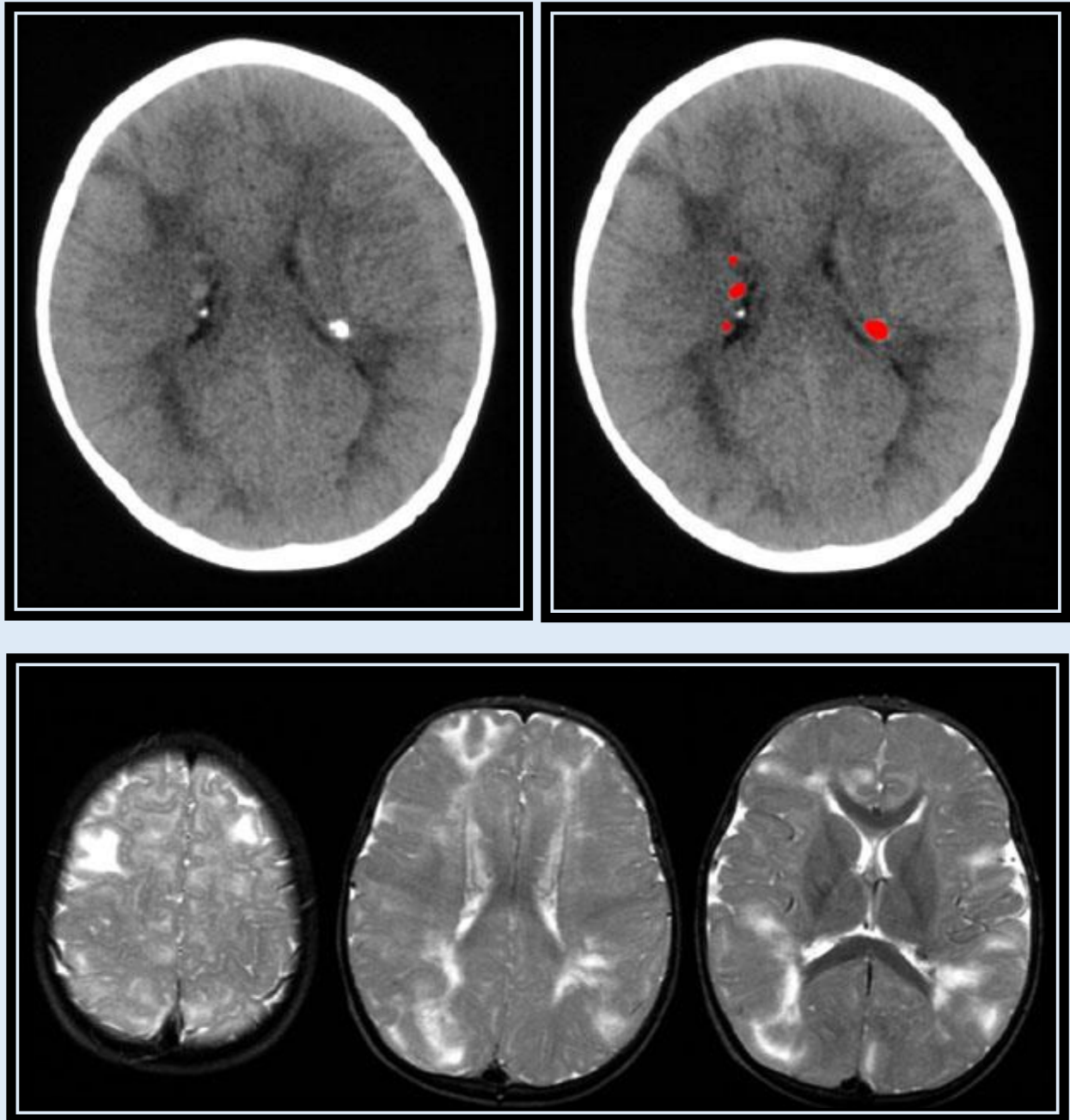
In contrast, NF2 patients present typically in adulthood, characterized by bilateral acoustic schwannomas. Other lesions include meningiomas, gliomas, and neurofibromas.



NF2 with bilateral VIII schwannomas, right optic nerve meningioma, and posterior meningioma.

Tuberous Sclerosis

The classic triad of seizures, mental retardation, and adenoma sebaceum is associated with tuberous sclerosis (TS), another autosomal dominant disorder. The most common imaging finding are tubers, which are hamartomas along the subependymal surface and cortex. These lesions tend to calcify. White matter glial abnormalities may also be present.





Precontrast CT, Giant Cell Astrocytoma

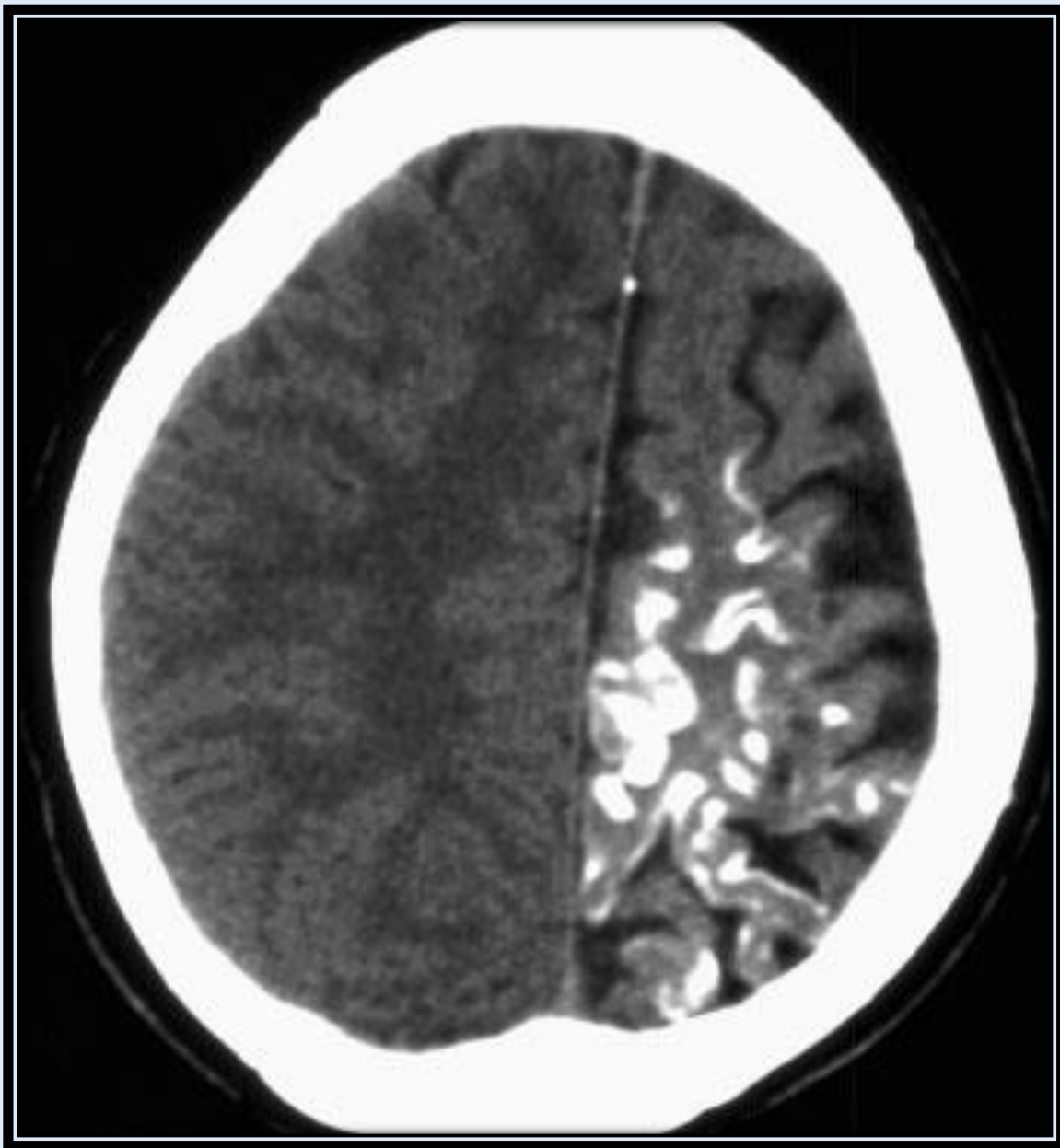


Postcontrast CT, Giant Cell Astrocytoma

A tuber near the foramen of Monro may rapidly enlarge and lead to obstructive hydrocephalus, referred to as a subependymal giant cell astrocytoma.

Sturge-Weber Syndrome

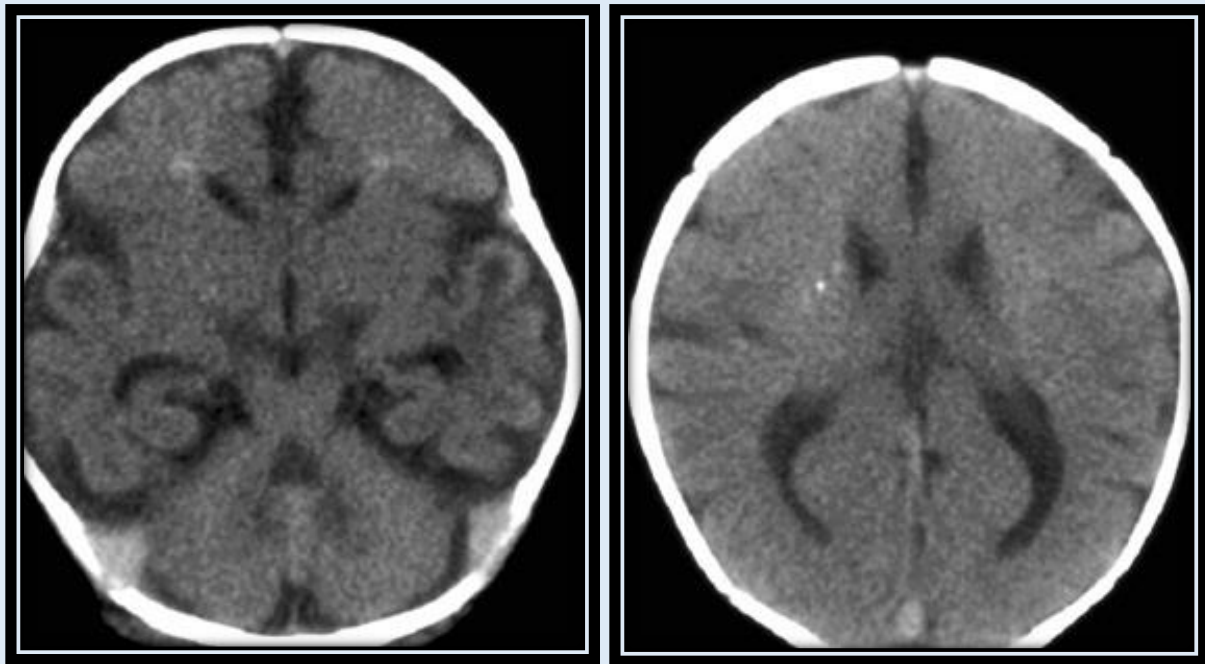
Sturge-Weber syndrome is also called encephalotrigeminal angiomatosis and is characterized by low flow vascular malformations in the trigeminal nerve distribution. On the skin, the port wine nevus is the abnormality. Intracranially, the low flow state in the leptomeninges results in chronic ischemic injury leading to atrophy of the involved gyri. Clinical manifestations include seizures, mental retardation, and hemiparesis. Serpiginous calcifications are seen overlying the involved segment of parenchyma.



Infection

Congenital infections

Congenital infections such as TORCH can affect the CNS. Imaging typically demonstrates calcifications. The most common TORCH to involve the CNS is cytomegalovirus (CMV). CMV may be associated with periventricular calcifications, migrational abnormalities, cerebellar hypoplasia, and ventricular enlargement. Toxoplasmosis is the second most common. The calcifications are typically more variable in location. Imaging findings of HIV may include diffuse atrophy, delayed myelination, and calcifications most commonly in the basal ganglia and subcortical white matter of the frontal lobes.



TORCH calcifications

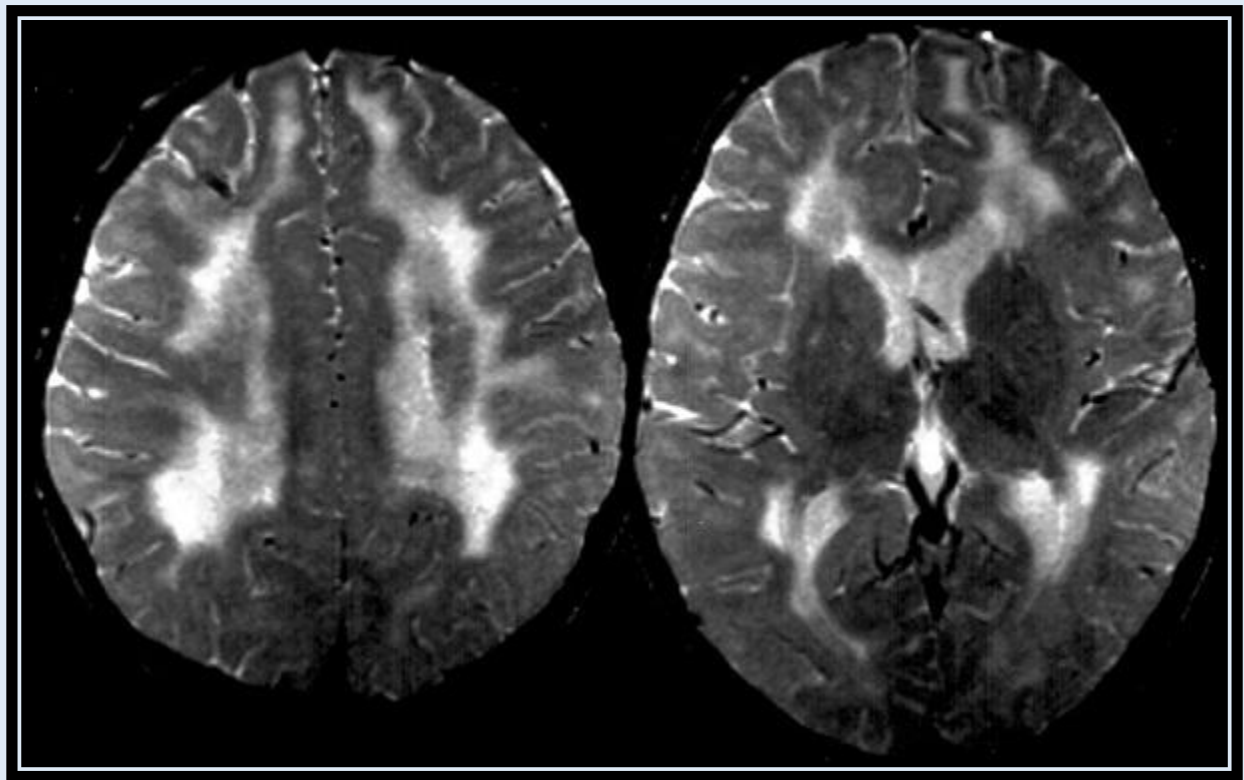
Typically CNS infections in children image similar to adults.

Encephalitis

Encephalitis is inflammation of the brain and may be seen with meningeal inflammation. Herpes encephalitis, when it occurs as a secondary reactivation as seen in adults, typically affects one or both of the temporal lobes as abnormal cortical high T2 signal on MRI, possibly hemorrhagic. In neonates who get the infection during birth, Herpes can involve any part of the brain.

Subacute sclerosing panencephalitis

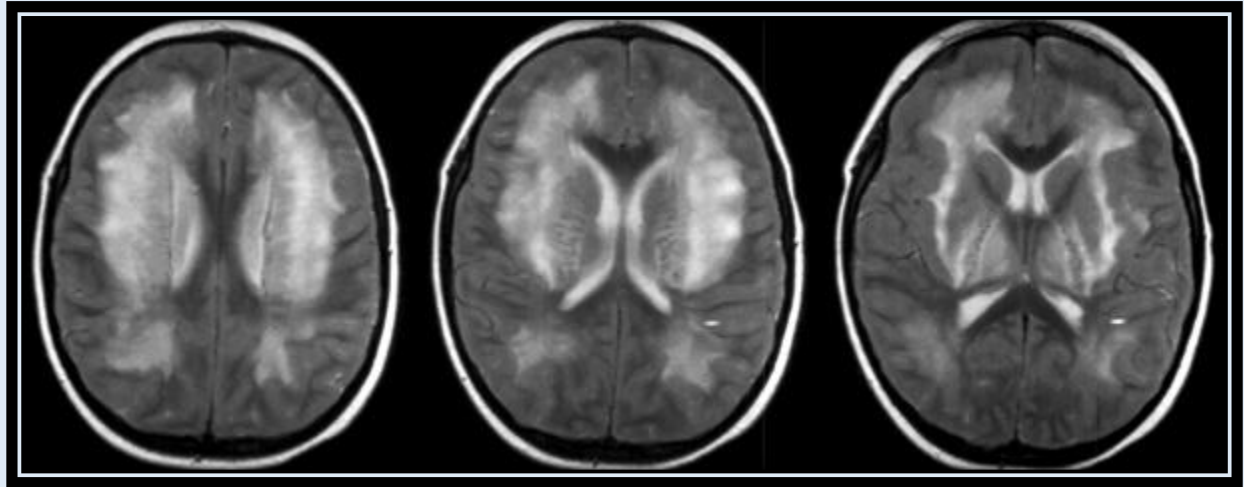
Subacute sclerosing panencephalitis (SSPE) is thought to be an encephalitis secondary to reactivation of a latent measles infection. Imaging demonstrates nonspecific atrophy and increased T2 signal within cerebral white matter.



SSPE

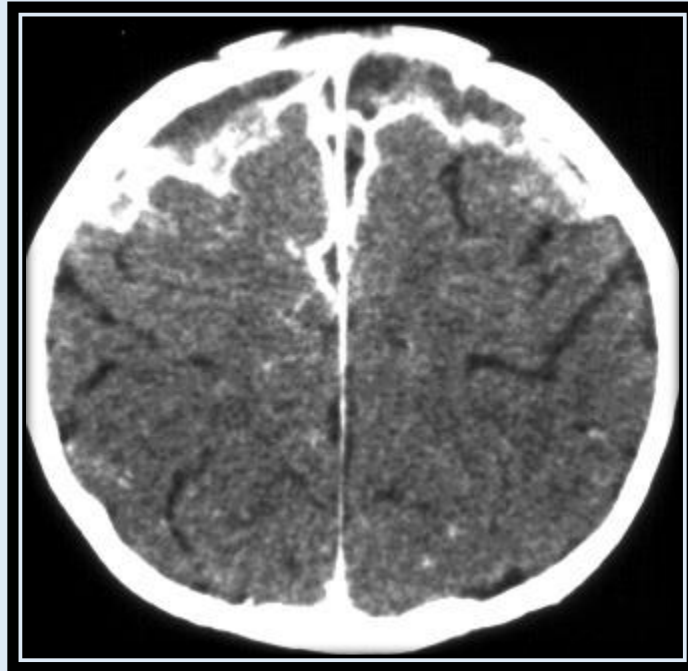
Acute disseminated encephalomyelitis

Acute disseminated encephalomyelitis (ADEM) is an immunologic disease that occurs in response to a recent viral infection or immunization. Increased T2 signal is typically seen in the white matter, brainstem, and cerebellum.



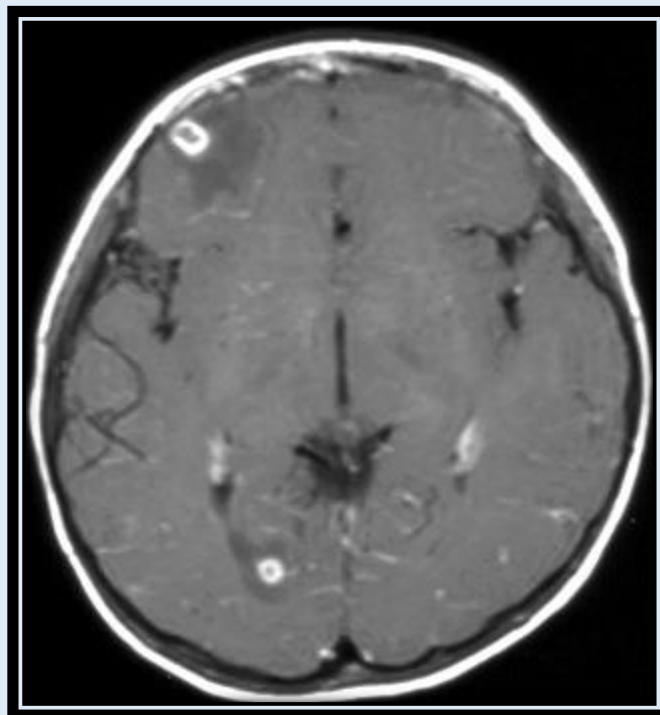
ADEM

Meningitis



Meningitis with frontal subdural enhancing effusions

Cysticercosis



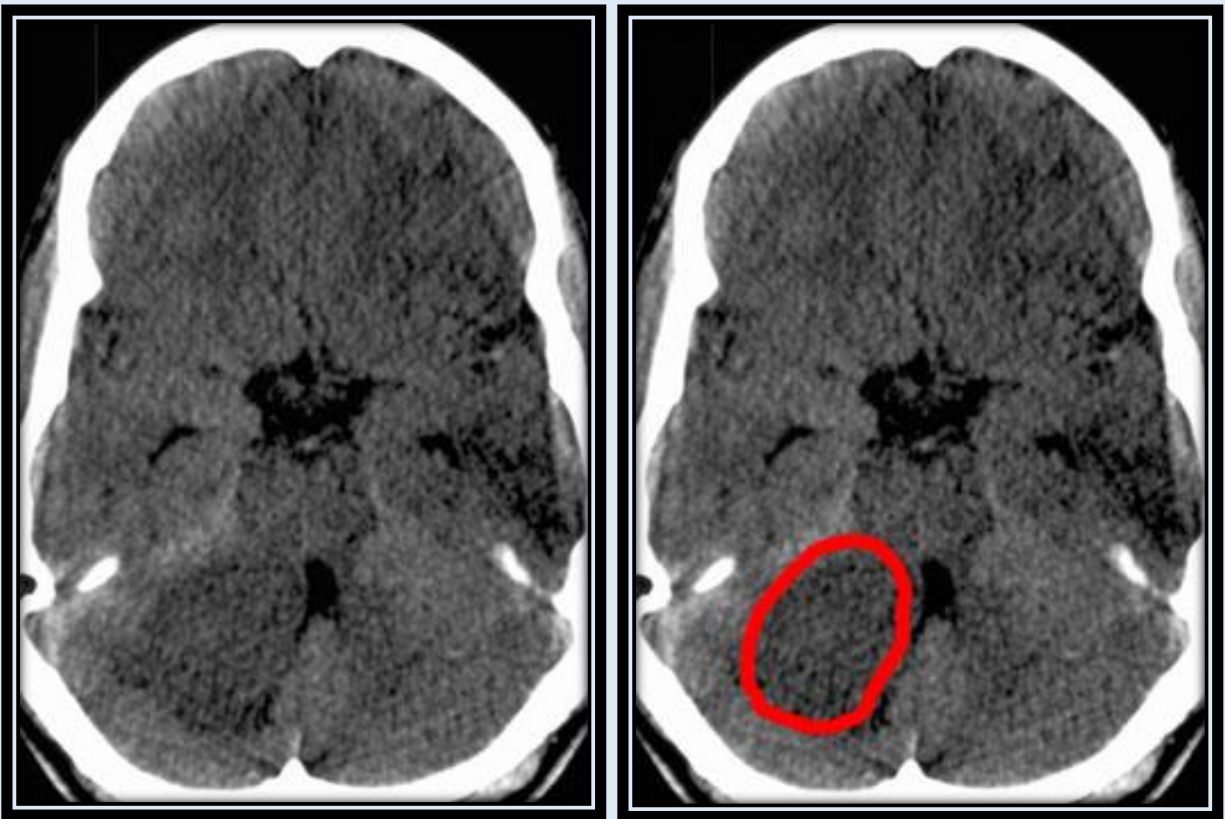
Cysticercosis with ring enhancing lesions on enhanced MRI

Posterior Fossa Tumors

CNS tumors are the most common solid malignancy of childhood. Tumors of the posterior fossa are more common in children than in adults. Posterior fossa tumors often present with obstructive hydrocephalus secondary to compression of the fourth ventricle. The differential diagnosis for posterior fossa tumors in children is limited with the most frequent being juvenile pilocytic astrocytoma, medulloblastoma, brainstem glioma, and ependymoma.

Cerebellar Astrocytoma

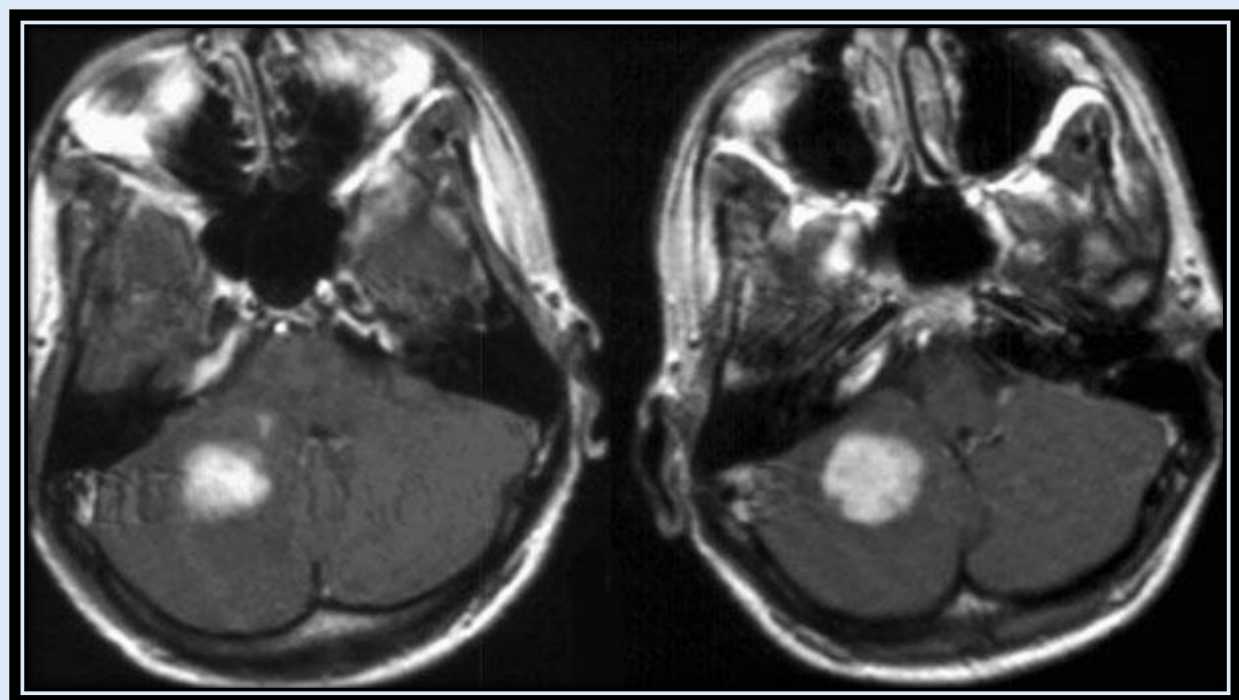
The most common posterior fossa tumor is an astrocytoma, typically a low-grade pilocytic type. Imaging can be variable, but the lesions are usually well defined with anterior displacement of the fourth ventricle. Lesions can be cystic with an enhancing mural nodule or solid with heterogeneous enhancement. Lesions typically do not demonstrate calcification or hemorrhage.



Head CT



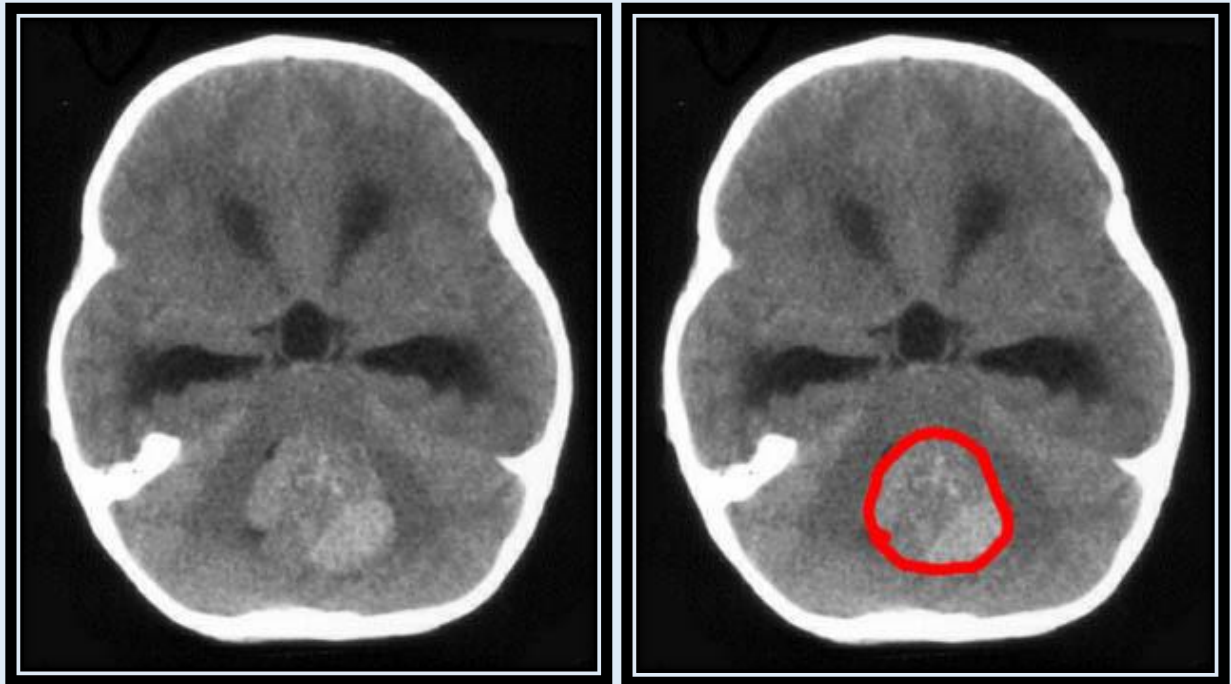
MRI T2-weighted



Post contrast MRI

Medulloblastoma

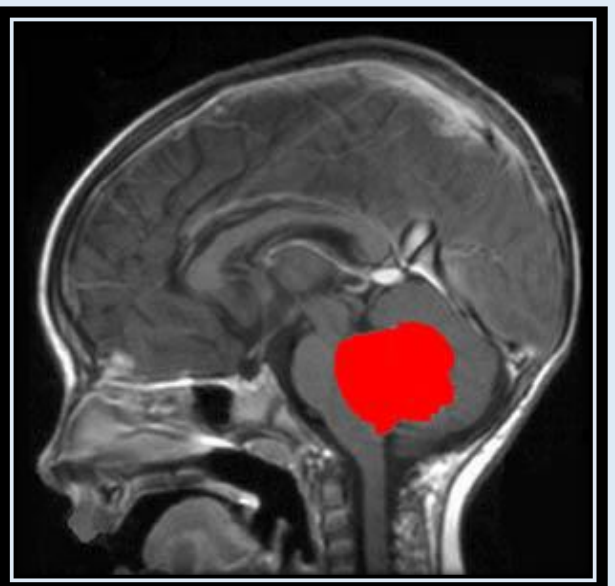
The most malignant and the second most common posterior fossa tumor, medulloblastoma is considered a primitive neuroectodermal tumor (PNET) and arises from the inferior medullary velum of the cerebellar vermis. The tumor invades the fourth ventricle and is typically a poorly defined mass. Lesions are hypercellular and are typically hyperdense on unenhanced CT, enhancing diffusely and homogeneously. On MRI, lesions also tend to be more homogeneous. CSF spread/seeding can occur both intracranially and as drop metastases to the intraspinal CSF.



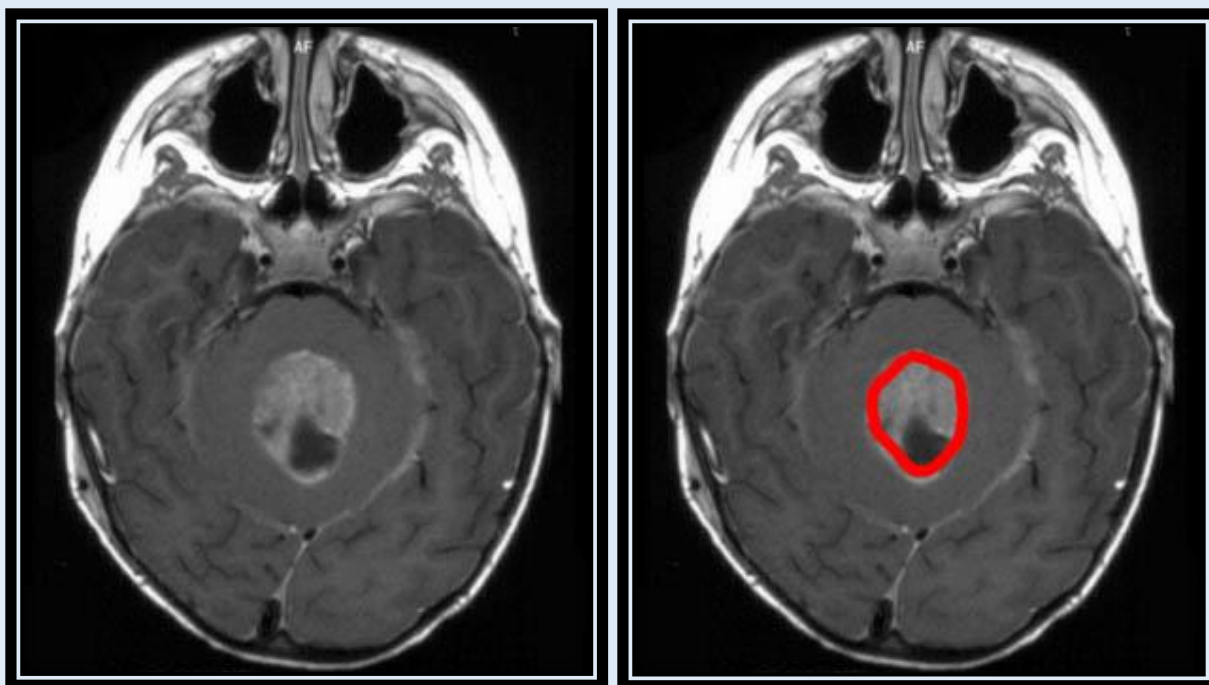
Head CT without contrast



Head CT with contrast



Sagittal MRI with contrast



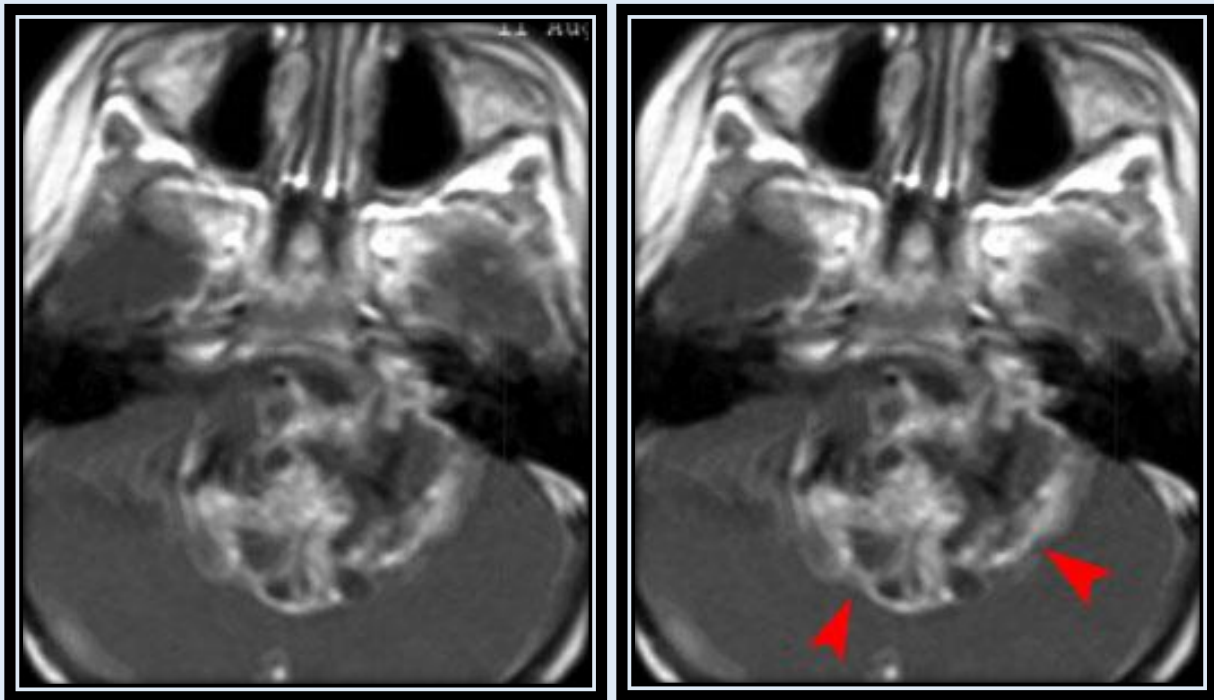
Axial MRI with contrast

Brainstem Glioma

Brainstem gliomas typically present with cranial nerve abnormalities, pyramidal tract signs, or cerebellar dysfunction. Most commonly, these astrocytomas arise in the pons and are moderately aggressive. Lesions may be exophytic, but typically will circumferentially enlarge the brainstem. MRI imaging tends to demonstrate high signal on T2 with rare enhancement. A cystic component may be present in 10% of cases. If large enough the fourth ventricle will be displaced posteriorly from the lesion.

Ependymoma

These tumors are typically slow growing, arising from ciliated ependymal cells. Two thirds of ependymomas occur in the fourth ventricle arising from the floor of the ventricle. Sometimes called a toothpaste lesion, they may fill the fourth ventricle and grow out into the cisterna magna and spinal canal through the foramen of Luschka or Magendie. Lesions appear heterogeneous on imaging, exhibit heterogeneous enhancement, and are usually well defined with lobulated margins.



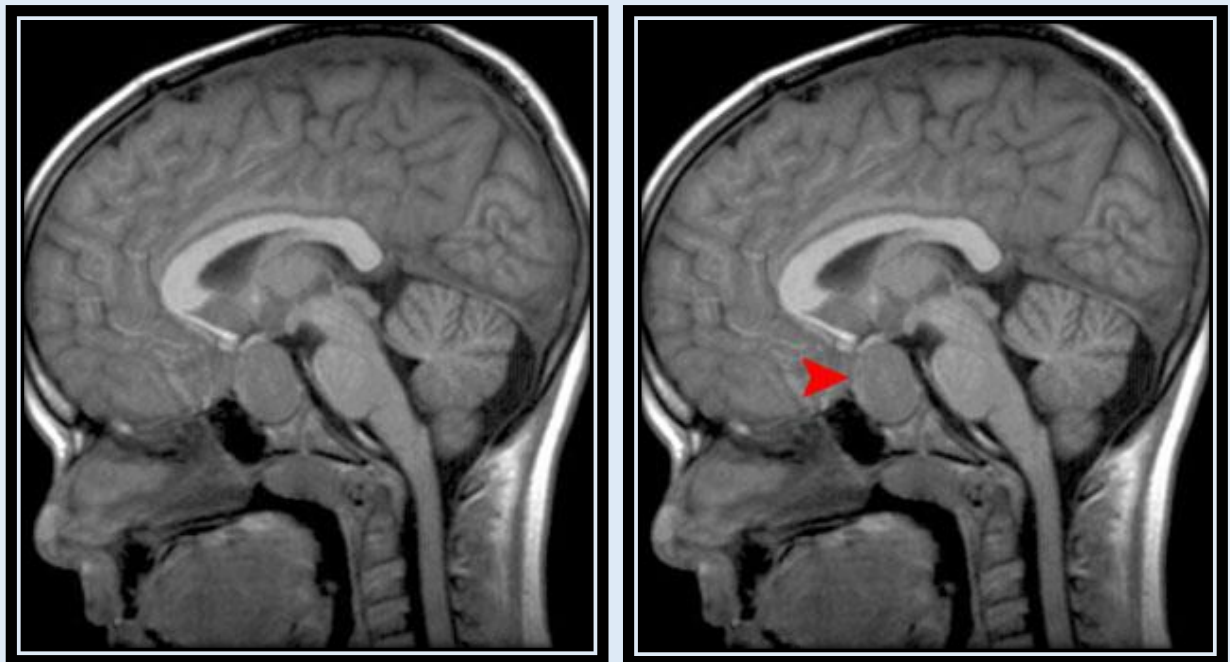
Axial MRI with contrast

Supratentorial Tumors

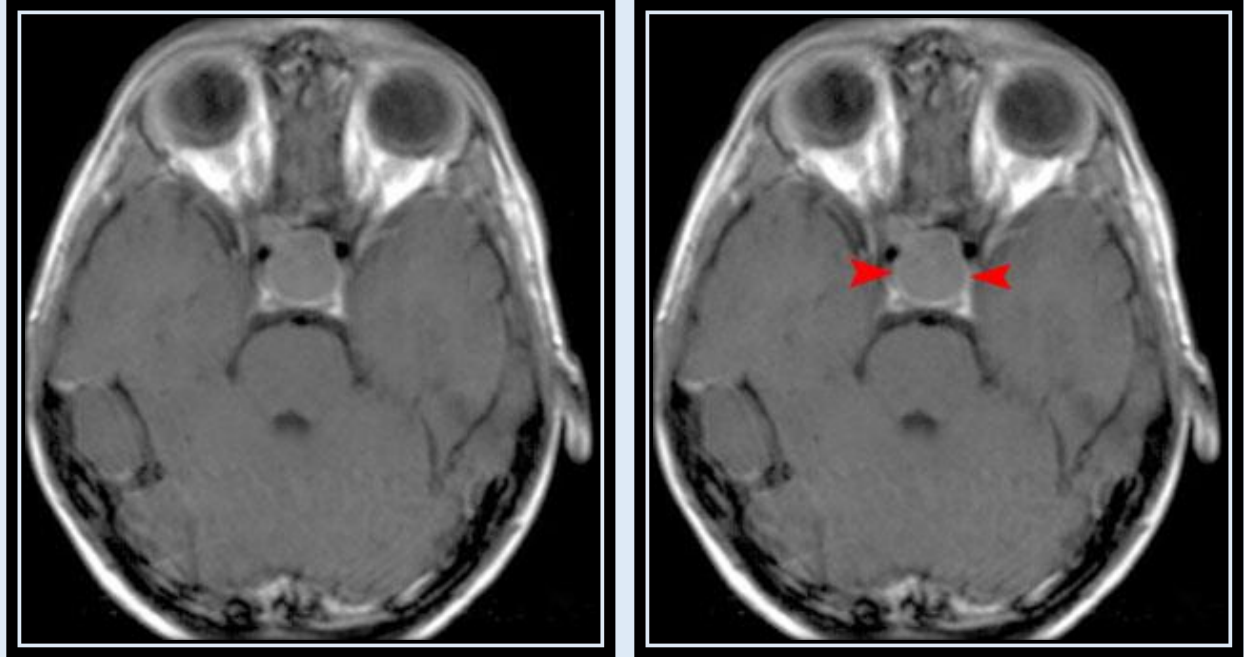
Cerebral tumors are less common than tumors of the posterior fossa in children. The imaging appearance of the lesion does not always correlate to the histologic grade. Approximately 25% of pediatric brain tumors arise in the parasellar region, accounting for nearly half of all supratentorial tumors.

Craniopharyngioma

The most common parasellar mass lesion in childhood, craniopharyngiomas account for about 10% of childhood intracranial tumors. The most common presenting symptom is headache, often with nausea and vomiting. Half of children will have visual symptoms, most commonly bitemporal hemianopsia, decreased acuity, and double vision. They arise from persistence and proliferation of squamous epithelial cells within the tract of the embryologic structure, the craniopharyngeal duct. They may be entirely cystic or solid but most commonly are a combination of both. The cystic fluid may be high signal on all MRI sequences because of proteinaceous material. Eighty percent of cases demonstrate calcification on CT. Solid components typically enhance.



Sagittal MRI with contrast

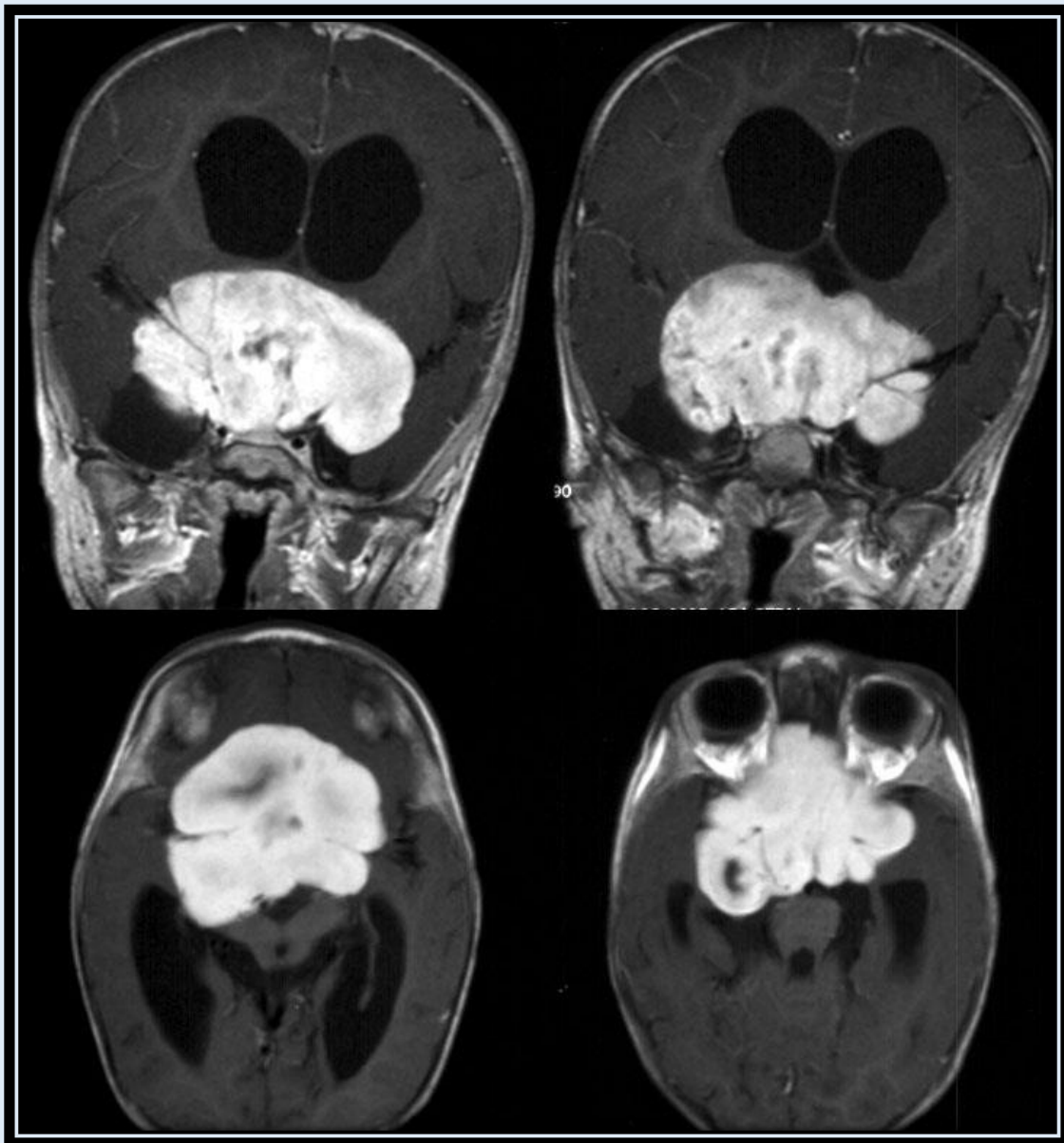


Axial MRI with contrast

Note: Sometimes difficult to differentiate from a craniopharyngioma, Rathke's cleft cyst can also occur in the same location and appear very similar on imaging and histology. Rathke's cleft cysts are remnants of Rathke's pouch between the pars distalis and the pars nervosa of the pituitary. In contrast to craniopharyngioma, Rathke's cleft cysts do not calcify or enhance. Growth is unlikely and if present typically indicates a craniopharyngioma.

Suprasellar astrocytoma

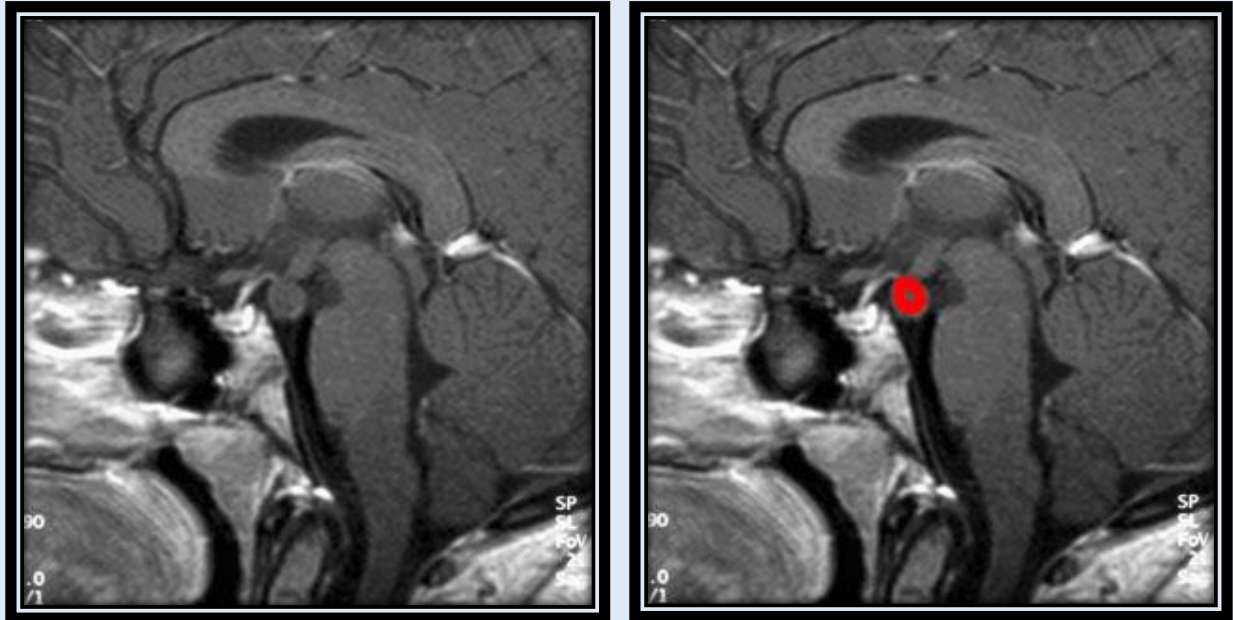
Gliomas of the optic pathways and hypothalamus are among the most common suprasellar neoplasms in children second to craniopharyngioma. Optic gliomas are the most common intracranial neoplasm in neurofibromatosis type I (NF1). However over half of children and adults with optic gliomas will not have NF1. Optic gliomas may occur at any point along the visual pathways. Hypothalamic astrocytomas are generally similar histologically but are less likely to be associated with NF1.



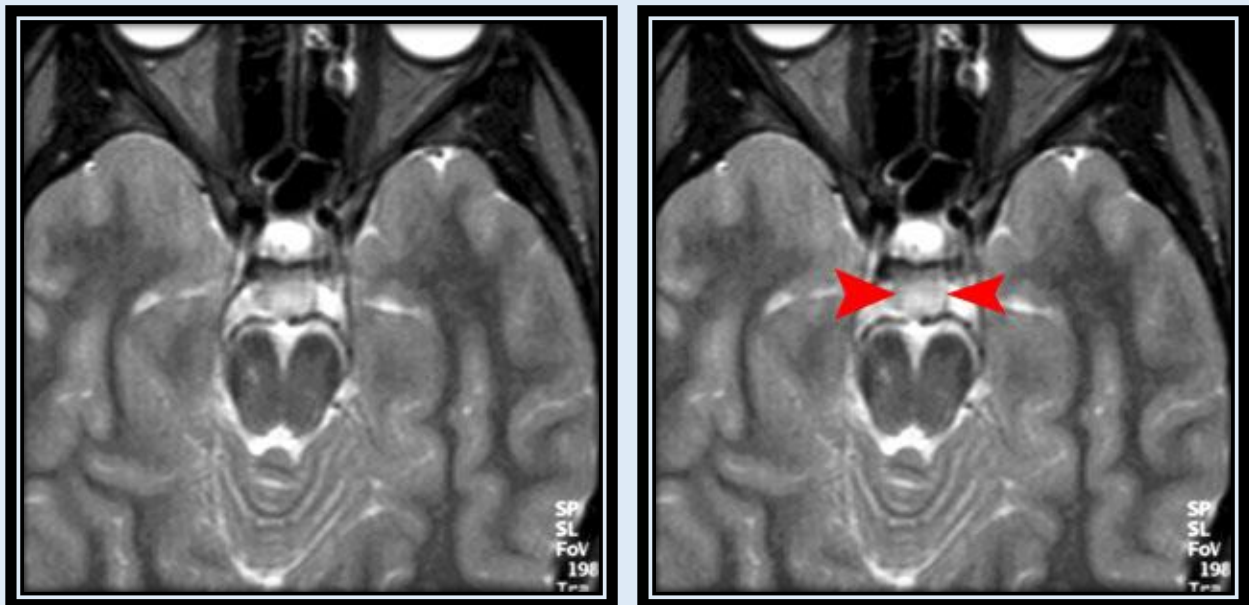
Chiasmatic/hypothalamic astrocytoma enhancing with contrast

Hypothalamic hamartomas

Hypothalamic hamartomas present with a suprasellar mass and may behave as a neoplasm clinically. However, the most common presenting symptom is precocious puberty or a gelastic seizure characterized by fits of laughter. No enhancement has been reported with this lesion.



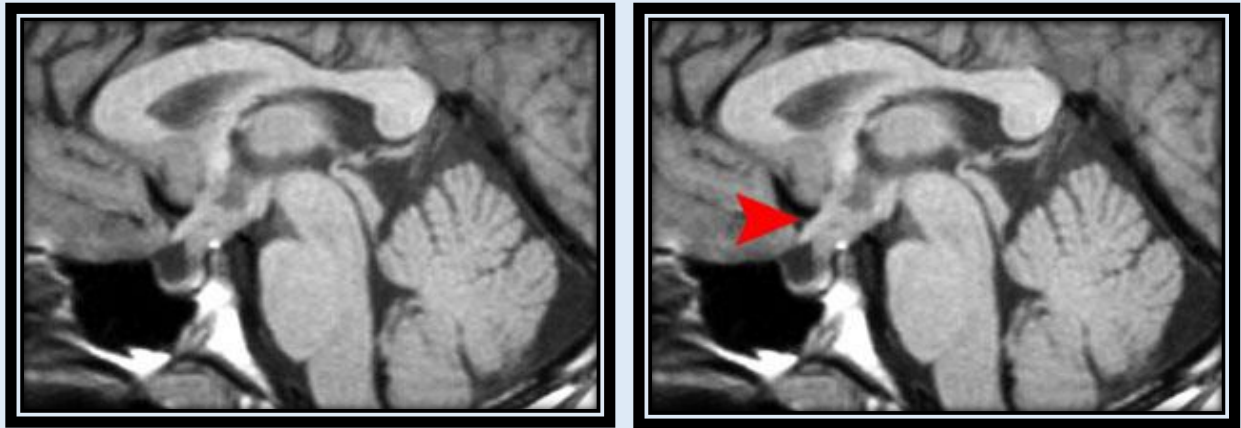
Sagittal T1 MRI post contrast



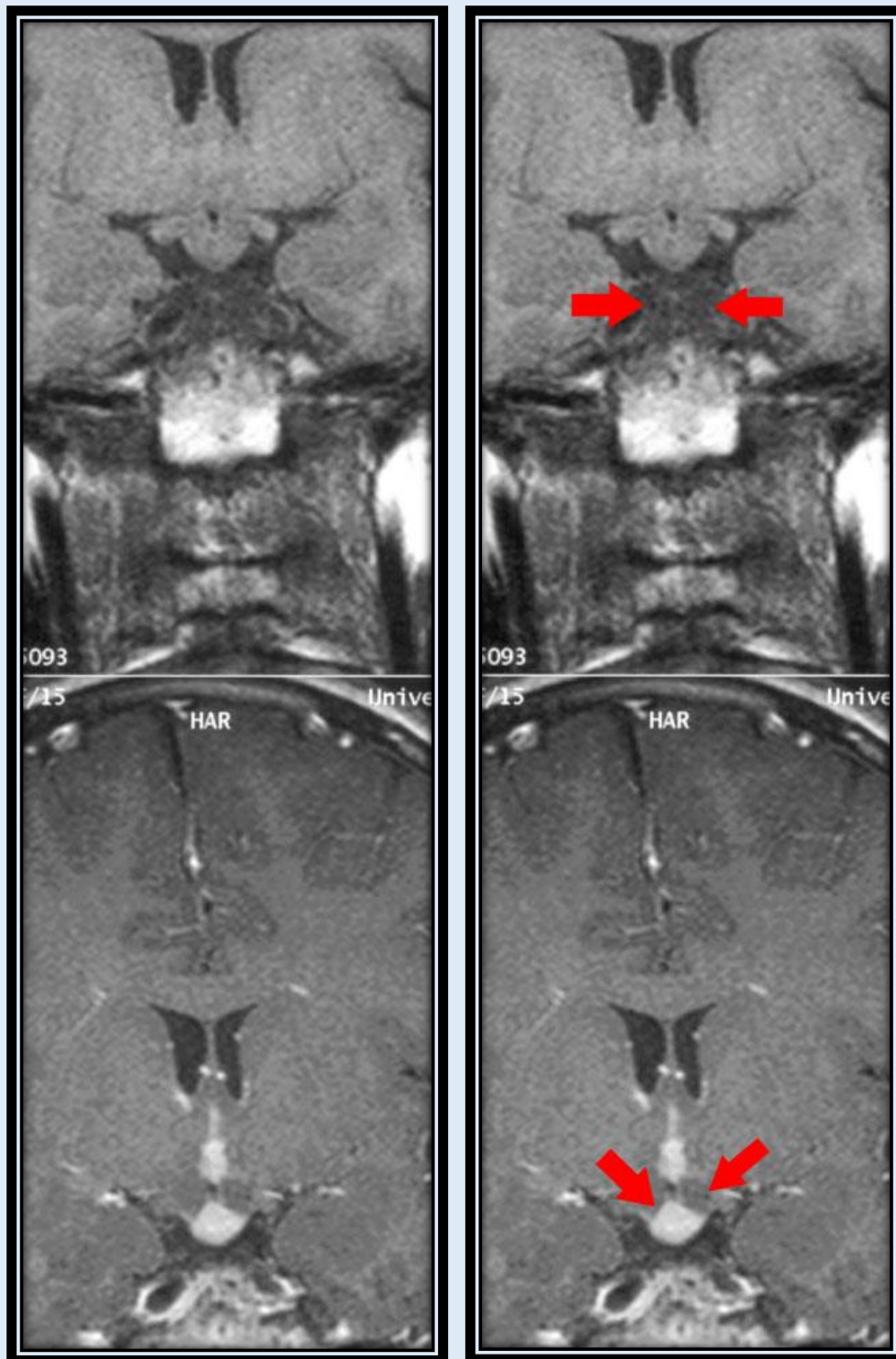
Hamartoma of the tuber cinereum

Germ Cell Tumors

This group of tumors includes germinomas, embryonal carcinomas, teratomas, endodermal sinus tumors, choriocarcinomas, and mixed tumors. Most germ cell tumors occur most frequently at the pineal gland with the exception of germinoma. Fatty tissue or calcification may be seen in teratomas. Histologically, germinomas range from more benign processes to highly malignant and can metastasize throughout the CSF spaces. The imaging appearance does not aid in determining aggressiveness. Lesions uniformly enhance.



Sagittal T1 MRI post contrast



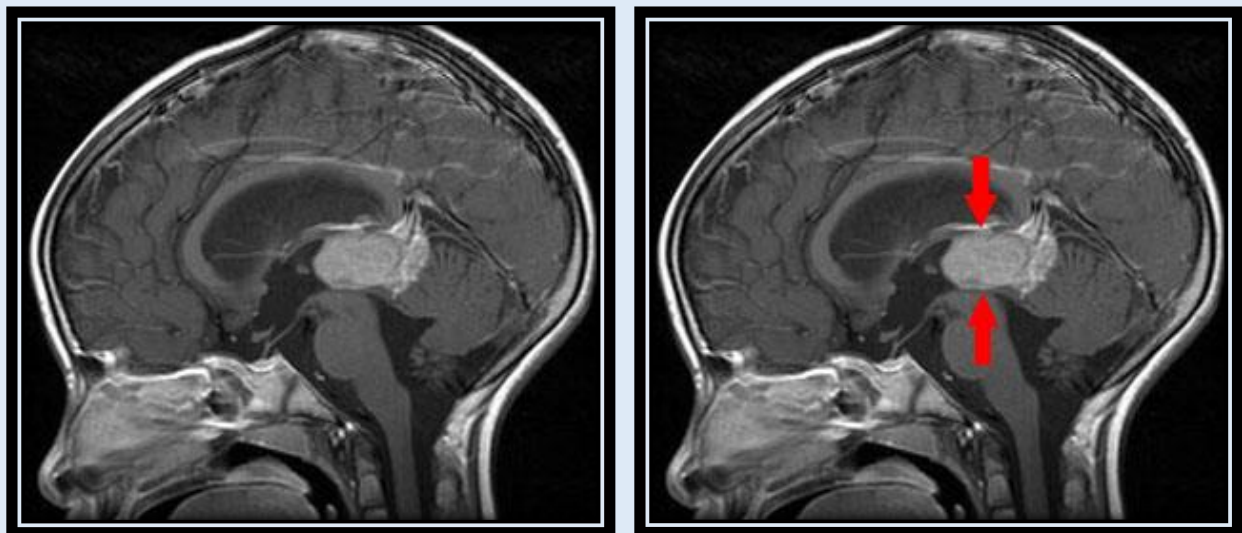
Germinoma

Pineal Region Tumors

The pineal region is the second most common location for CNS neoplasms of the supratentorial space in children. Regardless of histology, lesions cause symptoms related to compression of the cerebral aqueduct or invasion of the tectum. The classic feature of a pineal mass is Parinaud's sign, paralysis of conjugate upward gaze. Physiologic calcification within the pineal gland is increasingly common in the second decade of life. However, pineal calcification in a child less than 6 years old must be considered suspicious for pathology.

Pineocytomas and pineoblastomas

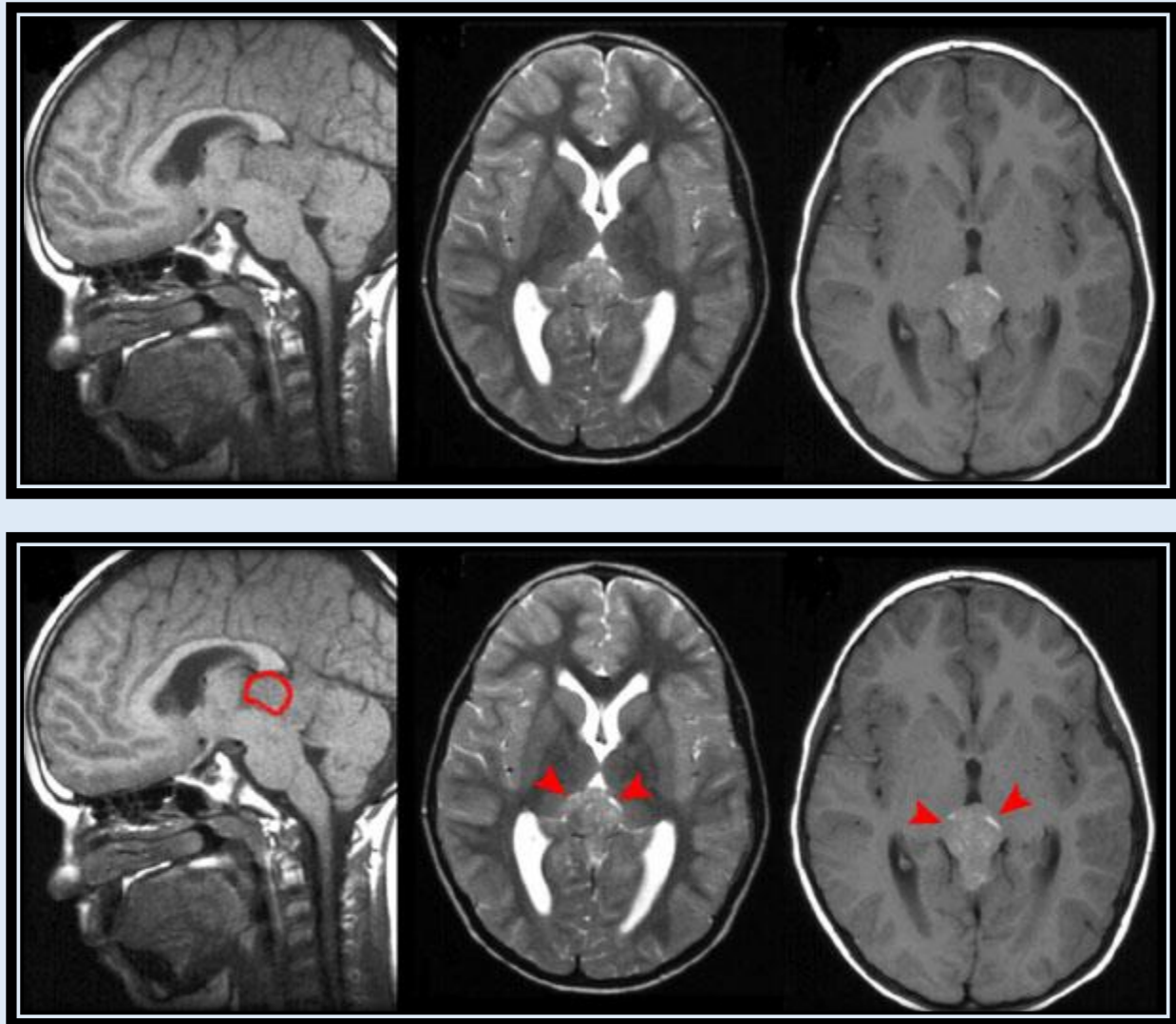
Pineocytomas are well-circumscribed tumors whereas pineoblastomas are typically diffuse with CSF spread and drop metastases. Lesions are nonspecific on imaging, demonstrate enhancement, and may appear sharply margined despite their aggressiveness.



Pineoblastoma

Germinomas

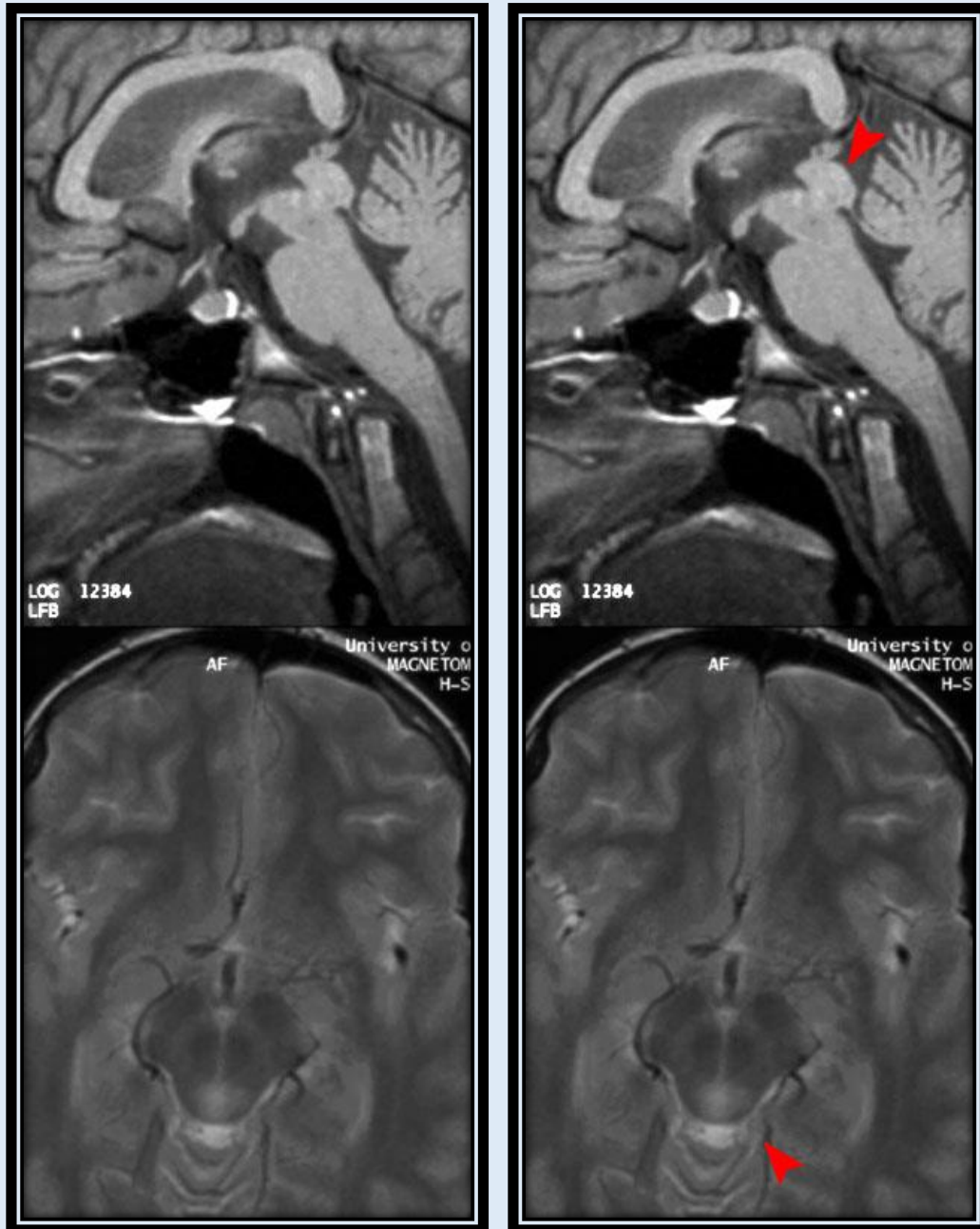
Germinomas are the most frequent tumors in the pineal region in children and imaging is similar to suprasellar germinomas. Teratoma is the second most common pineal region germ cell tumor in children. Other germ cell tumors rarely exist in pure form, with the majority of nongerminoma germ cell tumors containing a mixture of cell types.



Pineal region germinoma

Tectal glioma

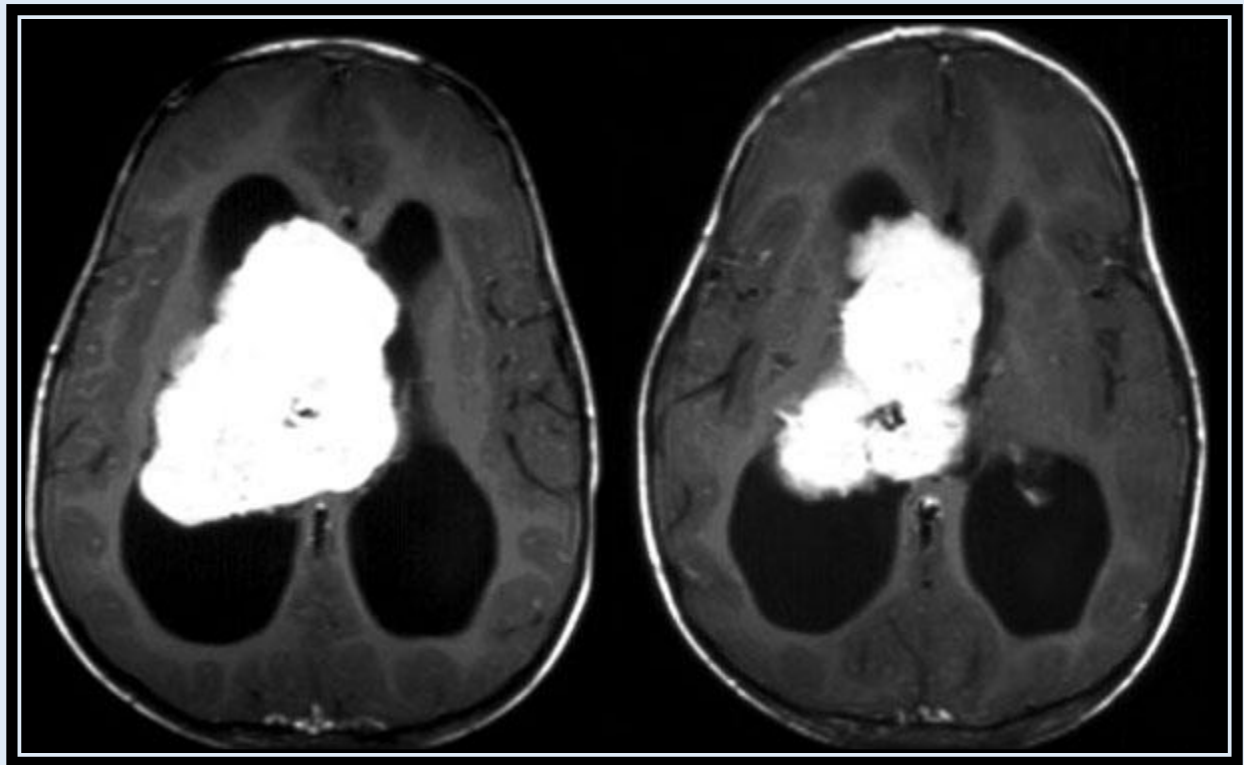
Glial tumors in the pineal region tend to have a good prognosis. Most midbrain glial tumors are low-grade astrocytomas. Signs and symptoms are related to hydrocephalus caused by obstruction at the cerebral aqueduct and in general, eye findings are conspicuously absent.



Tectal glioma

Intraventricular Masses

Tumors of the lateral and third ventricles constitute a small portion of supratentorial masses in children. Choroid plexus tumors account for less than 5% of all pediatric intracranial tumors but 10-20% of those occurring in the first year of life. The majority of tumors represent benign papillomas, though malignant lesions can also be seen. Males are more affected than females and the left lateral ventricle is disproportionately affected. Communicating hydrocephalus may occur from overproduction of CSF from the tumor itself, though obstructive hydrocephalus is more common. Less common to arise in a supratentorial location is an ependymoma, much more frequent in the posterior fossa.



Choroid plexus carcinoma

A glial tumor at the foramen of Monro is typically associated with tuberous sclerosis and is called a subependymal giant cell astrocytoma. With progressive growth ventricular obstruction occurs. The diagnosis can be inferred if calcified subependymal tubers are present.



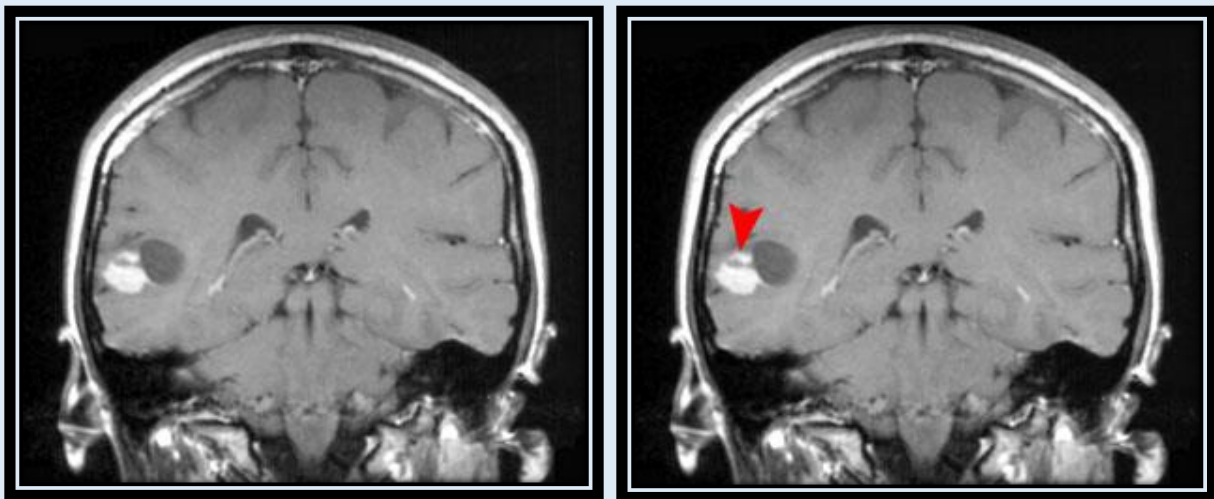
Precontrast, Subependymal giant cell astrocytoma



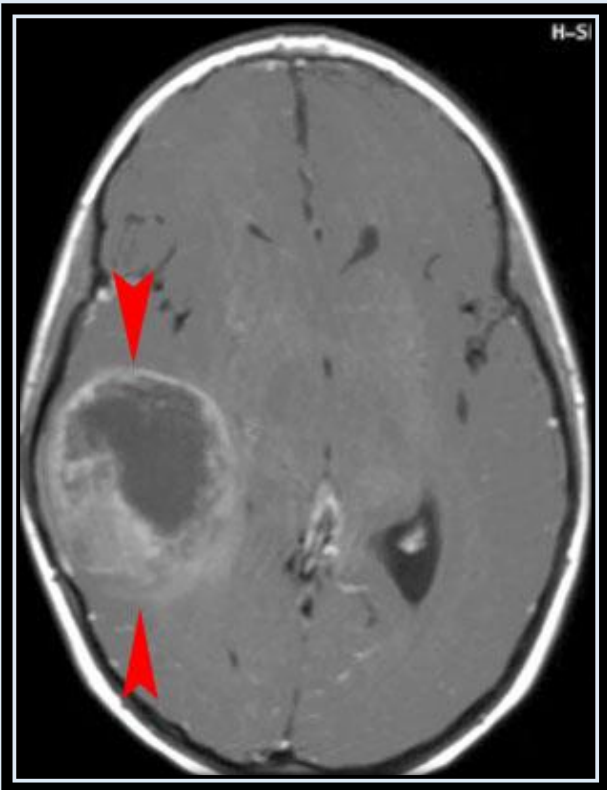
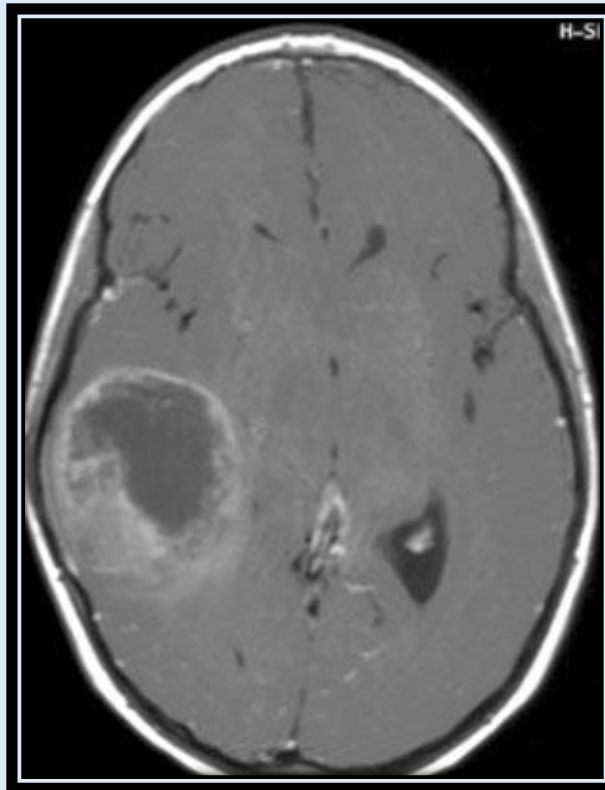
Postcontrast, Subependymal giant cell astrocytoma

Hemispheric Tumors

Nearly half of all supratentorial tumors in children are glial tumors arising from the cerebral hemispheres. Symptoms of hemispheric tumors include headaches, seizures, focal neurologic deficits, and behavioral or cognitive changes. Astrocytomas are the most common source of brain neoplasms. Grading and identification of histology by imaging is not prudent based on enhancement as more rare relatively benign tumors such as pleomorphic xanthoastrocytoma (PXA) may show considerable enhancement. Astrocytomas can range from low-grade neoplasms to highly malignant glioblastoma multiforme. One third of ependymomas are supratentorial and unlike the posterior fossa ependymomas, the majority of lesions are extraventricular within brain parenchyma. Oligodendrogliomas can occur at any age but are typically tumors of young adults. Ganglioglioma, gangliocytoma, and dysembryoplastic neuroepithelial tumor (DNET) are relatively benign tumors seen in the cerebral hemispheres.



PXA



Oligodendroglioma



Ganglioglioma

Pediatric Neurology Quiz Part I

Q_1: On the parasagittal image in head ultrasound, germinal matrix hemorrhage is differentiated from choroid plexus by:

- A. Location, the choroid plexus is anterior to the caudothalamic groove and hemorrhage is posterior.
- B. Location, the choroid plexus is posterior to the caudothalamic groove and hemorrhage is anterior.

Q_2: Grade III germinal matrix hemorrhage is differentiated from grade II by:

- A. The presence of intraparenchymal hemorrhage.
- B. The presence of ventricular dilatation.
- C. The presence of intraventricular extension.
- D. The presence of cystic spaces in the periventricular white matter.

Q_3: The lacunar skull seen in patients with Chiari II malformations is directly related to the degree of hydrocephalus.

- A. True
- B. False

Q_4: Imaging findings seen in Chiari II malformations include all of the following except:

- A. Kinked medulla.
- B. Enlarged massa intermedia.
- C. Tectal beaking.
- D. Posterior fossa cyst.
- E. Hydrocephalus

Q_5: Alobar holoprosencephaly is characterized by the lack of cleavage of the two cerebral hemispheres, a monoventricle, an absent falx cerebri, and partially separated thalami.

- A. True
- B. False

Q_6: Schizencephaly can be differentiated from a porencephalic cyst by:

- A. The cleft being lined by gray matter.
- B. The cleft being lined by white matter.
- C. Focal increased T2 signal in the parenchyma.
- D. The two entities are the same.

Q_7: Abnormal neuronal migration may lead to all of the following except.

- A. Agyria.
- B. Heterotopia.
- C. Pachygyria.
- D. Hydranencephaly.

Q_8: In hydranencephaly, the cerebellum and thalami are typically spared because.

- A. They are fed by the vertebrobasilar system.
- B. The falx cerebri had not developed at the time of injury.
- C. They are myelinated at birth.
- D. Perinatal infections are treated by maternal antibodies.

Q_9: One cause of high output congestive heart failure in the newborn is a vein of Galen malformation.

- A. True
- B. False

Q_10: Myelination patterns are best demonstrated with CT of the head.

- A. True
- B. False

Answers

Q_1: On the parasagittal image in head ultrasound, germinal matrix hemorrhage is differentiated from choroid plexus by:

Location, the choroid plexus is posterior to the caudothalamic groove and hemorrhage is anterior.

Q_2: Grade III germinal matrix hemorrhage is differentiated from grade II by:

The presence of ventricular dilatation.

Q_3: The lacunar skull seen in patients with Chiari II malformations is directly related to the degree of hydrocephalus.

False

Q_4: Imaging findings seen in Chiari II malformations include all of the following except:

Posterior fossa cyst.

Q_5: Alobar holoprosencephaly is characterized by the lack of cleavage of the two cerebral hemispheres, a monoventricle, an absent falx cerebri, and partially separated thalami.

False

Q_6: Schizencephaly can be differentiated from a porencephalic cyst by:

The cleft being lined by gray matter.

Q_7: Abnormal neuronal migration may lead to all of the following except:

Hydranencephaly.

Q_8: In hydranencephaly, the cerebellum and thalami are typically spared because:

They are fed by the vertebrobasilar system.

Q_9: One cause of high output congestive heart failure in the newborn is a vein of Galen malformation.

True

Q_10: Myelination patterns are best demonstrated with CT of the head.

False

Pediatric Neurology Quiz Part II

Q_1: All of the following are true except:

- A. Subacute sclerosing panencephalitis (SSPE) is thought to be secondary to reactivation of a latent measles infection.
- B. The most common imaging finding in TORCH infections are calcifications.
- C. Imaging findings in CNS infections in children differ from adults because the brain is not typically completely myelinated until approximately 16 years of age.
- D. Acute disseminated encephalomyelitis (ADEM) is an immunologic disease in response to a recent viral infection or immunization.

Q_2: Supratentorial ependymomas in children:

- A. Account for the majority of ependymomas.
- B. Behave similarly to posterior fossa ependymomas.
- C. Are typically extraventricular within brain parenchyma.
- D. Are the result of CSF spread from posterior fossa ependymomas.

Q_3: The most frequent tumor in the pineal region is:

- A. Pineoblastoma.
- B. Craniopharyngioma.
- C. Subependymal giant cell astrocytoma.
- D. Germinoma.

Q_4: The four most common posterior fossa masses in children include all of the following except:

- A. Juvenile pilocytic astrocytoma.
- B. Brainstem glioma.
- C. Gangliocytoma.
- D. Medulloblastoma.
- E. Ependymoma.

Q_5: Intracranial calcifications seen in Sturge-Weber syndrome are:

- A. Premalignant lesions.
- B. Vascular calcifications from a slow flow state.
- C. Secondary to prenatal infection.
- D. The result of treatment.

Q_6: Most patients with neurofibromatosis 2 present as newborns with multiple nerve sheath tumors.

- A. True
- B. False

Q_7: The most common imaging finding in neurofibromatosis 1 are NF1 spots in the basal ganglia, cerebellum, brainstem, and splenium that typically regress after age 12.

- A. True
- B. False

Q_8: An optic glioma is pathognomonic for having NF1.

- A. True
- B. False

Q_9: Bilateral acoustic schwannomas are pathognomonic for NF2.

- A. True
- B. False

Q_10: Glial tumors in the cerebral hemispheres can be accurately graded by imaging characteristics.

- A. True
- B. False

Answers

Q_1: All of the following are true except:

Imaging findings in CNS infections in children differ from adults because the brain is not typically completely myelinated until approximately 16 years of age.

Q_2: Supratentorial ependymomas in children:

Are typically extraventricular within brain parenchyma.

Q_3: The most frequent tumor in the pineal region is:

Germinoma.

Q_4: The four most common posterior fossa masses in children include all of the following except:

Gangliocytoma.

Q_5: Intracranial calcifications seen in Sturge-Weber syndrome are:

Vascular calcifications from a slow flow state.

Q_6: Most patients with neurofibromatosis 2 present as newborns with multiple nerve sheath tumors.

False

Q_7: The most common imaging finding in neurofibromatosis 1 are NF1 spots in the basal ganglia, cerebellum, brainstem, and splenium that typically regress after age 12.

True

Q_8: An optic glioma is pathognomonic for having NF1.

False

Q_9: Bilateral acoustic schwannomas are pathognomonic for NF2.

True

Q_10: Glial tumors in the cerebral hemispheres can be accurately graded by imaging characteristics.

False

Ped Radiology Post-Test

Ped Radiology Post-Test

Q_1: The "double bubble" sign signifies a dilated stomach and duodenal bulb and is seen with duodenal atresia.

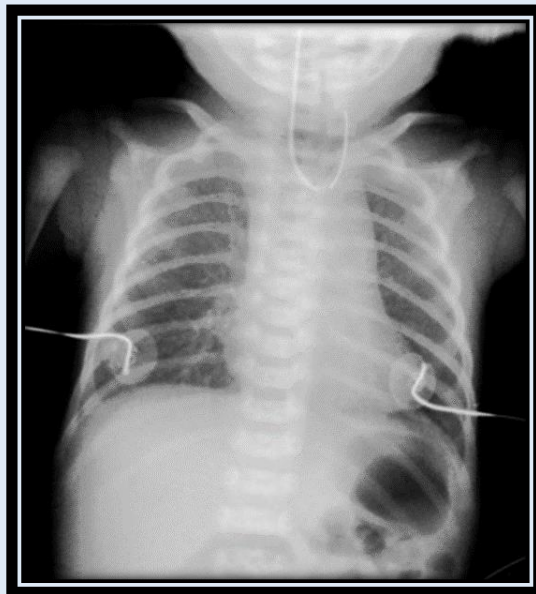
- A. True
- B. False

Q_2: All of the following are true regarding meconium ileus EXCEPT:

- A. "Soap bubble" appearance of bowel, usually in the right lower quadrant
- B. Small bowel obstruction
- C. The presenting symptom in 85% of cystic fibrosis patients
- D. Volvulus and ileal stenosis are complications, although rare

Q_3: Problem: inability to pass NG tube. What is the diagnosis?

- A. Esophageal atresia with a tracheoesophageal fistula
- B. Esophageal atresia without a tracheoesophageal fistula
- C. Tracheoesophageal fistula without esophageal atresia
- D. None of the above



Q_4: In Hirschsprung disease the most common transition site is the rectosigmoid colon.

- A. True
- B. False

Q_5: Appendicitis can present with which of the following?

- A. Small bowel obstruction
- B. Appendicolith
- C. Right lower quadrant pain, McBurney's sign
- D. All of the above

Q_6: What is the diagnosis?

- A. Necrotizing enterocolitis
- B. Meconium Ileus
- C. Duodenal atresia
- D. None of the above.



Q_7: In hypertrophic pyloric stenosis, all of the following are true EXCEPT:

- A. Pyloric length > 14mm
- B. Pyloric muscle wall thickness > 3 - 4mm
- C. Exaggerated peristaltic waves
- D. Bilious vomiting

Q_8: Treatment of intussusception includes air or fluid enema under fluoroscopic guidance, or surgery if these methods fail.

- A. True
- B. False

Q_9: Where is the coin lodged?

- A. Trachea
- B. Esophagus
- C. Carina
- D. None of the above



Q_10: Malrotation with midgut volvulus is a surgical emergency because it may lead to bowel necrosis.

- A. True
- B. False

Q_11: The umbilical venous catheter tip should be within 1 cm of the diaphragm, in the IVC.

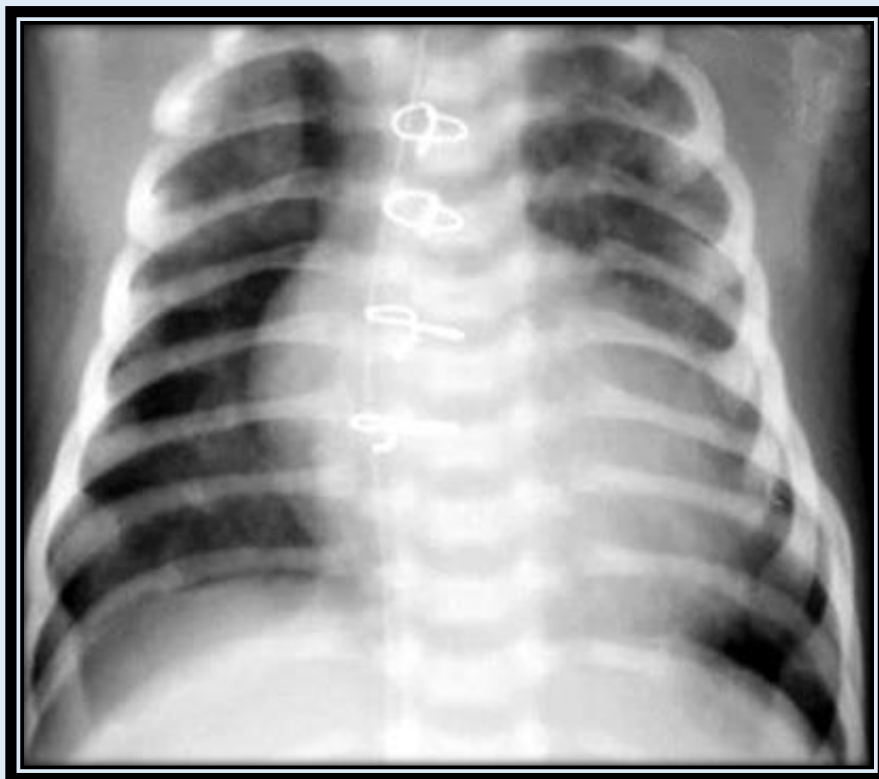
- A. True
- B. False

Q_12: If there is a question of pneumoperitoneum on a supine x-ray, the following x-ray's can be obtained for confirmation:

- A. Prone or cross table lateral
- B. Left side down decubitus or cross table lateral
- C. Left side down decubitus or prone
- D. None of the above

Q_13: What is the diagnosis?

- A. Pneumoperitoneum
- B. Pneumothorax
- C. Pneumonia
- D. None of the above



Q_14: Transient tachypnea of the newborn is characterized by all of the following EXCEPT:

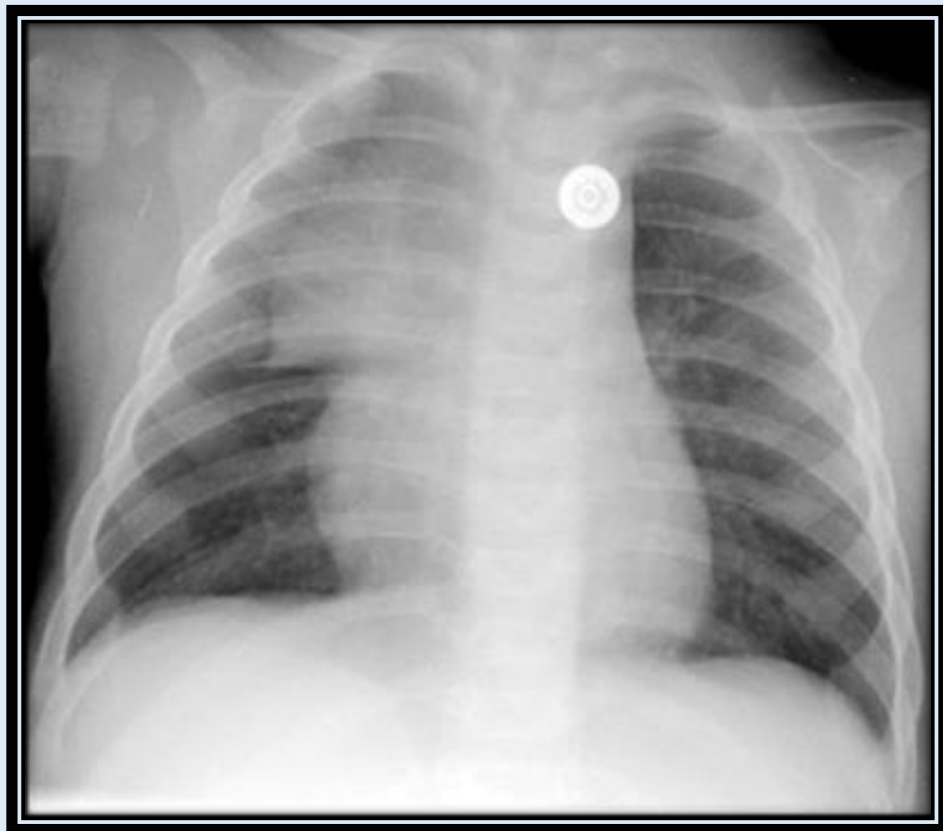
- A. Presents 4 - 6 hours after birth with respiratory distress
- B. Typically affects premature infants
- C. Due to delayed clearance of fetal pulmonary fluid
- D. Usually clears by 48 - 72 hours

Q_15: Congenital diaphragmatic hernia can be diagnosed on prenatal ultrasound.

- A. True
- B. False

Q_16: What is the image depicting?

- A. Right upper lobe collapse
- B. Right upper lobe mass
- C. Normal thymus
- D. None of the above



Q_17: Primary tuberculosis can present with all of the following EXCEPT:

- A. Hilar adenopathy
- B. Pleural effusion
- C. Diffuse, small uniform nodules
- D. Focal consolidation

Q_18: Thickening of the epiglottis in acute epiglottitis, as seen on the lateral view, is called the thumb sign.

- A. True
- B. False

Q_19: What is the most likely diagnosis?

- A. Mycoplasma pneumonia
- B. Pneumothorax
- C. Cystic fibrosis
- D. None of the above



Q_20: The deep sulcus sign is diagnostic of a pneumothorax.

- A. True
- B. False

Q_21: The early filling film in a voiding cystourethrogram (VCUG) allows visualization of a ureterocele, if present.

- A. True
- B. False

Q_22: You identify vesicoureteral reflux while performing a VCUG on a 2 year-old boy. The patient's siblings do not need to be screened for vesicoureteral reflux

- A. True
- B. False

Q_23: What grade of reflux is being depicted?

- A. Grade 1
- B. Grade 2
- C. Grade 3
- D. Grade 4
- E. Grade 5



Q_24: All of the following are true regarding autosomal recessive polycystic kidney disease EXCEPT:

- A. Renal enlargement
- B. Echogenic kidneys on ultrasound due to numerous cysts throughout the cortex and medulla
- C. Associated with hepatic fibrosis
- D. Associated with intracranial aneurysms

Q_25: Hydronephrosis is the most common cause of an abdominal mass in the neonate.

- A. True
- B. False

Question 26: What is the diagnosis?

- A. Hydronephrosis
- B. Multicystic dysplastic kidney
- C. Autosomal dominant polycystic kidney disease
- D. None of the Above



Q_27: Mesoblastic nephroma can be reliably differentiated from a Wilms tumor on imaging.

- A. True
- B. False

Q_28: Most neuroblastomas arise from the adrenal gland and present with a palpable abdominal mass.

- A. True
- B. False

Question 29: What is the diagnosis?

- A. Wilms tumor
- B. Neuroblastoma
- C. Mesoblastic nephroma
- D. None of the above



Q_30: Wilms tumor can invade the renal vein / IVC and displace vessels whereas neuroblastoma encases vessels.

- A. True
- B. False

Q_31: All Salter-Harris fractures involve the growth plate.

- A. True
- B. False

Q_32: Radiographic findings suggestive of non-accidental trauma include:

- A. Metaphyseal corner fractures
- B. Posterior rib fractures near the costovertebral junction
- C. Multiple fractures at different stages of healing
- D. All of the above

Question 33: What is the diagnosis?

- A. Slipped capital femoral epiphysis
- B. Legg-Calve-Perthes disease
- C. Bone cyst
- D. Hip dislocation



Q_34: All of the following are true regarding Developmental Dysplasia of the hip EXCEPT:

- A. More prevalent in males than females
- B. Clinical findings include shortened leg, asymmetric gluteal folds, and hip clicks
- C. Alpha angle < 60 degrees
- D. Ultrasound is preferred if the patient is < 6 months old

Q_35: A child presents with a fever and a painful hip. It is important to exclude septic arthritis because of the unfavorable sequelae if undiagnosed and untreated.

- A. True
- B. False

Question 36: What is the diagnosis?

- A. Patellar tendon rupture
- B. Osteochondroma of the tibial tuberosity
- C. Osgood-Schlatter disease
- D. None of the above



Q_ 37: Classic radiographic findings of Langerhans cell histiocytosis include:

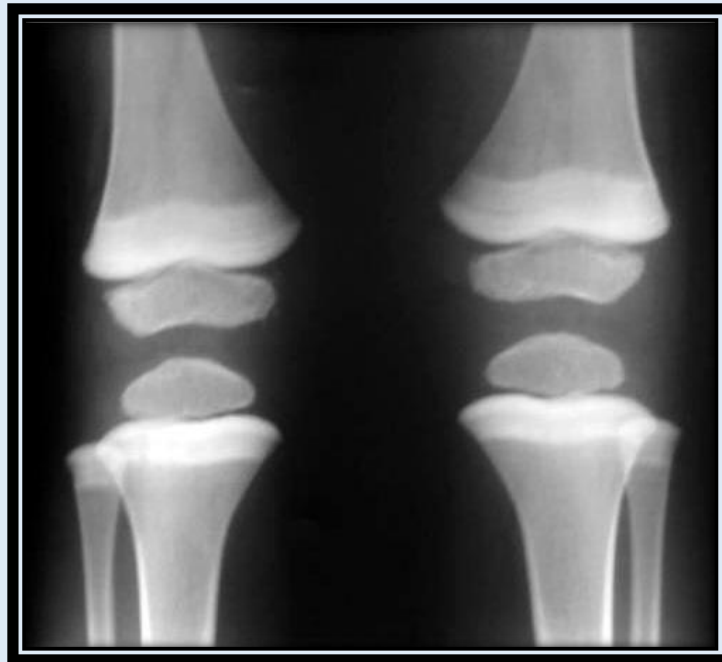
- A. Punched out lytic skull lesions
- B. Vertebra plana
- C. Floating teeth appearance in the mandible
- D. All of the above

Q_38: Achondroplasia results in a pelvis with tall flared iliac wings and increased acetabular angles whereas mucopolysaccharidoses result in rounded iliac wings with decreased acetabular angles.

- A. True
- B. False

Question 39: What is the diagnosis?

- A. Lead poisoning
- B. Normal variant
- C. Leukemia
- D. None of the Above



Q_40: Radiographic findings of Osteogenesis Imperfecta include all of the following EXCEPT:

- A. Multiple fractures at different stages of healing
- B. Wormian bones within the skull
- C. Metaphyseal corner fractures
- D. Osteopenia

Q_41: Grade IV germinal matrix hemorrhage is parenchymal hemorrhage from direct extension of a germinal matrix hemorrhage.

- A. True
- B. False

Q_42: Associated findings of Chiari I malformation include hydrocephalus and hydrosyringomyelia (syrinx).

- A. True
- B. False

Q_43: What is the diagnosis on this sagittal head ultrasound?

- A. Germinal matrix hemorrhage
- B. Periventricular leukomalacia
- C. Normal
- D. None of the Above

Q_44: All of the following are true regarding a vein of Galen malformation EXCEPT:

- A. Arteriovenous fistula between one or more cerebral arteries and the vein of Galen
- B. Typical presentation is high output congestive heart failure
- C. Imaging shows a mass in the region of the posterior 3rd ventricle
- D. Treatment is surgical removal

Q_45: An arachnoid cyst in the posterior fossa will exert mass effect on the underlying cerebellum.

- A. True
- B. False

Question 46: What is the diagnosis?

- A. Sturge-Weber syndrome
- B. Meningitis
- C. Subacute sclerosing panencephalitis
- D. None of the above



Q_47: All of the following can be present in Tuberous sclerosis, EXCEPT:

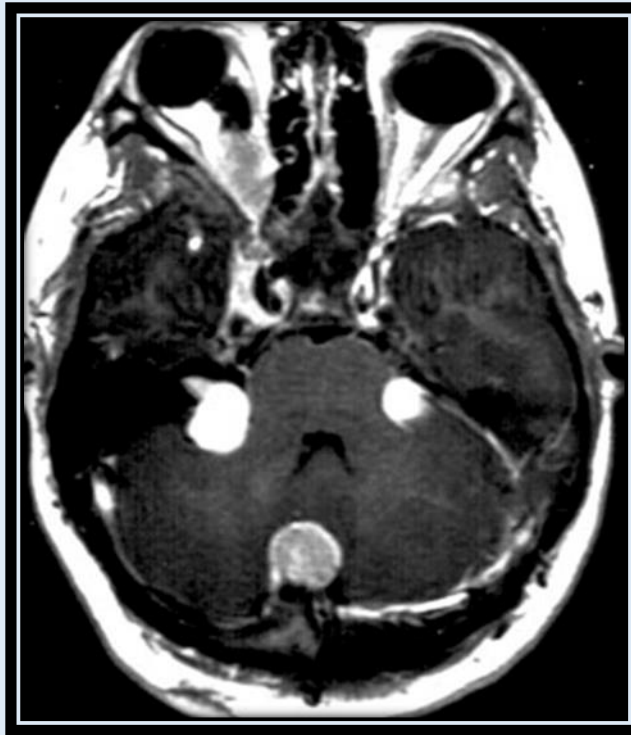
- A. Subependymal and cortical tubers
- B. Bilateral acoustic schwannomas
- C. Giant cell astrocytoma
- D. Classic triad of mental retardation, seizures, and adenoma sebaceum

Q_48: Herpes encephalitis *typically* affects the temporal lobes in neonates who get the infection during birth.

- A. True
- B. False

Q_49: What is the diagnosis?

- A.** Neurofibromatosis 1
- B.** Neurofibromatosis 2
- C.** Neurofibromatosis 3
- D.** None of the Above



Q_50: Ependymomas typically arise from the floor of the 4th ventricle whereas medulloblastomas arise from the roof of the 4th ventricle.

- A.** True
- B.** False

Answers

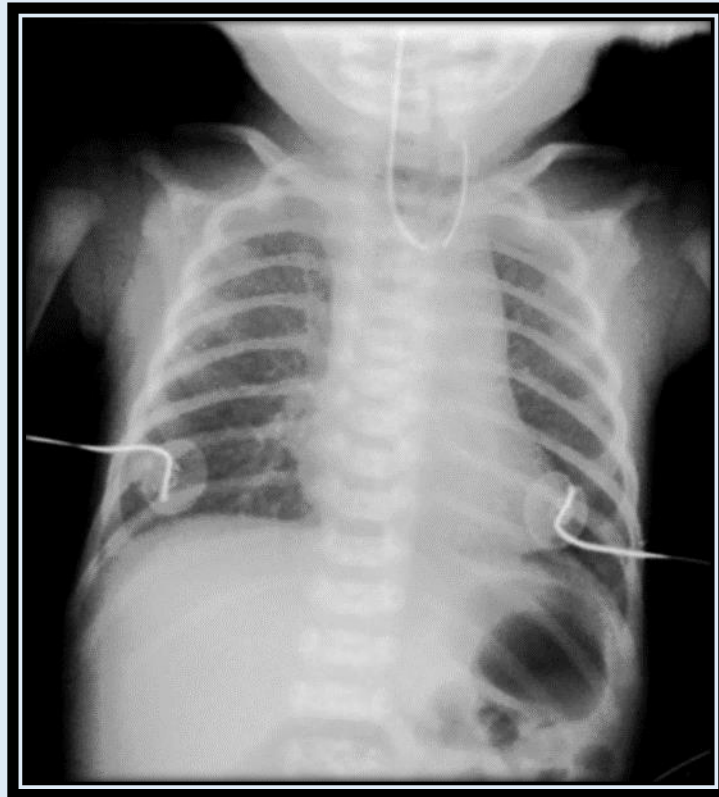
1) The "double bubble" sign signifies a dilated stomach and duodenal bulb and is seen with duodenal atresia.

True

2) All of the following are true regarding meconium ileus EXCEPT:

The presenting symptom in 85% of cystic fibrosis patients, rather 10-15% of patients with CF present with meconium ileus.

3) Problem: inability to pass NG tube. What is the diagnosis?



Esophageal atresia with a tracheoesophageal fistula.

The NG tube is looped within the esophageal pouch. Air is in the stomach indicating presence of a tracheoesophageal fistula.

4) In Hirschsprung disease the most common transition site is the rectosigmoid colon

True.

The transition zone is the junction between the proximal normally innervated colon and the distal aganglionic segment. The normally innervated proximal colon becomes dilated.

5) Appendicitis can present with which of the following?

All of the above.

It can present with small bowel obstruction, an appendicolith and right lower quadrant pain

6) What is the diagnosis?



Necrotizing enterocolitis.

There is extensive pneumatosis (air in the bowel wall) seen as bubbly lucencies overlying the bowel. This is the most definitive radiographic finding of NEC.

7) In hypertrophic pyloric stenosis, all of the following are true EXCEPT

Bilious vomiting.

Patients with this entity present with **nonbilious** projectile vomiting.

8) Treatment of intussusception includes air or fluid enema under fluoroscopic guidance or surgery if these methods fail

True.

Note that the choice of studies performed varies among institutions.

9) Where is the coin lodged?



Esophagus.

A coin in the esophagus has its widest dimension on the AP view and a coin lodged in the trachea has its widest dimension on the lateral view

10) Malrotation with midgut volvulus is a surgical emergency because it may lead to bowel necrosis

True

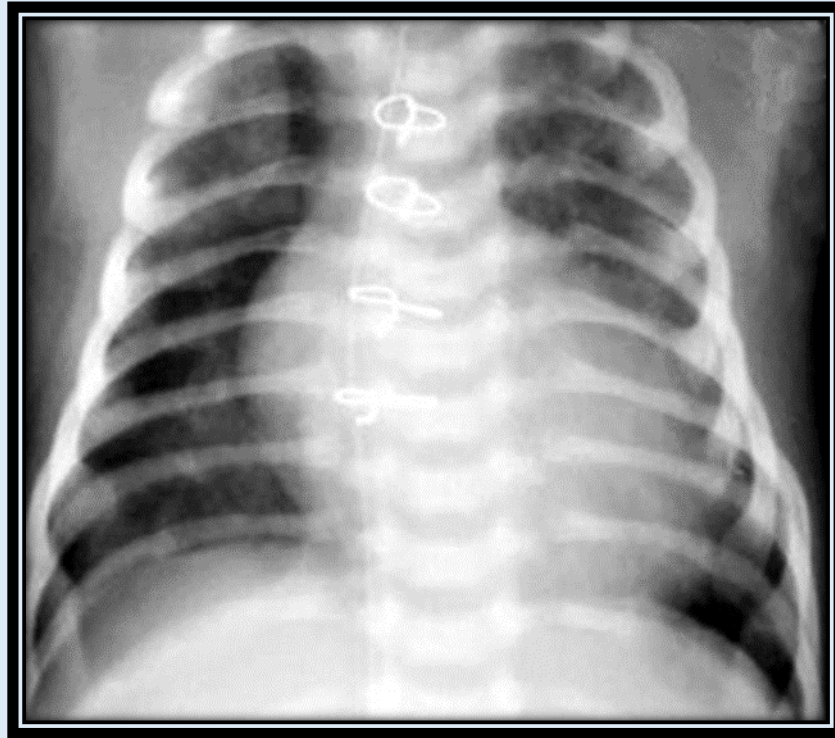
11) The umbilical venous catheter tip should be within 1 cm of the diaphragm, in the IVC

True

12) If there is a question of pneumoperitoneum on a supine XR, the following XRâs can be obtained for confirmation

Left side down decubitus or cross table lateral.

13) What is the diagnosis?



Pneumothorax.

The right heart border is sharp in appearance and the right costophrenic angle is hyperlucent, diagnostic of a pneumothorax.

14) Transient tachypnea of the newborn is characterized by all of the following EXCEPT

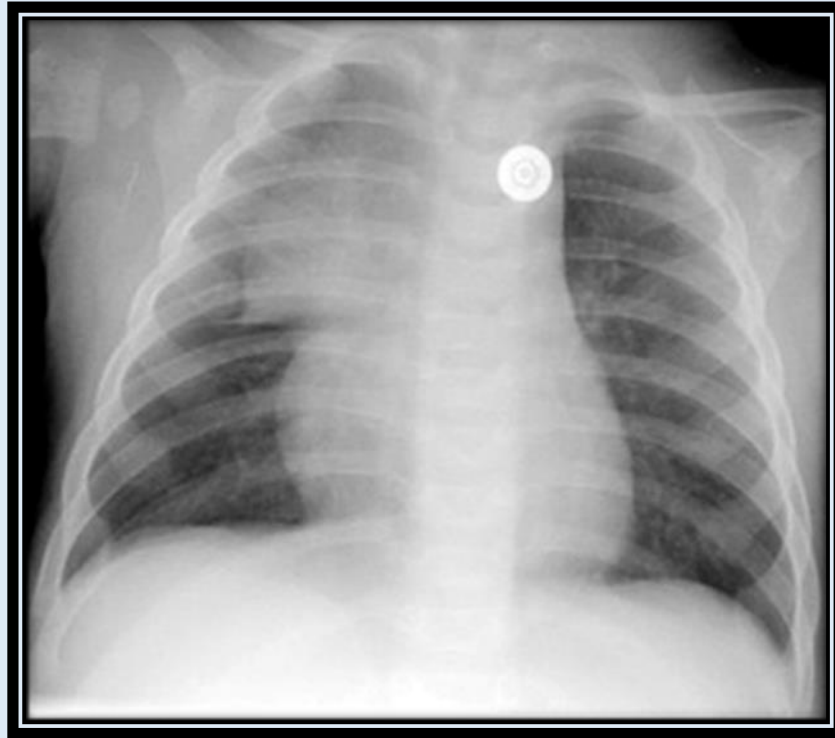
Typically affects premature infants.

TTN usually affects neonates born at term.

15) Congenital diaphragmatic hernia can be diagnosed on prenatal ultrasound

True

16) What is the image depicting?



Normal thymus.

Note the sharp, well-defined lateral and inferior borders of the normal appearing thymus projected along the right superior mediastinum

17) Primary tuberculosis can present with all of the following EXCEPT

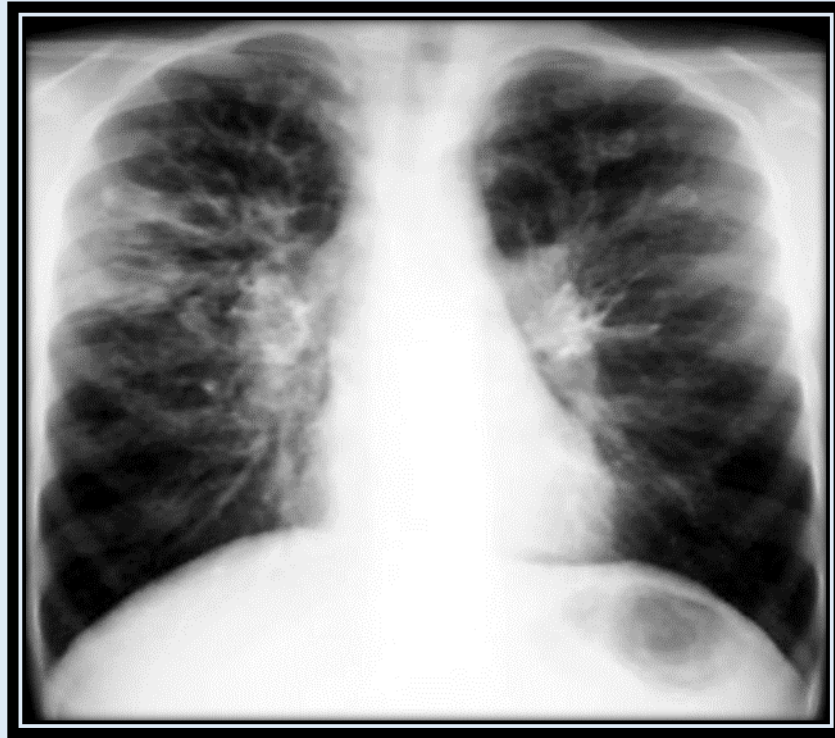
Diffuse small uniform nodules.

Miliary TB results from secondary infection and is characterized by diffuse small uniform nodules in the lungs.

18) Thickening of the epiglottis in acute epiglottitis, as seen on the lateral view, is called the "thumb sign"

True

19) What is the diagnosis?



Cystic fibrosis.

The CXR demonstrates bronchiectasis, mucous plugging and hyperinflation consistent with CF.

20) The deep sulcus sign is diagnostic of a pneumothorax

True

21) The early filling film in a voiding cystourethrogram (VCUG) allows visualization of a ureteroceles, if present

True

22) You identify vesicoureteral reflux while performing a VCUG on a 2 year-old boy. The patient's siblings do not need to be screened for vesicoureteral reflux

False.

There is an increased incidence of vesicoureteral reflux in siblings of children with VUR, in children of parents who had VUR, and in non-African Americans as opposed to African American children.

23) What grade of reflux is being depicted?



Grade 5.

There is severe hydronephrosis and tortuosity of the ureter.

24) All of the following are true regarding autosomal recessive polycystic kidney disease EXCEPT

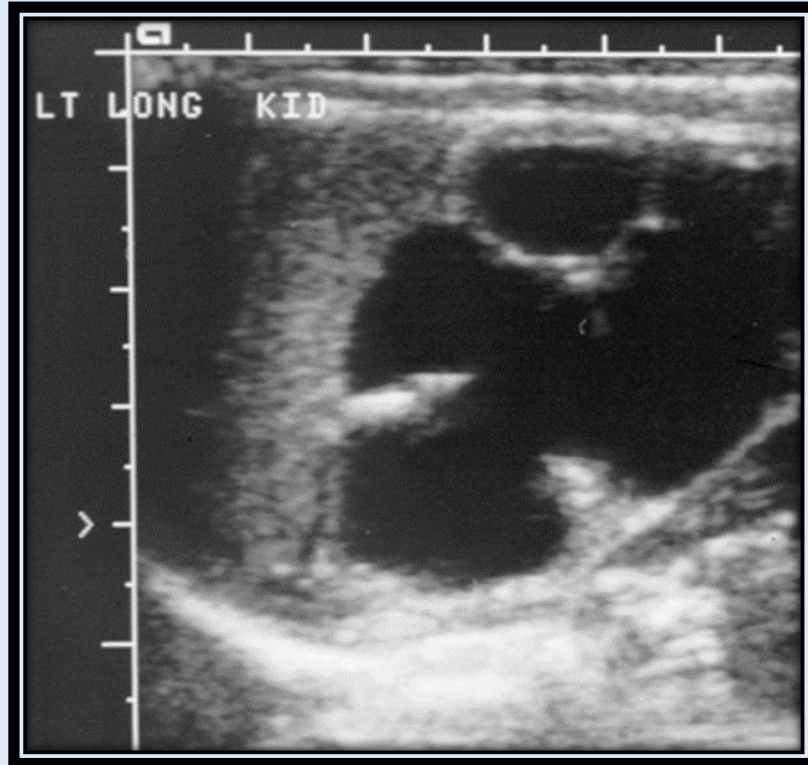
Associated with intracranial aneurysms.

Autosomal *dominant* polycystic kidney disease is associated with intracranial aneurysms.

25) Hydronephrosis is the most common cause of an abdominal mass in the neonate

True

26) What is the diagnosis?



Hydronephrosis.

The cystic appearing spaces communicate in hydronephrosis as opposed to multicystic dysplastic kidney where the large cysts do not communicate.

27) Mesoblastic nephroma can be reliably differentiated from a Wilms tumor on imaging

False.

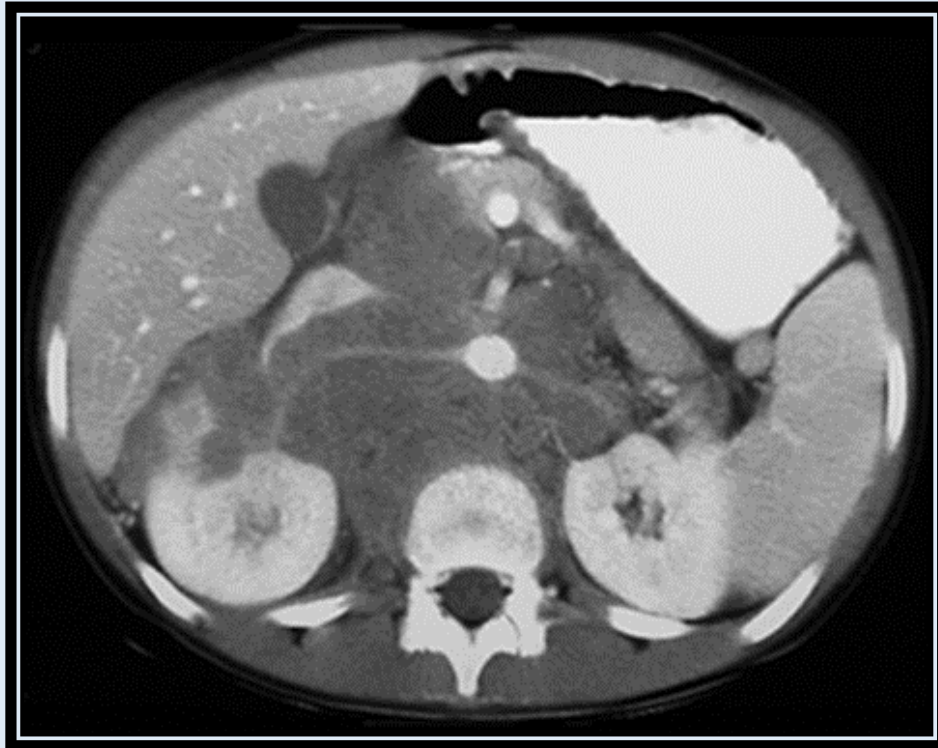
Because imaging cannot differentiate mesoblastic nephroma from a rare early Wilms tumor, it must be surgically removed

28) Most neuroblastomas arise from the adrenal gland and present with a palpable abdominal mass

True.

Neuroblastomas can arise anywhere along the course of the sympathetic chain, but most commonly do so from the adrenal gland.

29) What is the diagnosis?



Neuroblastoma.

There is a large hypodense mass crossing the midline and encasing the aorta and its branches. It does not arise from the kidney (absent "claw sign").

30) Wilms tumor can invade the renal vein/IVC and displace vessels whereas neuroblastoma encases vessels

True

31) All Salter-Harris fractures involve the growth plate

True.

In addition, Salter-Harris fractures are divided into 5 types based on whether there is also metaphyseal, epiphyseal or solely physeal involvement.

32) Radiographic findings suggestive of non-accidental trauma include

Metaphyseal corner fractures, posterior rib fractures near the costovertebral junction, and multiple fractures at different stages of healing.

33) What is the diagnosis?



Legg-Calve-Perthes disease.

The subchondral lucency in the femoral epiphysis represents the *crescent sign* seen in LCP disease.

34) All of the following are true regarding Developmental Dysplasia of the Hip EXCEPT

More prevalent in males than females.

It is more prevalent in females than males (9:1).

35) A child presents with a fever and a painful hip. It is important to exclude septic arthritis because of the unfavorable sequelae if undiagnosed and untreated

True.

If septic arthritis is left untreated, it can lead to joint destruction.

36) What is the diagnosis?



Osgood-Schlatter disease.

There is fragmentation of the tibial tuberosity, thickening of the inferior patellar tendon, and soft tissue swelling inferior to the patella

37) Classic radiographic findings of Langerhans cell histiocytosis include

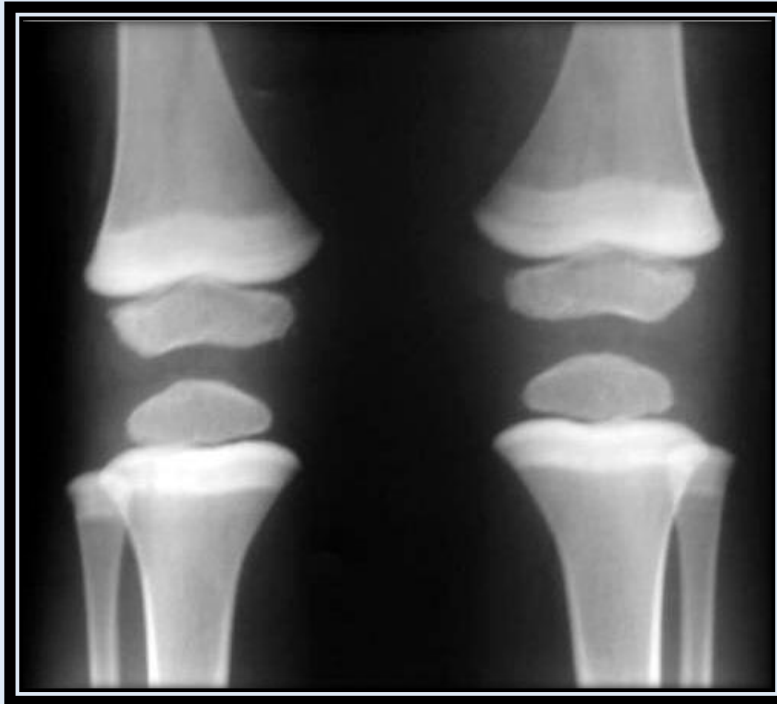
Punched out lytic skull lesions, vertebra plana, and "floating teeth" appearance in the mandible.

38) Achondroplasia results in a pelvis with tall flared iliac wings and increased acetabular angles whereas mucopolysaccharidoses result in rounded iliac wings with decreased acetabular angles

False.

The reverse is true. The pelvis in achondroplasia has a "tombstone" appearance with rounded iliac wings and decreased acetabular angles.

39) What is the diagnosis?



Lead poisoning.

This is a classic example of lead poisoning with sclerotic metaphyseal bands involving the distal femurs, proximal tibias and proximal fibulas. The dense metaphyseal bands seen in normal variants do not typically involve the proximal fibula. Leukemia causes lucent metaphyseal bands.

40) Radiographic findings of Osteogenesis Imperfecta include all of the following EXCEPT

Metaphyseal corner fractures.

These are highly specific for non-accidental trauma.

41) Grade IV germinal matrix hemorrhage is parenchymal hemorrhage from direct extension of a germinal matrix hemorrhage

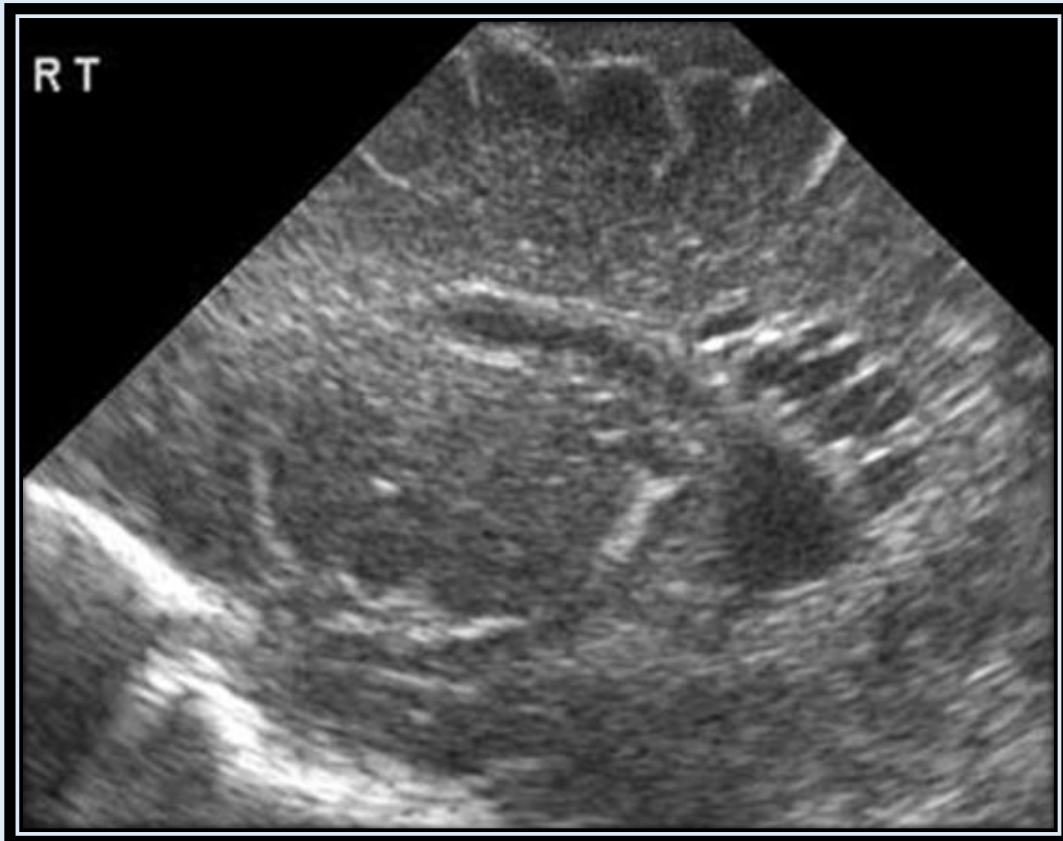
False.

Grade IV hemorrhage is a parenchymal venous infarction hemorrhage rather than extension from a germinal matrix hemorrhage.

42) Associated findings of Chiari I malformation include hydrocephalus and hydrosyringomyelia (syrinx)

True.

43) What is the diagnosis on this sagittal head ultrasound?



Periventricular leukomalacia.

Cystic changes along the right lateral ventricle represent PVL.

44) All of the following are true regarding a vein of Galen malformation EXCEPT

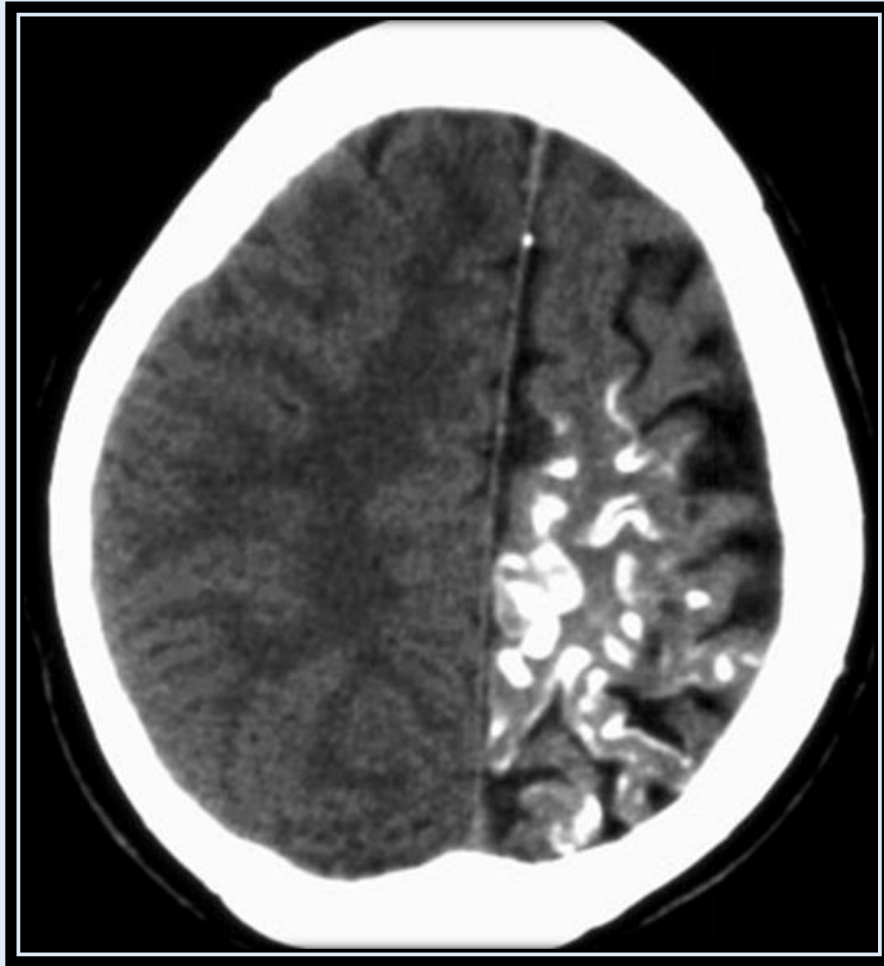
Treatment is surgical removal. Rather, treatment is typically arterial embolization.

45) An arachnoid cyst in the posterior fossa will exert mass effect on the underlying cerebellum

True.

A mega cisterna magna does not exert mass effect on the adjacent brain.

46) What is the diagnosis?



Sturge-Weber syndrome.

Note the atrophic left hemispheric gyri with serpiginous calcifications.

47) In Tuberous sclerosis all of the following can be present EXCEPT

Bilateral acoustic schwannomas.

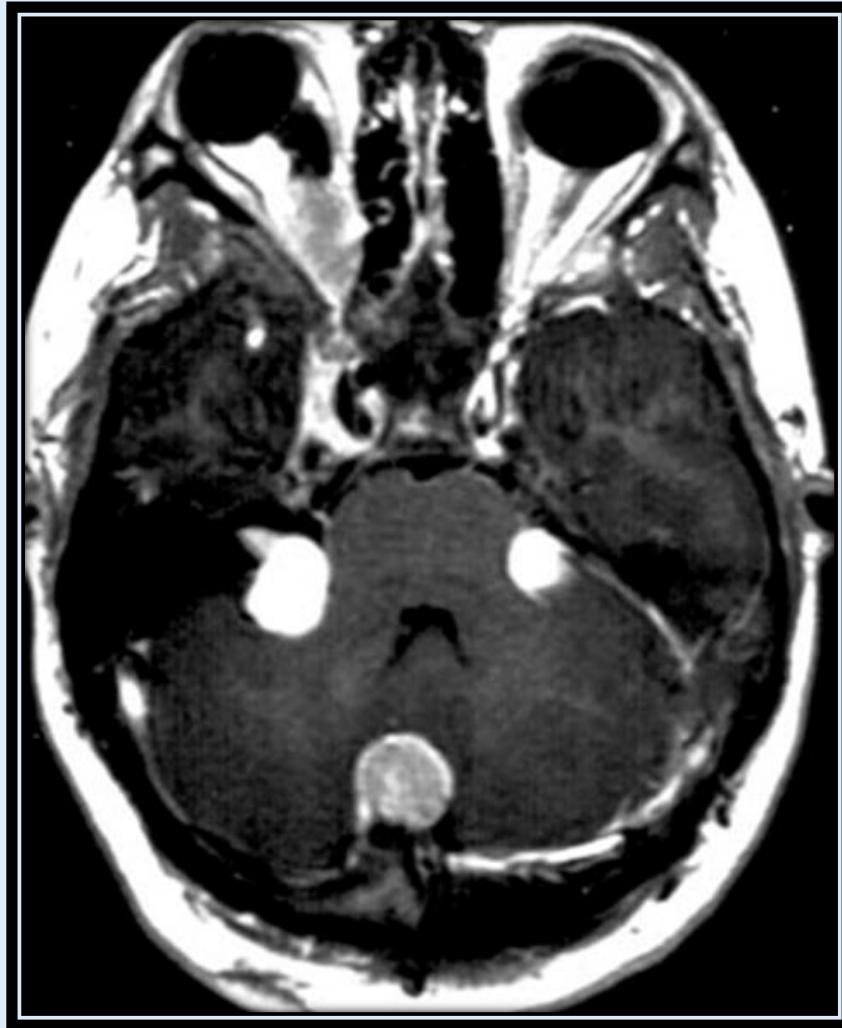
These are seen in Neurofibromatosis 2.

48) Herpes encephalitis *typically* affects the temporal lobes in neonates who get the infection during birth

False.

Any part of the brain can be affected under these circumstances.

49) What is the diagnosis?



Neurofibromatosis 2.

There are bilateral acoustic schwannomas, right optic nerve meningioma, and posterior meningioma.

50) Ependymomas typically arise from the floor of the 4th ventricle whereas medulloblastomas arise from the roof of the 4th ventricle

True.

References:

Texts:

- Blickman JG: Pediatric Radiology The Requisites, 1994, Mosby-Year Book, Inc.,
- MI. Donnelly LF: Fundamentals of Pediatric Radiology, 2001, W.B. Saunders Company,
- PA. Kirks DR, editor: Practical Pediatric Imaging, 1998, Lippincott-Raven Publishers, NY.
- Siegel MJ: Pediatric Body CT, 1999, Lippincott Williams and Wilkins, PA.
- Siegel MJ, editor: Pediatric Sonography, 2002, Lippincott Williams and Wilkins, PA.
- Weissleder R, Rieumont MJ, Wittenberg J: Primer of Diagnostic Imaging, 1997, Mosby, Inc.,

Websites:

- Auntminnie.com
- emedicine.com, Clubfoot article by Chung,
- E MedPix Radiology Teaching File and Medical Imaging Database

Articles:

- Glotzbecker MP, Carpentiere DF, Dormans, JP: Langerhans Cell Histiocytosis: Clinical Presentation, Pathogenesis, and Treatment from the LCH Research Group at the Children's Hospital of Philadelphia, Volume 15 spring 2002, pages 67-73